Hyperglycaemia is Associated with Male Infertility and Activin Dysregulation in Type 1 Diabetes

Doctoral thesis submitted in accordance with the assigned joint award doctoral programme

in fulfilment of the requirements for the degree of
Doctor of Human Biology (Doctor biologiae hominis - Dr. biol. hom.)
at the Faculty of Medicine of the Justus-Liebig-University Gießen

and

in fulfilment of the requirements for the degree of
Doctor of Philosophy (PhD)
at the Faculty of Medicine of Monash University Melbourne

Submitted by Constanze Christin Maresch
born on 17.04.1987
in Borna, Germany

Gießen (2016)

From the Clinical Research Unit at the Medical Clinic and Polyclinic III at the
Justus-Liebig-University Gießen led by Prof. Dr. Thomas Linn

Examiners: Prof. Dr. Thomas Linn
Prof. Dr. Andreas Meinhardt
Prof. Serge Nef
Dr. Catherine Itman

Day of thesis defence: 26.04.2017

„ A scientist in his laboratory is not a mere technician: he is also a child confronting natural phenomena that impress him as though they were fairy tales.“

Marie Curie

Copyright Notices

Notice 1

Notice 2

Table of Contents

1 Introduction

Diabetes mellitus (DM) is one of the most prominent public health threats in modern societies with a rapidly rising prevalence. In 2000, the World Health Organization (WHO) reported that there were 177 million people living with DM and predicted that this number will increase to at least 300 million by 2025 [287]. This is further supported by a report from Wild et al., which predicts an increase in individuals affected by DM of 37 % by the year 2030 [289]. This increase will not only affect the older population, but also an increasing number of individuals, especially men, in their reproductive age, since there is a rise in the number of childhood and adolescent males with type 1 (T1D) and type 2 (T2D) diabetes mellitus [246]. Moreover, the great majority of T1D patients are diagnosed before the age of 30 years [3].

To date, several clinical studies have reported a negative impact of DM on male reproductive function leading to erectile dysfunction and ejaculation dysfunction, as well as a reduction in semen volume, sperm counts, sperm motility, and abnormal sperm morphology [12]. Furthermore, the unique characteristics of glucose metabolism within testicular cells make them prone to changes under diabetic conditions. It is likely that the glucose sensing machinery as well as the hormonal control within these cells to counteract hyper- und hypoglycaemia play a crucial role in the subfertility and/or infertility associated with DM [12,141,248].

Focusing on the molecular mechanism responsible for DM-induced changes in male fertility numerous clinical and animal studies have been conducted to address this issue, yet still little is known and much remains to be evaluated further.

Activins are members of the transforming growth factor-β (TGF-β) superfamily and have recently been reported to play an important role in glucose metabolism by regulating the differentiation and activity of the insulin-producing pancreatic β-cells, as well as the response of insulin on target cells [49]. Additionally, these mechanisms have been proposed to modulate events involved in insulin sensitivity in a tissue dependent manner and therefore regulate whole-body insulin responsiveness [104]. Therefore, the involvement of the activins in the development and onset of diabetes related male subfertility and/or infertility seems likely.

In the studies described in this thesis, the *mev-1* (methyl viologen sensitive) mutant of the nematode *Caenorhabditis elegans* (*C. elegans*), the *Ins2*$^{Akita+/-}$ mouse

model, as well as cultured Sertoli cells were used to investigate the effects of hyperglycaemia and insulin deficiency on the biological actions of the activins, specifically in male reproduction. The *mev-1* mutant of the nematode *C. elegans* was shown to be a valuable model organism in the study of glucose-induced cell toxicity, and thus the study of hyperglycaemic effects of DM [71,84]. It carries a mutation within the cytochrome b subunit of succinate dehydrogenase resulting in excessive mitochondrial superoxide production and premature death [121]. This in turn closely resembles the metabolic situation of diabetic patients who exhibit a deficiency in the signalling of reactive oxygen species (ROS) leading to the initiation of autoimmune diabetes as well as diabetes induced morphological changes in mitochondria, which are closely linked to the presence of superoxide anion [159,266].

The Akita mouse is a model of T1D that results from a mutation in the *Ins2* gene. This mutation leads to a misfolded protein product, which accumulates in the endoplasmic reticulum (ER), causing ER stress and, ultimately, death of the insulin producing β-cells of the pancreas [282]. The diabetic Akita mouse is thus similar to humans with T1D, which is caused by an autoimmune destruction of the β-cells of the pancreas [1,12]. Akita mice are a unique model to study infertility as they display a sudden and severe onset of diabetes at 4-6 weeks of age similar to untreated diabetes in human adolescents and without concern of drug-induced toxicity to both pancreas and testis[125].

My hypothesis is that hyperglycaemia will induce local low-grade inflammation regulated by activins and their binding protein follistatin. Therefore, the aim of this thesis is to investigate the impact of T1D on male reproductive function in the context of low-grade inflammation using *mev-1* mutant nematodes, heterozygous *Ins2*^{Akita} (*Ins2*$^{Akita+/-}$) mice, and cultured Sertoli cells. I will give an overview about diabetes, the male reproductive tract, and a detailed description of the actions of the activins as members of the TGF-β superfamily. This is followed by material and methods, results and discussion.

1.1 Diabetes mellitus

Diabetes is a group of chronic, metabolic diseases characterized by hyperglycaemia resulting from defects in insulin secretion and/or insulin action [1]. First described in ancient times, the name diabetes mellitus was coined by the Greek/Roman doctor Araetus of Cappodocia (ca. 81-133 A.D.) deriving from the Greek word

"diabenein" meaning "straddling" and the Latin word *"mellitus"* for honey sweet. Both words marked the most pronounced symptoms of the disease, namely the urge to pass urine frequently and a sweet taste of the urine, the latter being one of the earliest diagnostic methods [4].

Left untreated, diabetes leads to chronic hyperglycaemia, which is associated with long-term damage, dysfunction, and failure of different organs, especially the eyes, kidneys, nerves, heart, and blood vessels [1,12,61,115,154,232,273].

The development of DM involves several pathogenic processes, including autoimmune destruction of pancreatic β-cells with consequent insulin deficiency together with abnormalities that result in insulin resistance. The latter in turn leads to inadequate insulin secretion and/or diminished tissue responses to insulin at one or more points in the complex pathways of hormone action, affecting not only carbohydrate, but also fat, and protein metabolism [1,22].

Symptoms of severe hyperglycaemia include polyuria, polydipsia, weight loss, and in some cases also polyphagia, blurred vision, growth impairment, and susceptibility to certain infections. Furthermore, uncontrolled DM can lead to acute, life-threatening consequences with ketoacidosis or the non-ketotic hyperosmolar syndrome. Additionally, DM is complicated by retinopathy with potential loss of vision, nephropathy leading to renal failure, peripheral neuropathy with risk of foot ulcers, amputations, Charcot joints, autonomic neuropathy causing gastrointestinal, genitourinary, cardiovascular symptoms, and sexual dysfunction. Moreover, patients with DM have an increased incidence of atherosclerotic cardiovascular, peripheral arterial, and cerebrovascular disease, accompanied by hypertension and abnormalities of lipoprotein metabolism [1,22].

The great majority of diagnosed cases of DM are classified as T1D (discussed in greater detail below) or T2D. Patients suffering from T1D, caused by an absolute deficiency of insulin secretion, can often be identified by measuring circulating antibodies against pancreatic islets, as well as by genetic markers [1,178,196].

T2D is much more prevalent than T1D and is caused by a combination of insulin resistance and inadequate compensatory insulin secretion. A marked feature of this condition is its presence for a long period of time before it is detected. This is due to varying degrees of hyperglycaemia sufficient to cause pathologic and functional changes in various target tissues, without clinical symptoms. However, measurement of plasma glucose in the fasting state or after a challenge with an oral glucose load can

demonstrate an abnormality in carbohydrate metabolism during this asymptomatic period [1,135].

Further classifications of DM include neonatal diabetes mellitus, genetic defects of the β-cell, also referred to as maturity onset diabetes of the young (MODY), genetic defects in insulin action, diseases of the exocrine pancreas, endocrinopathies, drug- or chemical-induced diabetes, and gestational diabetes mellitus. Furthermore, it is known that certain infections, such as congenital rubella, adenovirus, and mumps are associated with β-cell destruction and can therefore lead to the development of DM. Besides these classifications, there are also uncommon forms of immune-mediated diabetes, including the stiff-man syndrome or diseases that lead to the production of anti-insulin receptor antibodies. Other genetic syndromes that are sometimes associated with diabetes include the chromosomal abnormalities of Down syndrome, Turner syndrome, and Klinefelter syndrome [1,29,83,147,158,212,257].

To date, there is no simple cure for DM. Thus, disease management concentrates on the regulation of blood glucose levels using insulin as the main therapeutic agent. However, especially in T2D patients, adequate glycaemic control can also be achieved by weight reduction, exercise, and/or oral glucose lowering agents. Hence, these patients do not require insulin in the early stages of their diabetes but may require it as they age. The degree of hyperglycaemia reflects the probability of future complications. Hence, monitoring and targeted treatment of the glycaemic status of each patient is crucial [1,147].

1.1.1 Prevalence and incidence of diabetes mellitus

Worldwide the number of people with diabetes is increasing due to a variety of factors such as population growth, aging, urbanization, and increasing prevalence of obesity and physical inactivity. Unfortunately, the epidemiological data regarding diabetes mellitus and its associated diseases are often underreported and most data sources do not distinguish between T1D and T2D in adults. Therefore it is not possible to present data for certain countries, such as Germany, as well as for the subtypes of diabetes separately [289].

The World Health Organizations Global Burden of Disease Study provided estimates for the global prevalence of DM in the year 2000, including projections for the year 2030. Prevalence is defined as the proportion of individuals in a population

having a disease or characteristic. According to WHO, there were 171,228 million people in the year 2000 suffering from diabetes [287]. This number will rise by 37 % until the year 2030 with up to 363,212 million diabetic people in the world. The prevalence of diabetes is similar in men and women. However, since age is an important impact factor, prevalence is slightly higher in men over 60 years of age and in women at older ages. Furthermore, a report from Wild et al. found that even though the prevalence of diabetes is higher in men, there are more women with diabetes. Besides age, ethnicity is an important impact factor [289]. Hence, in developing countries, the majority of people with diabetes are in the 45- to 64-year age range, whereas, the majority of people with diabetes in developed countries are over 64 years of age. According to Wild et al. and based on the WHO estimates the number of people with diabetes over 64 years of age will be more than 82 million in developing countries and more than 48 million in developed countries [287,289].

This increase in individuals affected by diabetes is predicted to be mainly due to an increase in cases of T2D. However, since about 10 % of all cases suffer from T1D, by the year 2030 about 36 million people will be affected worldwide. Since the great majority of T1D patients is diagnosed before the age of 30 and there is a rise in the number of children and adolescents with T1D, not only the older population will be affected, but also an increasing number of individuals, especially men, in their reproductive age [3,246]. Therefore, this study will focus on T1D and will include a general description of T1D, including its etiology, diagnosis, and pathogenesis. Furthermore, T1D as an inflammatory disease and the impact of T1D on male reproductive function will be discussed.

1.1.2 Type 1 diabetes mellitus

Type 1 diabetes mellitus can be further differentiated into immune-mediated T1D and idiopathic T1D.

Immune-mediated T1D accounts for 5-10 % of all diabetes cases and was previously known as insulin dependent, or juvenile-onset diabetes. It commonly occurs in childhood and adolescence, but can also develop at later ages. It results from a T-cell mediated autoimmune destruction of the pancreatic β-cells and can be detected by measurement of immunological markers, such as islet cell autoantibodies, autoantibodies to insulin, autoantibodies to glutamic acid decarboxylase (GAD65), and

autoantibodies to the tyrosine phosphatases IA-2 and IA-2b, as well as autoantibodies to the zinc transporter 8 (ZnT8). In patients, if all classes of antibodies are present, this results in a nearly 100 % progression to clinical T1D given enough time. These markers are present in 85-90 % of the patients [1,178].

Although the causes for T1D remain unknown, certain risk factors have been identified. Amongst these, certain variants of genes belonging to the human leukocyte antigen (HLA) complex, such as HLA-DQA1, HLA-DQB1, and HLA-DRB1, were found to be either predisposing or protective. The HLA complex is part of the immune system and involved in the recognition of proteins on the surface of cells [1,178].

The onset of this form of diabetes differs between individuals, since the rate of β-cell decay varies from being rapid in some patients (mainly infants and children) and slow in others (mainly adults). Moreover, some individuals develop ketoacidosis as their first manifestation of the disease, whereas in others, the disease begins with modest fasting hyperglycaemia that can rapidly change to severe hyperglycaemia and/or ketoacidosis in the presence of infection or other stress. Furthermore, it is not unusual that some individuals retain residual β-cell function, which is sufficient to prevent ketoacidosis for many years. Nevertheless, at a latter stage eventually, when little or no insulin secretion remains, these individuals become dependent on insulin for survival and are at risk of ketoacidosis [1,22,120].

Immune-mediated destruction of the pancreatic β-cell is known to have multiple genetic predispositions and is also related to environmental factors that are still poorly defined. While patients with this form of T1D are rarely obese, the presence of obesity is not incompatible with the diagnosis. Due to the autoimmune origin of the disease, these patients are also prone to other autoimmune disorders such as Graves' disease, Hashimoto's thyroiditis, Addison's disease, vitiligo, celiac sprue, autoimmune hepatitis, myasthenia gravis, and pernicious anaemia [1,22,120].

While immune-mediated T1D accounts for most T1D cases, in some cases of T1D no antibodies directed against β-cells can be found. This is known as idiopathic T1D, which is strongly inherited, lacks immunological evidence for β-cell autoimmunity, and is not HLA associated. In some patients there is manifestation of permanent deficient insulin secretion by pancreatic β-cells (insulinopenia) with a predisposition for ketoacidosis, whereas others suffer from episodic ketoacidosis with varying degrees of insulin deficiency between episodes. Hence, permanent monitoring for optimal disease treatment is crucial and an absolute requirement for insulin

replacement therapy in affected patients may be intermittent [1,152,271].

1.1.3 Treatment of diabetes mellitus

To date, there is no cure for DM, therefore therapeutic strategies concentrate on the regulation of glucose metabolism in order to retain normal blood glucose levels and avoid diabetic complications and long-term damage. Treatment strategies involve either medical or transplantation therapy [201].

Medical therapy can be treatment with oral anti-diabetica (OAD), such as biguanide, glitazone, or sulphonylureas and can be used in about 40 % of all patients [87]. Another form of medical treatment is insulin therapy, which is vital in most individuals with T1D. Insulin was first isolated in 1921 by Frederic Banting and Charles Best and resulted in a revolution in the treatment of diabetes [31]. Clinical studies have shown that treatment of DM by intensive insulin therapy lowers glycated hemoglobin (HbA1c) levels, a long-term blood glucose marker, and subsequently reduces the incidence of strictly glucose-dependent complications such as diabetic retinopathy, nephropathy, and neuropathy [46,139]. Intensive insulin therapy (IT) only became feasible through self-management trainings for patients and has increased their life span significantly. In contrast to conventional insulin therapy, IT comes with increased insulin blood levels and higher incidence for hypoglycaemia. At present, most caregivers and patients acknowledge that the benefits of IT outweigh its adverse events [46]. Insulin treatment varies from additive substitution of basal insulin to full insulin substitution to insulin pump therapy [142]. Since insulin plays a central role in the development and onset of diabetes, biosynthesis as well as mutations of the gene encoding insulin will be described in greater detail below.

However, the therapeutic goal of the normalisation of blood glucose cannot be attained in a significant number of patients due to individual restrictions and risk of adverse events, such as hypoglycaemic incidents. Pancreas or pancreatic islet transplantation was demonstrated to reduce the burden of multiple glucose measurements and daily insulin injections, but these interventions are invasive and subject the patient to many risks, such as the need to use continuous immunosuppressive medication [201,210]. Hence, treatment for DM is far away from a definitive cure and can still be optimized.

1.1.4 Type 1 Diabetes as an autoimmune disease

As described in section 1.1.2 immune mediated T1D is the most common form of T1D resulting from a T-cell mediated autoimmune destruction of the pancreatic β-cells. For a better understanding of this interaction, this section will give a brief description of the immune system and its endocrine control, as well as of the special role of T-lymphocytes in the development of T1D.

1.1.4.1 Immune system - general principles

The immune system provides protection from invading organisms within complex animal species and is comprised of a complex series of cells that identify and eliminate invading pathogens. In vertebrates the immune system consists of an innate and an adaptive immune system, which overlap in many of their cellular and molecular mechanisms. The main cellular components of the immune system are the leukocytes, or white blood cells. These cells, as well as their products, circulate continuously through the blood, lymph, and tissues in both surveillance and effector mode [109].

The **innate immune system** generally recognizes uniquely conserved patterns expressed by various pathogens. It comprises mainly of mononuclear phagocytes (monocytes and macrophages) and granulocytes or polymorphonuclear leucocytes such as neutrophils, eosinophils, basophils, and mast cells. Furthermore, it also involves natural killer (NK-) cells and dendritic cells, which themselves are closely aligned to the adaptive immune system. The innate immune system provides the first line of defence against external threats through an inherent ability to recognize and rapidly respond to a broad range of pathogens and other immunogens, and by initiating inflammation [6,109].

The activation of the immune response involves the so-called pattern recognition receptors, which recognize specific motifs produced by bacterial, viral, fungal, and protozoan pathogens. These receptors belong to a family of transmembrane receptors, known as Toll-like receptors (TLR), which are expressed on cell surfaces and intracellular endosomes, especially in macrophages, monocytes, and dendritic cells. Upon activation of pattern recognition receptors, corresponding immune cells are activated leading to inflammation [52,109,281]. Besides the activation of immune cells, this inflammatory response involves further major changes such as fever, increased blood flow at the site of inflammation, as well as enhanced pain sensitivity. Apart from specific pathogens, the inflammatory process can also be triggered by tissue injury,

insoluble particles, activation of the plasma complement and clotting protease pathways, immune complexes, and intracellular components released by tissue damage. While monocytes and macrophages are involved in the initial inflammatory response, mast cells regulate vascular permeability, vasodilation, and leukocyte recruitment thereafter, followed by a neutrophil response in which extracellular pathogens are being removed [52,109,222,281]. During this process, a targeted expression of pro-inflammatory cytokines, pro-inflammatory prostaglandins and leukotrienes, neuropeptides, chemokines, and adhesion molecules, allows circulating neutrophils, monocytes, and lymphocytes to specifically target and enter the affected tissue. After the initial pro-inflammatory response, anti-inflammatory cytokines, prostaglandins, late-acute-phase proteins, and anti-inflammatory corticosteroids from the hypothalamic-pituitary-gonadal (HPG) axis resolve the inflammatory response. The long-term effects of inflammation include increased tissue fibrosis and persistent alterations in the number, type, and activity of leukocytes in the target tissue. Furthermore, the activation of the innate immune response leads, in turn, to the activation of the adaptive immune response [52,109,161].

The **adaptive immune system** recognizes molecular patterns that are foreign to the host and involves lymphocytes, such as T-cells, B-cells and NK-cells, as well as antigen presenting cells (dendritic cells and macrophages). Through complex cellular interactions the adaptive immune system requires more time to become active than the innate immune system. These interactions, however, also provide efficacy, specificity, and memory to the immune response [109]. It is activated by the recognition of antigens, usually associated with proteins, which are foreign to the host and indicate an external threat. This recognition process relies on the unique ability of lymphocytes to generate a wide range of cell-surface receptors that are able to bind almost any foreign molecule, without having encountered it before. B-cells display surface bound immunglobulins, whereas the receptor on T-cells (TCR) is structurally related to immunglobulins and is a complex of interacting surface proteins itself. B-cells interact directly with the antigen, whereas immune responses involving T-cells are more precise and determined by proteins of the highly polymorphic major histocompatibility complex (MHC). This complex is expressed on the surface of antigen-presenting cells and binds to the TCR leading to the activation and proliferation of the T-cell. Recognition of the MHC is facilitated by co-expression of the receptor proteins CD4 or CD8 as part of the TCR. Furthermore, activation of the T-cell requires the physical interaction between co-

stimulatory ligand pairs, such as CD40/CD40LG and CD80/CD86, and the production of either type 1 or type 2 cytokines. Type 1 cytokines enhance cellular immune responses and include the interleukins (IL) IL-2, IL-12, and interferon γ (IFN γ), whereas type 2 cytokines augment antibody responses and include IL-4, IL-5, IL-10, and IL-13. Due to this complex interaction and depending on the molecules that are involved, there is a great variety of outcomes of the T-cell activation, leading to the production of either type 1 helper cells (Th1) or type 2 helper cells (Th2) [64,107,109,251].

The absence of the appropriate co-stimulatory molecule and/ or the presence of anti-inflammatory or immunosuppressive cytokines can lead to the inactivation of T-cells as well as to the deletion or the production of regulatory T-cells (T-reg), which are responsible for regulating antigen-specific immunity and maintaining peripheral immune tolerance [109,298].

Reactions of the adaptive immune system are also responsible for an autoimmune reaction, which can lead to chronic inflammation and, dependent on the target tissue, the development of diseases such as T1D [109,176,178]. The autoimmune process leading to T1D is described in greater detail in section 1.1.4.2.

1.1.4.2 Autoimmunity in type 1 diabetes

Autoimmune diseases generally represent a failure of tolerance or a disruption in the recognition of host antigens [109]. In T1D the clinical onset is preceded by the appearance of autoantibodies against β-cell antigens, which leads to the specific destruction of the pancreatic islet β-cells and eventually results in a complete dependency on exogenous insulin. This specific destruction is initiated by the activation of T-cells through autoantibodies leading to either a Th1 or a Th2 response. The Th1 response is initiated through activation of CD4 positive T-cells by β-cell antigens and antigen-presenting cells (APCs), such as dendritic cells, B-cells, and macrophages. This interaction leads to the production of pro-inflammatory cytokines and free radicals, which are toxic to the β-cell. Furthermore, the production of cytokines attracts T- and B-cells, which in turn proliferate in the islet of Langerhans leading to insulitis. Moreover B-cells mediate further damage to β-cells by producing antibodies against released β-cell antigens. As a consequence of the activation of CD8 positive T-cells, β-cells carrying the target auto-antigens are attacked directly [1,107,178].

As discussed in section 1.1.2, T-cell activating autoantibodies include antibodies directed against insulin (IA), GAD65, insulinoma antigen-2 (IA-2) or ZnT8 [1,80,178].

As a trigger for the development of autoimmunity in T1D, genetic polymorphisms in the HLA complex, as well as non-HLA polymorphisms have been considered [80].

Polymorphisms in the HLA complex are thought to explain more than half of the genetic influence in T1D. Located on chromosome 6p21 the HLA complex contains a variety of genes related to the immune system. It can be divided into three classes, of which class II is the major genetic susceptibility determinant for T1D. This class includes heterodimeric proteins coded for at the DP, DQ, and DR loci. Interestingly, specific alleles at the DRB1, DQA1 and DQB1 loci are particularly associated with T1D. These proteins were shown to be expressed on APCs and to have a strong peptide-binding activity by which they bind to T-cells after recognition. Depending on the haplotype, these proteins were found to be either predisposing or protective. Besides class II proteins, HLA class I proteins, such as HLA-A and HLA-B, also contribute to the development of T1D, although to a lesser extent. These proteins act by directing CD8 positive T-cells towards cells that have been infected with a virus, as virus peptides are presented on class I heterodimers [80,187].

Besides HLA genes, a number of non-HLA genes have been associated with autoimmunity and disease risk in T1D. These genes contribute either to the risk of islet autoimmunity or to the progression to clinical onset in subjects who had developed islet autoimmunity. One of the strongest non-HLA genes is protein tyrosine phosphatase non-receptor type 22 (PTPN22), which inhibits the T-cell receptor signalling and therefore downregulates the immune response. Single-nucleotide polymorphisms (SNP) within this gene are believed to promote progression to diabetes [44,80]. A further non-HLA gene is the interleukin-2 receptor-α (IL2RA). This receptor is expressed on T-cells, which require IL-2 for their growth and survival. Genetic variants of this receptor were shown to impair T-cell function and therefore lead to autoimmunity [300]. Moreover, recent studies on the interferon-induced with helicase C domain 1 (IFIH1), also known as MDA5 (melanoma differentiation-associated protein 5), have been linked to a reduced expression of this domain with T1D. IFIH1 recognises viral RNA and mediates the innate immune response. IFIH1 variants were shown to be either protective or predisposing for T1D [77,183].

Furthermore, insulin is a key β-cell autoantigen in T1D. Hence it is not surprising that polymorphisms of the insulin gene (*Ins*) contribute to disease susceptibility. The *Ins* gene is located on chromosome 11 and shows polymorphism in

its promoter region. Predisposition to T1D is dependent on a variable number of tandem repeat polymorphisms, with shorter repeats conferring risk and longer repeats providing protection [80,176].

Since insulin plays a central role in the development and onset of T1D, insulin biosynthesis and insulin gene mutations, as well as the role of insulin as an autoantigen will be discussed below.

1.1.5 Insulin biosynthesis and insulin gene mutations

Insulin is mainly synthesized within the pancreatic β-cells of Langerhans, but is also produced in other organs, such as the brain or the testis [92,253]. The first translational product from the insulin gene is preproinsulin (shown in Fig. 1-1), which is a 110 amino acid polypeptide with the 24 amino acid signal peptide.

During further synthesis, the signal peptide is bound by the signal-recognition particle (SRP), which then interacts with its receptor in the membrane of the endoplasmatic reticulum. The ER is a membrane-bound organelle that supports the biosynthesis of approximately one-third of the cellular proteins [185]. Binding of the signal peptide to the ER membrane activates the penetration of preproinsulin into the ER lumen, where the proteolytic cleavage of the signal peptide from preproinsulin yields proinsulin. This process was first discovered by Steiner et al. [185,254,255]. Subsequently, proinsulin undergoes protein folding as well as formation of disulphide bonds. After appropriate folding, proinsulin is transferred into the Golgi apparatus where it is sorted into constitutive or regulatory pathways [185,254,255].

Thereafter, the transformation of proinsulin into insulin and C-peptide occurs within secretory granules by enzymatic removal of C-peptide at the sites of dibasic amino acids. This is achieved by two prohormone convertases (PC1/3 and PC2) that cleave proinsulin either at the connecting site between the insulin beta-chain (PC1/3) or at the insulin alpha-chain (PC2) and the connecting peptide (C-peptide). Finally, the remaining basic amino acids are removed by carboxypeptidase E [182,185,254,255].

Humans carry a single insulin gene consisting of three exons of which exon 1 (42 bp) contains only the 5'-untranslated region, exon 2 (204 bp) encodes the signal peptide, the B-chain and part of the C-peptide, and exon 3 (219 bp) encodes the rest of the C-peptide as well as the A-chain [74,185].

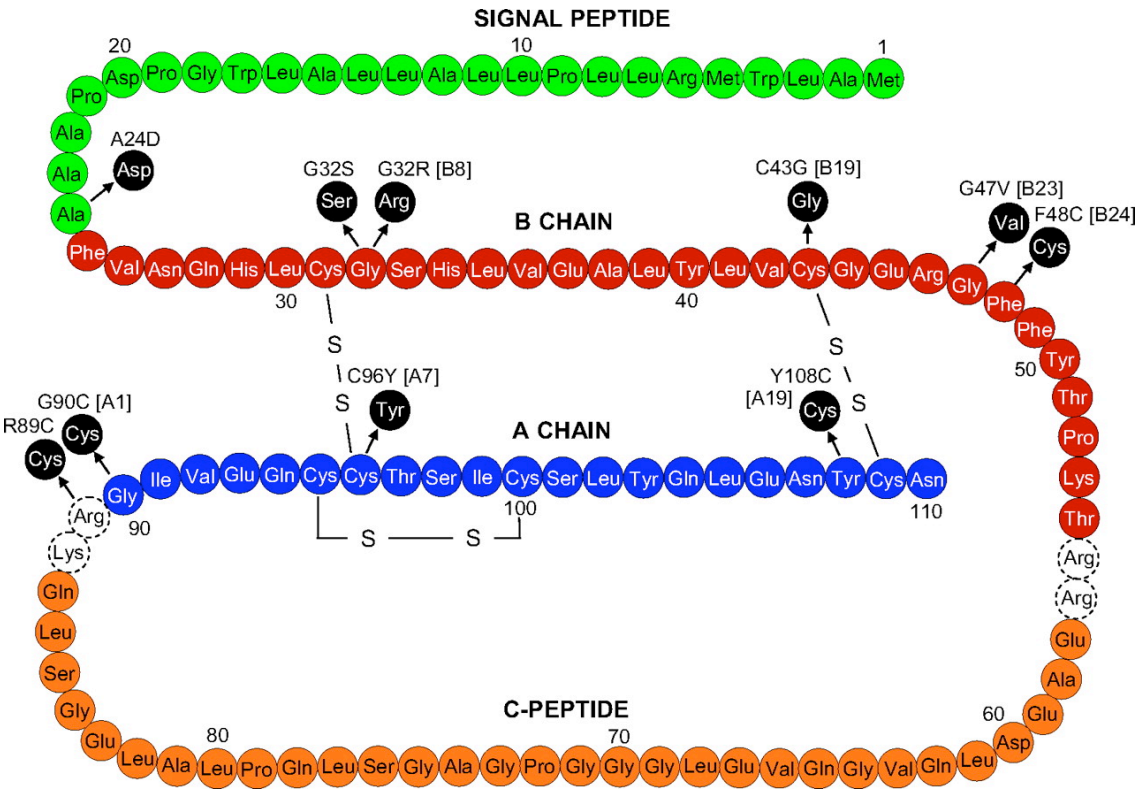

Fig. 1-1. The human preproinsulin molecule.

Diagram representing the human preproinsulin molecule showing locations of mutations causing neonatal DM [257] with permission.

So far, three distinct mutant insulins have been identified in humans, however, not all individuals with mutant insulin develop diabetes due to the presence of normal alleles. In those cases, an overproduction of normal insulin will compensate for the deleterious effect of the mutant insulin. This effect can, however, in turn be influenced by several factors that are likely to cause insulin resistance or pancreatic β-cell secretory dysfunction (i.e. aging) [102,179,185,261]. Besides insulin gene mutations that lead to structural abnormalities within the insulin molecule itself, there are four known gene mutations that effect the conversion of proinsulin to insulin [56,185,302].

In contrast to humans, insulin in rodents is derived from a two-gene system consisting of preproinsulin 2 (*Ins2*), which is orthologous to the insulin gene in humans and other mammals, and preproinsulin 1 (*Ins1*), which is a rodent specific retrogene. Both *Ins*2 and *Ins*1 are expressed in the pancreas and encode proinsulin peptides built of a signal peptide, a B-chain, a C-peptide, and an A-chain [241].

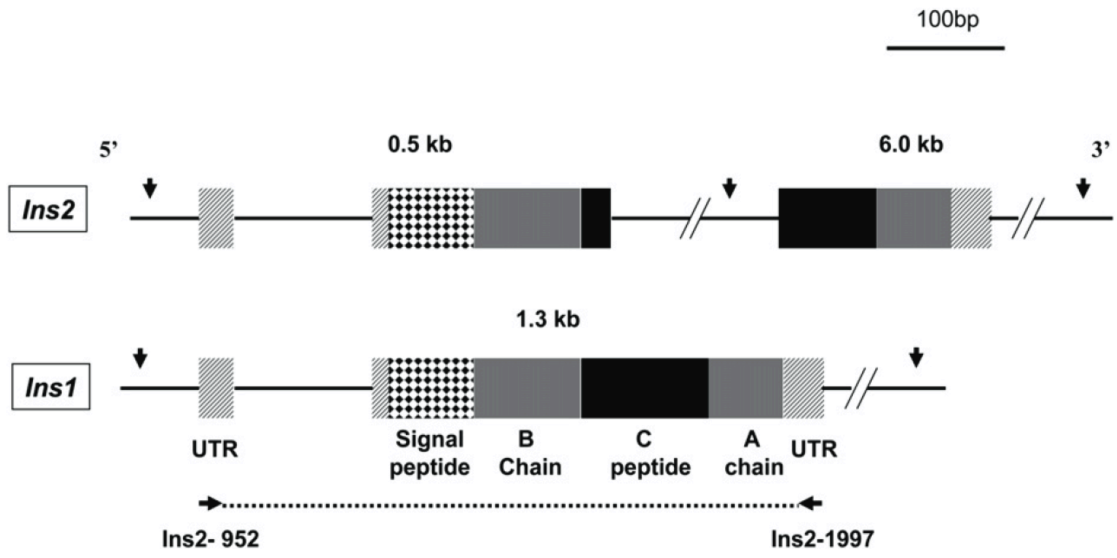

Fig. 1-2. Gene structure of *Ins2* and *Ins1* in the house mouse (mus musculus).
Gene structure of *Ins2* and *Ins1* in the house mouse (mus musculus) [241] with permission.

Ins1 was found to originate from a reverse-transcribed, partially processed mRNA of *Ins2* and therefore retains only one of the two introns, which is homologous to the first intron of *Ins2* (Fig. 1-2). Further, *Ins1* carries homologous regulatory regions with *Ins2* from aberrant transcription. This is partially due to processes where the mRNA was transcribed from the upstream region of *Ins2* and hence contains not only the gene itself, but also the regulatory regions. Within the mouse genome *Ins1* is located on chromosome 7 and *Ins2* is located on chromosome 19, whereas in other rodents, such as the rat, both genes are located on the same chromosome [241].

Murine insulin knockout models have revealed that both genes exert functional differences. This is supported by findings from Babaya et al. who showed that the two insulin genes have different null phenotypes related to the etiology of diabetes. Hence, without the presence of *Ins2* alleles, *Ins1*-carrying mice were affected by the resultant insulin deficiency that accelerated the onset of T1D. Whereas, in mice carrying *Ins2* alleles, no decrease in insulin content was detected [27]. This suggests that *Ins1*, which evolved after the *Ins2* gene, might exert some negative effects on glucose metabolism, some of which could worsen the diabetic syndrome [27,241].

1.1.6 Mouse models of type 1 diabetes

To date several rodent models of T1D have been established and especially the

mouse models are widely used. These include genetic models such as the NOD, the *Ins2*^{Akita}, or the Munich mouse, and toxin-induced mouse models such as the Streptozocin (STZ) treatment model [137,146,153,185].

The NOD mouse, descriptive for non-obese diabetic mouse, is the premiere model for T1D and was first described by Makino et al. [160]. The NOD mouse is an inbred mouse strain developed in the course of a breeding program to establish a cataract-prone sub line (CTS) from non-inbred ICR mice [145]. These mice show an autoimmune destruction of the pancreatic β-cells accompanied by several organ specific pathologies. Showing an abrupt onset of diabetes, as indicated by leukocyte infiltration into the pancreatic islets (insulitis), between 90 and 120 days (equivalent to early adolescence period in humans), hyperglycaemia, glycosuria, hypercholesterolemia, ketonuria, polydipsia, polyuria, and polyphagia, the clinical features of the diabetes syndrome in NOD mice are quite similar to human T1D [146,160]. These mice require daily insulin injections in order to survive, once diabetes is established. Hence, it is difficult to maintain aging colonies of this strain to further investigate the development of diabetic complications [146].

The *Ins2*^{Akita} mouse, a monogenic diabetic model, was first established by Yoshioka and colleagues in a colony of C57Bl/6N mice [146,282]. Since this mouse model was used in this study, it will be described in greater detail below.

A further genetic model for T1D is the Munich *Ins2*^{C95S} mouse, which was first identified in 2007 as a novel non-obese diabetic mouse by the screening of N-ethyl-N-nitro-sourea (ENU) mouse mutagenesis project. This model carries a mutation at the C95S residue resulting in a disruption of the intra-chain disulphide bond of the insulin alpha-chain. This mutation causes hypoinsulinaemic hyperglycaemia by the age of one month. Similar to the *Ins2*^{Akita} model these mice were shown to have a decreased number and size of insulin granules, enlarged ER and swollen mitochondria in the pancreatic islets consistent with ER stress related to the abnormally folded mutant insulin molecules [112,185,236].

Besides genetic mouse models, toxin induced mouse models for T1D are widely used. These include high dose alloxan (ALX) and STZ models and multiple "Low Dose" STZ models. Alloxan and STZ are small molecules resembling glucose and binding the GLUT-2 glucose transporters in both pancreatic β-cells and the liver. Both molecules disintegrate in aqueous solution, leading to the production of free radicals. This in turn, damages β-cells, which in contrast to other epithelial cells, are known for

their low cytoplasmic concentrations of antioxidant enzymes, such as superoxide dismutase or catalase [148]. However, besides the aimed effect of diabetes development, these substances bear a high risk of undesired side effects and toxin-induced mice also display a high mortality, as well as a high inter-strain variability in the level of hyperglycaemia that they develop [146].

Other models for T1D include knockout and transgene, as well as viral infection models [146].

A detailed literature review on reproductive dysfunction in T1D animal models is given in Table B-7.

1.1.7 The *Ins2*^{Akita} mouse model

The *Ins2*^{Akita} mouse model carries an autosomal dominant mutation at the *Mody* region and develops hyperglycaemia with notable pancreatic β-cell dysfunction [282]. The following section will discuss the origin of this mouse model as well as its application and use for studies of T1D. The particular features regarding the research into reproductive abnormalities in this mouse model are discussed in section 1.2.6.

1.1.7.1 Establishment of the *Ins2*^{Akita} mouse model

The monogenic diabetic model called the *Ins2*^{Akita} mouse was first established in a colony of C57Bl/6N mice by Yoshioka and colleagues in 1997 in Akita, Japan [146,282]. Originally this model was referred to as *Mody4* due its dominant inheritance presenting with early juvenile onset of hyperglycaemia, since it also resembles the Maturity Onset of Diabetes in the Young (MODY) in humans, which is inherited in an autosomal dominant manner and characterized by a primary dysfunction of pancreatic β-cells [282]. A spontaneous missense mutation in the *Ins2* gene is found at the distal end of chromosome 7 and resulting in the conversion of cysteine Cys96 (TGC) into a tyrosine (TAC) codon at the seventh amino acid on the A chain of proinsulin. This leads to a conformational change of the protein due to the inability to form a disulphide bridge between the corresponding residues A7 and B7. This defect in protein folding leads via a so-called unfolded protein response to the induction of endoplasmic reticulum stress and β-cell apoptosis [282].

Mice homozygous for the mutation exhibit high early mortality, which is why heterozygous mutants are commonly used for most studies. “To avoid the complications

of diabetic pregnancies wild type females are usually mated to young, heterozygous mutant males to produce litters with a 50:50 ratio of mutants and wild type controls" [146]. Furthermore, recent studies have shown that the penetration of the dominant genotype can vary and is dependent on background strain and sex [125]. Hence, both sexes of the *Ins2*^{Akita} model develop hyperglycaemia at weaning, however, loss of β-cells and diabetes are more pronounced in heterozygous males than in females. Akita mice develop T1D by the age of approximately 4 to 5 weeks, manifesting with severe hyperglycaemia, hypoinsulinemia, polydipsia, and polyuria in male mice, while female mice show less severe symptoms with less impairment in β-cell function [199,235].

As the mice age, the β-cell mass decreases, which is accompanied by a decline in plasma and pancreatic insulin levels. Nonetheless, insulin can still be detected in a small number of β-cells remaining in the residual islets by immunostaining. In those surviving β-cells, insulin molecules are made up from the two functional *Ins1* alleles on chromosome 19, present in 25 % of the total insulin, and the one normal *Ins2* allele on chromosome 7. This allows heterozygous chronically hyperglycaemic mice of both sexes to survive beyond six month of age, thereby distinguishing this model from other genetic T1D mouse models [146]. Moreover, other than many other monogenic diabetes mouse models, the *Ins2*^{Akita} mouse is lean and its pancreatic β-cell dysfunction does not result in pancreatic invasion of immune cells [282].

1.1.7.2 Differences of the *Ins2*^{Akita} mouse model to human type 1 diabetes

The characteristics of a human T1D were discussed in 1.1.2.

Although *Ins2*^{Akita} mice exhibit several features of MODY in humans, which is inherited in an autosomal dominant manner and characterized by a primary dysfunction of pancreatic β-cells, the mutation in the mouse model is different from humans [185,257,282]. Humans were found to have several point mutations resulting in amino acid substitutions within the proinsulin molecule. Patients exhibiting this mutation were found to be heterozygous for the defective gene and show a high incidence of glucose intolerance with usually mild and late-onset symptoms and, in some cases even normal glucose tolerance, due to the co-production of wild type insulin. Furthermore, hyperinsulinemia or hyperproinsulinemia is a common symptom in human subjects. Hyperinsulinemia results from a reduced clearance rate of mutant insulin molecules through insulin-receptor mediated uptake and degradation because of the low binding potency of the mutant insulin to the receptor. Hyperproinsulinemia on the other hand

reflects a decreased cleavage or altered subcellular sorting of mutant proinsulin. Thus, in human MODY significant amounts of both wild type and mutant (pro)insulin are being secreted from the islets [282].

In contrast, Wang et al. state that Akita mice have diabetes with a severe decrease in insulin secretion (hypoinsulinemia) and a 100 % penetrative phenotype [282]. However, this penetrance is in contrast to the Akita mice bred in the animal facility at Mannheim (Germany) for more than 30 generations, with a prevalence of 50 % of a severe hyperglycaemic, hypoinsulinaemic diabetic phenotype. These mice will not gain weight with age and display reduced fat and lean body mass compared to non-diabetic littermates. According to insulin blood levels, heterozygous Akita mice are comparable to T1D patients with about one-tenth residual insulin secretion capacity. Therefore, hyperglycaemic mice will survive 24 weeks and more so that long-term diabetic complications can be investigated. Littermates with near-normal glycaemia (<11.1 mmol/l non-fasting blood glucose concentrations) or severe hyperglycaemia (>33.3 mmol/l) can be compared. Although it remains to be elucidated, this heterogeneous phenotype of the *Ins2*$^{Akita+/-}$ mice might arise from a different mutation of the *Ins2* gene. Therefore, it is possible that mice with a fasting blood glucose of <11.1 mmol/l have sufficient remaining circulating insulin to prevent the animal from developing diabetes.

1.1.7.3 Applications of the *Ins2*^{Akita} mouse model

After its establishment the *Ins2*^{Akita} mouse model has been used for the study of several diabetes-related complications, such as diabetic nephropathy, retinopathy, neuropathy, and diabetes-induced osteoporosis. Furthermore, the impact of T1D on reproduction has been studied by several groups using this mouse model, which will be discussed in greater detail in section 1.2.6.

Diabetic nephropathy is a major complication in both T1D and T2D patients, being a leading cause of end-stage renal disease (ESRD) in approximately 50 % of all cases [130,154]. Mice with a mutation in the *Ins2* gene exhibit features of human diabetic nephropathy, such as decreased body and heart weight, as well as increased kidney to body weight and kidney weight to tibia length ratio, and increased plasma glucose, plasma triglycerides, and thiobarbituric acid reactive substances in plasma. Further, they have a significantly increased renal albumin excretion, resulting in albuminuria. These are accompanied by a drastic increase in the albumin/creatinine ratio, a decrease in nephrin expression and glomerular filtration rate [25,130,154].

Diabetic retinopathy (DR), a sight-threatening consequence of diabetes, is mainly characterised by neural retinal degeneration together with microvascular dysfunction [115]. As diabetic retinal retinopathy is accompanied by a progressive loss of inner retinal neurons, including the amacrine and retinal ganglion cells, similar observations have been noted in the *Ins2*^{Akita} model. Thus, Akita mice have been shown to develop very early DR-related retinal abnormalities, including increased vascular permeability, retinal ganglion cell (RGC) apoptosis, reduced retinal thickness, decreased retinal blood flow, as well as abnormal electroretinographic responses resulting in vision loss. Using a scopic electroretinogram (ERG), a diagnostic test that measures the electrical activity generated by neural and non-neuronal cells in the retina in response to a light stimulus, neuropathic abnormalities were evaluated within the Akita mouse model. *Ins2*^{Akita} mice show ERG abnormalities and neuropathic lesions including degeneration of cone photoreceptors at early stages of the disease, and severe ERG defects, loss of synaptic structures in second order neurons, such as the outer plexiform layer, and decreased number of amacrine cells and RGCs at later stages. Further, these changes are accompanied by early thinning of the neurosensory retina within outer retinal layers, progressing towards the inner retina with the duration of the disease [100,115].

It is well known that diabetes adversely affects the skeleton, which is why bone mineral loss is a further serious complication of T1D. *Ins2*^{Akita} mice were shown to have significantly less bone mineral density compared to wild type controls [130]. Furthermore, when severe hyperglycaemia has developed, these mice show diminished bone formation and suppressed periosteal bone appositions, which is mainly due to alterations in the calcium signalling of osteocytes [199].

Diabetic neuropathy is the most common, but still poorly studied complication of diabetes, and is known to affect approximately 60 % of all patients. It results in cardiovascular, genitourinary, sudomotor and alimentary symptoms or subclinical disease in humans and manifests in sensory loss, electrophysiological measures of nerve impairment and anatomical evidence of nerve fibre loss [232,259]. Studies of the neuropathological features in the *Ins2*^{Akita} mouse model have shown controversial results. On the one hand, male *Ins2*^{Akita} mice exhibit unambiguous, spontaneous, rapidly developed neuropathology similar to that found in humans. These are characterised by progressively developed markedly swollen axons and dendrites in the prevertebral superior mesenteric and celiac ganglia with an overall increase in presynaptic axon

terminal cross sectional area [232]. Supporting these neuronal findings, Choeiri et al. have shown that a decrease in the sensory nerve conduction velocity occurs together with an increase in gait disturbances. These results were further shown to become more severe with age [63]. Apart from these findings, *Ins2*^{Akita} mice showed no defect in the procession of spatial memory [63]. On the other hand, Sullivan et al. suggested that *Ins2*^{Akita} mice at 24 weeks show only minimal signs of diabetic neuropathy based on heat sensation and nerve conduction velocity analysis [130,259]. This is supported by findings from Yaguchi et al., who undertook neuropathological examinations, which failed to show remarkable abnormalities in the brain, spinal cord or sciatic nerve of Akita mice up to 48 weeks of age [299].

1.1.8 Other models of type 1 diabetes

Other than the mouse models described above, various genetic rat models and toxin-induced diabetic rats are frequently used models for the study of T1D [118,306]. Besides these models, the nematode *Caenorhabditis elegans* was shown to be a valuable model organism in the study of glucose-induced cell toxicity, and thus the study of hyperglycaemic effects of DM [71,84]. This model organism was used to study glucose toxicity on reproductive function, which will be described in section 3.1.

1.2 Testis biology

The testis is a specialized organ and site of the production of spermatozoa and androgens. It is composed of two distinct compartments: the seminiferous epithelium, where spermatogenesis occurs nourished by the Sertoli cells, and the interstitium [122]. This section will provide a short overview about the male reproductive tract, followed by a more detailed description of the Sertoli cell, including an insight into spermatogenesis and spermiogenesis. Furthermore, steroidogenesis and the reproductive complications associated with T1D will be discussed.

1.2.1 Anatomy of the male reproductive tract

In mammals the male reproductive tract (Fig. 1-3) is composed of testes (Fig. 1-4), epididymides, ductus deferentes, accessory sex glands, and penis [239].

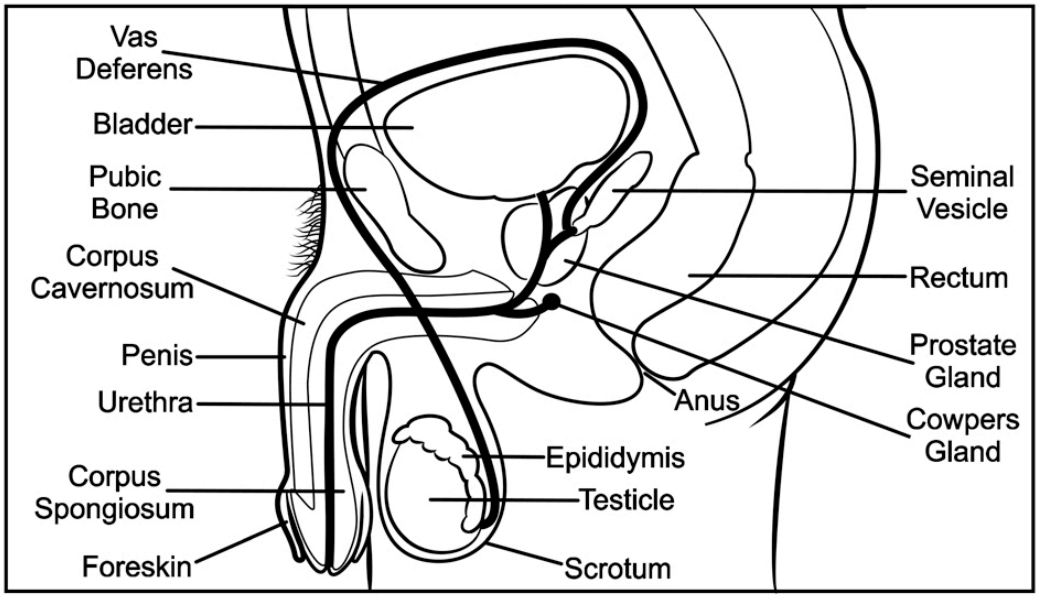

Fig. 1-3. Anatomy of the human male reproductive tract.
Anatomy of the male reproductive tract [108].

The development of the testis from the gonads starts after migration of sexually indifferent germ cells into the bipotential genital ridge. This process takes place in the first quarter of gestation in humans and in the third quarter of gestation in mice and is triggered by the expression of the sex-determining region of the Y chromosome (SRY) by the Sertoli cells. In contrast, in females not SRY, but Wnt4 is expressed, resulting in the differentiation of female gonads into ovaries. In the initial phase of testicular development, pre-Sertoli cells migrate into the developing gonad, where they aggregate to form the sex cords between which the endothelial and interstitial cells are found. The sex cords progress to subsequently form the seminiferous tubules.

The interstitial spaces between the seminiferous tubules contain blood and lymphatic vessels, macrophages, nerves, fibroblast cells, lymphocytes, as wells as Leydig cells. Leydig cells play a crucial role in male fertility since they are the sites of testosterone production both during development of the testis and later during pubertal development to adulthood. The steroidogenic function of the Leydig cells is critically dependent on the pituitary-derived luteinizing hormone (LH) [32,190,239]. The seminiferous tubules are the site of sperm production (spermatogenesis) and sperm maturation (spermiogenesis) and contain various germ cells, as well as somatic Sertoli cells. The

latter have essential nutritive and physiological functions essential for the developing germ cells. The tubules themselves are enclosed by a peritubular tissue comprising a basement membrane and myoepithelial cells or myofibroblasts, further interspersed with layers of collagen fibres and glycosaminoglycan and proteoglycan matrices. The peritubular tissue comprising of peritubular myoid cells is capable of contracting and these contractions facilitate transport of fluid, secreted by the Sertoli cells, together with the spermatozoa in the seminiferous tubules into the rete testis and further into the efferent ducts and the epididymis. The contractions are initiated in response to oxytocin, vasopressin, prostaglandin $F_{2\alpha}$, and endothelin [239].

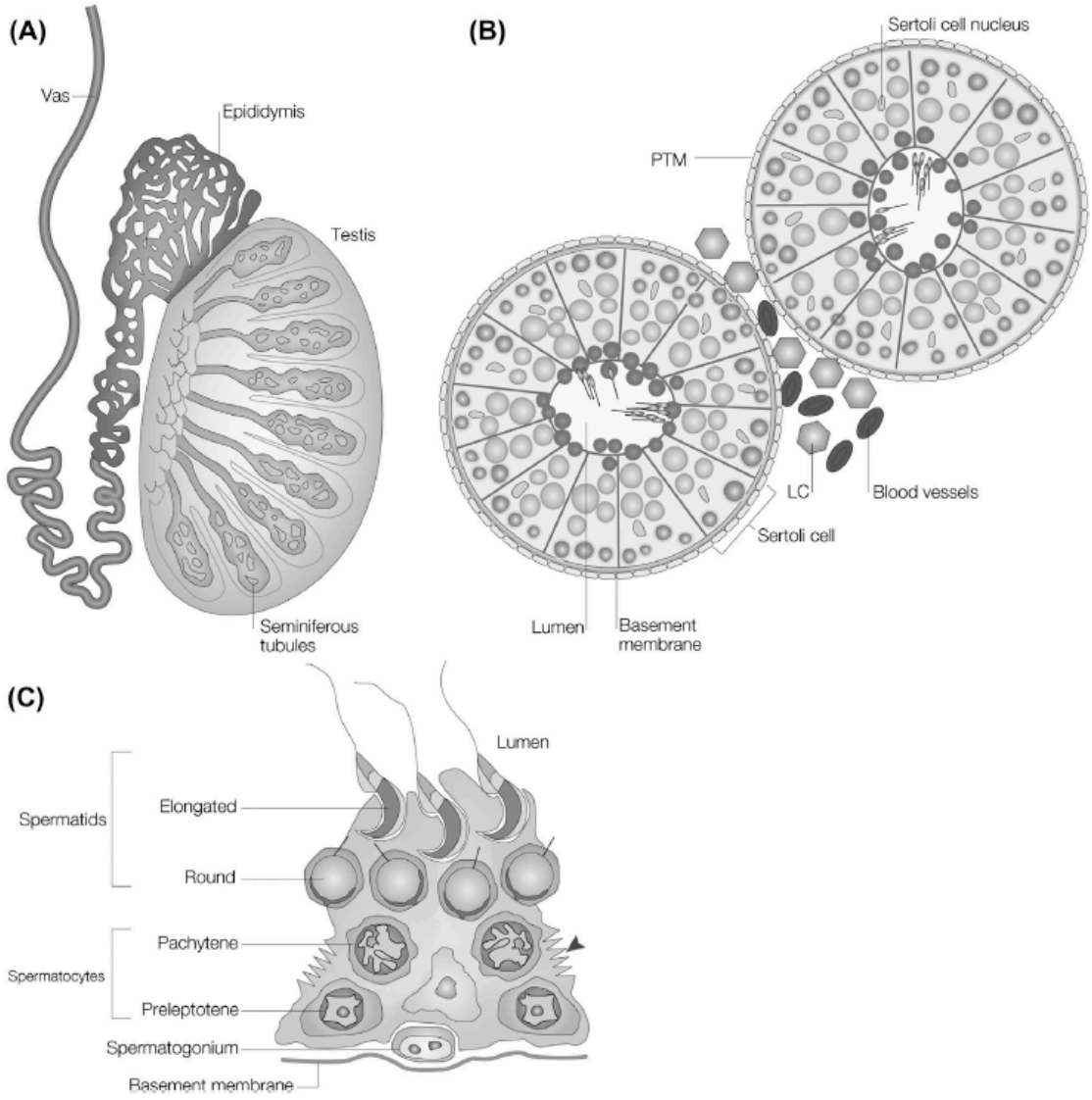

Fig. 1-4. Structure of the testis, seminiferous tubule, and Sertoli cell.

Structure of the testis (A), the seminiferous tubule (B), and the Sertoli cells (C) [65] with permission.

The basic structure of the testis is reached by eight weeks post fertilization in humans and by fourteen days in mice. Enlargement of the seminiferous tubules is due to proliferation of Sertoli cells and germ cell expansion resulting in growth of testis size [190].

Masculinization of the embryo is triggered by the expression of anti-müllerian hormone (AMH) by Sertoli cells and androgens from Leydig cells. Furthermore, fetal testis development is mainly characterized by Sertoli cell proliferation and androgen production of the Leydig cells, which makes both cell types crucial for male fertility. Following this, the primordial germ cells which are initially centrally placed in the seminiferous cords then migrate towards the basement membrane of the seminiferous tubules and give rise gonocytes that in turn develop into the spermatogonial stem cells (SSC) from which full spermatogenesis develops during the hormonal induction of puberty. The process of spermatogenesis is described in section 1.2.4. At puberty, LH secretion by the pituitary gland stimulates Leydig cell precursors to form the adult population of Leydig cells and increase levels of testosterone. Testosterone stimulates germ cells to initiate spermatogenesis and is thus required for fertility and normal male behaviour. During the same period, Sertoli cells proliferate to increase their numbers and then cease mitosis and undergo a maturation process in which they form the blood-testis-barrier (BTB) dividing the seminiferous epithelium into a basal and an adluminal compartment [190]. Both the role of Sertoli cells as well as of the BTB is extensively described in section 1.2.3.

After completion of fetal testicular development, secretion of androgens by intra-testicular Leydig cells induces differentiation of the mesonephric (or wolffian) duct into the epididymis and ductus deferens as well as some of the accessory sex glands. It is also responsible for the development of the indifferent external genitalia into a penis and a scrotum [32,190,239].

During fetal life, the testes migrate from their initial site close to the kidneys caudally into a scrotum, which provides the optimal lower temperature for the process of spermatogenesis and also for sperm storage. This process is referred to as testicular descent and is further divided into two stages: transabdominal migration and inguino-scrotal phase. While the transabdominal migration is completed early during fetal development, the inguino-scrotal phase occurs late in fetal life in humans, and after birth in mice. Besides the testis itself, both the cranial suspensory ligament and the gubernaculum are involved in the descent of the testis. The gubernaculum runs between

the testis and the inguinal area and will eventually lead to an outpouching of the peritoneum forming a sac, the processus vaginalis. This vaginal process is surrounded by fibres of the cremaster muscle that enables the testis to be retracted into the peritoneal cavity in rodents through the inguinal canal. The processus vaginalis remains patent in rodents throughout life but closes in humans after birth. The nephric replacement is a tightly controlled process regulated by various factors such as insulin-like growth factor 3 (Insl3), calcitonin gene-related peptide (CGRP), AMH, and androgens [239].

The testes are surrounded by a tough fibrous capsule called the tunica albuginea, which consists of an outer layer of visceral peritoneum built of mesothelial cells and an inner layer consisting of fibroblasts, collagen fibres, and smooth muscle cells [239].

"Both ends of each seminiferous tubule open into the tubuli recti and then into the rete testis through short transitional zones lined by cells resembling Sertoli cells, which appear to form a valve or a plug" [239]. It is known that in humans up to six seminiferous tubules can join a single tubulus rectus, whereas in mice the total number of these cords is between 12 and 18. In mice, as in most rodents, the rete testis is located on one side of the testis, whereas in humans it lies alongside one edge of the testis in a fibrous mediastinum. Therefore, in humans the rete testis can be divided into a septal, tunical, and extratesticular region. The rete testis is connected to the epididymal duct through efferent ducts that coil to form the caput epididymis. The epididymal duct arises from the mesonephric duct. It is arranged in lobules and can, according to the structure of the epithelium and the gross morphology, be divided into caput, corpus, and cauda, with the latter terminating in the vas deferens. The epididymal duct is lined by an epithelium consisting of principal, apical, narrow, light, and basal cells, as well as by intraepithelial leucocytes. Distally, the epididymis joins the vas deferens, an unconvoluted duct which distally joins the prostatic urethra [190,239].

Similar to the epididymal duct, accessory sex glands arise from the mesonephric duct, but also in part from the prostatic and penile urethra. They comprise vesicular, ampullary, bulbourethral, and prostate glands. The secretion of the accessory sex glands contains various substances, such as fructose, citric acid, zinc, and acid phosphatase, which are added to the semen at ejaculation. In mice the secretion from these glands forms a large, hard, copulatory plug within the vagina, which is thought to fulfil several functions such as prevention from sperm leakage, facilitation of sperm transport, facilitation of gradual release of sperm within the female tract, and prevention of

subsequent fertilizations by other males [239].

Semen is then eventually deposited in the female reproductive tract by an intromittent organ, the penis [239].

1.2.2 Steroidogenesis in the adult male

Since inter- and intra-cellular processes in spermatogenesis are driven by signals originating from hormones, it is important to discuss molecular mechanisms of steroidogenesis in this context.

Spermatogenesis is driven by three major hormones, namely, LH and follicle-stimulating hormone (FSH), which are both derived from gonadotrophs in the anterior pituitary, and testosterone, which is mainly secreted by testicular Leydig cells. These hormones work in concert to promote the initiation of spermatogenesis, as well as germ cell proliferation, development, and differentiation. For this, FSH acts on Sertoli cells to activate gene expression and signalling pathways that support the process of sperm production, whereas LH acts on Leydig cells to promote the production of testosterone. To stimulate testosterone, LH binds to its cognate receptor, luteinizing hormone–chorionic gonadotropin receptor (LHCGR), on Leydig cells, which in turn activates the production of enzymes that is required for the biosynthesis of testosterone [250].

Biosynthesis of testosterone and of all other steroids starts with the cleavage of cholesterol to pregnenolone, which is the common precursor of all other steroids (Fig. 1-5). This first step, as well as all following steps, is catalysed by various steroidogenic enzymes, which can be divided into three categories. The first category contains the cytochromes P450, including mitochondrial (CYP11A1, CYP11B1, CYP11B2), microsomal (CYP17A1, CYP21A2, CYP19A1), and redox proteins (FDX1, FDXR, POR, CYB5A). Cytochromes P450 are steroid hydroxylases and their names derive from the specific enzymatic function. For instance CYP17A1 (P450c17, steroid 17-hydroxylase/17,20-lyase) is named after its role in the cleavage of cytochrome *b*5 (CYB5A) in the 17,20-lyase reaction. The second category comprises the oxidoreductases, such as hydroxysteroid dehydrogenases (HSD) 17βHSDs, 11βHSDs, 3βHSDs, and 3αHSDs, and 5α-reductases. The third category comprises conjugating enzymes (sulfotransferases, sulfatases, uridyldiphosphate, glucuronyltransferases) and steroidogenic acute regulatory protein (StAR), which mobilizes cholesterol into the steroidogenic pathways [23].

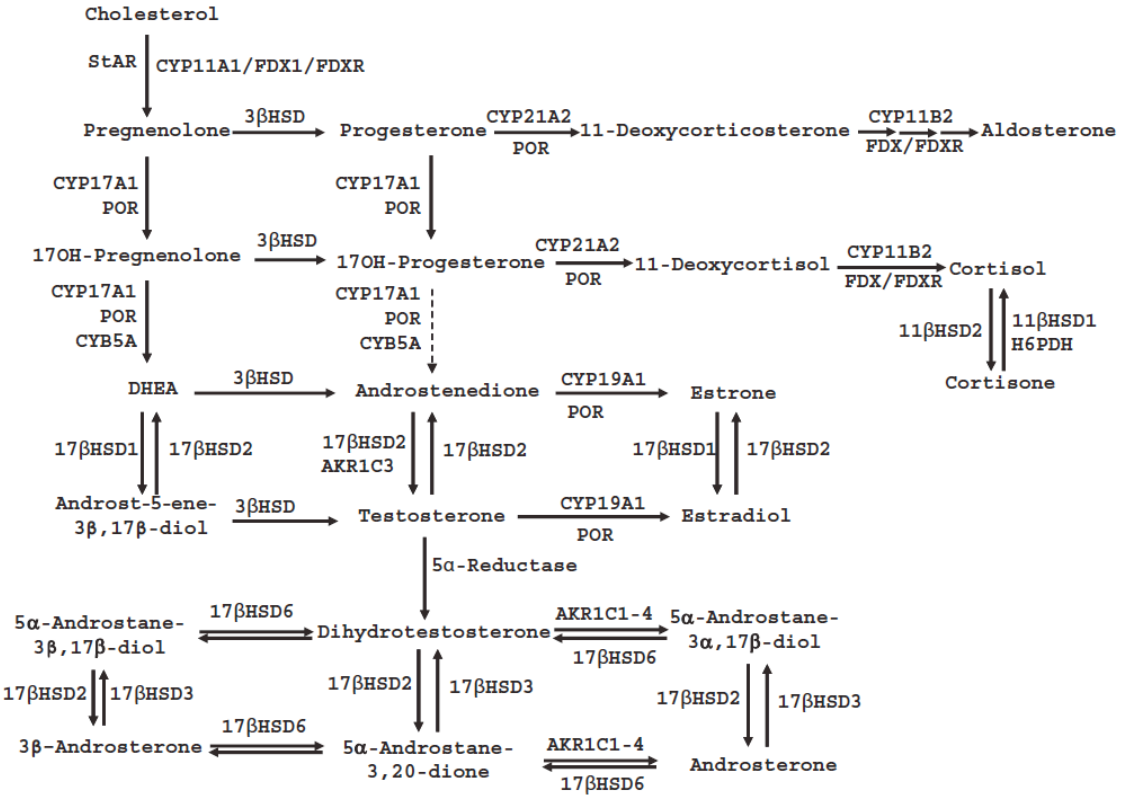

Fig. 1-5. Human steroidogenesis.
Human steroidogenesis [23] with permission.

Most of the steps in steroidogenesis are irreversible transformations. Thus, the cytochrome P450-catalyzed oxygenations, such as the 3βHSD/$\Delta^5 \rightarrow \Delta^4$-isomerase (3βHSD) reactions, and the 5α- and 5β-reductase reactions proceed only in one direction, whilst the 3α-, 3β-, 11β-, 17β-, and 20αHSD reactions are reversible [23].

During steroidogenesis, testosterone arises from the cleavage of the side chain of cholesterol by CYP11A1, leading to the formation of pregnenolone after loss of six carbon atoms. Pregnenolone can be further converted into progesterone via 3βHSD or 17OH-pregenenolone via CYP17A1. Thereafter, CYP17A1 catalyses the formation of 17OH-progesterone from progesterone or of didehydroepiandrosterone (DHEA) from 17OH-pregnenolone. These products will then further be converted into androstendione via 3βHSD or CYP17A1. In the final (reversible) step, androstendione is reduced by 17βHSD to yield testosterone. Another pathway for the yielding of testosterone is the conversion of DHEA to Androst-5-ene-3β-17β-diol, which is then irreversibly reduced to testosterone via 3βHSD.

Testosterone is secreted by Leydig cells in a pulsatile manner, which is due to

the pulsatile stimulation of the Leydig cells by episodic LH secreted by the anterior pituitary gland, since LH activates cholesterol transfer via StAR. Testosterone acts via the androgen receptor (AR) in somatic cells and is essential for maintaining spermatogenesis and has a crucial role in the process of masculinization and the maintenance of male secondary sexual characteristics. It further supports spermatogenesis by acting upon Sertoli and other testicular cells to regulate gene expression and the activation of signalling pathways [250].

Moreover, testosterone is also released into the bloodstream, where it acts to regulate LH secretion by the pituitary through a negative feedback loop. Hence, increased circulating testosterone concentrations feed back at the level of the hypothalamus and pituitary to suppress LH secretion by the pituitary, which subsequently reduces LHCGR-mediated stimulation of Leydig cells and thereby reduces testosterone production. Equally, a reduction in circulating testosterone concentrations induces LH secretion by the pituitary and a concomitant increase in testosterone production by the Leydig cells [250]. This communication between hypothalamus, pituitary and testicular cells is also known as hypothalamic-pituitary-gonadal (HPG) axis.

1.2.3 The Sertoli cell

First discovered in 1865 by the Italian physiologist and histologist Enrico Sertoli, the eponymous Sertoli cell was described as the non-spermatogenic "mother cell" of the seminiferous tubules (Fig. 1-4). Sertoli found that these cells do not produce spermatozoa, based on the finding that firstly spermatozoa have been observed in only a few extensions of these cells, secondly that spermatozoa are only found in extensions, where it would be possible for them to have entered accidentally, and lastly that the formation of spermatozoa is not associated with neither the form of the branched cells, nor with the constant position inside the tubule, nor their tendency to enclose the seminiferous cells among their branches, nor their communication with one another through the extensions [285].

Today it is known that Sertoli cells serve two distinct functions: first the formation of the seminiferous cords, and second the provision of nutritional and structural support of developing germ cells during spermatogenesis (discussed in section 1.2.4) [264]. Their number increases exponentially during fetal development,

followed by a further postnatal increase. During this time, Sertoli cells build the foundation of normal adult testicular function. Thus, in the fetus Sertoli cells support testis formation by coordinating the migration and differentiation of all other cell types. This starts with the differentiation of the primordial gonad into a testicular phenotype through the expression of the sex-determining region of the Y (SRY) chromosome gene, followed by the regulation of the proliferation, differentiation, and function of all other cell types, such as primordial germ cells, somatic Leydig cells, and peritubular myoid cells [264]. Moreover, during testicular development Sertoli cells induce the regression of Müllerian ducts via secretion of AMH [264]. Hence, Sertoli cells play a central role in testicular development. At this time, Sertoli cells are undifferentiated and responds to FSH, which promotes proliferation, and thyroxine, which inhibits the proliferative activity of the Sertoli cells [264]. Until recently, Sertoli cells were thought to reach their final, non-proliferative, state at puberty with Sertoli cell numbers per testis reaching about 3 x 10^6 in rodents and 1800 x 10^6 in humans [190]. Hence, any damage to the Sertoli cell environment was thought to be a cause of infertility, displayed as spermatogonial arrest [308]. However, several studies show that Sertoli cells express a mixture of proliferation inducing and inhibiting genes in an adult stage, making them different from other terminally differentiated quiescent cells [5,35,36,60]. This in turn suggests, that Sertoli cells rather resemble arrested proliferating than terminally differentiated somatic cells. Moreover, observations in Sertoli cells of hamsters and mice have now suggested that under pathological conditions, Sertoli cells might regain their proliferative capabilities due to hormonal changes and a disruption in spermatogenesis, further supporting that non-proliferative Sertoli cells are more likely to display a proliferation arrest rather than a final differentiation [5,263].

At puberty, the role of Sertoli cells switches to the support of germ-cell differentiation, meiosis, and spermatid transformation. This functional change is initiated by alterations in protein expression and gene transcription, and the formation of a functional BTB. The latter takes place through the formation of highly specialized tight junctions between adjacent Sertoli cells thereby preventing inter-cellular transport of macromolecules. Thus, the Sertoli cells control the intertubular environment as all germ cells other than spermatogonia and preleptotene spermatocytes, are located internal to the Sertoli cell tight junctions playing an important role for intra-testicular immune system and intra-tubular immunity [32]. The formation of the BTB is an essential step in the development of spermatogenesis and any delay will prevent the onset of

meiosis, whereas disruption of the BTB will lead to infertility due to an inability of the spermatogonia to differentiate into spermatocytes [190].

In order to study Sertoli cells function *in vitro*, many researchers use isolated primary Sertoli cells [290] or Sertoli cell lines, that were generated using different models and methods [144,168,172,203,225,237,279]. Within this study, primary mouse Sertoli cells and the WL-3 Sertoli cell line were used to determine diabetes-induced changes in Sertoli cell function with respect to activin metabolism, which will be discussed in section 1.3.

1.2.4 Spermatogenesis

Spermatogenesis is a highly conserved progression of cellular maturation steps, which allows male germ cells to develop into mature spermatozoa (Fig. 1-6). This process takes places within the seminiferous tubules of the adult testis, where the spermatogonial stem cells are maintained by regular mitosis, at intervals entering the process of meiosis to develop into spermatocytes, and lastly undergoing spermiogenesis, where the morphological transformation of haploid round spermatids into elongated spermatids is completed. Following this last step of spermatogenesis, spermatozoa are released into the tubule lumen and transit towards the excurrent ducts [32].

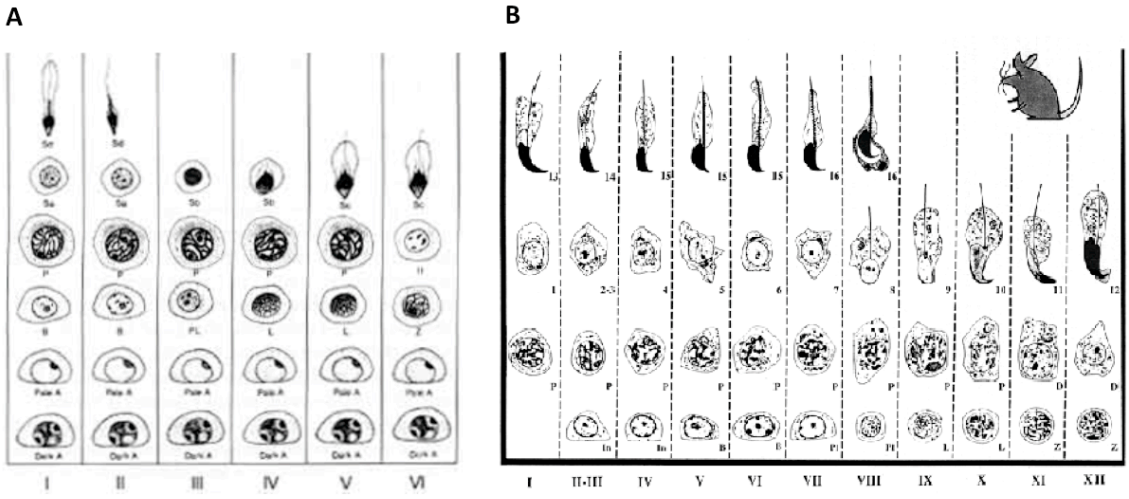

Fig. 1-6. Schematic presentation of spermatogenesis.
Spermatogenesis in the human (A) [245 with permission] and in mice (B) [223].

Throughout adult life, spermatogenesis is preserved by spermatogonial stem cells (SSCs), which can be grouped into type A_{single} (A_S) spermatogonia in mice and type

A_{pale} ($_{AP}$) and A_{dark} (A_d) spermatogonia in humans. Loss of spermatogonial stem cell receptors, such as glial-cell-derived neurotrophic factor (GDNF), Gfr1a and c-ret, as well as gradual reduction in neurogenin 3 marks the first steps of maturation. Differentiation is completed when the SSCs completely loose their ability to function as stem cells and concurrently express the cell surface signalling receptor tyrosine kinase kit. SSCs are now being referred to as A1, A2, A3, A4, In and B spermatogonia. For further maturation spermatogonia undergo mitosis. Following mitosis, spermatogonia enter meiosis to become primary spermatocytes, that undergo sister chromatid exchange and a nuclear division during the first phase of meiosis to yield secondary spermatocytes. Subsequently, the second meiotic division produces four haploid round spermatids from each progenitor, which further undergo chromosomal remodelling to bundle the genetic content and to initiate formation of mature sperm including formation to the tail from a pair of centrioles through the process termed spermiogenesis [32,69]. Sertoli cells together with the contractile peritubular myoid cells build the basement membrane of the seminiferous tubules. The contractions of the myoid cells allow spermatozoa to transit through the seminiferous tubule lumen towards the epididymis [32]. Since each Sertoli cell supports the maturation of a definite number of germ cells, the number and function of the Sertoli cells formed prior to puberty determine the adult sperm output [32,69].

1.2.5 Type 1 Diabetes and reproduction

Since diabetes mellitus is a major public health problem it has been reported to cause not only serious complications such as retinopathy, nephropathy, and neuropathy, but also impairment in fertility in women and men. Hence, women suffering from diabetes were shown to have a high prevalence of sexual dysfunction with a mixed pattern of sexual symptoms, including loss of sexual interest or desire, arousal or lubrication difficulties, painful intercourse (dyspareunia), and loss of the ability to reach orgasm [78]. Additionally, T1D in pregnant women was shown to also affect the child during pregnancy, resulting in placental transfer of maternal excess glucose leading to fetal hyperinsulinaemia and accelerated fetal growth [216].

However, since the prevalence of patients suffering from T1D is steadily increasing, affecting many more men during their reproductive age, this study concentrates on the impact of diabetes on male reproductive health. A large number of

studies in diabetic men, as well as in animal models have indicated that diabetes mellitus disrupts fertility at various levels including altered spermatogenesis, degenerative and apoptotic changes in testes, altered glucose metabolism in Sertoli cells, reduced testosterone synthesis and secretion, erectile dysfunction, ejaculatory dysfunction, reduced libido, and impotence [12,124]. When studying sperm parameters and sperm quality markers, the literature shows some conflicting results, with evidence for alterations in sperm morphology and motility in some studies [141,173], but not in others [2,3,162]. Interestingly, in many studies that reported normal semen parameters, a higher degree of sperm microstructure damage, such as alterations in mitochondrial DNA (mDNA), was observed, indicating that DM is more likely to affect male fertility at a molecular level [2,3,131,162].

The interpretation of clinical results is, however, exacerbated by inconsistent study design with many clinical studies concentrating on T2D patients or, when both types of diabetic patients were recruited, results not distinguishing between T1D and T2D. Moreover, these studies seem to mainly focus on the clinical significance, rather than the molecular mechanisms underpinning DM-induced alterations of male fertility. Additionally, factors such as the glycaemic control, the type of treatment, as well as all the comorbidities associated to DM can mask the outcomes of the studies that relate with DM and male fertility. This exacerbates the interpretation of how much of the observed disrupted fertility is due to changes in glycaemic status and which is attributed to other factors, such as body weight/ adipose tissue and DM related comorbidities. Hence, the use of animal models, which allow investigations under tightly controlled conditions, are crucial for the study of DM-induced male infertility [12].

In accordance with the clinical data, many animal studies have reported a reduced fertility, gonadal dysfunction, and alterations in sperm motility and morphology. Moreover, these studies also reported altered sexual behaviour, reduced testicular weight and sperm content, as well as reduced epididymal sperm content [30,106]. To date, several animal experiments have also aimed to investigate the underlying molecular mechanisms that cause diabetes-induced infertility, but comprehensive studies remain scarce. One proposed mechanism is the disruption of the HPG axis, since DM is known to cause changes in the HPG axis, such as altered levels of FSH and LH, which in turn can be related to diabetes-induced impotence [30,166,235]. Also atrophic changes within the epididymis, resulting in the loss of spermatozoa in the epididymal lumen and oxidative stress, affecting both testis and epididymis, have been proposed to

contribute to DM-induced disruption in male fertility [252].

A more detailed review of the literature on the impact of T1D on male reproductive health is given in Table B-6 and Table B-7.

Nevertheless, molecular mechanisms beyond glucose deregulation remain poorly investigated and most of the biochemical changes involved in DM-induced infertility remain unknown. Hence, it is crucial to evaluate the molecular mechanisms of testicular insulin and glucose regulation to determine the impact of DM on male reproductive function.

Optimal glycaemic control in diabetic individuals is crucial to reduce and avoid DM-related complications and comorbidities, since hypo- and hyperglycaemia lead to molecular alterations, which in turn can also lead to detrimental effects on male reproductive health [12,221]. Moreover, it was shown that disease onset and disease duration are important impact factors in this matter [141,186,229,248]. Indeed, the actions of insulin on the male reproductive tract has been studied since the early 1980's, showing that not only insulin itself, but also insulin-like growth factor-1 (IGF-1) and insulin receptors are involved in the regulation of the energy metabolism of Sertoli cells by regulating the uptake of nucleotides (ATP, GTP, UTP), and the secretion of transferrin, pyruvate, and lactate. Therefore, insulin is actively involved in initiation and maintenance of spermatogenesis [41,95,129,249]. This is further supported by findings, which show that insulin not only regulates glycine metabolism, but also lipid metabolism within Sertoli cells by regulating the biosynthesis of arachidonic acid [195]. Further studies imply that insulin secreted from Sertoli cells acts in an autocrine-paracrine manner [94,202]. Recent studies suggest, that insulin may also be involved in male reproductive function via regulation of the HPG-axis [235]. Lastly, there is also evidence that insulin can regulate human sperm fertilization capacity through regulation of glucose metabolic pathways during sperm acrosome formation and capacitation [17].

Glucose is an energy substrate required to maintain spermatogenesis, a metabolically active process, which depends upon tight cooperation among testicular cells. In this context, Sertoli cells play a crucial role in providing pyruvate and glycolytic converted lactate for developing germ cells [129]. Thus, disturbance in glucose metabolism, as in diabetic individuals, can lead to major disruptions in the cellular organisation, ranging from vacuolization to a high degree of degeneration. This in turn, has dramatic consequences for the cellular interaction during spermatogenesis [12].

These findings show that a deregulation of the insulin and glucose metabolism

plays a significant role in DM-induced male infertility and/or subfertility.

1.2.6 Reproduction in the *Ins2*^{Akita} mouse model of type 1 diabetes

Various studies have shown that male mice homozygous for the mutation within the *Ins2* gene show testicular atrophy starting by the age of 5 weeks with an observed reduction in testis size, reduction in seminal vesicle weight, arrested spermatogenesis, and an absence of mature spermatozoa as well as a decreased numbers of spermatocytes and spermatids. By the age of 7-8 weeks these mice exhibit infertility [136,235,236]. Data on heterozygous *Ins2*^{Akita} mice is conflicting, with one study stating that these mice become infertile at the age of approximately 24 weeks and cease to sire pups after the age of 4 to 6 month [235] and another study showing that these mice maintain fertility [236]. The latter is also supported by findings from Fox et al., who showed that testicular morphology of heterozygous Akita mice did not differ from wild type mice [86].

By the age of 8 to 9 weeks the seminiferous tubules of homozygous mice display an intact BTB, show, however, a marked atrophy, characterized by a loss of germ cell populations and an increase in the presence of large, multinucleated cells as well as vacuolization. This is accompanied by fewer germ cells in the epididymis. Additionally, sperm from homozygous Akita mice fertilize fewer embryos, and those embryos that get fertilized show developmental damage at blastocyst stage, such as fragmentation and poor embryo development. This is likely to be due to the observed increased amount of DNA damage in germ cells within the seminiferous tubules of these mice [136,235,236].

Schoeller et al. went on to investigate molecular mechanisms behind the observed testicular damage and showed that these mice, despite having a reduction in testis size as well as abnormal testis and sperm morphology, do not display any increase in ER stress in the testis. This suggests, that the observed testicular phenotype of homozygous Akita mice is not caused by ER stress, but by diabetes itself [235]. Furthermore, both the testes and sperm of homozygous Akita mice show an increase in apoptotic germ cells as well as a lower number in motile and progressively and rapidly moving sperm. Investigations from Schoeller et al. on sperm morphology revealed that sperm from homozygous mice lack acrosomes, show membrane blebbing and numerous detached sperm heads, as well as abnormal mitochondria [235]. Moreover, Schoeller et al. observed decreased serum levels of testosterone and LH, which could be partially

rescued by exogenous insulin. This suggests that the observed testicular phenotype might be due to a disruption within the HPG-axis [235]. The finding that homozygous *Ins2*^{Akita} mice show reduced levels of leptin further supports this view [236]. Leptin has been shown to play a role in the HPG-axis by acting upon the hypothalamus, thus inducing the secretion of testosterone within the testis [143].

To further support the impact of diabetes on the reproductive outcome in those mice, Kim and Moley investigated the glucose metabolism in these mice. Thus, Akita mice exhibit a reduced expression in the glucose transporter SLC2A8 within the testes and a loss of expression in SLC2A9b within testes and sperm. Also, expression of SCL2A9b was found to be significantly lower within the acrosome and principal piece of Akita sperm. All together these findings indicate that the expression of glucose transporters may be regulated by insulin signalling and/ or hyperglycaemia and that therefore diabetes in Akita mice has an important impact on sperm maturation and fertilization [136].

Moreover, O'Neill et al. proposed the involvement of oxidative stress in the diabetes-induced disruption of fertility in heterozygous Akita mice, since they showed an increase in the advanced glycation endproduct CML within the testes, epididymides and sperm. Moreover, the receptor for advanced glycation endproducts (RAGE) was found to be present on the developing acrosome and epididymal sperm, with the latter showing an increase in nDNA damage [189].

Within the present study the heterozygous *Ins2*^{Akita} model was used to investigate long-term effects of diabetes on male reproductive functions with focus on the regulation of the activins.

1.3 Activin and the TGF-β superfamily

Many testicular functions, such as formation and programming of sexually indifferent germ line cells for spermatogenesis, as well as spermatogenesis itself, require progressive, interactive instructions between multiple cell types. Members of the TGF-β superfamily play a crucial role in this system by providing a complex, interactive system, allowing different cell types to communicate with one another [305].

The TGF-β superfamily compromises approximately 40 structurally related proteins, including 3 TGF-β homodimeric proteins (TGF-β-1, -2 and -3), several activins, Nodal, over 15 bone morphogenetic proteins (BMPs), AMH, growth and

differentiation factors (e.g. GDF9, also named BMP15), and the divergent GDNF subfamily [305]. It was named after its first member TGF-β1, which was first described in 1983 [21].

The following section will discuss the signalling processes of the TGF-β superfamily, with a particular focus on activin signalling and the role of activins in male reproduction.

1.3.1 Activin and Inhibin

Activin and inhibin are both recognized as pleiotropic growth factors, which were first described based on their ability to regulate FSH synthesis and secretion by the anterior pituitary [32,72]. Both are highly conserved across different species, and have conserved functions. Activins are homodimers formed by dimerization of two β subunits, whereas inhibins are heterodimers formed by dimerization of an α-subunit (encoded by the *Inha* gene) and one β-subunit. To date, four different β subunits, including β_A (*Inhba*), β_B (*Inhbb*), β_C (*Inhbc*) and β_E (*Inhbe*) have been described in mammals.

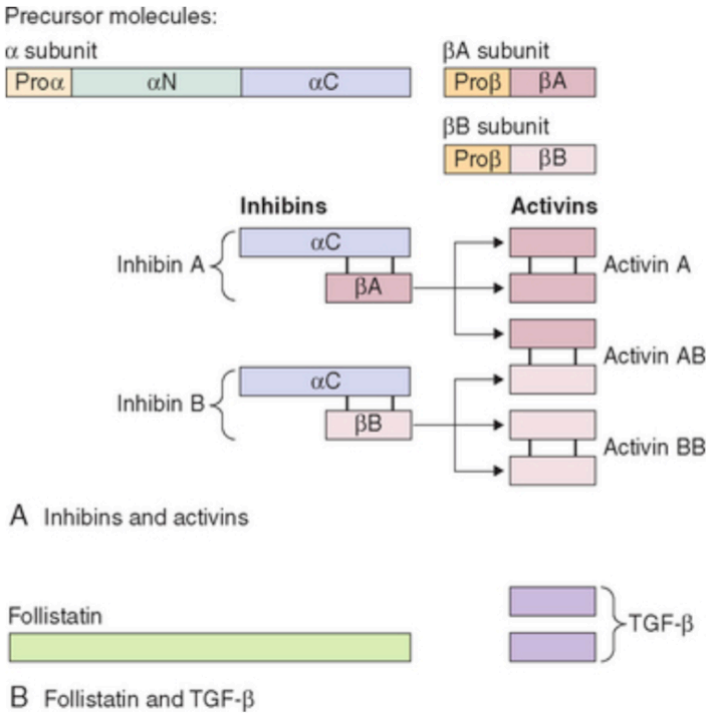

Fig. 1-7. Activins, inhibins, follistatin, and TGF β .

A schematic representation of the formation of different dimeric proteins from three basic subunits [99].

Originating from a precursor protein, which consists of a pro-region and a C-terminal mature peptide, the biologically active mature protein is formed after disulphide-bonded dimerization and cleavage of the pro-region. Each of the mature subunits forms three intra-molecular disulphide bonds and two subunits are joined by a further disulphide bond resulting in activin A (β_A: β_A homodimer), activin B (β_B: β_B homodimer) or activin AB (β_A: β_B heterodimer) or inhibin A or B. Activins A and B are the bioactive forms, while activins C and E are weak agonists or antagonists. For the formation of inhibin A the α subunit binds to the β_A subunit, whereas for the formation of inhibin B it binds to the β_B subunit. The inhibins are antagonists of activin A and B. Additionally, *in vitro* studies of the β_C subunit showed that it can either form a homodimer or heterodimers with the β_A and β_B subunits resulting in a functional inhibitory protein of activin A *in vivo* [32,156,305]. A scheme of the structure of activins, inhibins, and their precursor molecules is shown in Fig. 1-7.

1.3.2 TGF-β superfamily signalling – The Smad pathway

Members of the TGF-β superfamily are known to signal through the formation of a multimeric receptor complex. This receptor complex is formed of two distinct receptor subunit classes, which are common to nearly all TGF-β superfamily ligands. The first subclass is termed type I receptors and contains receptors termed anaplastic lymphoma kinase (ALK) 1 to ALK7. The second subclass is termed type II receptors, known as TGFBR2, ActRIIA (Acvr2a), and ActRIIB (Acvr2b), with two subunits that hold intrinsic serine/threonine kinase activity [32,156,305].

Activins signal through binding to the type II receptor subunit, either ActRIIA or ActRIIB, which further enables the phosphorylation of the type I receptor via the constitutively active kinase domain. Distinct receptor binding affinities, such as TGFBR2 and ALK1 or 5 for TGF-βs and Acvr2a or 2b plus ALK2, 4 or 7 for activins, BMPs and Nodal allow a crosstalk between the ligands at the level of receptor utilization. Furthermore, it provides a structural basis for signalling intensity and duration. Thus, after binding to the type II receptors activin A activates the type I receptor ALK4, whereas activin B activates ALK4 and ALK7. Inhibins, on the other, can recruit another receptor type, known as type III receptors (TGFβRIII, betaglycan), which then binds to the type II receptor and prevents activin receptor type I and II dimerization and signalling [32,156,305].

Thereafter, the receptor kinase activity of the type I receptors leads to the recruitment and phosphorylation of downstream signalling molecules such as regulatory Smads (R-Smads) 2 and 3, which are typically activated by activins, Nodal and TGF-βs, or Smads 1, 5 and 8, which are used by BMPs. Being phosphorylated these Smads are able to bind to the common Smad4 in order to build a complex which can translocate into the nucleus to affect gene transcription [32,156,305].

This pathway can be negatively regulated by either inhibitory Smads on an intracellular level or by cell surface antagonists. The inhibitory Smads 6 and 7 can bind to R-Smads to inhibit their signalling. Negative regulation by cell surface antagonists, such as inhibin, Bambi, follistatin, noggin, gremlin, and chordin, was shown to be either due to direct binding of the receptor ligands or by competitive binding to the type II receptors [32]. A scheme of the Smad signalling pathway is shown in Fig. 1-8.

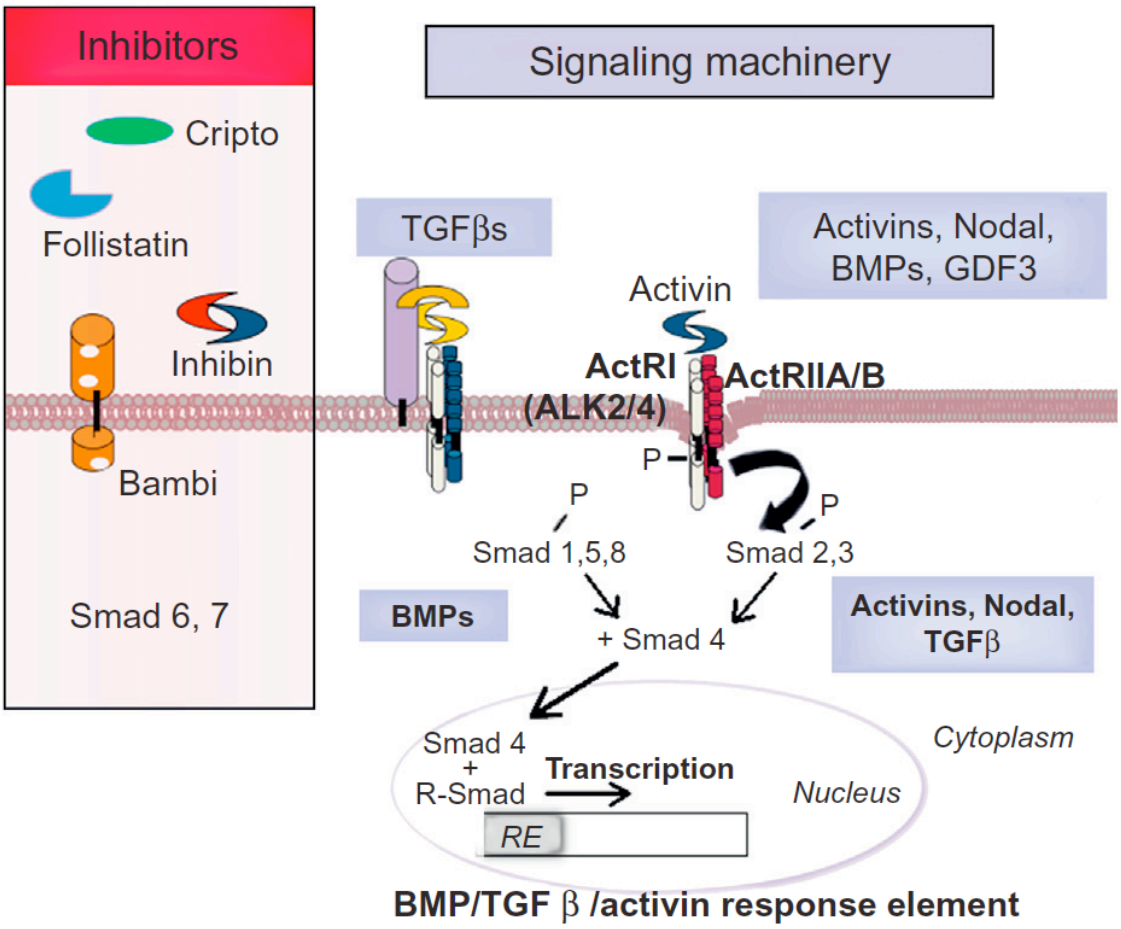

Fig. 1-8. Smad signalling pathway.
Smad signalling pathway [156] with permission.

Bambi, also known as BMP and activin membrane-bound inhibitor, is a

transmembrane glycoprotein related to the type I receptors. It exerts its actions as a pseudo-receptor, lacking an intracellular serine/threonine kinase domain required for signalling. Thus, it allows binding of the receptor ligands without processing the signal further, since it prevents the formation of the receptor complexes [194].

Follistatin (FST) is a glycosylated monomeric protein, which antagonises activins by binding to the β-subunits to form a stable complex that effectively prevents the activins from interacting with the type II receptor. Through alternative splicing multiple transcript variants that encode multiple follistatin isoforms are being built. These include FST315 and FST288 (comprised of 315 and 288 amino acids, respectively), which differ at their C-terminus, and have different affinities for cell surface heparan sulphate-containing glycoproteins. Another isoform, FST303, is thought to be produced by proteolytic cleavage of FST315. While FST315 is a freely circulating protein, FST288 is largely tissue-bound, and FST303 appears to be gonad-specific [258].

Noggin, gremlin, and chordin are glycosylated proteins known for their inhibitory effects on BMP. Thus, they inhibit BMP signalling by blocking the molecular interfaces of the binding epitopes for both type I and type II receptors by sequestering its ligand in an inactive complex [116,205,226].

The crosstalk amongst all ligands of the TGF-β superfamily is understood to be a tightly regulated system and will finally determine the response within the signalling cascade [32,156,305]. It is therefore important to identify which components of this signalling cascade are present in each cell and within every physiological context to fully understand how cell respond to its activation.

1.3.3 The role of activin in reproduction

Since male reproductive function depends on the production of hormones from the HPG axis, it is of great importance that activin serves both paracrine and autocrine actions in each organ of this axis. Activin is known to stimulate GnRH release from the hypothalamus and FSH release from the pituitary. It can further increase the number of GnRH receptors on the surface of gonadotropes and augment the GnRH-mediated transcriptional activation of GnRH receptors in order to enhance the pituitary response to GnRH [32].

In the testis itself, the local production of activin and the control of its signalling

pathway are critical for germ and Sertoli cell development as well as for adult testis function [32]. However, activins were also shown to be of great importance during testis development, since the gonad shows a sexually dimorphic response to activin and its inhibitors [32,156,305].

1.3.4 The role of activin in diabetes

To date, several studies have proposed an important role for several members of the TGF-β superfamily in maintaining β cell function under physiological conditions and that they hence play a crucial role in the pathology of diabetes. Specifically, activins A and B, as well as their binding protein follistatin, have been shown to be involved in the regulation of glucose metabolism and inflammation [15,62,104,191,260,293]. Moreover, since gene expression of the activin βB subunit as well as that of the canonical activin receptors ALK4, ActRIIA, and ActRIIB has been demonstrated in the pancreatic bud in mice [73], and the activin βA subunit was localized in α, β, and δ cells of the pancreatic islet [192,303], the involvement of activins in the development and onset of diabetes seems likely.

Hashimoto and Funaba reported that activins A and B are regulators of the differentiation and activation of pancreatic β-cells and that they are moreover involved in controlling the response of insulin target cells [104]. Additionally, they have been proposed to modulate events involved in insulin sensitivity in a tissue dependent manner and therefore regulate whole-body insulin responsiveness [104]. Hence, activin A is capable of reducing target tissue sensitivity to insulin, while activin B was shown to enhance insulin gene transcription [104,295]. This is further supported by the finding that activin enhances glucose stimulated insulin secretion (GSIS), and augments the expression of genes characteristic to mature β-cells, such as insulin, solute carrier family 2 (Scl2a2 or GLUT2), and PC2, which suggests that activin is actively involved in β-cell differentiation.

With regard to diabetes, many studies focus on the interaction of activin activity and T2D. This is due to the fact that activin A was shown to affect inflammation in adipose tissue by stimulating macrophage formation from a pro- into an anti-inflammatory phenotype. This is supported by the finding that toll like receptor 4 signalling is increased in recently diagnosed T2D patients and that activin A was shown to be activated through this mechanism [295]. Additionally, activin A was shown to be

released by murine bone marrow derived neutrophils after stimulation with tumor necrosis factor (TNF-α), a response that was abolished after pre-treatment with insulin [293]. This supports the hypothesis that activin A is directly involved in inflammation associated with T2D and that insulin directly impacts activin A release. Furthermore, these data suggest that a loss of insulin sensitivity could lead to an increase in activin A levels and inflammation, and thereby exacerbating the disease.

Focussing on the role of activin in T2D, Wu et al. found that, although serum levels of activin A or follistatin in diabetic patients did not differ from control patients or patients with impaired glucose tolerance, activin A and/ or B measures could still be positively correlated to parameters of insulin resistance and T2D, such as fasting glucose, fasting insulin, and HbA1c [295]. Furthermore, they found that serum levels of activin A, but not activin B or follistatin, were positively correlated with age in control, but not in diabetic subjects. This indicates that increasing levels of activin A with age are necessary to maintain a healthy metabolism and that this mechanism is disrupted in diabetic patients, despite the fact that acute changes of glucose and insulin did not alter activin A and B levels [295]. In contrast to this finding, Chen et al. did not confirm a correlation between serum activin A levels and fasting glucose, fasting insulin, or M-value for insulin sensitivity, while they showed a positive correlation for activin A with age in T2D men [62]. However, they were able to show an association between circulating plasma activin A levels in T2D men without cardiovascular complications and myocardial glucose metabolism as well as left ventricular mass/ volume (LVMV)-ratio. This indicates that activin has a potential role in early human diabetic cardiomyopathy [62]. Further support for a role of activin A in diabetic cardiomyopathy was provided by Blumensatt et al. who showed that activin A release from epicardial adipose tissue in T2D patients inhibits proper function of insulin by inhibiting the Akt pathway, a signal transduction pathway that promotes survival and growth in response to extracellular signals. Hence, insulin-stimulated glucose uptake is reduced [38]. Adding to investigations on the role of activin A in diabetic cardiomyopathy, Andersen et al. established that activin A levels are positively correlated with abnormal glucose regulation in patients with acute myocardial infarction (MI). This involved a correlation for blood activin A levels with glucose levels at admission, glucose levels during and oral glucose tolerance test (OGTT), HbA1c, as well as insulin and C-peptide. Furthermore, they showed that glucose enhanced activin A release in endothelial cells, whereas activin A in turn attenuated the release of the inflammatory cytokine IL-8, while concurrently enhancing

levels of the anti-oxidative enzyme metallothionine. Thus, they proposed an anti-inflammatory role for activin A in this context, a view further supported by findings that activin weakened the suppressive effect of IL-8 on insulin release in islet cells [15].

Taken together, these results suggest that, even though there seems to be no difference in circulation serum activin A levels in diabetic and non-diabetic men, activin A does play an important role in glucose metabolism. This mainly involves the regulation of differentiation and activation of pancreatic β -cells and controlling of the response of insulin target cells [110].

Besides the involvement of the activins in diabetes and diabetes-induced complications, recent studies have also focussed on the regulation of the downstream signalling pathway of the activins. Thus, Smad 3 was shown to promote hepatic gluconeogenesis during T2D, while inhibition of Smad 3 signalling suppressed endogenous glucose production [297]. Moreover, phosphorylation of the Smad 2/3 complex was shown to be enhanced in T2D animals, which is likely accompanied by a diminished expression of the inhibitory Smad 7 [150,301].

A detailed literature review on the role of activin in DM is given in Table B-8.

1.4 Hypothesis and aims of the study

The previous chapters demonstrate that there is evidence linking T1D and male reproductive dysfunction, however, the underlying mechanisms are still poorly understood. In this study, I hypothesize that hyperglycaemia will induce local low-grade inflammation regulated by activins and their binding protein follistatin. Thus, the aim of this study is to identify this interaction as novel underlying mechanism of diabetes-induced male reproductive dysfunction, providing new insights into this field of research.

To accomplish this, I used *mev-1* mutant nematodes, heterozygous *Ins2*^{Akita} (*Ins2*$^{Akita+/-}$) mice, and cultured Sertoli cells to investigate the following research objectives:

1) To investigate the effect of hyperglycaemia on the brood size of *mev-1* mutant nematodes and to delineate the impact of high glucose treatment on Sma/Mab pathway genes in *mev-1* nematodes, which are closely related to the TGF-β signalling pathway in mice and humans

2) To assess the reproductive phenotype of *Ins2*$^{Akita+/-}$ mice
3) To assess the regulation of activins and their signalling pathway in *Ins2*$^{Akita+/-}$ mice
4) To study the effects of high glucose and high activin on cultured Sertoli cells

Results from these investigations will give insights into the role of activins and their signalling pathway in diabetes-induced male infertility allowing for a better understanding of the pathogenesis of male reproductive dysfunction in diabetic males.

2 Material and Methods

In order to investigate the impact of T1D and high glucose levels on male reproduction, with focus on the activin signalling pathway, animal experiments were carried out using the *C. elegans* strain *mev-1*, as well as C57Bl/6J and heterozygous *Ins2*^{Akita} (*Ins2*$^{Akita+/-}$) mice. Further, *in vitro* experiments using primary Sertoli cells as well as a Sertoli cell line (WL-3) were conducted in order to evaluate the influence of altered insulin and glucose on Sertoli cell function. This section will describe the handling of these animals and cells as well as the methods used. Section A will give a detailed list of consumables, instruments, chemicals and reagents, buffers and solutions, and software used in these studies.

2.1 *C. elegans* experiments

Studies on the *C. elegans* model organism were carried out in the laboratory of Prof. Dr. Uwe Wenzel at the Institute for Molecular Nutritional Research of the Justus-Liebig-University.

Nematodes used in the present study were N2 (wild type, Caenorhabditis Genetics Center (CGC) University of Minnesota, Minneapolis, USA) and *mev-1* (constructed in the lab of Dr. Kai Lüersen, University of Kiel), both generously provided by Prof. Uwe Wenzel.

According to the methods of Stiernagle et al., *C. elegans* were cultured on nematode growth medium (NGM) agar plates seeded with concentrated Escherichia coli *(E. coli*) OP50 (obtained from the CGC) liquid culture at 20°C [256]. OP50 seeded NGM agar plates were kindly prepared by Eva Czynski and Alexandra Neeb. All steps for the production of *E. coli* OP50 cultures as well as their transfer onto NGM-agar-plates were carried out under sterile conditions using a sterile fume hood. Worms were transferred regularly to fresh plates before starving.

2.1.1 Cultivating *E. coli* OP50 on 2xYT-agar plates

Prior to cultivation bacterial cultures (with or without RNAi) were stored as glycine cultures at -20°C. In order to cultivate *E. coli* OP50, bacterial smears were plated onto 2xYT-agar-plates using a sterile inoculation loop. Further, annealing of the

inoculation loop allowed isolation of bacterial colonies as shown in Fig. 2-1. Plates were sealed with Parafilm and incubated for 12 to 16 h at 37°C. Afterwards plates were stored at 4°C.

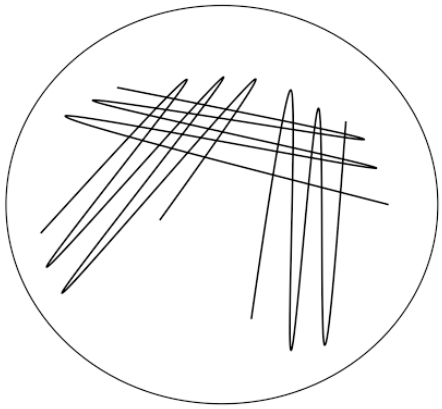

Fig. 2-1. Isolation of bacterial colonies.

2.1.2 Generation of an *E. coli* OP50 over culture

In order to generate an *E. coli* OP50 overnight culture 3 ml 2xYT-medium were pipetted into a tissue culture tube. Using a sterile pick a single colony of the *E. coli* culture is taken from the 2xYT-agar-plate and added into the medium. Thereafter, the tube was incubated overnight at 37°C, shaking at 300 rpm. To ensure oxygen supply within the tube, the lid was placed loosely on top.

2.1.3 Generation of an *E. coli* OP50 day culture

In order to generate an *E. coli* OP50 day culture 200 ml 2xYT-medium were inoculated with 500 μl overnight culture in an 500 ml Erlenmeyer flask. The flask was closed for sterility and incubated for 6 h at 37°C, shaking at 300 rpm.

2.1.4 Concentrating an *E. coli* OP50 day culture on NGM-agar-plates

For further use of the day culture, 4 x 45 ml of the day culture were transferred into a 50 ml centrifuge tube and centrifuged for 5 minutes at 5000 x g. The supernatant was discarded and the pellet resuspended in 4.5 ml 2xYT-medium. This concentrated suspension was stored at 4°C until use.

NGM-agar plates were overlaid with either 100 µl (55 mm plates) or 600 µl (100 mm plates) OP50 day culture, swayed and air dried under sterile conditions. Thereafter, plates were stored at room temperature (RT).

2.1.5 Synchronization of *C. elegans* using egg-prep

For all experiments, synchronous *C. elegans mev-1* populations were used.

Age synchronous populations of L1-larval nematodes were obtained by the collection as described by Donkin and Williams [75]. To obtain homogeneous populations of L4-larval nematodes worms were synchronized by bleaching. For this, 2 to 5 ml M9 buffer were pipetted onto NGM-agar-plates that were fully grown with gravid nematodes. Plates were shaken gently and nematodes, that were now swimming within the buffer, were washed into 15 ml centrifuge tubes. If necessary, plates were rinsed once more with M9 buffer to collect remaining worms. In order to obtain adult worms, centrifuge tubes were filled to 14 ml with M9 buffer and centrifuged for 2 minutes at 1200 rpm. When the adult worms had settled and the supernatant (13.5 ml), containing bacteria and larvae, was discarded. Thereafter, the worms were washed using 13.5 ml M9 buffer, followed by centrifugation for 2 minutes at 1200 rpm. Washing was repeated until the supernatant was clear (generally, 2 times). After the last washing step, worms were centrifuged for 2 minutes at 1200 rpm and the supernatant was discarded, leaving a remainder of 3.5 ml within the tube. Thereafter, worms were lysed by adding 1.5 ml bleaching solution (0.45 N NaOH, 2 % HOCl) into the tube, followed by intense shaking for 5 minutes. This procedure allows the eggs to be set free. Afterwards, this tube was filled to 14 ml with M9 buffer, followed by centrifugation as described above. In order to remove the bleaching solution, the supernatant was discarded, leaving a remainder of 0.5 ml within the tube that was washed for 3 times as described above. After the last washing step 10 ml of M9 buffer and 10 µl cholesterol were added into the tube, which was then left for incubation in an overhead shaker overnight at 20°C. During this time the larvae hatched.

On the following day, the tube was centrifuged for 2 minutes at 1200 rpm, the supernatant was discarded and leaving a remainder of 1 ml. This was washed as described above. Hereafter the larvae were raised in NGM-liquid-media under experimental conditions.

2.1.6 Raising synchronized larvae in NGM-liquid-media

For all experiments synchronised L1 larvae were grown in liquid NGM with bacteria in 96 well microtitre plates. For this, 2x 150 μl of a concentrated OP50 day culture were pipetted into a 1.5 ml Eppendorf tube and centrifuged for 2 minutes at 10000 rpm. The supernatant was discarded and the pellet resuspended and vortexed in 2 ml NGM medium. Thereafter, the optical density (OD_{600}) of the bacterial suspension was measured against NGM-liquid-media. The anticipated OD_{600} was 1.0 ± 0.1, which corresponds to 8 x 10^8 bacteria/ ml.

In a volume of 10 µl M9 buffer about 10 larvae were transferred to each well. To each well 44 μl NGM-bacteria-solution were added. Outer wells were spared and filled with 200 μl MilliQ H_2O to avoid desiccation. Thereafter, nematodes were grown for three days protected from evaporation within a cardboard box at 20 ° C and shaking at 150 rpm.

In order to investigate the role of the activin and BMP pathway in the reproductive outcome of *C. elegans mev-1* nematodes, worms were incubated using zmp-2-RNAi (Source Bioscience, Cambridge, UK) for *dbl-1* (BMP-5 in humans), *sma-2* (Smad-1 in humans), *sma-3* (Smad-5 in humans), *sma-6* (BMPRIB in humans). When grown in zmp-2RNAi-NGM-medium instead of OP50 medium, worms were grown for four days.

2.1.7 Incubation with treatment media and assessment of brood size

In order to assess the effect of glucose treatment on brood size in *mev-1 C. elegans* nematodes, worms were incubated with RNAi or control NGM-liquid medium and treated with either glucose or M9-buffer alone (control) for a period of 24 h. To determine a suitable glucose concentration, a pilot experiment using 10 mM or 100 mM was carried out. For this, 6 μl of the 100 mM glucose solution (10 mM treatment), 6 μl of the 1 M glucose-solution (100 mM treatment) or 6 μl M9-buffer (control) were added into the wells of the 96-well microtiter plate. The following day, worms of each treatment group were transferred into 15 ml centrifuge tubes containing 7 ml M9-Tween20 washing buffer. Worms were allowed to settle for 10 minutes, then the supernatant was discarded, leaving a remainder of 1 ml. 50 μl of the worm suspension were pipetted onto a fresh NGM-OP50-agar plate and air dried for 30 minutes. Brood

size was assessed by placing treated or control nematodes in groups of 5 onto individual culture plates. The pilot experiment showed no effect of the treatment with 10 mM glucose, whereas 100 mM glucose significantly decreased brood size. Hence, 100 mM glucose were chosen for all further treatments and a total of 8 plates per treatment group were used during each experiment. The examined nematodes were transferred to a new well every day for a total of three days. The total number of eggs released on the plates was counted. At least 24 independent replicates were performed for statistical purposes.

2.2 Mouse handling

Ins2$^{Akita+/-}$ mice were obtained from the Mannheim colony (Mannheim, Germany) bred for more than 30 generations on a C57Bl7/6J background. Blood glucose was monitored consecutively over the study period. At 8 weeks of age, approximately half of these mice had permanent blood glucose levels greater than 14.0 mmol/l and were classified as having severely hyperglycaemic, insulin-dependent diabetes according to criteria for diabetic ketoacidosis [93]. Insulin was occasionally administered subcutaneously to prevent critical weight loss. Non-diabetic *Ins2*$^{Akita+/-}$ mice, defined as having on-going blood glucose levels <14.0 mmol/l, were included in all experiments as phenotypic controls with an identical genetic background. Adult (12- and 24-week-old) male C57Bl/6J mice were obtained from Charles River Laboratories (Sulzfeld, Germany) as wild type controls. All animals were housed in groups of 3 to 4 animals (Type II macrolon cages) at a temperature of 21±1°C with a 12 h light–dark cycle. At the end of experimental period, animals were killed by cervical dislocation under intra-peritoneal ketamine (75 mg/kg body weight) + xylazine (10 mg/kg body weight) anaesthesia. 200 – 500 μl non-fasting blood was collected from the retro-orbital venous plexus from all mice and HbA1c was determined as described previously [204]. Serum for biochemical determinations was generated by whole-blood centrifugation at 1300 rpm for 10 minutes. Mice had free access to food and water and were obtained following approval from the Animal Ethics Committee, in accordance with German Animal Welfare Act for the care and use of laboratory animals and the rules of the regulatory authorities in Baden-Württemberg (Regierungspräsidium Karlsruhe, Germany). Unless stated otherwise, all reagents were obtained from Sigma-Aldrich Chemie GmbH (Seelze, Germany).

2.2.1 Tissue Isolation

12- and 24-week old C57Bl/6J mice as well as 12- and 24-week diabetic and non-diabetic *Ins2*$^{Akita+/-}$ mice were killed by Ketamine-Xylazine euthanasia, followed by cervical dislocation. Thereafter, the abdomen was opened and testes and epididymides were excised. Generally, one organ was used for immunohistochemistry and processed as described in section 2.5, whereas the other organ was snap-frozen in liquid nitrogen for further protein or gene analysis as described in section 2.6.

2.2.2 Sperm analysis

In order to perform morphological sperm analysis fresh epididymides from C57Bl7/6J or *Ins2*$^{Akita+/-}$ mice were placed in Petri dishes containing 1 ml of high saline bicarbonate (HSB) buffer and milked using forceps to release stored sperm. Sperm were then incubated at 37°C until assessment of sperm count and sperm morphology according to WHO criteria [292] by Dr. Agnieszka Paradowska-Dogan and colleagues, which followed shortly after excision. Briefly, 10 μl of the sperm solution were streaked onto an objective slide and left to air-dry. Sperm were then stained with Schorr solution for morphological evaluation. For this, slides with sperm were incubated in 100 % EtOH for 10 min., 70 % EtOH for 1 min., hematoxylin for 10 min. and 30 sec., H_2O for 3 min., 70 % EtOH for 10 sec., 95 % EtOH for 10 sec., Schorr solution for 1 min., 95 % EtOH for 10 sec. (twice), 100 % EtOH for 1 sec (three times), and xylol for 5 min. (twice). After Schorr staining 100 sperm per sample were evaluated on a cell counter (Assistent Counter AC-15, P+W Medizintechnik, Germany).

2.3 Cell culture

2.3.1 Primary mouse Sertoli cells

In order to isolate cells for the primary Sertoli cell culture at the Hudson Institute of Medical Research (Melbourne, Australia), C57Bl/6J (from Monash Animal Services) mice were killed at 21 days of age by CO_2 euthanasia, followed by cervical dislocation. Thereafter, the abdomen was opened and testes were excised, placed into DMEM-medium, and processed as follows.

Testes of 21 days old C57Bl/6J mice (n=10 animals per isolation) were decapsulated by tearing the tunica albuginea from the tubules using two forceps. Tubules were chopped finely with a scalpel blade and placed into a 50 ml centrifuge tube. For the first digestion step 5 ml collagenase/DNAse solution (1 mg/ ml collagenase) were added. Then the tube was sealed with Parafilm and the tissue was allowed to dissociate in a 34ºC water bath for 20 minutes, shaking at 60 cycles/ min. The tube was then filled to about 40 ml with Dulbecco's Modified Eagle's Medium (DMEM)/F12. The tubules were allowed to settle for 5 minutes and the supernatant (containing interstitial cells) was discarded. This washing step was repeated twice for a further two times. Thereafter, the tubules were resuspended in 5 ml Trypsin/DNAse solution. The tube was sealed with Parafilm and the tubules were allowed to dissociate in a 34ºC water bath for 20 minutes, shaking at 60 cycles/ min. During this step the tubules dissociated and the intra-tubular cells were set free. Subsequently, 5 ml SBTI/DNAse solution were added and the solution was incubated for 5 minutes at RT in order to let the cells settle down. The supernatant, containing peritubular cells, was collected into a 50 ml centrifuge tube. The cells were washed twice with DMEM/F12, every time allowing the cells to settle for 5 minutes and collecting the supernatant, containing peritubular cells.

After the second washing step, the pellet, containing the tubules, was resuspended in 5 ml hyaluronidase/DNAse solution. The tube was sealed with Parafilm and the tubules were allowed to dissociate in a 34ºC water bath for 15 minutes, shaking at 60 cycles/ min. Thereafter, the cells were resuspended gently within this solution using a 5 ml pipette. About 10 ml of DMEM/F12 were added to dilute the hyaluronidase, followed by centrifugation as described above. The supernatant was discarded and the pellet was resuspended in DMEM/F12. The cell suspension was then filtered through a 100 μm cell strainer to remove clumps. The filtered solution was diluted to 20-30 ml with DMEM/F12 and centrifuged as before. Thereafter, cells were resuspended in 1 ml DMEM + 0.1 % BSA. Following this step, Sertoli cells were counted within a Neubauer counting chamber, diluted 1:2 with trypan blue. Viable cells were counted in 5 squares and calculated as follows:

Cell count x 5 (5 squares counted in a total of 25) x 2 (dilution factor in trypan blue) x 10^4 = X cells/ ml

Following counting, Sertoli cells were resuspended to a concentration of $1x10^6$ cells/ ml in DMEM + 0.1 % BSA. 500 μl cell suspension ($0.5x10^6$ cells) were seeded in a 48-well chamber slide and incubated at 37°C with 5 % CO_2 for 48 h. The medium was aspirated and 300 μl of hypotonic Tris solution (20 mM) were added for 1.5 minutes to each well. This would destroy most of the germ cells, leaving mainly Sertoli cells within the well. The hypotonic solution was removed and the cells were washed with 300 μl DMEM and then incubated with 500 μl DMEM + 0.1 % BSA at 37°C with 5 % CO_2 for 24 h. Thereafter, cells were ready for experimental treatment. These studies were performed in accordance with the Australian National Health and Medical Research Council Guidelines on Ethics in Animal Experimentation and were approved by the Monash Medical Centre Animal Experimental Ethics Committee.

2.3.2 WL-3 cell line

WL-3 mouse Sertoli-cells were kindly provided by Dr. Lutz Konrad (Giessen, Germany) and were originally established by Mueller and Korach [172]. Cells were cultured in DMEM-F12 (Thermo Fisher Scientific Inc., MA, USA), supplemented with 10 % fetal bovine serum (FBS) (Thermo Fisher Scientific Inc.) and 1 % penicillin-streptomycin (PenStrep) (Thermo Fisher Scientific Inc.). The cells were grown in the suspensions at a temperature of 37 °C in 5 % CO_2. Before the experiments, cells were grown in a single tissue culture flask angled neck and vented cap. Medium was changed before the start of each experiment and it was not changed during the treatments. Cell viability was assayed with Trypan blue staining. Cell viability was always above 80 %. Exposure experiments were repeated in triplicates.

2.3.3 Dose response experiments

In order to determine suitable and effective concentrations for the individual treatments, dose response experiments on WL-3 and primary Sertoli cells were carried out in 48-well plates according to the scheme shown in (Fig. 2-2). All treatments were done in triplicates per experiment. Cells were seeded at a confluence of 1.5 x 10^5 cells/ ml in the culture medium and were allowed to attach overnight. For glucose and mannose dose responses cells were cultured in glucose free DMEM (Thermo Fisher Scientific Inc.) supplemented with 10 % FBS, 1 % PenStrep and 1 mM Sodium-pyruvate. A stock of 100 mM was used for further dilutions. DMEM-F12 medium

served as diluent for testosterone, insulin, and hr-FSH. A stock of 1 mg/ml, 5 mg/ml, and 5000 mIU/ml was used for testosterone, insulin, or FSH respectively. Supernatant was collected at 24 and 48 h for measurement of the activin A and inhibin levels.

Vial	A	B	C	D	E	F
Volume of diluent (ml)	25	37,5	42.5	45	47.25	50
Volume and source of Glc/ Man (ml)	25 of stock	12.5 of stock	7.5 of stock	5 of stock	2.75 of stock	0
Final Glc/ Man concentration (mM)	50	25	15	10	5.5	0
Volume of diluent (μl)	4495	3600	3375	3375	3375	3375
Volume and source of testosterone (μl)	5 of stock	900 of vial A	1125 of vial B	1125 of vial C	1125 of vial D	1125 of vial E
Final testosterone concentration (ng/ml)	1000	200	50	12.5	3.125	0.78
Volume of diluent (μl)	3992	3500	3500	3500	3500	4000
Volume and source of insulin (μl)	8 of stock	500 of vial A	500 of vial B	500 of vial C	500 of vial D	0
Final insulin concentration (ng/ml)	10000	1250	156.25	19.53	2.44	0
Volume of diluent (μl)	3600	3375	3375	3375	3375	3375
Volume and source of FSH (μl)	900 of stock	1125 of vial A	1125 of vial B	1125 of vial C	1125 of vial D	1125 of vial E
Final FSH concentration (IU/ml)	1000	250	62.5	15.6	3.9	0.98

Fig. 2-2. Pipette scheme for dose response treatment on Sertoli cells.

2.3.4 Measurement of transepithelial resistance (TER)

For the measurement of TER WL-3 Sertoli cells were plated at $0.25x10^6$ cells/cm^2 at 37°C in Matrigel (BD Biosciences, Bedford, MA)-coated Millicell PCF bicameral chambers (12-mm diameter, 0.4 μm pore size, 0.6 cm^2 surface area; Millipore, Bedford MA) in 24-well culture plates. Culture medium was DMEM/F12, supplemented with 10 % FBS and 1 % PenStrep, unless otherwise indicated. WL-3 cells were cultured overnight before addition of treatment media. The treatment media was glucose free DMEM, supplemented with 10 % FBS, 1 % PenStrep and 1 mM Sodium-pyruvate. Cells were then cultured at glucose concentrations of either 5 or 25 mM in the absence or presence of recombinant activin A (50 ng/ml; R&D Systems, Minneapolis MN). Treatments were added to both the basal and apical compartments. All treatments were done in triplicates per experiment. To assess inter-Sertoli cell TJ assembly, the TER across the Sertoli cell epithelium was quantified using a Millipore Millicell-electrical resistance system (Merck Millipore, Germany), with measurements taken daily at 37°C commencing from the day of treatment (d 0). For this, the cell culture plate was placed on a heat pad within the cell culture hood and the cells were allowed to adjust for 15 minutes before the first measurement. An electrode was placed into the chamber wells, measuring the resistance between the basal and apical compartments. Each well was measured three times and the electrode was washed in ethanol, 1X PBS, and glucose free medium between wells.

2.4 RT-PCR

Reverse transcription combined with the polymerase chain reaction (RT-PCR) was used to quantify gene expression in tissue and cell culture samples.

2.4.1 Principle

The method of real time PCR was first mentioned in 1993 by Higuchi et al. [113]. Starting from as little as one copy of a specific gene sequence, the PCR generates copies of a DNA template in an exponential manner. This reaction results in a quantitative relationship between the amount of starting target sequence and the amount of PCR product accumulated at any particular cycle. In order to quantify the resulting PCR products double-stranded (ds)DNA-intercalating agents (DNA-binding dyes) (i.e.

SYBR® Green 1) are used. These reagents are bound by dsDNA, which results in the fluorescence of the reagent. The intensity of the fluorescence signal is dependent on the quantity of the dsDNA in the reaction. At the end of each elongation step of each PCR cycle fluorescent measurements are performed to monitor the increasing amount of amplified DNA [19].

2.4.2 Protocol

RNA isolation

In order to purify total RNA from cultured cell and tissue, samples were processed using the RNeasy Mini kit from Qiagen (Qiagen, Hilden, Germany) according to the manufacturers instructions. For this purpose, cultured cells were harvested and disrupted using RLT-buffer with 1 % β-Mercaptoethanol. Snap-frozen tissue (one testis per animal) was homogenized in 1 ml RLT-buffer. The homogeniser was sterilized first with RO water and then with 70 % ethanol between each step. Homogenised tissue was then centrifuged at 13000 rpm for 10 minutes and the supernatant was transferred into a new centrifuge tube. This step was repeated (generally three times) until the supernatant appeared clear. 350 μl of the lysate (cells or tissue) were then mixed with 350 μl of 70 % ethanol in a 2 ml collection tube. 700 μl of the lysis solution were then transferred into an RNeasy spin column and centrifuged for 1 minute at 13000 rpm. Thereafter, the flow through was discarded and 500 μl of RW1 buffer were added into the column, followed by centrifugation as described above. Following this, the flow through was discarded again and 500 μl of RPE buffer were added into the column, followed by centrifugation as described above. Then, the flow through was discarded and the sample was washed by adding 500 μl of 80 % ethanol, followed by centrifugation as described above. Thereafter, the spin column was placed into a fresh 1.5 ml collection tube, 20 μl of RNase free water were added and samples were centrifuged for 2 minutes at 13000 rpm. The purified RNA remained now within the 1.5 ml collection tube and was stored at -80°C until further processing.

Finally, prior to translation into cDNA, the RNA yield was quantified using a NanoDrop spectrophotometer. Each sample was measured twice to yield a mean RNA amount.

Generation of cDNA

In order to generate first-strand cDNA for the use in real-time quantitative RT-PCR (qRT-PCR) 1 µg of total RNA was reversed transcribed in 20 µl reactions using the Superscript III VILO Kit (Invitrogen, Carlsbad, California, United States).

From the measured RNA yield the amount of sample needed for 1 µg RNA in a total volume of 8 µl was calculated as follows:

Amount of sample (1 µg RNA) = 1000/ mean RNA yield in ng/ µl

Amount of RNase free water (µl) = 8 - Amount of sample (1 µg RNA)

Sample and water were mixed in a 200 µl PCR reaction tube. Then 1 µl of DNAse I reaction buffer and 1 µl DNAse I amplification grade was added, followed by centrifugation for 8 seconds at 13000 rpm. The following steps were carried out on a VWR thermocycler. DNA digestions was carried out at 37°C for 15 minutes. Then, 1 µl of 25 mM EDTA was added to the sample, followed by centrifugation as described above. Samples were incubated for 25 minutes at 65°C. Finally, a master mix of 4 µl 5x First strand buffer + 2 µl 0.1 m DTT + 1 µl 10 mM dNTP mix + 1 µl 0.5 ng/ µl Oligo dTs + 1 µl Superscript III was added to the sample, followed by another centrifugation step. The reverse transcription was then carried out at 50°C for 50 minutes and 72°C for another 15 minutes.

PCR products were diluted 1:20 (20 µl CDNA + 380 µl RNase free water) in a 0.5 µl PCR reaction tube.

Primer verification

Primers were selected using Primer3 and BLAST [181], two programmes, that provide primers specific to the PCR template sequence, including primer pair specificity checking against a selected database. Desalted primers were diluted with RNase free H_2O to 10 times of the molecular weight, vortexed, and incubated for 10 minutes. Thereafter, equal volumes of the forward and the reverse primer were added into a fresh centrifuge tube to make up a 1:1 primer set dilution. For final use, a 1:10 dilution was made up of 40 µl 1:1 diluted primer set and 360 µl RNase free H_2O.

Primer efficiency was tested using the slope of a standard curve generated from a dilution series (1:5; 1:10; 1:15; 1:20) of 1 µg RNA template concentration from a C57Bl/6J testis sample of a 24 week old animal. The log of each concentration (-0,70; -

1,00; -1,18; -1,30) was then plotted against the Ct value for that concentration. From the resulting standard curve the slope was derived and used to calculate the primer efficiency[37] using the following equation:

$$\textbf{Efficiency (E\%)} = (10^{(-1/\text{slope})} - 1) * 100$$

The primer efficiency for each primer used in this work is shown in Table 2-1.

Table 2-1. Primer sequences.

Gene	Forward primer (5'-3')	Reverse primer (5'-3')	E%
β-Actin	CCTAGGCACCAGGGTGTGAT	GCTCGAAGTCTAGAGCAACA	77.5
ppiA	GCAAGCATGTGGTCTTTGGG	TTGATGGGTAAAATGCCCGC	64.2
Inhba	GGAGAACGGGTATGTGGAGA	TGGTCCTGGTTCTGTTAGCC	84.1
Inhbb	CTGCCAGTGTTTCAGGGTATAA	CCTTCACTCCACCAGTCATTT	35.9
Inha	CTCCTTTCCTGGTAGCCCAC	CCAAAAACAGGGGCTGAACC	66.8
FST (total)	CCACTTGTGTGGTGGATCAG	AGCTTCCTTCATGGCACACT	82.1
FST 288	CTCTCTCTGCGATGAGCTGTGT	GGCTCAGGTTTTACAGGCAGAT	72.0
FST 315	CTCTCTCTGCGATGAGCTGTGT	TCTTCCTCCTCCTCCTCTTCCT	69.1
Acvr1b	CCAACTGGTGGCAGAGTTAT	CTGGGACAGAGTCTTCTTGATG	73.3
Acvr2a	GGGACGCATTTCTGAGGATA	TCCTGGAGGCATCCTACTCA	75.5
Acvr2b	CGACTTTGTGGCTGTGAAGA	TCGTTCCACGTGATGATGTT	47.2
TNF-α	CATCTTCTCAAAATTCGAGTGACAA	TGGGAGTAGACAAGGTACAACCC	58.9
SOX-9	CGGAGGAAGTCGGTGAAGA	GTCGGTTTTGGGAGTGGTG	87.4
IL-1 β	CAACCAACAAGTGATATTCTCCATG	GATCCACACTCTCCAGCTGCA	90.7
IL-1α	TTCTGCCATTGACCATCT	AATCTTCCCGTTGCTTGA	58.3
IL-10	GCTCTTACTGACTGGCATGAG	CGCAGCTCTAGGAGCATGTG	83.8
FSH-R	AAACAGGAGCAGGCTGTGAT	TCTTGGTGTCGCTTGATGAG	-
Vimentin	CAGCAGTATGAAAGCGTGG	GGAAGAAAAGGTTGGCAGAG	-
Occludin	CCAGGTGAGCACCTTGGGAT	TTCAAAAGGCCTCACGGACA	-
N-cadherin	GGAATCCCGCCTATGAGTGG	CGTCTAGCCGTCTGATTCCC	-
Claudin-11	CTACGTGCAGGCTTGTAGAGC	GGCACATACAGGAAACCAGATG	-
GATA-4	CACCCCAATCTCGATAT	GCACAGGTAGTGTCCCGTC	-
ZO-1	GGAGCTACGCTTGCCACACT	GGTCAATCAGGACAGAAACACAG	-
AMH	ACCCTTCAACCAAGCAGAGA	CCTCAGGCTCCAGGGACA	-
AR	GCTCAAGGATGGAGGTGCAGT	TAGTCTCCTGCCTCTGCTGTA	-

qRT-PCR

Total RNA was extracted after sampling using the RNeasy Mini Kit from Qiagen according to the manufacturer's instructions. RNA yield was quantified using a NanoDrop spectrophotometer (NanoDrop products, DE, USA). Total RNA (1 μg) was reversed transcribed in 20 μl reactions using the Superscript III VILO Kit (Invitrogen). Real-time PCR amplifications were performed using the IQ SYBR Green Supermix (Bio-Rad Laboratories GmbH, Munich, Germany) on the StepOne Plus real-time polymerase chain reaction system (Applied Biosystems, Waltham, MA, USA). Each well contained 5 μl SYBR Green, 3.2 μl RNase free H_2O, 0.3 μl primer (set of forward and reverse) and 1.5 μl cDNA template. Cycling conditions were 95 °C for 10 min followed by 40 cycles at 95 °C for 15 sec, 60 °C for 30 sec and 72 °C for 30 sec. After amplification, a melting curve analysis was performed to analyse the specificity of the products using the following conditions: 95 °C for 30 sec, 60 °C for 30 sec followed by 80 cycles at 60 °C for 10 sec. The expression of each of the genes was measured in triplicate for each animal tissue and cell culture sample. PCR signal of the target transcript was normalized to the geometric mean of two reference genes. In order to find the most suitable reference gene for the analysis, a housekeeping gene panel (Mouse housekeeping gene primer set; McLab; Cat#: mHKG-120, MCLAB, USA) was run on the testis samples. Evaluation of the panel suggested *β-Actin* and *peptidylprolyl isomerase A* (*ppiA*) as the most suitable genes. Thus, both reference genes were used within the study with beta-actin giving Ct values of 20.59 ± 1.40 and ppiA giving Ct values of 17.56 ± 1.25. In order to reduce the standard deviation of the primers even further, the mean of both primers was used with a Ct of 19.02 ± 0.87. PCR signal of the target transcript was normalized to the geometric mean of two reference genes and expression levels were assessed through relative quantification using the $2^{-\Delta\Delta Ct}$ method [37]. For this the gene expression data was organised in an excel file as shown in Table 2-2. Briefly, Ct values for *β-Actin* and *ppiA* were assessed for each sample in triplicates and the geometric mean was calculated. Thereafter, Ct values for each target gene were assessed for each sample in triplicates and the mean was calculated. The ΔCt value was calculated by subtracting the mean Ct value of the reference genes from the mean Ct value of the target gene from each sample. For the wild type control samples a mean ΔCt value was generated for each age group to allow the assessment of the fold-change in gene expression relative to wild type control transcripts. The ΔΔCt for each sample was calculated by subtracting the mean ΔCt wild type control value from the ΔCt value

of that sample. The fold change in gene expression levels was then calculated as $2^{-\Delta\Delta Ct}$. In order to normalise the data, the mean fold change was calculated for wild type control samples of each age group and the fold change of each samples was then divided by that value.

Table 2-2. Organisation of gene expression data in Excel for $2^{-\Delta\Delta Ct}$ calculation and example calculation.

Age	Sample no.	Mouse strain	Mouse number	Ct β-Actin	Ct mean β-Actin	Ct ppiA
12 weeks	1	C56Bl/6J	6	20.88/ 20.03/ 21.13	20.68	17.01/ 16.48/ 16.86
Ct mean ppiA	pooled Ct of β-Actin and ppiA	Ct target gene	Ct mean target gene	ΔCt to mean HKG	mean ΔCt wild type control	ΔΔCt
16.78	18.73	32.27/ 31.55/ 31.40	31.74	13.01	11.82	1.19
$2^{-\Delta\Delta Ct}$ (fold change) - mean HKG	mean fold change	Normalised fold change	mean normalised fold change	SD normalised fold change	Grubbs G value	
1.41	6.02	0.23	1.00	1.41	0.54	

After assessment of the $2^{-\Delta\Delta Ct}$ value, normalised data were analysed for normality distribution using the Shapiro-Wilk normality test (see section 2.7). When normal distribution was confirmed, data was corrected for outliers using the Grubb's test. For this, the mean and the standard deviation (SD) of the normalised fold change were calculated for each group and the respective Grubb's value was calculated with the following equation:

Grubb's value = (mean normalised fold change of the respective group - normalised fold change of the sample)/ SD of the normalised fold change of the respective group

Outliers were then identified according to the number of animals in the respective group. Data are expressed as the fold-change in gene expression relative to wild type control transcripts.

2.5 Histology and Immunohistochemistry

2.5.1 Fixation, sectioning, and staining of organs

Whole-mouse testes were fixed in Bouin's fluid for 8 h (C57Bl/6J wild type controls) or, after optimization according to Fig 11, 24 h (*Ins*2$^{Akita+/-}$). The separated epididymides were fixed for 4 h in 3.7 % paraformaldehyde. Tissues were dehydrated in a graded series of ethanol as follows: 80 % EtOH for 30 min., 96 % EtOH for 45 min., 99.6 % EtOH for 45 min., EBE I for 60 min., EBE II for 60 min., EBE III for 30 min., and EBE IV for 30 min. Thereafter tissues were kept in paraffin (46°C – 48°C) overnight at 50°C, followed by 2 h at 46°C the next day before they were embedded in paraffin. 5 µm thick sections were processed for Harris' hematoxylin or antibody staining.

Prior to antibody staining sections were de-paraffinised and rehydrated as follows: 5 min. Rotihistol I, 5 min. Rotihistol II, 2x3 min. 99.6 % EtOH, 2x3 min. 96 % EtOH, 2x3 min. 70 % EtOH, 3 min. RO water.

Thereafter antigen retrieval was carried out using citrate buffer. Localization of the Sertoli cell marker protein SRY-Box-9 (SOX-9) was performed using a polyclonal ChIP Grade antibody (diluted 1:300, ab3697, Abcam, Cambridge, U.K.). goat-anti-rabbit IgG was used as secondary antibody (diluted 1:500, Vector Laboratories, CA, USA). The sections were counterstained with Harris' haematoxylin and mounted under DPX. To localize the β A-subunit of activin (mouse monoclonal antibody (E4), diluted 1:100, supplied by Oxford Brookes University, Oxford, U.K.) [138], sections were de-paraffinised and rehydrated as described above prior to antigen retrieval using the mouse-on-mouse-HRP-polymer-bundle kit according to the manufacturers instructions (ZYTOMED Systems GmbH, Berlin, Germany). The sections were counterstained with Harris' haematoxylin and mounted under DPX (BDH Laboratory Supply, Poole, U.K.). Cell death was analysed using the TUNEL (TdT-mediated dUTP-biotin nick end labelling) assay (Millipore, Merck KGaA, Darmstadt, Germany) on paraffin-embedded testis sections according to the manufacturers instructions. Specific signal was visualized by treatment with sheep peroxidase-conjugated anti-digoxigenin antibodies (Vectastain® Elite ABC Kit, Vector Laboratories, CA, USA) followed by diaminobenzidine (DAB) development. Both the evaluation of the staining and the

measurement of seminiferous tubule diameter were done using ImageJ software (open source image processing program) [233]. For the determination of the seminiferous tubule diameter all tubules within one testicular cross-section were selected for the analysis.

Fixative / Time	5h	8 h (capsule cut after 1 h)	24 h (capsule broached after excision)
Bouin's Fixative	• Weak fixation • Loose structure of the tubules • Many spaces within the tubules	• Fixation gets weaker towards the center of the tubule • Very good fixation in the layers close to the tunica albuginea (layers 1-3/4) • Clear dertermination of spermatogenesis only in well fixed tubules possible	• Very good fixation • Compact tissue throughout the whole tubule • Clear determination of spermatogenesis is possible
3.7 % paraformaldehyde	-	-	• Weak fixation • Loose structure of the tubules • Many spaces within the tubules

Fig. 2-3. Fixation optimization for *Ins2*$^{Akita+/-}$ testis.

Using hematoxylin stained testicular sections, the state of spermatogenesis in the seminiferous tubules was evaluated by the spermatogenesis index (SI) using the Johnsen's score [127], adapted for the mouse testis [140]. For this, serial light microscopic pictures from each testis sample were taken at a 10x magnification. Using ImageJ a stationary grid with 11x9 squares was applied to each picture and a fixed area of 5x5 squares was marked in which tubules were counted (Fig. 2-4). A Score from 1 to 10 was given to each tubule cross-section according to the cell types present. Score 1: No cells present in tubule cross-section; Score 2: Sertoli cells only; Score 3: Sertoli cells and spermatogonia only; Score 4: Sertoli cells, spermatogonia, few spermatocytes and no spermatozoa or spermatids; Score 5: Only spermatids and spermatozoa absent; Score 6: Only spermatozoa absent, but few spermatids; Score 7: Only spermatozoa absent, with numerous spermatids; Score 8: Reduced spermatozoa only; Score 9: Numerous spermatozoa present in lumen, but seminiferous epithelium disorganized; Score 10: Complete spermatogenesis with numerous spermatozoa.

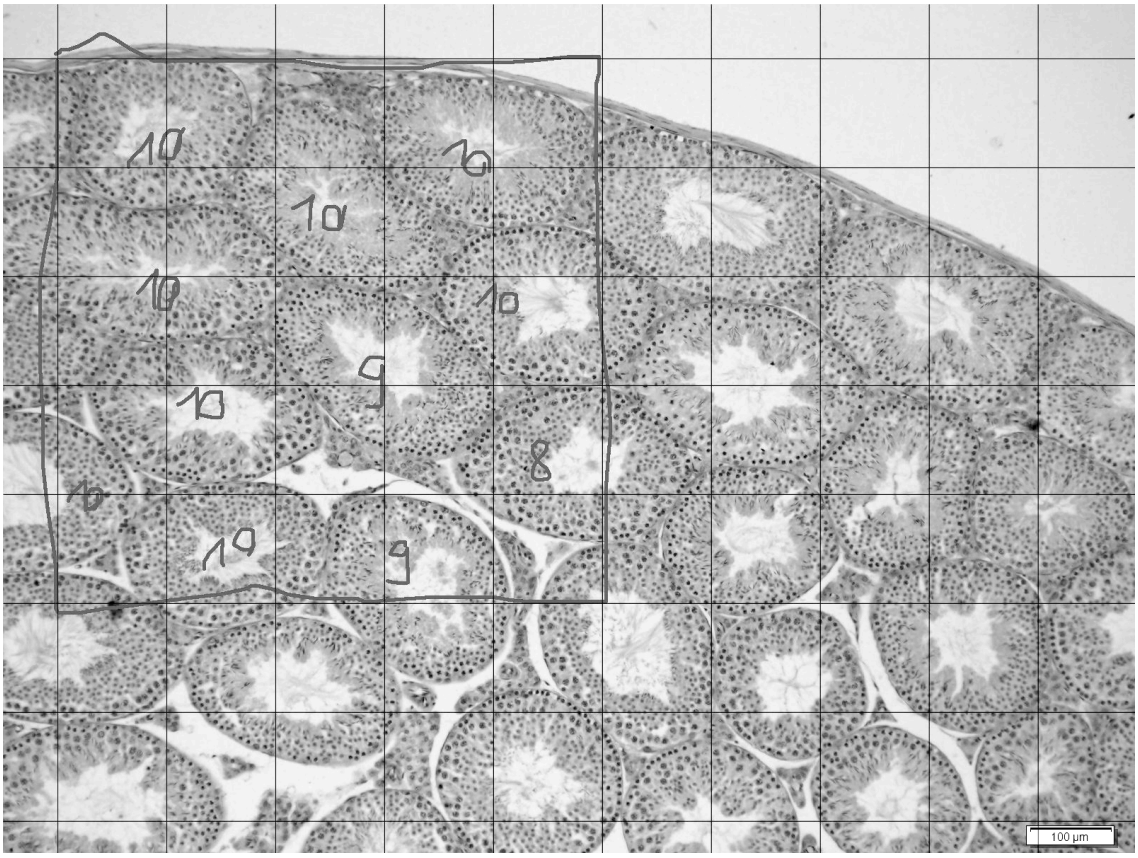

Fig. 2-4. Assessment of the Johnsen score in mouse testicular tissue sections using ImageJ.

Example picture for the assessment of the Johnsen score in mouse testicular tissue sections. An area of 5x5 squares was evaluated per picture. Scale = 100 μm.

2.6 Protein methods

2.6.1 Lysis of tissue and cells and protein concentration determination

Tissues (testes or epididymis) were excised and kept at 4°C (if homogenized immediately) or frozen in liquid nitrogen and stored at -80°C until needed. All steps of the tissue lysis were conducted on ice. For this purpose an Eppendorf tube was weighed and zeroed. Then the tissue was added into the Eppendorf tube and weighed and tissue weight was recorded. Thereafter a Protease Inhibitor Cocktail (Sigma, P8340) was mixed with cold PBS (0.01 M, pH 7.4) at a dilution of 1:200 and was then added at a volume 10 times the wet weight of the tissue onto the tissue contained in an Eppendorf tube. The tissue was then homogenized at low speed for about 20 seconds (B. Braun

Potter S, Sartorius, Germany). After each sample the probe was washed with 70 % EtOH and then PBS. The homogenised tissue was then centrifuged at 13000 rpm at 4°C for 10 minutes and the supernatant was frozen at -20°C until measurement.

From the cell culture samples, the treatment medium was collected into 1.5 ml Eppendorf tubes and kept frozen at -20°C until measurement. Adherent cells were washed with PBS and then lysed using RIPA buffer + Protease/Phosphatase Inhibitor (dilution 50:1) (Cat# 539134, Calbiochem, Merck, Germany) per well for 5 minutes. The lysate was then transferred into a 1.5 ml Eppendorf tube and centrifuged at 13000 rpm for 30 min at 4°C. The remaining supernatant was collected into a fresh 1.5 ml Epi and stored at -80°C until analysis.

The Pierce™ BCA protein assay kit (#23225, Pierce Biotechnology, IL, USA) was used to measure total protein concentrations according to the manufacturer's instructions for the microplate procedure. Briefly, diluted bovine serum albumin (BSA) standards were prepared according to the scheme shown in Table 2-3. The working reagent (WR) was prepared by mixing 50 parts of BCA Reagent A with 1 part of BCA Reagent B (50:1, Reagent A:B). Thereafter 25 μl of each standard or unknown sample were pipetted in duplicate into a well of a 96-Well plate (Thermo Fisher Scientific Inc.). 200 μl of the WR were added to each well and the plate was mixed thoroughly on a plate shaker (Ratek Instruments, Australia) for 30 seconds. Thereafter, the plate was covered and incubated at 37°C for 30 minutes. Finally, the plate was allowed to cool to RT prior to measurement of the absorbance at or near 562 nm on a plate reader (Benchmark microplate reader, Bio-Rad Laboratories).

Table 2-3. Preparation of diluted albumin (BSA) standards.

Vial	Volume of diluent (MilliQ) (μl)	Volume and Source of BSA (μl)	Final BSA Concentration (μg/mL)
A	0	300 of stock	2000
B	125	375 of stock	1500
C	325	325 of stock	1000
D	175	175 of vial B dilution	750
E	325	325 of vial C dilution	500
F	325	325 of vial E dilution	250
G	325	325 of vial F dilution	125
H	400	100 of vial G dilution	25
I	400	0	0 = Blank

2.6.2 Milliplex MAP Kit assay

The MILLIPLEX MAP Human TGFβ Signaling Magnetic Bead Panel 6-plex (Cat# 48-614MAG, Merck Millipore), was used in order to detect changes in phosphorylated Smad2 (Ser465/Ser467), phosphorylated Smad3 (Ser423/Ser425), ERK (Thr185/Tyr187), and Akt (Ser473), as well as total protein levels of TGFbRII and Smad4 in tissue lysates using the Luminex® system (Luminex Corporation, TX, USA).

Principle

The MILLIPLEX MAP method is based on the Luminex® xMAP® technology, which uses colour coded magnetic beads that are coated with specific detection antibodies. Hence, analytes within test samples are captured by the bead. Thereafter, a biotinylated detection antibody is introduced and incubated with a Streptavidin-PE conjugate, in order to complete the reaction on the surface of each microsphere. When the microspheres are illuminated, the internal dyes fluoresce. A second illumination source then excites the Streptavidin-PE conjugate. Finally, high-speed digital-signal processors identify each individual microsphere and quantify the result of the bioassay based on fluorescent reporter signals.

Protocol

In order to start the Milliplex procedure, the reagents for the immunoassay were prepared. Firstly, the TGFβ Signaling magnetic beads (20X) stock solution was sonicated for 15 seconds and vortexed for 30 seconds. Beads were diluted to 1X by combining 0.150 mL beads with 2.85 mL of MILLIPLEX MAP Assay Buffer 2 using one of the Mixing Bottles provided. The captured 1X beads were vortexed for 15 seconds.

Secondly, the Biotin-Labelled Detection Antibody and Streptavidin-PE were prepared. For this, the 20X Detection Antibody stock was vortexed for 10 seconds, and briefly centrifuged thereafter. The Detection Antibody was then diluted to 1X by combining 0.150 mL of Detection Antibody with 2.85 mL of MILLIPLEX MAP Assay Buffer 2 using one of the Mixing Bottles provided. The MILLIPLEX MAP Streptavidin-Phycoerythrin (SAPE) 1:25 was vortexed for 10 seconds, before diluting it by combining 0.120 mL of Streptavidin-Phycoerythrin with 2.88 mL of MILLIPLEX MAP Cell Signaling Assay Buffer 2 using one of the Mixing Bottles provided.

Lastly the lyophilized MILLIPLEX MAP Cell Lysates (Catalogue # 47-229, 47-235, 47-216) were prepared, by reconstituting each of the lyophilized cell lysates in 100 µl of ultrapure water. This yielded 100 µl of lysate at a total protein concentration of 2 mg/mL for each vial. Then the lysates were vortexed and incubated for 5 min at RT (stored on ice). Thereafter, 150 µl of MILLIPLEX MAP Assay Buffer 2 were pipetted to each cell lysate vial and vortexed again.

After the preparation of the reagents for the immunoassay, the assay was started following the manufacturers instructions for the 96-well Plate and Hand-held Magnetic Separation Block. Hence, 10 μg of Protein from each sample were diluted in MILLIPLEX MAP Assay Buffer to make up a total volume of 25 μl. Then, 50 µl of Assay Buffer were added into each well of the plate. The plate was covered and mixed on a plate shaker for 10 minutes at RT (20-25°C). The Assay buffer was decanted and residual liquid was removed by inverting the plate and tapping it smartly onto absorbent towels several times. Then the 1X bead suspension was vortexed for 10 seconds before 25 μl were added to each well. Then 25 µl of Assay Buffer, reconstituted control cell lysates, and sample lysates were added to appropriate wells and incubate overnight at 2-8°C on a plate shaker (600-800 rpm) protected from light. On the following day the plate was shaken for 10 min (RT) (20-25°C) before it was attached to the handheld magnetic separation block to plate, allowing 60 seconds for beads to settle, and the samples and controls were then decanted. Thereafter, the plate was removed from the magnetic separation block and washed with 100 µl Assay Buffer per well. The washing buffer was decanted as described above. This was repeated for a total of two washes. Then, 25 µl/well of 1X MILLIPLEX MAP Detection Antibody were added, the plate was sealed, covered with the lid and incubated with agitation on a plate shaker for 1 hour at RT. Thereafter, the Detection Antibody was decanted as described above. For the detection 25 µl of 1X MILLIPLEX MAP SAPE were added to each well, the plate was sealed, covered with the lid and incubated with agitation on a plate shaker for 15 minutes at RT. Then 25 µl of MILLIPLEX MAP Amplification Buffer were added to each well and incubated for another 15 minutes as described before. Lastly, SAPE /Amplification buffer was decanted as described before and the beads were suspended in 150 µl of MILLIPLEX MAP Assay Buffer, and mixed on plate shaker for 5 minutes before analysis using the Luminex® system.

2.6.3 Radioimmunoassay (RIA)

Method background

Solomon Berson and Rosalyn Yalow from the Veterans Administration Hospital in New York first described RIA, or Radioimmunoassay, in 1960 for the measurement of endogenous plasma insulin. This method is a very sensitive technique, which uses radioactive labelled proteins and specific antibodies in order to detect antigens [47,149].

Test principle

In order to detect proteins by RIA either a competitive or a solid phase RIA can be used. Within the competitive RIA (i.e. FST, LH, FSH or Inhibin) a constant concentration of ^{125}I-Antigen (highly purified Inhibin, FST, LH, or FSH) and varying concentrations of unlabelled standard antigen or sample antigen compete for binding specifically to the antiserum. Here, immunocomplexes are precipitated after adding a secondary polyclonal antiserum followed by centrifugation. Unbound reagents are removed and the pellet is counted in a gamma counter. Within the solid phase RIA (i.e. testosterone), the specific antibody is adherent to the wall of the tube in which the assay is performed. The labelled tracer and the unlabelled antigen are added and compete for specific binding to the antiserum. The unbound fraction is pipetted off and the tubes are counted in the gamma counter. For both methods the standard curves are S-shaped (B/Bo plot) and are mathematically linearized by using a Log-Logit transformation, with LOGIT=Log(% Bound) / 100 - % Bound [47].

Protocol

To measure the concentrations of **testosterone** all samples were assayed in duplicates within a single assay using a direct testosterone RIA kit, following the manufacturer's instructions (RIA testosterone direct, Ref#IM1119, Beckman-Coulter, Inc., CA, USA). The lower limit of detection was 0.05 ng/ mL and the intra-assay variation was 8.5 %.

LH in serum was determined by a double-antibody radioimmunoassay using rLH-I-8 (AFP- 12066B) labelled with ^{125}I using the IODOGEN method for iodination. The hormone concentration was calculated using the mouse LH reference preparation (AFP-5306A) as the standard. Briefly, standards were prepared from mouse LH (AFP-5306A) (0.20 – 12.5 ng/ml) by preparing serial dilutions from a 25 ng/ ml stock

solution. Quality controls were rat LH RP-2 (QC1; dilutions 1:10, 1:20, 1:40, 1:80 prepared from a 30 ng/ ml stock solution), Hypox (QC2), mouse (QC3), female rat (QC4), rat 2015 (QC5), Wistar rat (QC6), Wistar rat + spike (QC7). 40 μl of standards, quality controls, and samples were added into tubes respective tubes in duplicates, followed by the addition of 40 μl assay buffer (0.01 M PBS (pH 7.4) + 0.5 % BSA) to all tubes (except total counts). Then, 40 μl of normal rabbit sera (Cat# 16120099, Thermo Fisher Scientific) were added to non-specific binding samples and blanks, while antisera (AFP-240580; 1:187.500 in 1:800 normal rabbit sera) was added to all remaining samples (except for total counts). The assay was incubated overnight at RT. The following day, 40 μl of tracer (9000 cpm/ 40μl) was added to all tubes and incubated overnight at RT. The next day, 40 μl of secondary antibody (goat anti rabbit IgG (GAR), GAR#12, MIMR, Monash University, diluted 1:40) were added to all samples (except for total counts). Then, 40 μl of serum from an hypophysectomised sheep (serum ovine hypox sera, Monash University, Australia) were added to standards and blanks, while 40 μl of assay buffer were added to neat samples. The assay was incubated overnight at 4°C. Lastly, 1.5 ml of saline were added to all tubes (except for total counts) before centrifugation at 2500 rpm for 30 minutes at 4°C. Before counting on a gamma counter (GENESYS LTI, Laboratory Technologies, USA) tubes were tipped and drained for approximately 5 minutes. The lower limit of detection was 0.092 ng⁄mL and the intra-assay variation was 7.6 %.

FST concentrations in mouse tissue homogenates were measured using a discontinuous RIA, as described previously [188], which detects "total" follistatin using a dissociating reagent that dissociates the activin–follistatin complex. The reagent has a working concentration of 20 % Tween-20 (Sigma), 10 % sodium deoxycholate (Pierce, Rockford, IL, USA), 0.4 % Sodium Dodecyl Sulphate (SDS Ultrapure Applichem), and 0.1 % sodium azide (BDH, Poole, Dorset, UK) prepared in Milli-Q water (TDS reagent). The antiserum (#204) was raised in rabbits against purified 35 kDa bovine follistatin. Human recombinant (hr) FS288 (AF Parlow NHPP Torrance, CA, USA) was used as Standard and Tracer, iodinated using Iodogen reagent (Pierce, Rockford, IL, USA). Immune complex precipitation was achieved using GAR.

The assay buffer was 0.01 M PBS containing 0.5 % BSA (Sigma A7906) and the samples were diluted appropriately in this buffer. Standard, Quality Controls and Samples were incubated with TDS reagent and the Antiserum (#204 1:8000 diluted in assay buffer with 1:1000 normal rabbit serum (NRS) (GIBCO) overnight at RT. Sample

and Buffer Blanks had no antisera added - only 1/1000 NRS. On day 2, the tracer was added at 10 000 cpm/50 μl in assay buffer and the assay incubated again overnight at RT. On day 3, 50 μl of second antibody GAR in assay buffer containing 0.05 M EDTA (BDH) was added. The assay was incubated for 3 hours at RT then 1.5 ml cold 0.9 % saline was added and the tubes were centrifuged in a Beckman Coulter JM19 at 2500 rpm for 35 minutes at 4ºC. The supernatant was decanted and the pellets counted on a Cobra 5005 gamma counter (Packard Instrument Co., Meriden, CT). A pool of mouse testis homogenate diluted in a dose-dependent manner was run parallel to the standard curve (data not shown). The Intra-assay %CV was 9.5 % and the Inter Assay CV% was 9.2 % (n=2) and the range of detection was <1.40 ng/ml (Effective dose (ED) 90) and >76 ng/ml (ED10).

Inhibin α-subunit-containing proteins were measured using a heterologous equilibrium RIA, as described previously [218], using a hr-inhibin standard and iodinated hr-inhibin as the tracer. The antiserum was raised in rabbits against bovine 31-kDa inhibin (#1989) directed to the inhibin alpha subunit and detects both dimeric inhibin A and inhibin B as well as free inhibin alpha subunit. GAR was used as second antibody. Gelding Sera was added back to the assay after the 2nd antibody. Samples and standards and QC's were diluted with assay buffer (0.5 % BSA-PBS). Male and Female Mouse Sera and various tissue homogenates have shown parallelism in this assay – assessed by comparison of slope values, and the recovery of spiked mouse samples was acceptable. Testicular Extracts and sera from inhibin knockout mice were measured and found to have no inhibin present using this assay.

Briefly, standards were prepared from human inhibin standard (0.3125 – 10 ng/ml) by preparing serial dilutions from a 10 ng/ ml stock solution. Quality controls were bovine follicular fluid (450IC), rat ovarian extract, RP – human male sera (low inhibin), mouse sera (medium – high inhibin), mouse testis homogenate pool.

Samples were assayed in 50 μl duplicates at a 1:2 dilution plus 50 μl antibody and processed by adding all solutions, except the 2nd Antibody, to the tube, followed by an overnight incubation. Then 2nd Ab/sera and 6 % PEG (polyethylene glycol) were added and left for a couple of hours, before centrifugation and counting. The average Intra Assay CV was 6 % (n=1). The lowest limit of detection was 0.25 ng/ml (ED90) and the limit of reading 20.61 ng/ml (ED10) read against a Human Inhibin Standard.

The RIA dose-response curves were linearized by logit log-dose transformation and analysed by parallel line statistics [50]. The sensitivity of the RIA's was based on the mean ED10 value of the standard curve.

2.6.4 Enzyme-linked immunoabsorbent assay (ELISA)

Method background

Based on the RIA method Peter Perlman and Eva Engvall conceptualized the ELISA, or Enzyme-linked immunoabsorbent assay, at Stockholm University in Sweden. This method differs from RIA by using enzyme rather than radioactive reporter labels and was first published in 1971, demonstrating a quantitative measurement of IgG in rabbit serum with alkaline phosphatase as reporter label [149].

Test principle

The ELISA method uses the quantitative sandwich-immunoassay technique. Therefore, a 96-well plate is coated with an immobilised, monoclonal antibody against the desired protein. A respective protein standard as well as the samples are pipetted in duplicates onto the plate. Hence, the protein contained in the standard or sample will bind to the immobilised, monoclonal antibody. Remaining unbound components are being removed by repeated washing steps. Within the next step, a substrate labelled detection antibody against the desired protein is pipetted into each well. After further washing to remove unbound antibody reagents the substrate is added and colour develops according to the protein content in the standard or sample. Finally, the colour development will be stopped and the optical density is measured using a photometric ELISA reader. The standard curve allows calculating the concentration of the samples assayed. Evaluation and calculation of the protein concentration from the ELISAs was done using the Genesis software (GENESYS LTI Laboratory Technologies).

Protocol

Activin A was measured using a specific ELISA [138] according to the manufacturer's instructions (Oxford Bio-Innovations, Oxfordshire, U.K.) with some modifications as described previously [188]. This assay measures total activin A. The coating antibody E4 (1.3 mg/ ml) was diluted in carbonate buffer (pH 9.6) for a total concentration of 650 ng/ 100 μl. A volume of 100 μl was added onto a 96-well plate

and incubated overnight at RT in a humidified box. The following day, the plate was washed with PBS and 0.05 % Tween 20 (Sigma-Aldrich) using an automated plate washer (Wellwash 4 Mk 2, Thermo Electron Corporation, Finland) and 300 µl blocking buffer (1 % BSA-Tris HCl) were added to each well and incubated for 1 hour. The recombinant activin A standard (1 ng/ 25 µl) [217] was diluted in 5 % BSA-PBS for tissue samples or in media blank for cell culture samples according to the scheme shown in Table 2-4.

Table 2-4. Preparation of recombinant activin A standards.

Vial	Volume of diluent (µl)	Volume and Source of activin A (µl)	Final activin A Concentration (pg/mL)
A	475	25 stock (1 ng)	2000
B	200	100 of vial A	666,67
C	200	100 of vial B	222,2
D	200	100 of vial C	74,074
E	200	100 of vial D	24,691
F	200	100 of vial E	8,230
G	300	0	0 = Blank

Tissue samples were diluted in 5 % BSA-PBS and media samples were assayed neat. 125 µl sample or tissue were pipetted into a glass tube and a 6 % SDS solution in 0.05 M PBS was added (3 % final concentration) followed by boiling for 3 minutes. The samples were allowed to cool before the addition of 20 µl 30 % H_2O_2 (2 % final concentration, Emsure Iso Hydrogen Peroxidase 30%, Merck KGaA, Germany) and subsequent 30 min incubation. The E4 (anti-βA-subunit) monoclonal antibody-coated plate was washed and plated with 25 µl of 20 % BSA-Tris Triton buffer prior to the addition of 100 µl standard or sample in duplicates. Thereafter, the plate was incubated with shaking (Ratek Instruments, Australia) for 1 hour at RT, before the addition of 25 µl detection antibody (E4-Biotin B in 5 % BSA-Tris Triton, 1:600) and incubation overnight at RT in a humid box. The next day, the plates were washed and 100 µl of poly HRP Streptavidin conjugated to Poly-Horseradish Peroxidase (HRP) (#M2051, Sanquin, Netherlands) was added to the wells and incubated at RT for 1 h. The poly HRP is made up in a 1 % Casein Colloid Buffer solution (#M2052, Sanquin) supplied with a 5 % solution (diluted 1/5 with PBS). After further washes, 100 µl of tetramethylbenzidine (TMB, Thermo Fisher Scientific Inc.) peroxidase substrate

solution (Invitrogen) was added to all wells and incubated shaking for 15–25 min at RT. Finally, 50 µl of 0.3 M HCL was added to stop the colour development and the absorbance values of each well were measured using an automated microplate reader (Benchmark microplate reader, Bio-Rad Laboratories, Hercules, CA, USA) with compatible software (Microplate Manager 5.2, Bio-Rad Laboratories), using a measurement wavelength of 450 nm and a reference wavelength of 620 nm. The limit of detection was 14.1 pg/mL and the average intra-assay CV was 4.0 %.

Activin B was measured using a specific ELISA [157] according to the manufacturer's instructions (Oxford Bio-Innovations) with some modifications and used a human recombinant Activin B standard. The coating antibody 46A/F (3.9 mg/ ml in PCS + azide) was diluted in carbonate buffer (pH 9.6) for a total concentration of 25 µg/ 10 ml. A volume of 100 µl was added onto a 96-well plate and incubated overnight at RT in a humid box. The following day, the plate was washed using an automated plate washer (Wellwash 4 Mk 2, Thermo Electron Corporation, Finland) and 300 µl blocking buffer (1 % BSA-PBS + 6 % sucrose) were added to each well and incubated for 1 hour. The recombinant human activin B standard (1.25 ng/ 25 µl) [157] was diluted in 5 % BSA-PBS for tissue samples or in media blank for cell culture samples according to the scheme shown in Table 2-5.

Table 2-5. Preparation of recombinant activin B standards.

Vial	Volume of diluent (µl)	Volume and Source of activin B (µl)	Final activin B Concentration (pg/mL)
A	475	25 stock (1,25 ng)	2500
B	200	100 of vial A	833,3
C	200	100 of vial B	277,8
D	200	100 of vial C	92,59
E	200	100 of vial D	30,86
F	200	100 of vial E	10,288
G	300	0	0 = Blank

For optimal recovery, tissue and media samples were diluted in PBS containing 5 % BSA at a dilution of 1 in 2. All diluted fluids and standards (150 µl) were mixed 1:1 with 150 µl 6 % SDS in water. Samples and standards were boiled for 3 min, and cooled for 10 min before 50 µl Triton assay diluent (TAD, Pierce, Rockford, IL, USA) made up in 500 ml 25 mm Tris, 0.15 m NaCl, pH 7.2, including 10 % BSA, 5 % Triton X-100 and 0.1 % sodium azide was added to samples and standard tubes. 50 µl of

freshly diluted biotinylated detection antibody 46A/F in TAD (1:800 to a final concentration of 0.5 μg/ml) was added to each well. Thereafter, 100 μl sample or standard was added to each well in duplicate, and the plate was incubated at RT for 1.5 h. The wells were washed with PBS and 0,05% Tween 20. Then 100 μl/well of freshly diluted streptavidin poly horseradish peroxidase (HRP, Mast Group Ltd, Bootle, Merseyside, UK) at 0.25 μg/ml in 1 % casein (1:4000) (Mast Group Ltd) was added for 1 h at RT. Wells were then washed with PBS and 0.05 % Tween 20. 100 μl of tetramethylbenzidine (TMB, Thermo Fisher Scientific Inc.) peroxidase substrate solution (Invitrogen) was added for 15–25 min at RT. The reaction was stopped by adding 100 μl/well of 0.3 M phosphoric acid. The absorbance values of each well were measured using an automated microplate reader (Benchmark microplate reader, Bio-Rad Laboratories) with compatible software (Microplate Manager 5.2, Bio-Rad Laboratories), using a measurement wavelength of 450 nm and a reference wavelength of 620 nm. The limit of detection was 23.0 pg/mL and the average intra-assay CV was 4.1 %.

IL-6 concentration in whole testis and epididymis was determined according to the manufacturers instructions using the BD OptEIA™ ELISA assay (555240, BD Biosciences Pharmingen, USA).

2.6.5 Western Blot

Method background

The Western blot or protein immunoblot was originally introduced in 1979 by Tobwin et al. and is an analytical technique used to identify specific proteins in tissue homogenates or extracts. Since then, Western blotting has become a common technique used in research laboratories worldwide for the immunodetection and quantitation of specific proteins in complex cell homogenates [269].

Test principle

In order to identify specific proteins the Western Blot method uses gel electrophoresis to separate proteins based on size. Thereafter, the gel is placed onto a membrane made of nitrocellulose or PVDF (polyvinylidene fluoride) onto which the proteins are transferred through an electrical current. In the final step, the membrane can

be further processed with specific antibodies to identify the target of interest, which is then visualized using secondary antibodies and detection reagents [59,269].

Protocol

The SDS–PAGE (SDS-polyacrylamide gel electrophoresis) was performed according to Laemmli (1970). The gel was made of 8 % SDS stacking gel and 10 % SDS separating gel as described below (Table 2-6). In order to enable access of the antibodies to all parts of the protein it is necessary to unfold it. Therefore, the samples were dissolved in 4x Laemmli buffer and RO H_2O and boiled for 5 min at 95°C to generate reduced, denatured proteins. Thereafter, the samples were centrifuged briefly before loading onto the gel. Per sample 30 μg of protein were loaded into each well. The electrophoresis was performed in 1x running buffer at 35 mA for about 80 minutes. When the dye molecule ("migration front") reached the bottom of the gel, the power was turned off. Thereafter, the gel was immediately preceded for transfer. Prior to wet transfer, PVDF membranes were soaked in methanol for 10 minutes, rinsed with RO H_2O and then soaked in 1x transfer buffer for 10 minutes. Concurrently, sponges and Whatman papers were soaked in 1x transfer buffer. Subsequently, samples were electrophoretically transferred from the gel onto a PVDF membrane. For this, the gels were first equilibrated in transfer buffer for 5 minutes and then placed in a sandwich cassette built up of the following: sponge, four layers of blotting paper, protein gel, PVDF membrane, three layers of blotting paper, sponge. The sandwich cassette was placed into a blotting chamber and submerged with ice-cold 1x SDS-free transfer buffer. The wet transfer was performed at 95 V for 80 minutes at 4°C.

In order to confirm the transfer of the proteins onto the membrane, it was stained for 10 min with Ponceau S stain. To visualize the proteins, the membrane was briefly washed with RO H_2O and to remove the dye the membrane was incubated in PBS-T.

Following this, the membranes were placed into a 120 ml container (Sarstedt, SA, Australia) and rinsed with 1x PBS. To prevent non-specific background binding of the primary and/or secondary antibodies the membrane was blocked for 1 hour at RT in Odyssey® blocking buffer. Subsequently, the primary antibody was incubated for 1 hour at RT, followed by rinsing in 1x PBS and washing with PBS-T three times for 5 minutes to remove residual primary antibody. Thereafter, the secondary antibody was incubated for 1 hour at RT followed by washing as described above to remove residual secondary antibody.

All antibodies were diluted in Odyssey® blocking buffer + 0.1 % Tween 20 at the dilutions given in Table 2-7.

Finally, the proteins were detected using the Odyssey® imaging system (LI-COR®). For quantification, the intensities of the total protein were normalised to β-tubulin.

Table 2-6. Preparation of SDS-PAGE gels.

Stock solution	8 % stacking gel (ml)	10 % separating gel (ml)
30 % (w/v) acrylamide	0.83	5
1.5 M Tris-HCl pH 8.8	-	3.75
1 M Tris-HCl pH 6.8	0.63	-
10 % SDS	0.05	0.15
10 % APS	0.05	0.15
TEMED	0.005	0.015
RO H_2O	3.4	5.93

Table 2-7. List of Western blot antibodies.

Antibody	Product number	Company	Dilution
Beta-tubulin	ab21057	Abcam, MA, USA	WB: 1:3000
Smad4	ab137861	Abcam, MA, USA	WB: 1:300
IRDye800CW (donkey anti goat IgG)	925-32214	LI-COR, NE, USA	WB: 1:15000
IRDye680RD (goat anti rabbit IgG)	925-68071	LI-COR, NE, USA	WB: 1:15000

2.7 Statistical analysis

Raw data from the project was entered using MS Excel® for Mac and the thesis manuscript was generated using MS Word® for Mac (Microsoft Office for Mac, version 2011, Microsoft Corporation, WA, USA).

Statistical analysis was performed using Graph Pad Prism 6 (GraphPad Software Inc., CA, USA). Values in tables and graphs are expressed as mean ± SEM (unless otherwise specified). Data were checked for normality of distribution using the Shapiro-Wilk normality test. Where data showed normal distribution unpaired t-test was performed for comparison between two groups and two-way ANOVA was used to test the effect of diabetes between several groups when multiple time-points were considered. Where the overall ANOVA showed significant differences among means, Tukey's *post-hoc* comparisons between treatments were performed. When one or more groups failed the

normality test, samples were analysed using the Kruskal-Wallis test. Where the Kruskal-Wallis test showed significance, Dunn's *post-hoc* comparisons between treatment and controls were performed. To test the correlation between two parameters Pearson correlation analysis was performed for normally distributed data. *P* value <0.05 was considered significant. Accordingly, significance was marked as * = P<0.05; ** = P<0.01; *** = P<0.001; **** = P<0.0001.

3 Results

In order to determine the impact of T1D on male reproductive function, experiments using the model organism *C. elegans*, the *Ins2*$^{Akita+/-}$ mouse model and *in vitro* studies on Sertoli cells were conducted. The results from these investigations are presented below.

3.1 Studies on *C. elegans*

3.1.1 High glucose affects brood size in *mev-1* strain *C. elegans*

The model organism *C. elegans* mutant in the *mev-1* gene was used in order to assess the general impact of high glucose on reproductive outcome. *mev-1* encodes the *C. elegans* ortholog of the succinate dehydrogenase cytochrome b560 subunit, an integral membrane protein that is a subunit of mitochondrial respiratory chain complex II (ubiquinol-cytochrome c reductase). Since this protein is required for oxidative phosphorylation, nematodes mutant for *mev-1* show an abnormal energy metabolism, increased sensitivity to oxidative stress and pathogen infections, as well as a shortened lifespan. Thus, *mev-1* mutant *C. elegans* nematodes are used as a model system to study the molecular mechanisms underlying diabetic hyperglycaemia-induced reduction in life-span. Since they were shown to exhibit analogies to the situation observed in T1D, they were used in this study to assess the effects of glucose on reproduction [84].

Pilot experiments were conducted to evaluate a suitable glucose concentration. For this, nematodes were grown in liquid NGM culture medium containing 0, 10 or 100 mM glucose and offspring were counted over a three-day period. A first assessment led to the conclusion, that a concentration of 100 mM glucose may induce significant glucose related effects on brood size (**p=0.0061) (Fig. 3-1). Hence, a concentration of 100 mM glucose was used for all further experiments. In these, treatment of *mev-1* strain *C. elegans* with 100 mM glucose resulted in a significant reduction in number of offspring per nematode compared to control (*p=0.0183, mean ± SD 124.2 ± 20.17 vs. 108.4 ± 20.21). In order to evaluate the impact of high glucose treatment on Sma/Mab pathway genes, which are closely related to the TGF-β

signalling pathway in mice and humans, nematodes were treated with siRNA before glucose incubation. Genes encoding *Smad-1* (*Sma-2*), *Smad-5* (*Sma-3*), *BMPRRIB* (*Sma-6*), and *BMP-5* (*dbl-1*) were targeted, but showed no significant effects on brood size (Fig. 3-2).

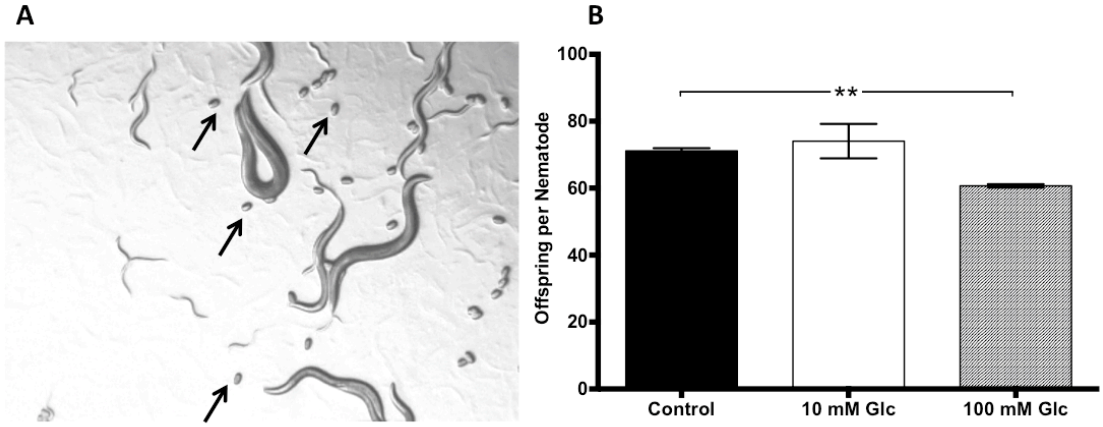

Fig. 3-1. Pilot experiment to determine the optimal glucose concentration for the treatment of *mev-1* nematodes.

mev-1 strain nematodes were grown in liquid NGM culture medium containing 0, 10 or 100 mM glucose and offspring were counted over a three-day period. (A) Arrows indicate *mev-1* eggs as counted for the analysis. (B) Number of offspring per nematode is significantly decreased after treatment with 100 mM glucose. Numbers in bars indicate numbers of experiments, n=2 experiments, **p=0.0061, unpaired t-test.

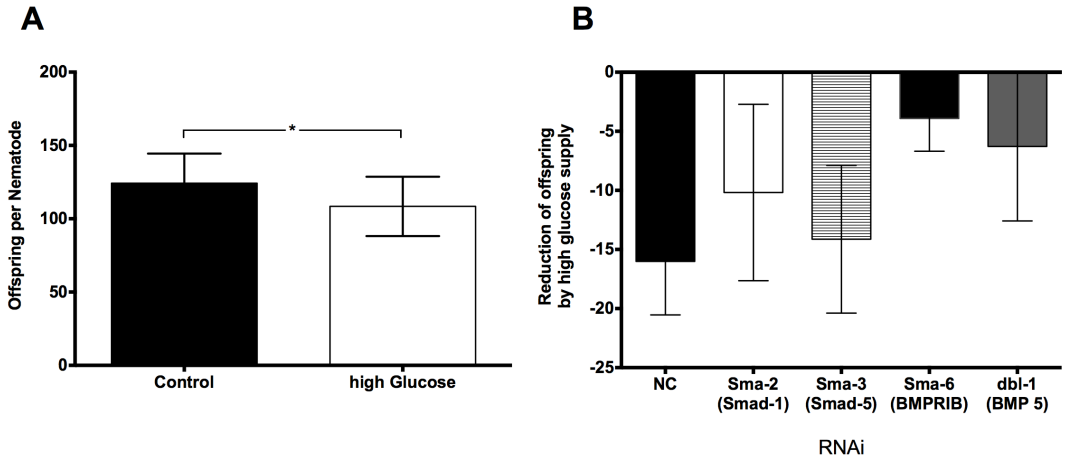

Fig. 3-2. Effect of high glucose on reproductive outcome in *mev-1* strain *C. elegans*.

(A) *mev-1* strain *C. elegans* were grown in liquid NGM culture medium in the presence or absence of 100 mM glucose. High glucose treatment significantly reduces brood size in *mev-1* strain *C. elegans*. *p=0.0183, unpaired t-test, n=3 experiments.

(B) *mev-1* strain *C. elegans* were grown in liquid NGM culture medium containing 100 mM glucose after treatment with siRNA targeting genes encoding *Smad-1* (*Sma-2*), *Smad-5* (*Sma-3*), *BMPRRIB* (*Sma-6*), and *BMP-5* (*dbl-1*). n=3 experiments.

3.2 *Ins2*$^{Akita+/-}$ mouse model

As described in section 1.1.8, *Ins2*^{Akita} mice develop T1D due to the accumulation of misfolded insulin within pancreatic β-cells. Recent studies have already shown that T1D is associated with testicular failure in young homozygous *Ins2*^{Akita} mice, with mice showing a reduction in testis size, reduction in seminal vesicle weight, arrested spermatogenesis, and an absence of mature spermatozoa as well as a decreased numbers of spermatocytes and spermatids starting by the age of 5 weeks. By the age of 7-8 weeks these mice exhibit infertility [235]. The long-term effects of T1D on male reproductive function in heterozygous *Ins2*^{Akita} have not been well-characterised, and were subjected to detailed investigation.

3.2.1 Assessment of general parameters in the *Ins2*$^{Akita+/-}$ mouse model

In order to characterise the heterozygous *Ins2*^{Akita} mouse model used in the present study, body weight (BW) and blood glucose (BG) were measured at 12 weeks and 24 weeks of age in a total of 34 non-diabetic mice and 45 diabetic mice, using genotype-matched wild type mice for comparison (Fig. 3-3). Testes and serum samples were available from 7-14 *Ins2*$^{Akita+/-}$ animals per group for detailed investigation of testicular function. Testis weight (TW) and HbA1c were assessed (Fig. 3-4). In general, non-diabetic *Ins2*$^{Akita+/-}$ mice (blood glucose <14.0 mmol/l) displayed higher body and testis weights compared to wild type. Non-diabetic *Ins2*$^{Akita+/-}$ mice exhibited significantly elevated blood glucose levels compared to wild type controls indicating a mildly diabetic phenotype.

Mean body weights of the diabetic mice were significantly decreased compared to non-diabetic *Ins2*$^{Akita+/-}$ mice at 12 weeks and to both non-diabetic control groups at 24 weeks of age. Mean blood glucose levels of diabetic mice were significantly elevated compared to both controls.

There was no difference in the mean testis weights of the mice at 12 weeks, but by 24 weeks, the non-diabetic mice showed larger testis weights than wild type

controls, while the diabetic mice displayed a 20 % reduction compared to wild type, and a 30 % reduction compared to non-diabetic mice (Fig. 3-4A). Testis weights in the *Ins2*$^{Akita+/-}$ mice showed a significant negative correlation with blood glucose (Pearson correlation coefficient of r^2=-0.2125, p = 0.0021) (not shown) and HbA1c levels (r^2=-0.4193, p=0.0002) (Fig. 3-4B), indicating that the severity and duration of hyperglycaemia was associated with reduced testis weight.

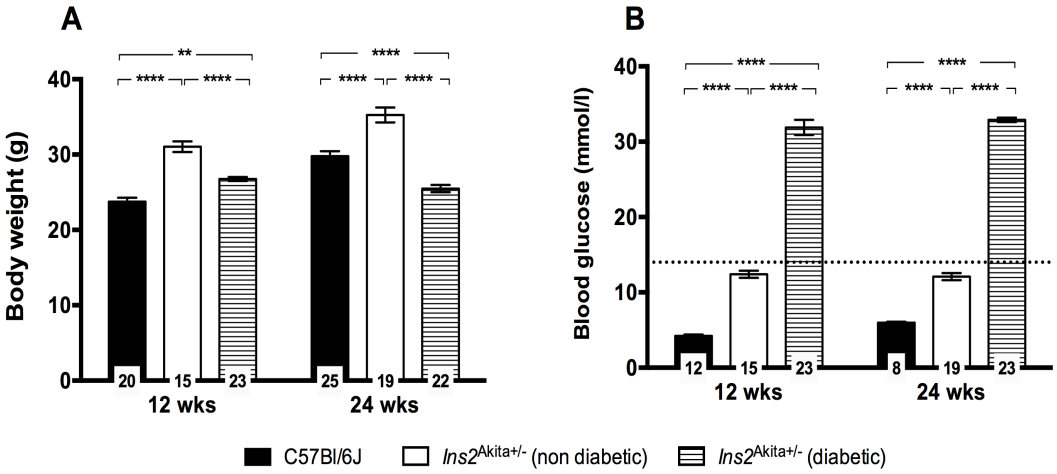

Fig. 3-3. Assessment of body weight (A) and blood glucose (B) in *Ins2*$^{Akita+/-}$ mice compared to wild type control.

Two-way ANOVA. Numbers in bars indicate numbers of animals per group. Dotted line indicates level of diabetes cut-off at 14.0 mmol/l.

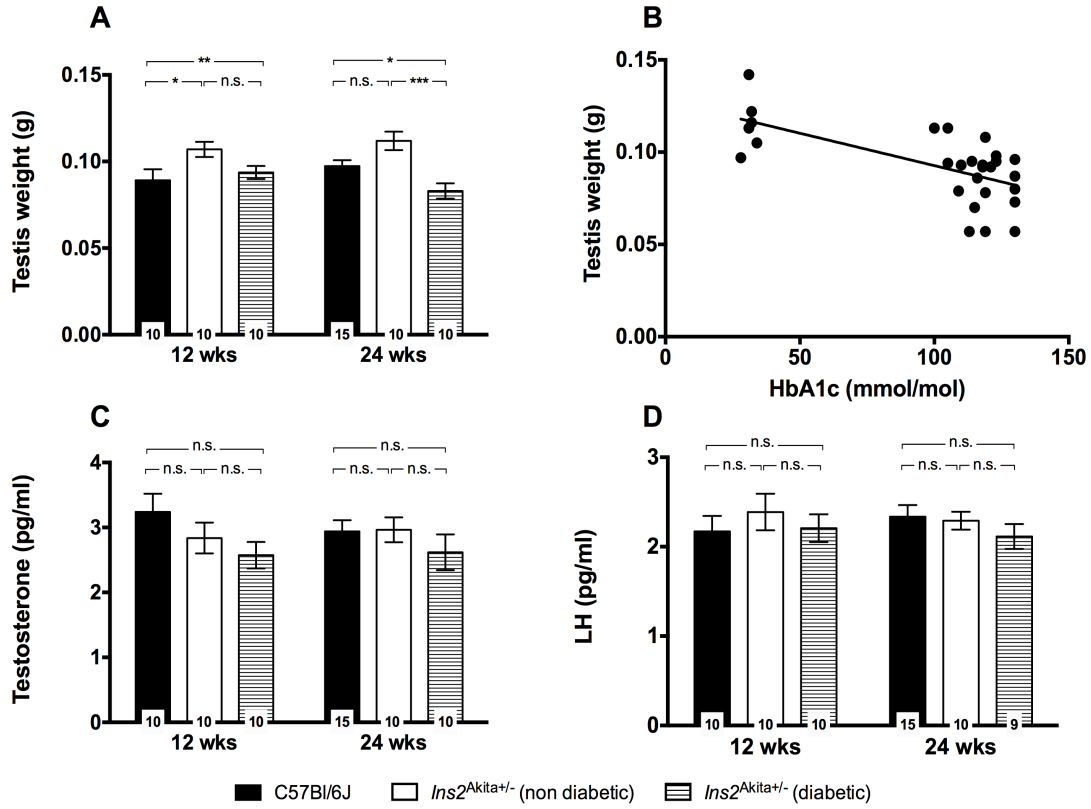

Fig. 3-4. Assessment of testis weight, HbA1c to testis weight correlation, testosterone, and LH in *Ins2*$^{Akita+/-}$ mice.

(A) Assessment of testis weight in *Ins2*$^{Akita+/-}$ mice compared to wild type control. Two-way ANOVA. Numbers in bars indicate numbers of animals per group. (B) Correlation of HbA1c to testis weight within *Ins2*$^{Akita+/-}$ mice (all mice from both age groups combined). (C & D) Testosterone and LH levels in mouse plasma as determined by RIA. Two-way ANOVA. Numbers in bars indicate numbers of animals per group.

3.2.2 Testicular atrophy of insulin-deficient *Ins2*$^{Akita+/-}$ mice

The observation that long-term diabetes reduced testis weight in diabetic *Ins2*$^{Akita+/-}$ mice indicated that testicular function was reduced. Histological examination of the testes showed features consistent with moderate spermatogenic disruption in these mice (Fig. 3-5A-F). On average, the seminiferous tubules of the diabetic *Ins2*$^{Akita+/-}$ mice (205.3 ± 20.26 μm) were 10 % smaller in diameter compared to non-diabetic (227.3 ± 9.29 μm) and 15 % compared to wild type controls (241.5 ± 14.43 μm) (p=0.0009, n = 6 mice/ group). Assessment of spermatogenesis using the Johnsen score revealed that the testes of 24 week old diabetic mice showed significantly less

normal tubules (score 10) as opposed to wild type (76.23 ± 3.95 vs. 66.86 ± 5.37 %, p=0.0006) and non-diabetic Akita mice (81.73 ± 1.70 vs. 66.86 ± 5.37 % , p<0.0001). Diabetic mice tended to show failure in spermatogenesis reaching scores below 5 more frequently, when compared to wild type or non-diabetic *Ins2*$^{Akita+/-}$ controls (Table 3-1). Pathological changes, such as vacuolisation, spermatogenic disruption, degenerating cells, and Sertoli-cell only pattern in some tubules were observed (Fig. 3-5C-F).

However, diabetic *Ins2*$^{Akita+/-}$ germ cells were not more frequently in a state of late apoptosis as revealed by TUNEL staining compared to controls (Fig. 3-6). In order to further distinguish the cause of the reduction in testis weight, testicular sections were stained for the Sertoli cell marker SOX-9 (Fig. 3-7A-F). All groups showed similar numbers of Sertoli cells within the seminiferous tubules at all ages analysed (Fig. 3-7G) (number of SOX-9 positive cells per tubule cross-section at 24 weeks of age: C57Bl/6J 15.25 ± 0.75; non-diabetic *Ins2*$^{Akita+/-}$ 14.95 ± 1.51; diabetic *Ins2*$^{Akita+/-}$ 15.29 ± 0.45). This is also resembled in SOX-9 mRNA expression levels (Fig. 3-7H).

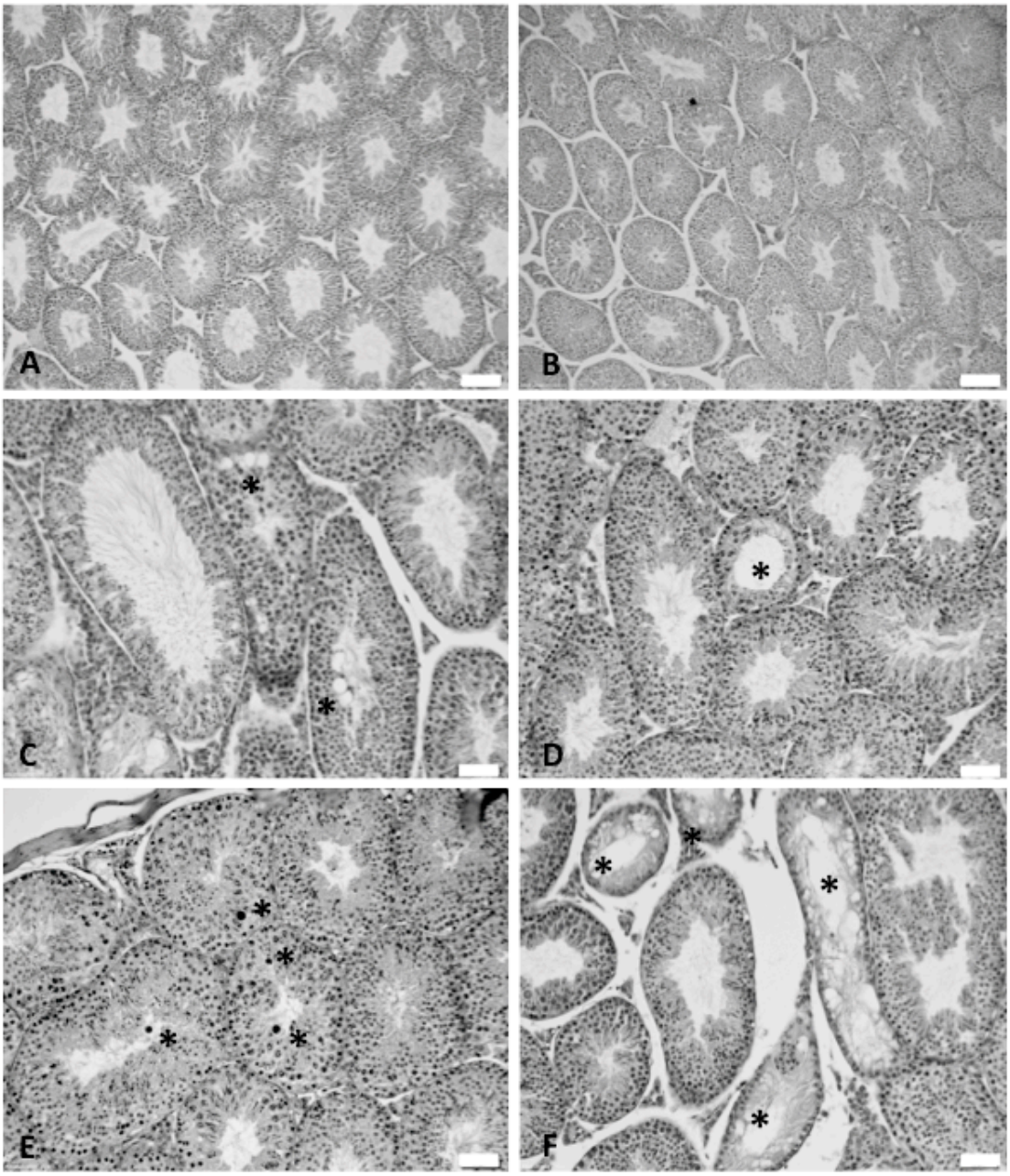

Fig. 3-5. Testicular morphology in *Ins*2$^{Akita+/-}$ mice compared to wild type control at 24 weeks of age.

Testicular sections from diabetic *Ins*2$^{Akita+/-}$ mice and controls at 24 weeks of age were processed for hematoxylin staining. (A) C57Bl/6J, (B) non-diabetic *Ins*2$^{Akita+/-}$ mice, (C-F) Pathological changes (asterixes) in diabetic *Ins*2$^{Akita+/-}$ mice: (C) vacuolisation (resembles Johnsen score 8); (D) spermatogenic disruption (resembles Johnsen score 3); (E) increased number of degenerating cells (resembles Johnsen score 9); (F) Sertoli-cell only tubules (resembles Johnsen score 2). (A & B) Scale bar = 100 μm. (C-F) Scale bar = 50 μm.

Table 3-1. Johnsen score count in testicular sections.

	12 weeks			24 weeks		
	C57Bl/6J	non-diabetic *Ins2*$^{Akita+/-}$	diabetic *Ins2*$^{Akita+/-}$	C57Bl/6J	non-diabetic *Ins2*$^{Akita+/-}$	diabetic *Ins2*$^{Akita+/-}$
	n= 3	n= 3	n= 5	n= 6	n= 3	n= 6
10	324	328	509	698	416	624
9	17	73	73	96	53	126
8	5	31	26	46	27	89
7	46	33	64	58	9	46
6	5	3	5	3	1	3
5	0	2	9	0	0	8
4	0	2	6	0	1	2
3	0	4	4	5	0	10
2	0	1	14	8	1	27
1	0	0	1	0	0	0
Mean Score	9.5	9.4	9.2	9.5	9.7	9.2

n = number of animals per group

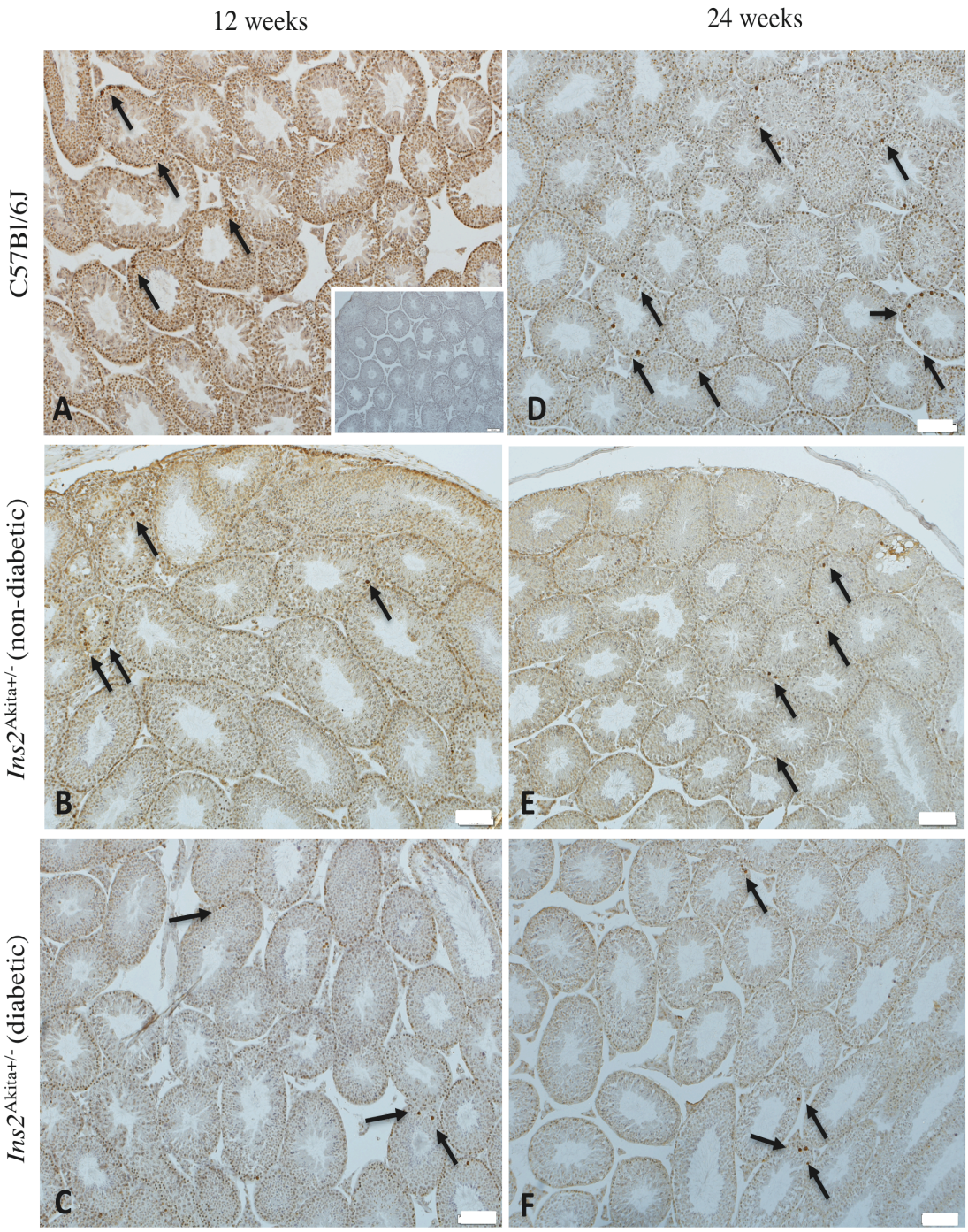

Fig. 3-6. TUNEL staining on testicular sections of *Ins2*$^{Akita+/-}$ mice compared to wild type control.

Testicular sections from diabetic *Ins2*$^{Akita+/-}$ mice and controls at 24 weeks of age were processed for TUNEL staining. Inserted picture in Fig. 3-6A indicates negative control sample. Arrows indicate TUNEL positive cells. Scale bar = 100 μm.

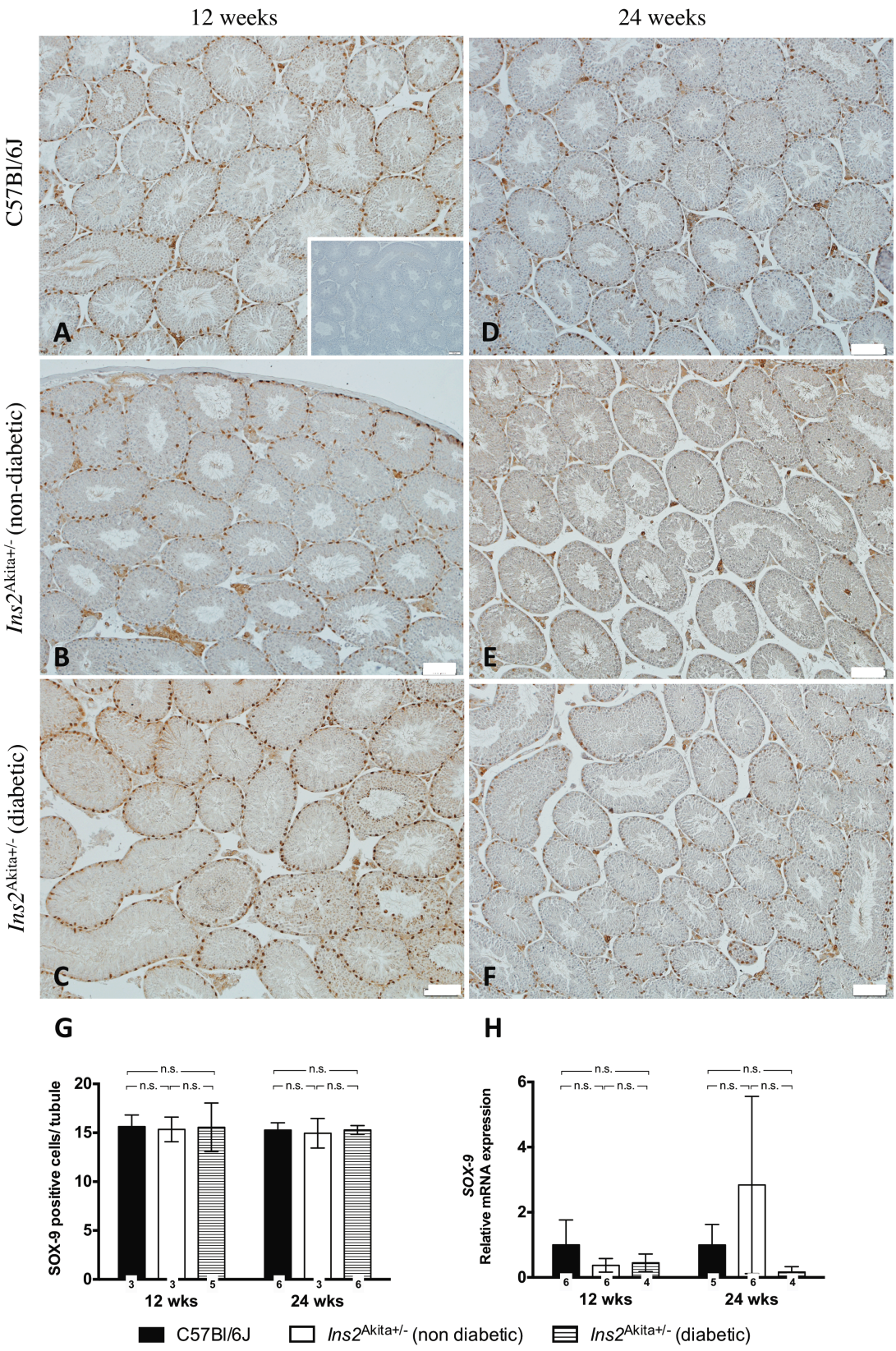

Fig. 3-7. Testicular SOX-9 in *Ins2*$^{Akita+/-}$ mice compared to wild type control.

(A-F) SOX-9 staining on testicular sections of *Ins2*$^{Akita+/-}$ mice compared to wild type control. Inserted picture in Fig. 3-7A indicates negative control sample. Scale bar =

100 μm. (G) Number of SOX-9 positive cells per tubule. Two-way ANOVA. Numbers in bars indicate numbers of animals per group. (H) qRT-PCR assessment of SOX-9 mRNA levels in mouse testis. Kruskal-Wallis test. Numbers in bars indicate numbers of animals per group.

3.2.3 Fertility in *Ins2*$^{Akita+/-}$ mice

To further evaluate the reproductive capacity of male *Ins2*$^{Akita+/-}$ mice sperm function from these mice was analysed in detail at 24 weeks of age.

Evaluation of the sperm morphology indicated that the overall sperm density was significantly lower in both non-diabetic and diabetic *Ins2*$^{Akita+/-}$ mice compared to wild type controls. Non-diabetic *Ins2*$^{Akita+/-}$ mice further show a significantly reduced number of normal sperm. Most interestingly, diabetic *Ins2*$^{Akita+/-}$ mice displayed a significantly increased number of sperm with head failure compared to both wild type and non-diabetic control (Fig. 3-8).

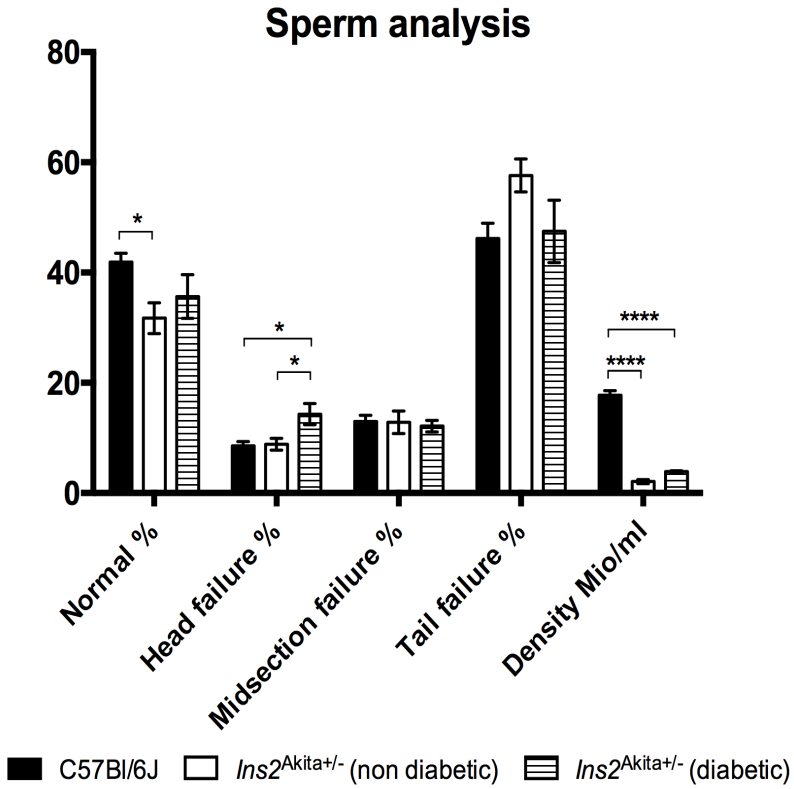

Fig. 3-8. Diabetic *Ins2*$^{Akita+/-}$ mice show decreased sperm density and increased sperm head failure at 24 weeks of age.

Sperm morphology parameters of epididymal sperm from 24 week old *Ins2*$^{Akita+/-}$ mice

compared to controls. n=4-5, one-way ANOVA.

3.2.4 The hypothalamic-pituitary-gonadal axis in *Ins2*$^{Akita+/-}$ mice

Measurement of testosterone in serum samples revealed a number of very high levels in the wild type mouse group, but similar levels of testosterone in non-diabetic and diabetic *Ins2*$^{Akita+/-}$ mice at 12 weeks of age and amongst all groups at 24 weeks of age (Fig. 3-4C). Measurement of LH in serum samples showed no difference between groups at any time (Fig. 3-4D).

3.2.5 Assessment of testicular inflammation in the *Ins2*$^{Akita+/-}$ mice.

Since activins mediate inflammatory responses within the testis [111,128,134], expression of several key inflammatory markers was examined (Fig. 3-9).

mRNA expression levels of IL-1α, IL-1β and TNF-α showed no changes in *Ins2*$^{Akita+/-}$ mice at any age. Moreover, the mRNA expression of the anti-inflammatory cytokine IL-10 was not altered in the testis of diabetic *Ins2*$^{Akita+/-}$ mice. This indicates that there was no induction of inflammatory processes within the testes of the *Ins2*$^{Akita+/-}$ mice. In contrast, testicular IL-6 protein production appeared to be increased at 12 weeks and 24 weeks in all *Ins2*$^{Akita+/-}$ mice (Fig 22 C). In contrast to IL-6 levels within the testis, epididymal IL-6 levels were not affected in neither non-diabetic nor diabetic *Ins2*$^{Akita+/-}$ mice at 12 weeks of age, but are significantly upregulated in diabetic *Ins2*$^{Akita+/-}$ mice at 24 weeks of age compared to non-diabetic *Ins2*$^{Akita+/-}$ and wild type control mice.

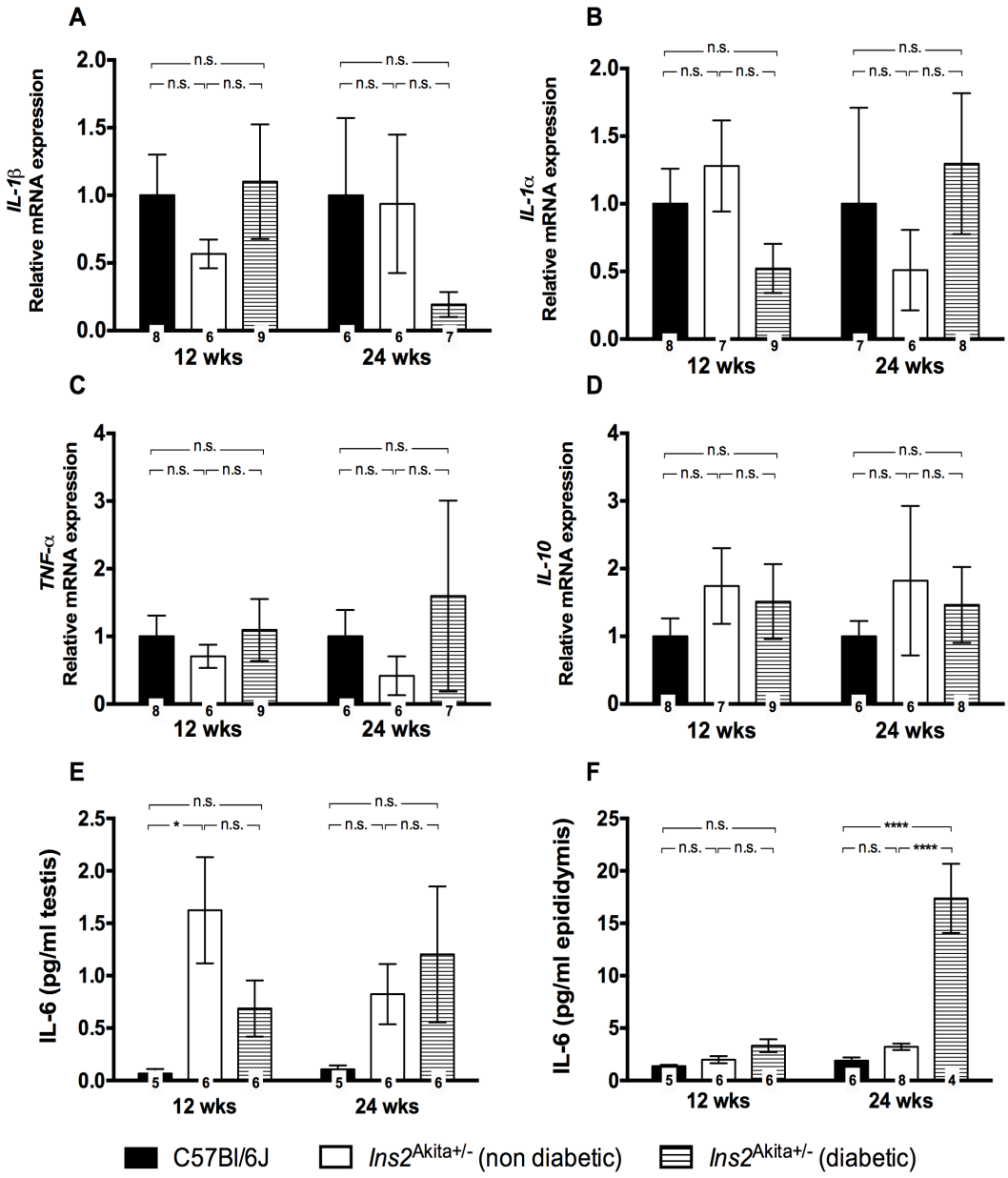

Fig. 3-9. Inflammatory markers in *Ins2*$^{Akita+/-}$ mice compared to controls.

(A-D) qRT-PCR assessment of IL-1α, IL-1β, TNF-α, and IL-10 mRNA levels in mouse testis. Numbers in bars indicate numbers of animals per group. Kruskal-Wallis test. (E & F) IL-6 levels in mouse testis (E) and epididymis (F) as determined by ELISA. Numbers in bars indicate numbers of animals per group. Two-way ANOVA.

3.2.6 Regulation of activins and their signalling pathway in the *Ins2*$^{Akita+/-}$ mice

Since activins and their antagonist play a major role in in the control of testicular function, protein and gene levels for activin A, activin B, inhibin, and follistatin were assessed.

Testicular levels of *Inhba* mRNA, encoding the βA subunit of activin A, were unchanged in the *Ins2*$^{Akita+/-}$ mice at all ages (Fig. 3-10C). However, at 12 weeks of age there was a very high variability in mRNA expression, suggesting that some animals did have elevated expression. In all three groups, staining for activin A protein on testis sections revealed a typical pattern of strong positive staining in Sertoli cells of the seminiferous tubules, as well as macrophages in the interstitium (Fig. 3-11).

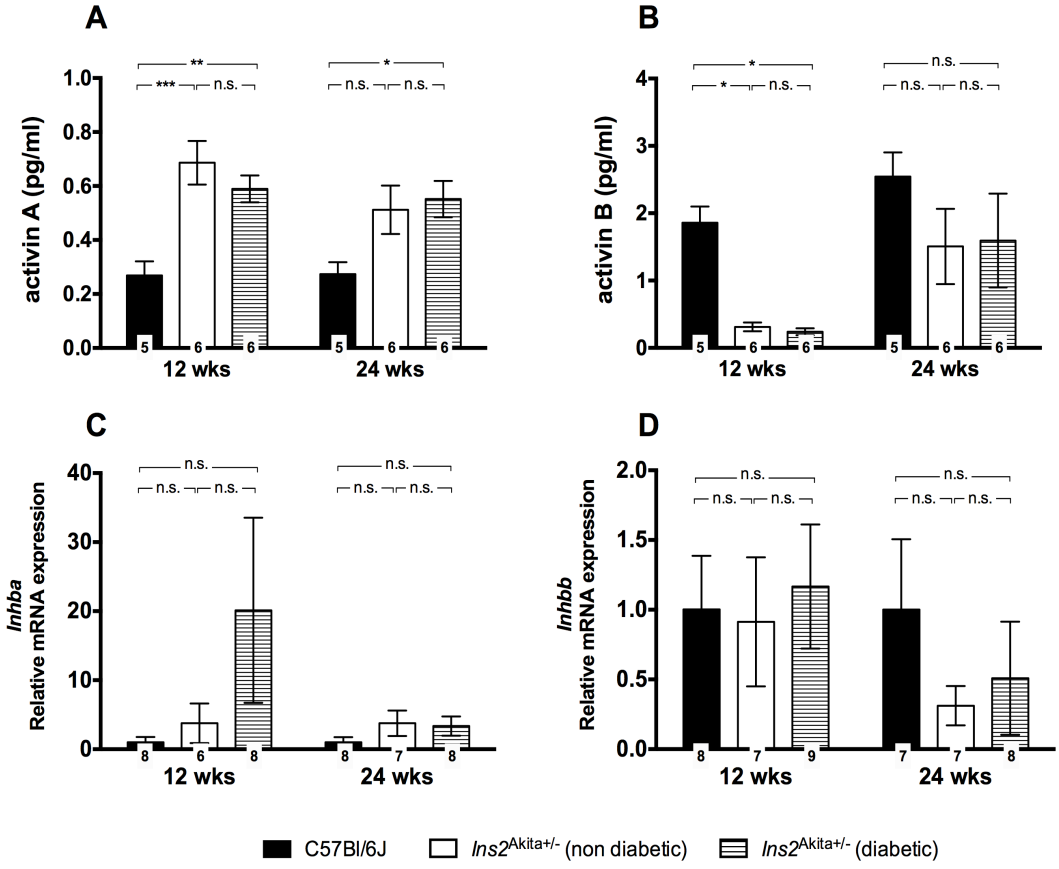

Fig. 3-10. Activins A and B in *Ins2*$^{Akita+/-}$ mice compared to controls.
(A &B) Assessment of activin A and activin B protein levels in mouse testis. Numbers in bars indicate numbers of animals per group. Two-way ANOVA. (C & D) qRT-PCR assessment of *Inhba* and *Inhbb* mRNA levels in mouse testis. Numbers in bars indicate numbers of animals per group. Kruskal-Wallis test.

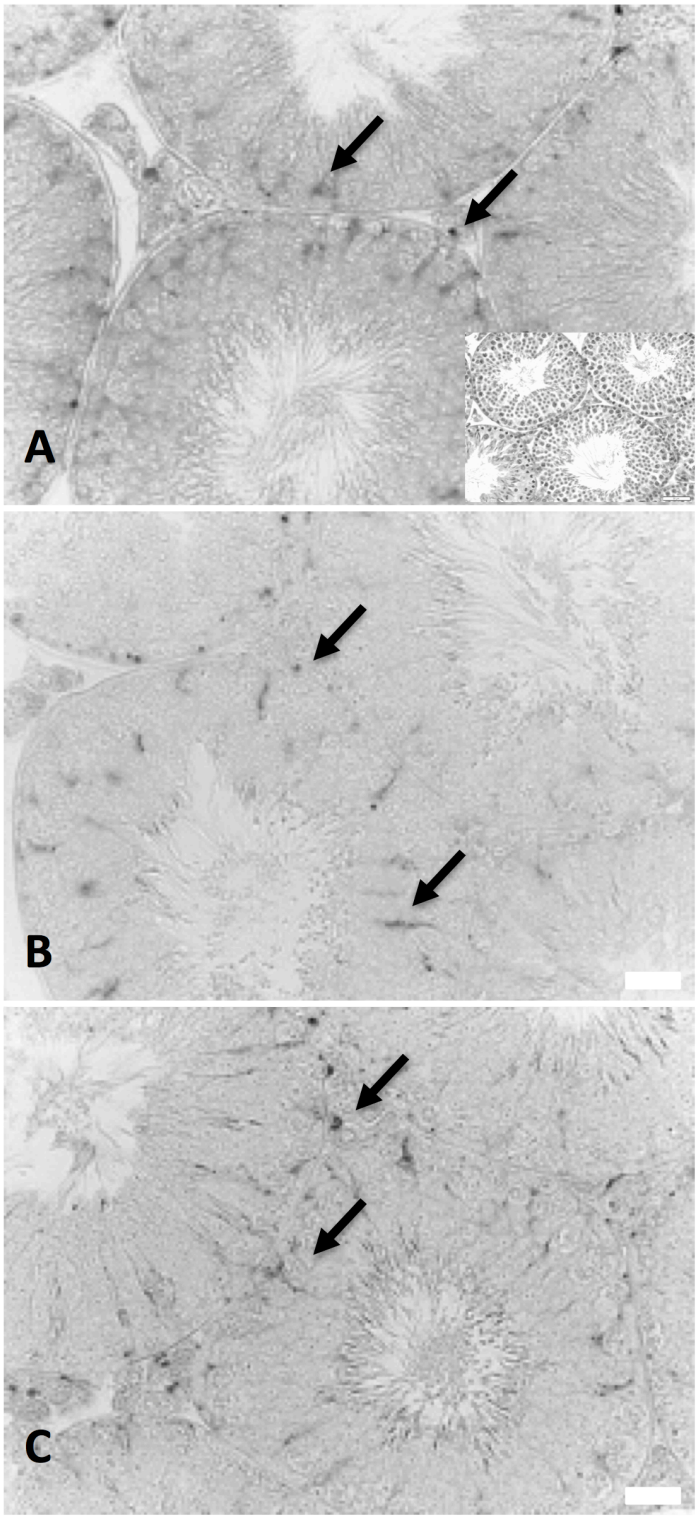

Fig. 3-11. Immunohistological staining for the activin β A subunit.

Testicular sections from diabetic *Ins*2$^{Akita+/-}$ mice and controls at 24 weeks of age were processed for activin βA subunit staining. Wild type (A), non-diabetic *Ins*2$^{Akita+/-}$ mice (B), and diabetic *Ins*2$^{Akita+/-}$ mice (C) at 24 weeks of age. Inserted picture in Fig. 3-11 A indicates negative control sample. Scale bar = 25 μm.

ELISA analysis was conducted in order to quantify activin A levels in testicular samples (Fig. 3-10A). These data showed that activin A protein was increased in both non-diabetic and diabetic *Ins2*$^{Akita+/-}$ mice at 12 and in diabetic mice at 24 weeks of age, when compared to wild type control. This suggests that within the testis of *Ins2*$^{Akita+/-}$ mice there is upregulation of activin A.

In order to further assess the role of activins within *Ins2*$^{Akita+/-}$ mice mRNA expression levels of *Inhbb*, encoding the inhibin βB subunit, were analysed. qRT-PCR results showed no changes in *Inhbb* mRNA levels at 12 weeks of age, but a trend towards a reduction in *Inhbb* expression in some Akita mice, when compared to wild type control (Fig. 3-10D). In contrast to these findings, activin B protein levels showed a significant downregulation at 12 weeks of age in both non-diabetic and diabetic *Ins2*$^{Akita+/-}$ mice, which seemed to recover at 24 weeks of age (Fig. 3-10B). This suggested that a higher proportion of the inhibin βB produced may have been diverted to the production of inhibin B within the *Ins2*$^{Akita+/-}$ testis. However, while there was an increase in *Inha* in some animals of the diabetic *Ins2*$^{Akita+/-}$ group at 12 weeks of age, overall qRT-PCR results for *Inha*, encoding the inhibin α subunit, showed no changes in mRNA expression in *Ins2*$^{Akita+/-}$ mice at any age (Fig. 3-12C). This finding was supported by the data of the measurements of total inhibin α-subunit containing proteins by RIA (Fig. 3-12A).

Evaluation of gene expression levels of the activin affinity binding protein, follistatin, revealed increased total follistatin (*FST* (total)) levels in some diabetic *Ins2*$^{Akita+/-}$ mice at 24 weeks of age, but no significant change in the overall expression level (Fig. 3-12D). This was also reflected in follistatin protein production measured by RIA (Fig. 3-12B).

To further assess the involvement of the TGF-β pathway signalling in T1D induced activin regulation, the expression of the relevant signalling receptors (Fig. 3-13A-C) was analysed. Gene expression in diabetic *Ins2*$^{Akita+/-}$ mice showed an upregulation of the type 1 activin receptor 1B (*Acvr1b*) at 12 weeks of age, which returns to baseline levels at 24 weeks of age. In contrast, in diabetic *Ins2*$^{Akita+/-}$ mice the type 2 activin receptor *Acvr2a* showed a marked downregulation at 24 weeks of age, while the type 2 activin receptor *Acvr2b* was markedly decreases at both 12 and 24 weeks of age.

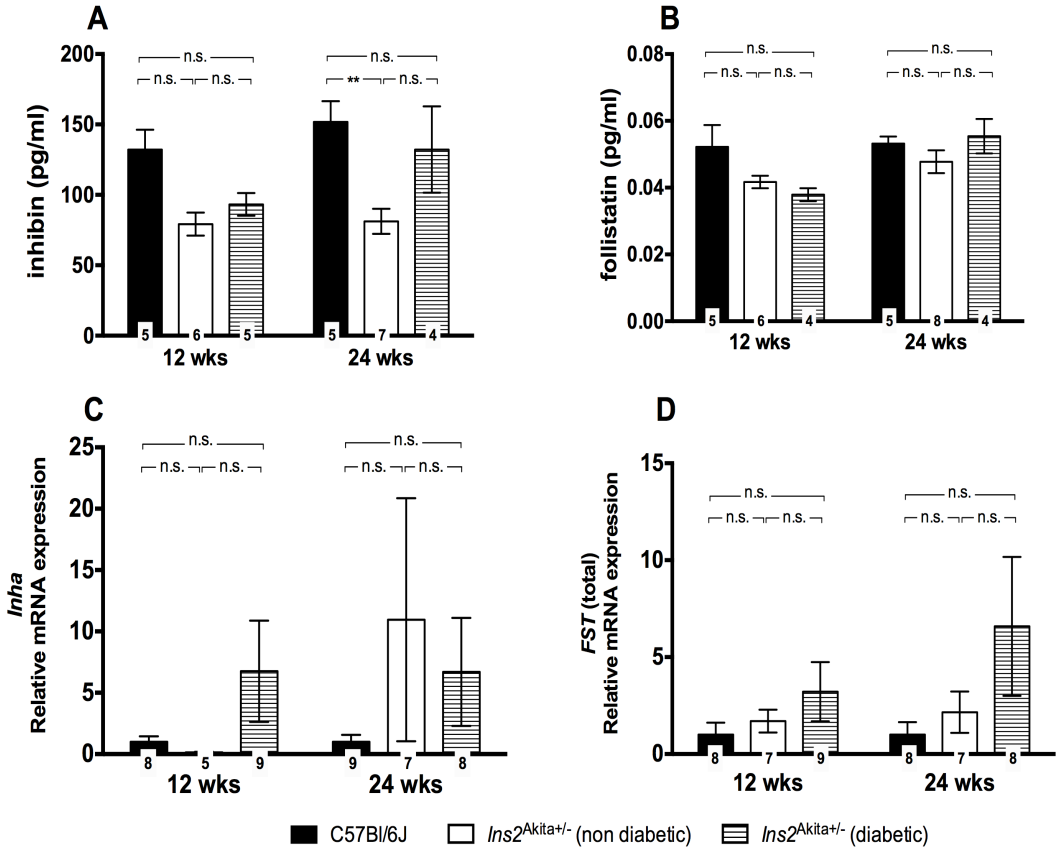

Fig. 3-12. Activin antagonists in *Ins2*$^{Akita+/-}$ mice compared to controls.

(A &B) Assessment of inhibin and follistatin protein levels in mouse testis. Numbers in bars indicate numbers of animals per group. Two-way ANOVA. (C & D) qRT-PCR assessment of *Inha* and *FST* mRNA levels in mouse testis. Numbers in bars indicate numbers of animals per group. Kruskal-Wallis test.

In order to determine if the Smad pathway was activated by changes in ligand expression in the testis, a multiplex analysis for phosphorylated Smad2 and 3, and Smad4 (Fig. 3-13D-E), as well as Western Blot analysis for Smad4 (Fig. 3-14) were undertaken. While pSmad2 appeared not to be regulated in *Ins2*$^{Akita+/-}$ mice, pSmad3 was significantly upregulated in diabetic *Ins2*$^{Akita+/-}$ mice at 24 weeks of age. Most interestingly, this upregulation occurred in parallel with an increase in Smad4 in diabetic *Ins2*$^{Akita+/-}$ mice at 24 weeks of age, when compared to non-diabetic *Ins2*$^{Akita+/-}$ mice and wild type control. This was also confirmed by Western Blot analysis (Fig. 3-14).

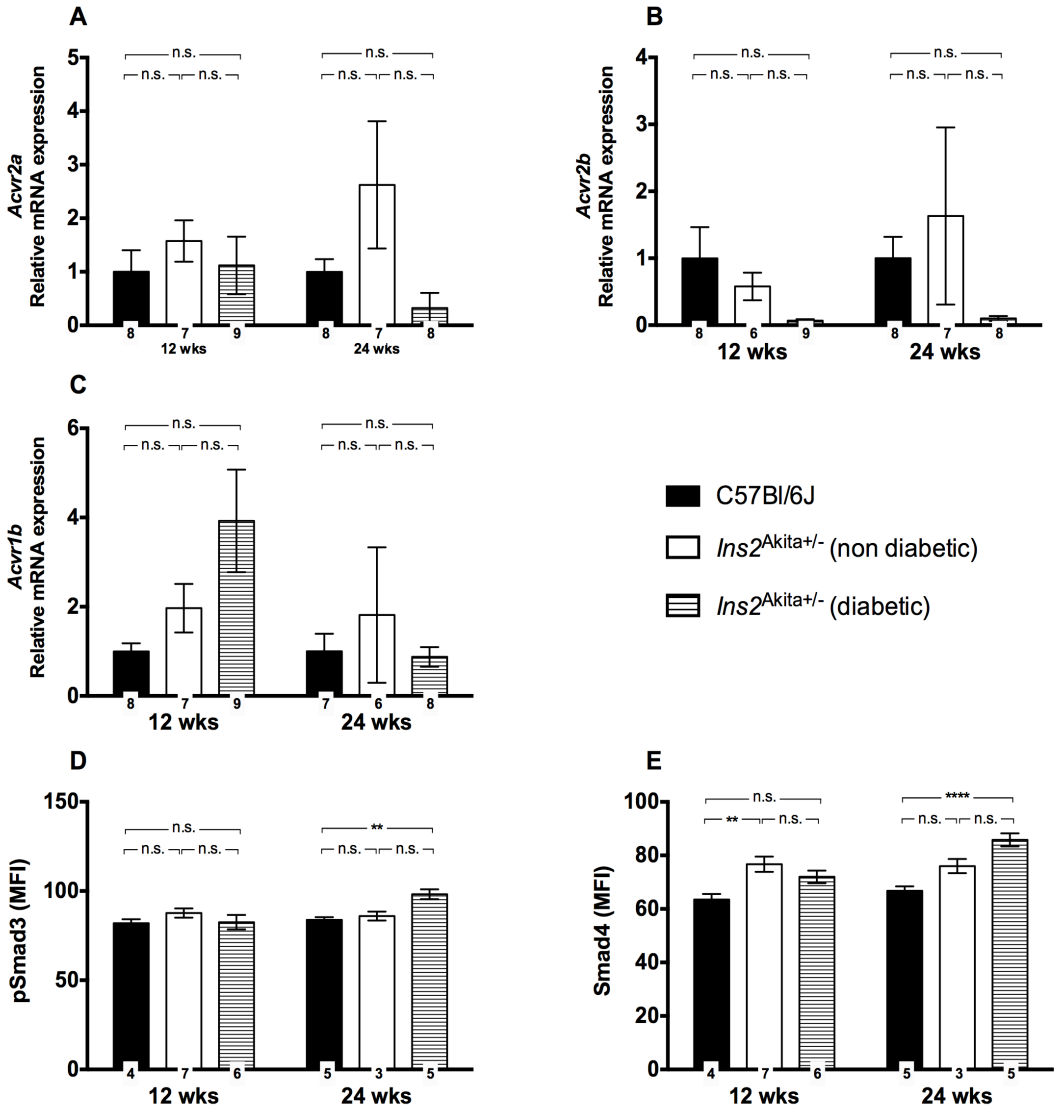

Fig. 3-13. Activin signalling in *Ins2*$^{Akita+/-}$ mice compared to controls.

(A-C) qRT-PCR assessment of *Acvr1b*, *Acvr2a*, and *Acvr2b* mRNA levels in mouse testis. Numbers in bars indicate numbers of animals per group. Kruskal-Wallis test. (D & E) Multiplex analysis of pSmad3 and Smad4 in mouse testis. Data expressed as median fluorescence intensity (MFI) ± SEM, numbers in bars indicate numbers of animals per group. Two-way ANOVA.

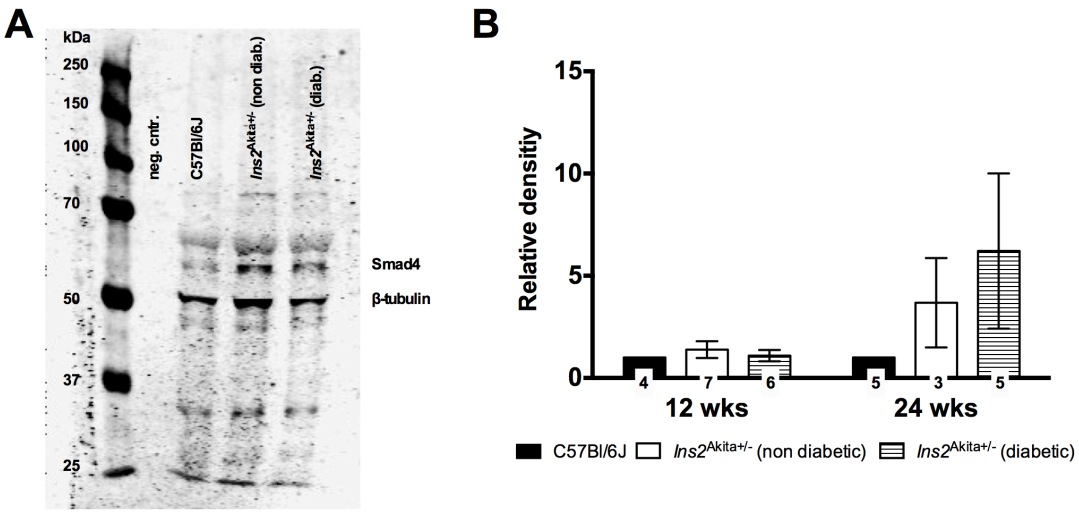

Fig. 3-14. Smad4 is elevated in the testis of diabetic *Ins2*$^{Akita+/-}$ mice.
Western Blot for Smad4 in 24 week old animals (A) and quantitative Smad4 protein analysis from Western Blot analysis (B) (n=6).

In order to determine if the effects of T1D on the production activin A, activin B, inhibin, and follistatin are also seen in the rest of the male reproductive tract, ELISA and RIA analysis was also conducted on epididymal samples from the three different groups of mice (Fig. 3-15). These data revealed that, in contrast to activin A production within the testis, epididymal samples showed a significant upregulation of activin A in diabetic *Ins2*$^{Akita+/-}$ mice compared to non-diabetic and wild type controls at 12 weeks of age and a significant upregulation compared to non-diabetic controls at 24 weeks of age.

Protein levels of activin B within the epididymis show a similar pattern to that seen within the testis, with a significant downregulation at 12 weeks of age in both non-diabetic and diabetic *Ins2*$^{Akita+/-}$ mice. This downregulation seems to recover at 24 weeks of age in non-diabetic *Ins2*$^{Akita+/-}$ mice only.

Similarly to the protein levels within the testis, epididymal levels of inhibin and follistatin were not affected by the diabetic conditions.

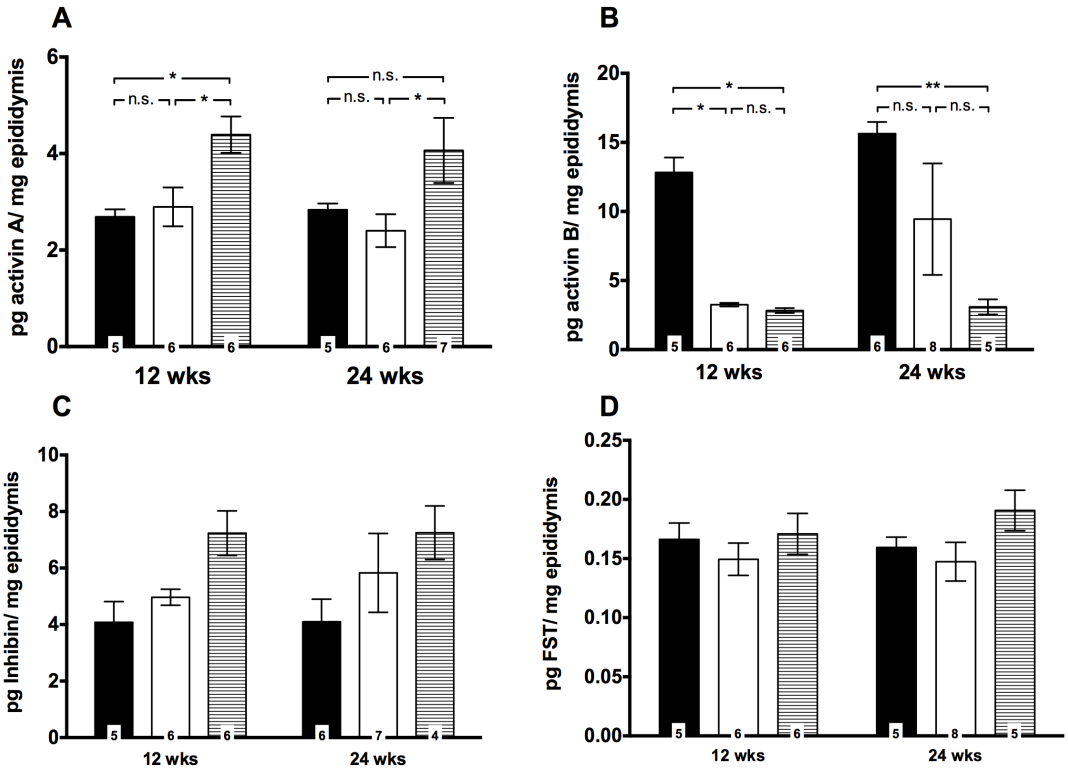

Fig. 3-15. Assessment of activin A, activin B, inhibin, and follistatin protein levels in mouse epididymis.

Numbers in bars indicate numbers of animals per group. Two-way ANOVA. (A & B) Activin A and B levels in mouse testis as determined by ELISA. (C & D) Inhibin and follistatin levels in mouse testis as determined by RIA.

3.3 Cell culture studies

Sertoli cells are the major sites for activin and inhibin production within the testis. In order to determine the direct impact of diabetic conditions, such as hyperglycaemia and hypoinsulinemia, on these cells and how these conditions regulate activin and inhibin signalling, *in vitro* experiments were carried out using primary mouse Sertoli cells generated from C57Bl/6J mice as well as an immortalized mouse Sertoli cell line (WL-3).

3.3.1 Confirmation of the Sertoli cell character in WL-3 mouse Sertoli cells

The WL-3 cell line was first established in 2001 by Mueller and Korach [172]. In order to confirm the Sertoli cell character that was described in the original

publication, qRT-PCR analyses for various Sertoli cell specific genes was carried out (Table 9). These experiments confirmed the expression for *Inha*, *Inhbb*, *vimentin*, *SOX-9*, *β-Actin*, and the androgen receptor (AR). Further, they confirmed the presence of *Inhba*, *N-Cadherin*, *Claudin-11*, *GATA-4*, *ZO-1*, and *AMH*. As already shown by Mueller and Korach these cells do not express the FSH receptor. Therefore, this gene analysis confirmed the Sertoli cell like character of this cell line, allowing further experiments within this study.

Table 3-2. Sertoli cell gene markers in WL-3 cells.

Gene	*Inha*	*Inhba*	*Inhbb*	*FSH-R*	*Vimentin*	*Occludin*	*N-Cadherin*	*Claudin-11*	*SOX-9*	*GATA-4*	*ZO-1*	*AMH*	*β-Actin*	*AR*	*ER-α*	*ER-β*	*Ck14*	*SGP-1*
Mueller and Korach	✓	n/a	✓	×	✓	n/a	n/a	n/a	n/a	n/a	n/a	n/a	✓	✓	✓	✓	✓	✓
Maresch et al.	✓	✓	✓	×	✓	×	✓	✓	✓	✓	✓	✓	✓	✓	n/a	n/a	n/a	n/a
Mean Ct value	28	19	25	×	24	×	35	31	33	34	31	35	21	36	n/a	n/a	n/a	n/a

n/a = non applicable

3.3.2 Establishment of treatment conditions using dose responses

In order to determine suitable treatment conditions for the diabetes experiments on Sertoli cells, dose response treatments for the single substances were carried out on primary mouse Sertoli cells (Fig. 3-16) and WL-3 cells (Fig. 3-17and Fig. 3-18). Single treatments with glucose, mannose (as an isoosmotic control for glucose), insulin, FSH, or testosterone were conducted over a period of 24 and 48 h and the protein levels of activin A were measured in order to determine Sertoli cell response.

Although Mueller and Korach as well as qRT-PCR data from the present study did not confirm the expression of the FSH receptor within the WL-3 cell line, dose response experiments were conducted in these cells. This was done in order to provide a comparable approach in both study systems as well as to provide evidence for the fact that, additionally to the qRT-PCR data, WL-3 cells are unresponsive to FSH. This is particularly necessary since recent data suggests that FSH also acts in a steroid-independent manner via Tgf- β , Hedgehog, Wnt and Notch signalling pathways [66]. In order to distinguish the impact of hyperglycaemia in Sertoli cells, WL-3 cells were

also analysed for inhibin production after glucose and mannose dose response treatment (Fig. 3-18).

Dose response treatments revealed that primary Sertoli cells and WL-3 cells reacted similarly to most of the various substances. In WL-3 cells there was a pronounced increase of activin A release at 48 h incubation with glucose or mannose as compared to glucose free medium (Fig. 3-17A). Interestingly, the plateau of activin A release was attained at physiologic glucose levels (5.5 mM) and did not further increase with hyperglycaemic glucose levels. In primary SC's this effect was not observed (Fig. 3-16).

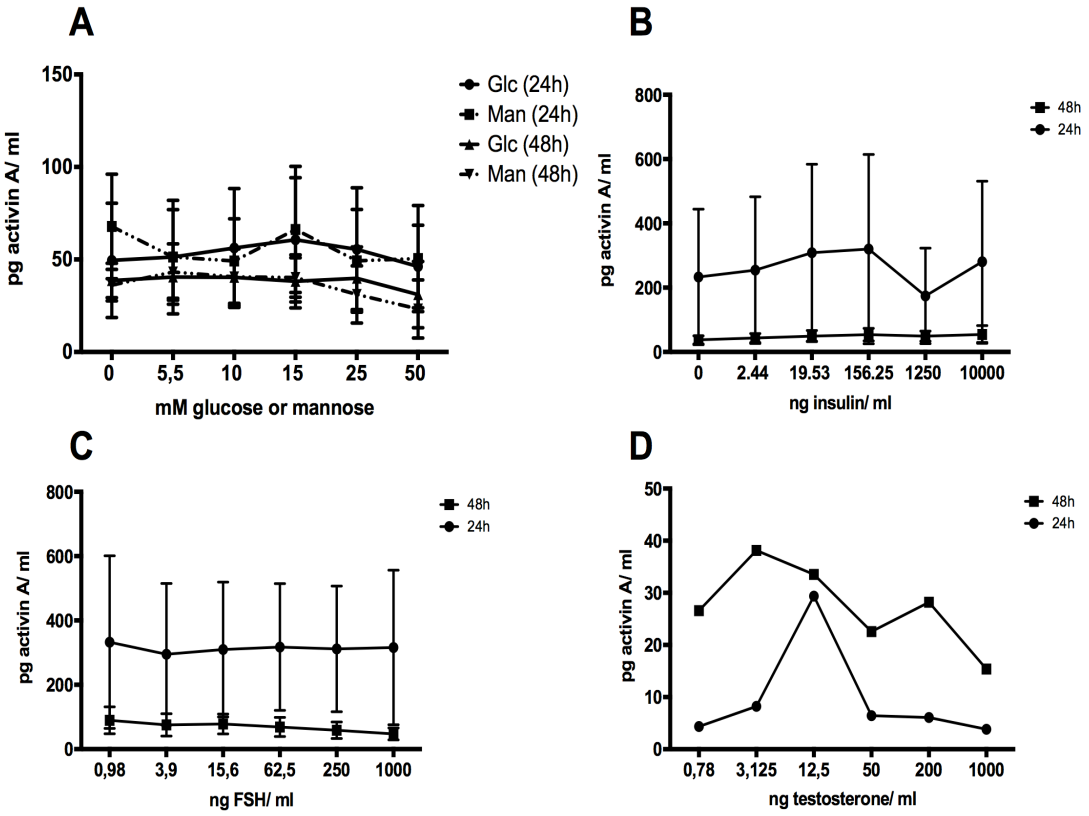

Fig. 3-16. Activin A production after dose response treatment in primary mouse Sertoli cells.

Activin A production in primary mouse Sertoli cells was measured via ELISA after treatment with (A) glucose or mannose, (B) insulin, (C) FSH, or (D) testosterone. (A-C) n=3 experiments, (D) n=1 experiment.

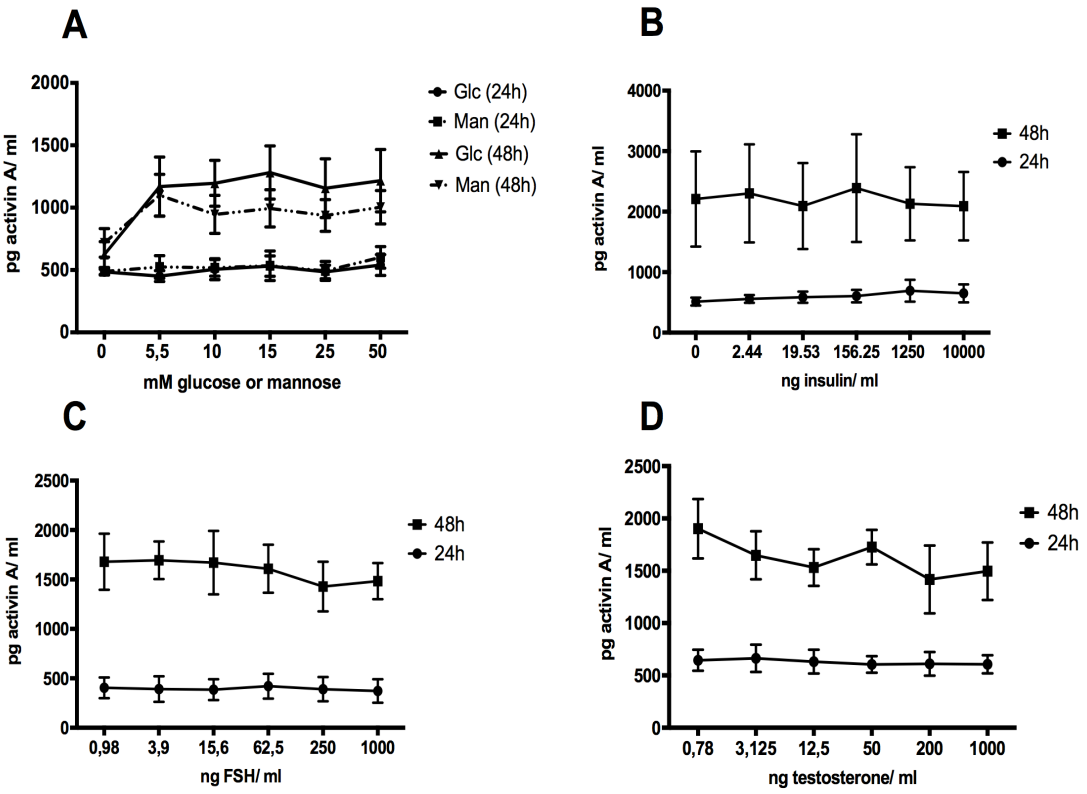

Fig. 3-17. Activin A production after dose response treatment in the WL-3 mouse Sertoli cell line.

Activin A production in the WL-3 mouse Sertoli cell line was measured via ELISA after treatment with (A) glucose or mannose, (B) insulin, (C) FSH, or (D) testosterone. n=3 experiments.

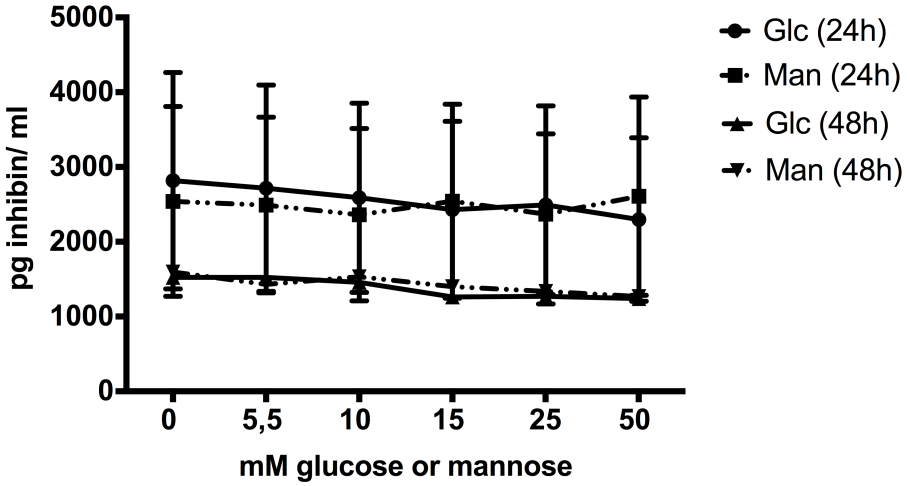

Fig. 3-18. Inhibin production after dose response treatment in the WL-3 mouse Sertoli cell line.

Inhibin production in the WL-3 mouse Sertoli cell line was measured via RIA after treatment with glucose or mannose for 24 or 48 h. n=1-2 experiments.

3.3.3 Evaluation of the effect of diabetic conditions on mouse Sertoli cells

Based on the evaluation of the dose response treatments (section 3.3.2) and review of the literature [55,68,79,126], combined treatments of glucose, insulin, and testosterone for both primary and WL-3 Sertoli cells were chosen as shown in Table 3-3.

Table 3-3. Treatment conditions for combined treatment on mouse Sertoli cells.

Treatment	1 (cntr)	2	3	4	5	6	7	8 (diab)
Glucose (mM)	5,5	25	5,5	25	5,5	25	5,5	25
Insulin (ng/ml)	5000	5000	2,44	2,44	5000	5000	2,44	2,44
Testosterone (ng/ml)	500	500	500	500	12,5	12,5	12,5	12,5

Additional concentrations of FSH were considered, but after review of the dose response treatments, which showed no effect, and review of the literature, which shows that under diabetic conditions FSH levels are not subject to change, no further

studies were performed on this topic. Hence, eight different treatment conditions were established, ranging from treatment 1 as physiological control treatment (cntr), over changing concentrations of glucose, insulin and testosterone to treatment 8, which can be considered as diabetic condition (diab). Cells were then treated over a period of 24 or 48 h and the culture medium analysed for production of activin A and inhibin (Fig. 3-19).

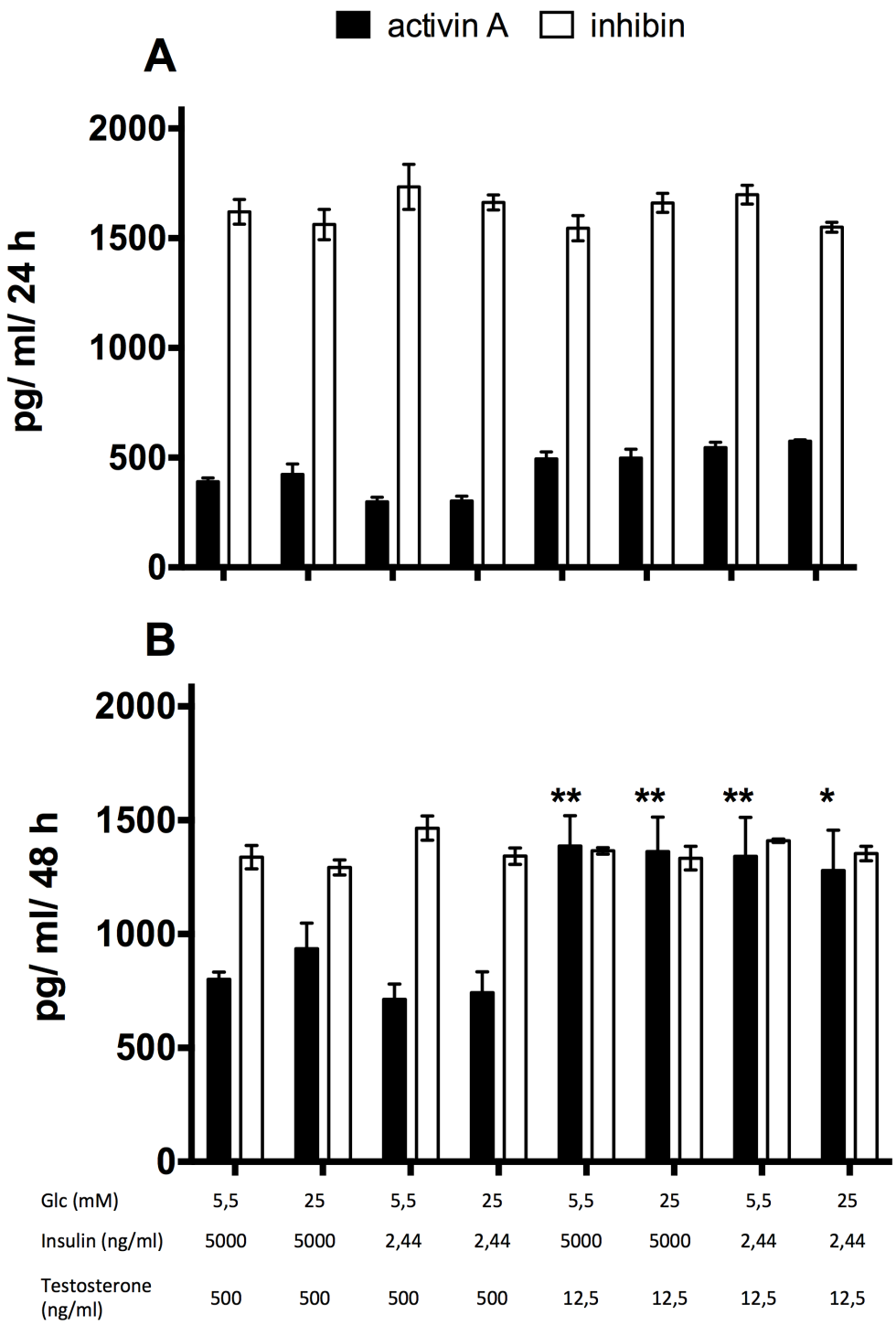

Fig. 3-19. Activin A and inhibin production after combined treatment on WL-3 cells.

Activin A and Inhibin production in the WL-3 mouse Sertoli cell line were measured via ELISA or RIA, respectively, after treatment with varying concentrations of glucose, insulin, and testosterone for (A) 24 h or (B) 48 h. n=3 experiments. Two-way ANOVA.

These results suggest that after 24 h of treatment there is only little effect with regard to activin A and inhibin, however after 48 h low concentrations of testosterone seem to induce a stronger activin A, but not inhibin response. This seems to be unaffected by changing conditions of glucose and insulin.

3.3.4 Evaluation of the effect of hyperglycaemia and increased activin A levels on mouse Sertoli cells

Since the combined treatment did not show a distinct effect of neither high glucose nor the diabetic condition on Sertoli cell function, further treatment options were considered. Results from the insulin-deficient *Ins2*$^{Akita+/-}$ mice had shown that activin A is upregulated in both non-diabetic and diabetic mice (Fig. 3-10), but only the mice that developed diabetes displayed testicular atrophy (Fig. 3-4). Hence, it was hypothesised that increased systemic activin A levels make Sertoli cells prone to glucose induced damage, and cells were treated with varying concentrations of glucose and a single dose of activin A for 24 and 48 h. The culture medium was then analysed for the production of activin A and inhibin (Fig. 3-20). While, after 48 h of treatment, activin A production showed an additive effect compared to 24 h treatment, there was no increase in production due to activin A treatment at any time point. Moreover, increasing glucose concentrations had no effect on activin A production at any time point. Other than activin A, inhibin levels remained constant over the time of treatment. Interestingly, after 48 h inhibin production was significantly downregulated by high glucose concentrations and this response was even more pronounced in the presence of activin A.

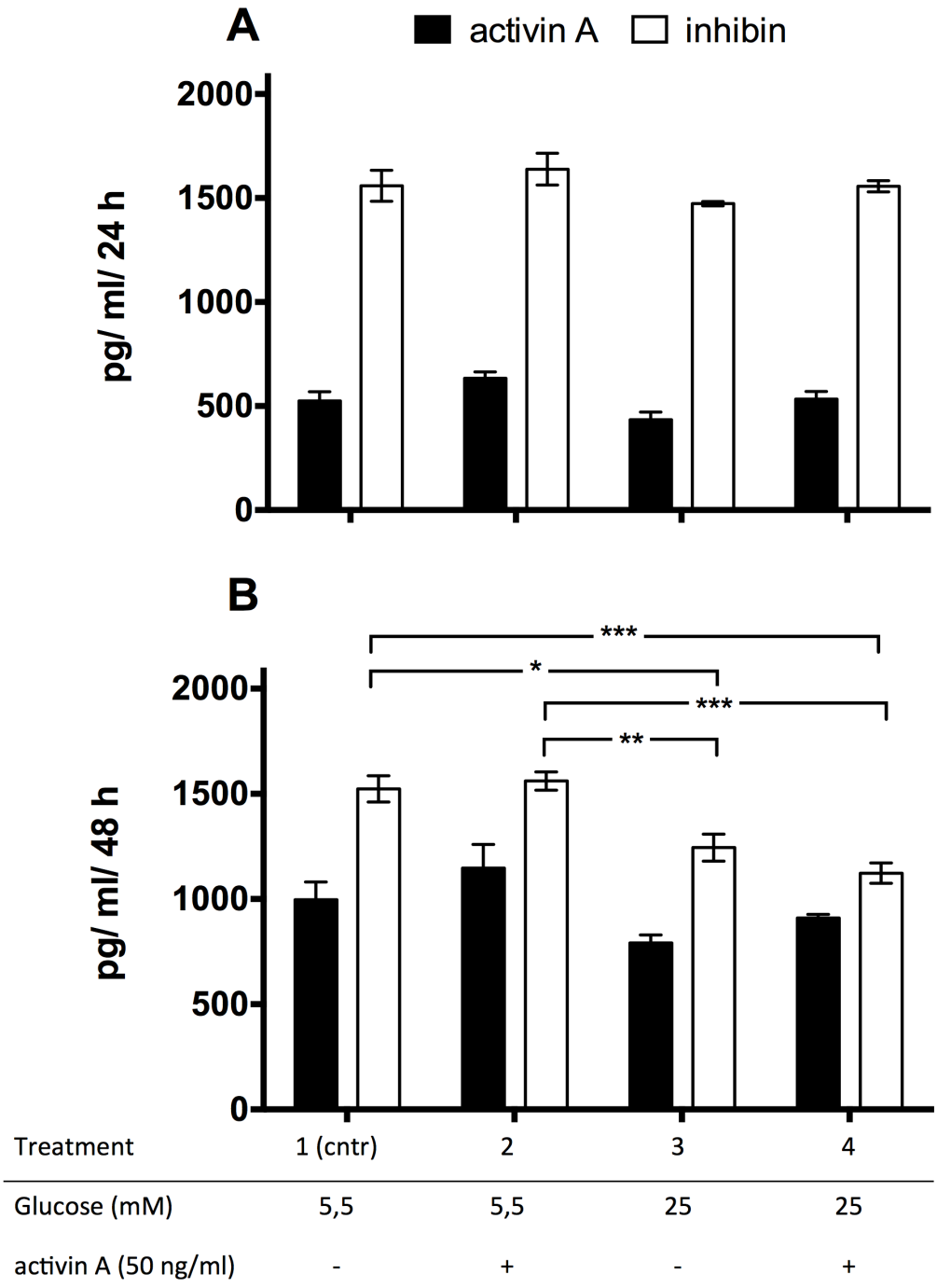

Fig. 3-20. Activin A and inhibin production after treatment with varying concentrations of glucose in the presence or absence of activin A on WL-3 cells.

Activin A and Inhibin production in the WL-3 mouse Sertoli cell line were measured via ELISA or RIA, respectively, after treatment with varying concentrations of

glucose in the presence or absence of activin A (50 ng/ml) for (A) 24 h or (B) 48 h. n=3 experiments. Two-way ANOVA.

To further investigate the impact of glucose and activin treatment on Sertoli cell function, the influence of this treatment combination on the formation of inter-Sertoli cell tight junctions was investigated by measurement of transepithelial resistance (TER). In order to determine optimal culture conditions for the measurement of TER pilot experiments were conducted using varying cell densities (0.25 and 0.5x10^6 cells per PCF insert) plated on PCF inserts with and without matrigel. Moreover, cells were monitored at different time points (-1, 0, 1, 2, 3 days) (Fig. 3-21).

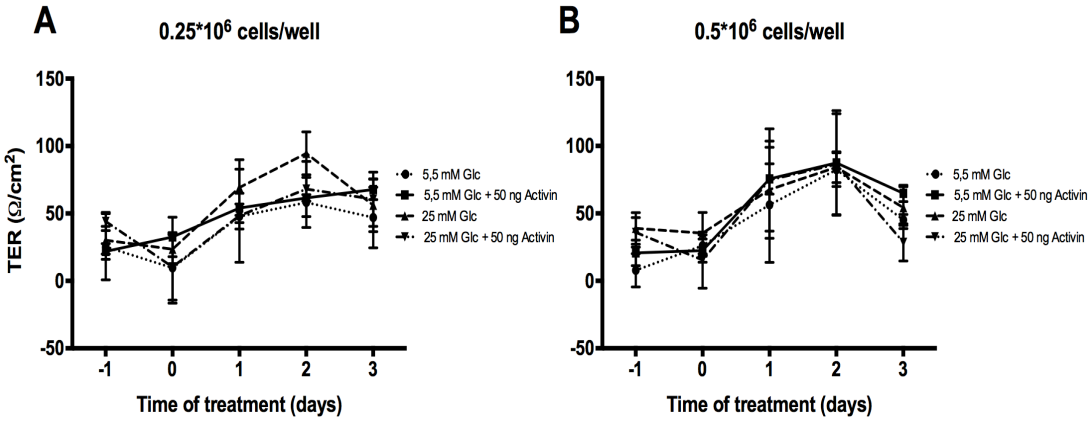

Fig. 3-21. Tight junction integrity in WL-3 cells after treatment with varying concentrations of glucose in the presence or absence of activin A.

(A and B) Tight junction integrity as determined by measuring transepithelial electrical resistance (TER) across a monolayer of WL-3 cells. WL-3 cells were seeded at 0.25x10^6 cells/well (A) or 0.25x10^6 cells/well (B). Following the formation of stable TJs for 24 h under control (medium alone) conditions WL-3 cell monolayers, cells were treated varying concentrations of glucose in the presence or absence of activin A (50 ng/ml). n=3 experiments.

A first assessment led to the conclusion, that cells grow better when the inserts are coated with matrigel. Further, a density of 0.25x10^6 cells allowed for a longer culture period. After monitoring the cells for up to 3 days after treatment, neither glucose nor activin treatment showed any difference with respect to TER. After treatment day 2, TER decreased, which was mainly due to apoptosis induced by

overgrowth. Therefore, the time points 2 and 3 days were neglected for further experiments.

To further optimize the treatment with activin A, two different treatment options were tested. In the first, activin A was added to the culture medium from the commencement of the treatment, in the second activin A was added at day 1. Moreover, cells were seeded in glucose free medium prior to the treatment (starvation). Results from this pilot run show a constant decrease in TER after treatment, regardless of the presence of activin A. Microscopic observation showed that cells were confluent at treatment day 2, however TER measurement suggests that there was no formation of tight junctions (Fig. 3-22).

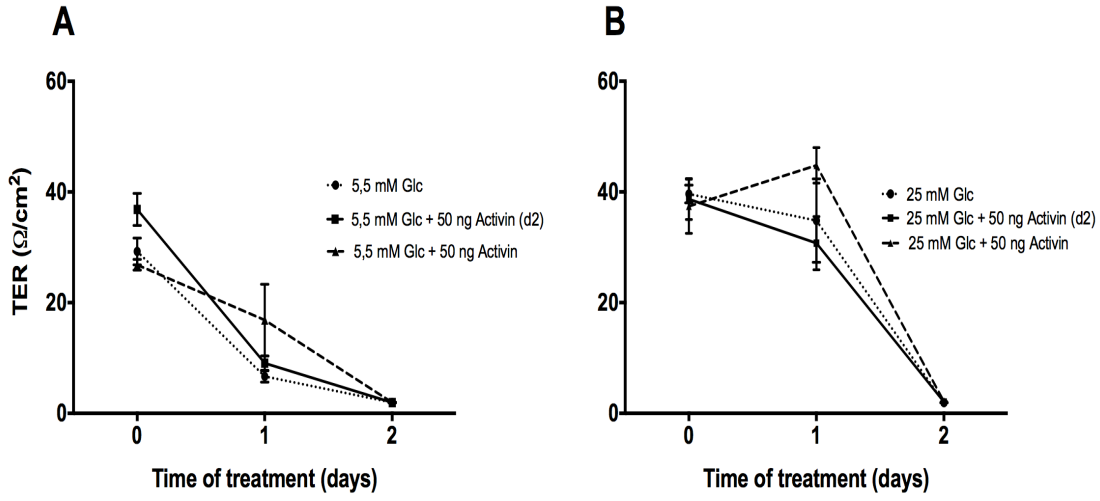

Fig. 3-22. Optimization of activin A treatment on W-3 Sertoli cells for the measurement of TER.

(A and B) Tight junction integrity as determined by measuring transepithelial electrical resistance (TER) across a monolayer of WL-3 cells. Following the formation of stable TJs for 24 h under control (medium alone) conditions WL-3 cell monolayers, cells were treated with 5.5 mM (A) or 25 mM (B) glucose in the presence or absence of activin A added at different time points. n=3 experiments.

4 Discussion

Type 1 diabetes is one of the most prominent public health threats in modern societies with rapidly rising prevalence. This is accompanied by a rise in the number of childhood and adolescent males with T1D affecting an increasing number of men in their reproductive age [246].

Up to the present time, a large number of studies have described a negative impact of T1D on male reproductive function leading to degenerative changes within the testis and epididymis, erectile dysfunction, ejaculatory dysfunction, as well as a reduction in semen volume, sperm counts, sperm motility, and altered sperm morphology [12,124]. However, the mechanisms responsible for T1D induced changes in male fertility remain to be elucidated.

Many studies in diabetic men, as well as in animal models, have indicated that T1D disrupts fertility at various levels including degenerative and apoptotic changes in spermatogenesis, altered glucose metabolism in Sertoli cells [11,136,209], reduced testosterone synthesis and secretion, erectile dysfunction, ejaculatory dysfunction, reduced libido, and impotence [12,124,136]. To date, several clinical studies as well as animal experiments have aimed to address the underlying molecular mechanisms responsible for diabetes-induced male infertility, but conclusive studies remain scarce. Suggested mechanisms include sperm DNA and mitochondrial damage [2,3], oxidative stress [164,166], atrophic changes within the epididymis [141], and a disruption of the hypothalamic-pituitary-gonadal axis [30,236].

Moreover, the unique characteristics of glucose metabolism within testicular cells make them prone to alterations under diabetic conditions. It is likely that the glucose sensing machinery as well as the hormonal control within these cells to counteract hyper- und hypoglycaemia play a crucial role in the subfertility and/or infertility associated to DM [12].

Besides its association with male reproductive function, T1D has recently been shown to have features of an inflammatory disease with levels of inflammatory markers correlating with the glycaemic status in T1D patients [111,134]. Moreover, the immune imbalance in autoimmune diseases such as T1D is known to cause inflammatory processes [20].

Along with their role in testicular physiology, activins are also known as growth

factors and cytokines that regulate inflammation and immunological mechanisms [109,111,128,134]. However, little is known about the role of the activins in diabetes mellitus. To this point, serum activin A levels were reported to positively correlate with blood glucose levels in diabetic patients and patients with myocardial infarction. Further, activins A and B, as well as their binding protein follistatin have been shown to be involved in the regulation of glucose metabolism by promoting the differentiation of insulin-producing and insulin-responsive cells, and regulating the function of the differentiated cells [15,62,104,191,260,293]. Hence, the activins could provide an important link between T1D and male infertility.

In the course of this work, the hypothesis that hyperglycaemia may affect testicular function by destabilizing the testicular equilibrium of the activin family of proteins and, thus, induces intratesticular inflammation was examined. To address this aim, hyperglycaemia induced changes within three different models were investigated: the model organism *C. elegans*, male heterozygous *Ins2*$^{Akita+/-}$ mice, and cultured Sertoli cells.

4.1 High glucose effects reproductive outcome in *C. elegans* nematodes

In the present work, the *C. elegans* mutant strain *mev-1* (methyl viologen sensitive) was used as model organism to study hyperglycaemia-induced infertility. These mutant nematodes carry a mutation within the cytochrome b subunit of succinate dehydrogenase resulting in excessive mitochondrial superoxide production and premature death [121]. This in turn closely resembles the metabolic situation of diabetic patients who exhibit a deficiency in the signalling of reactive oxygen species (ROS) leading to the initiation of autoimmune diabetes as well as diabetes induced morphological changes in mitochondria, which are closely linked to the presence of superoxide anion [159,266]. *C. elegans* exists as self-fertilizing hermaphrodite and as male, allowing easy generation and maintenance of homozygous populations with a large number of progeny, which made it a suitable model for the purpose of this study [9].

In order to simulate severe hyperglycaemia, which occurs as a consequence of β-cell destruction in T1D patients, nematodes were incubated in liquid NGM containing *E. coli* as food source as well as 100 mM glucose. The use of a liquid culture medium

ensured the adequate uptake of glucose through a continuous delivery to the intestinal tract by the pumping activity in the worm pharynx [103].

Most interestingly, glucose treatment resulted in a significant decrease in brood size, suggesting a functional role of glucose within the reproductive cycle of *C. elegans* nematodes. This effect, however, did not correlate with changes in Sma/Mab pathway signalling. This pathway is known to be involved in the regulation of body size, reproductive aging, the development of male-specific sensory rays as well as copulatory spicules, and is closely related to BMP subfamily ligands and signal transducers as they are found in mice and humans [98].

However, it is well known that between TGF-β secreting and receiving cells, the ligands do not simply diffuse to their receptors on the receiving cell, but are tightly regulated [98]. Hence, even though hyperglycaemia had no effect on the ligands and signal transducers themselves, it is possible that they interact via the extracellular regulation of ligand activity.

Besides the Sma/Mab pathway, the DAF-7 pathway is known as a further TGF-β signalling pathway in *C. elegans* nematodes. Still, although components of this pathway have common sequence features with the TGF-β/Activin/Nodal/GDF pathway components, it is mainly known for its regulatory role within the dauer/continuous development switch [98]. Only few studies have reported a role within the negative regulation of the proliferative pool of germ cells, involving an unknown downstream signalling pathway [98,200]. Hence, the DAF-7 pathway seems to play a minor role in the reproduction of *C. elegans* nematodes, leaving the Sma/Mab pathway as a more suitable target for investigation in the context of hyperglycaemia induced infertility.

Previous studies have shown, that hyperglycaemia induces a reduction in brood size in *C. elegans* nematodes [224,265], with recent work from Teshiba et al. suggesting, that this effect is dependent on serotonergic signalling [265].

Taken together these findings show that hyperglycaemia has a negative effect on the reproductive outcome in *C. elegans*, however, evidence that this is linked to disruptions within the TGF-β signalling pathway was not found. Therefore, a higher organism was used to investigate this interaction in more detail.

4.2 Reproductive changes in male *Ins2*$^{Akita+/-}$ mice

The Akita mouse is a model of T1D that results from a mutation in the *Ins2*

gene. This mutation leads to a misfolded protein product, which accumulates in the endoplasmic reticulum (ER), causing ER stress and, ultimately, death of the insulin producing β-cells of the pancreas [282]. The diabetic Akita mouse is thus similar to humans with T1D, which is caused by an autoimmune destruction of the β-cells of the pancreas [1]. The Akita model also displays a severe onset of diabetes, similar to untreated diabetes in human adults, and does not have the drug induced toxicity of a toxin-induced model, which makes the Akita mouse model a unique model to study diabetes induced male infertility.

In this study, the heterozygous *Ins2*^{Akita} mice, bred in a colony in Mannheim (Germany), were used to investigate long-term effects of insulin deficiency and hyperglycaemia on the function of the activins within the reproductive tract. These mice have a phenotype penetrance of 50 %, which makes this model unique as it allows to study the effects of long-term hyperglycaemia by comparison of mice from an identical litter with near-normal glycaemia (<14.0 mmol/l non-fasting blood glucose concentrations) or severe hyperglycaemia (>33.3 mmol/l).

In order to investigate the working hypothesis, C57Bl/6J wild type mice, as well as non-diabetic, and diabetic *Ins2*$^{Akita+/-}$ mice were analysed for general parameters, such as body weight, blood glucose levels, and HbA1c value. Moreover, reproductive parameters like testis weight, testicular morphology, and sperm morphology were assessed. To study the regulation of the activins, mRNA and protein content of targets of the activin family was investigated in testis and epididymis samples. Lastly, the involvement of inflammation and the HPG-axis was assessed by analysis of inflammatory cytokines in testis samples and hormones in serum.

The major finding of these studies was that prolonged exposure to elevated blood glucose was associated with progressive testicular disruption in *Ins2*$^{Akita+/-}$ mice, based on the observation that only the *Ins2*$^{Akita+/-}$ mice that developed diabetes exerted progressive decrease in testis weight and increased evidence of spermatogenic disruption with age. Immunohistochemical determination of the number of Sertoli cells present within the testis revealed that the testis phenotype is not due to differences in this parameter. However, it is possible that the density of Sertoli cells is unaffected, but the length of seminiferous tubules and, therefore, total Sertoli cell number is reduced. This, in turn, would influence testicular weight as well as sperm output. This hypothesis is further supported by sperm analysis data, revealing that the *Ins2*$^{Akita+/-}$ mice show a significantly lower number of sperm compared to wild type controls and that diabetic

*Ins*2$^{Akita+/-}$ mice have a higher percentage of misshaped sperm heads compared to both controls. However, in light of the testicular morphology, which appeared to be grossly normal, the drastic reduction in sperm number and the increase in sperm head failure seems surprising and suggests that further disruption takes place in distal parts of the reproductive tract. Since activin A protein was solely upregulated in the epididymides of diabetic *Ins*2$^{Akita+/-}$ mice, it could be that activin signalling is also dysregulated within the epididymis, further influencing sperm maturation, and, ultimately, sperm morphology and concentration. To examine this further, it would be of interest to investigate activin signalling within the epididymides of *Ins*2$^{Akita+/-}$ mice as well as changes in sperm themselves, such as DNA fragmentation or acrosome formation.

Further, data from the Johnsen score count demonstrates that diabetic *Ins2*$^{Akita+/-}$ mice exhibit an increase in lower score counts. These changes might be due to acute or chronic adverse effects of severe hyperglycaemia. However, even though there appear to be substantial changes in testicular function within the heterozygous *Ins*2^{Akita} mouse model, these changes seem not to result in complete infertility in these mice. This finding is in contrast to the studies of Schoeller et al. who reported infertility in heterozygous *Ins*2^{Akita} mice at the age of 24 weeks [235]. One explanation for these conflicting results might be the different genetic background, since mice on an FVB background were used previously, whereas mice on a C57Bl/6J background were used in the present study. Mouse strain differences have been implicated in the susceptibility of various factors [151,278]. Besides the involvement of moderate elevations of blood glucose concentrations, the reduction of effective circulating insulin levels could be another explanation for the observed effect within the testis. This is supported by recent findings that show that the diabetic genotype determines the balance of T-cell inflammatory vs. regulatory responses to insulin in peripheral blood of diabetic patients [177]. Hence, one could presume that insufficient insulin levels trigger inflammatory responses within the testis of *Ins2*$^{Akita+/-}$ mice. Moreover, it is known that the regulation of insulin levels directly impacts on the expression of the insulin receptor (InsR), as well as the receptor for insulin like growth factor 1 (Igfl1r), leading to the activation of downstream signalling pathways involved in proliferation, differentiation, metabolism, and cell survival [24,262]. Thus, upregulation of insulin results in the downregulation of InsR and Igfl1r, whereas downregulation of insulin might results in the upregulation of both receptors [88,89,275]. Recent studies suggest that this specifically affects Sertoli cell function. Thus, a downregulation of the insulin receptors results in a 75 % reduction in

testis size and daily sperm production in adult testes [206].

However, testicular disruption was only observed in mice with an extreme elevation of glucose (>14 mmol/l), while induction of inflammatory cytokines, as determined by Il-1α, IL-1β, TNF-α and IL-10 levels, was not found. This in turn suggests that the testicular damage is more likely to be related to the increased glucose rather than inflammation related to the insufficient insulin levels.

Activins have recently been reported to play an important role in glucose metabolism by regulating the differentiation and activity of the insulin-producing pancreatic β-cells, as well as the response of insulin target cells [15,48,49]. Additionally, they have been proposed to modulate events involved in insulin sensitivity in a tissue dependent manner and therefore regulate whole-body insulin responsiveness [38,293,294,296]. Moreover, our group has recently shown that activin A levels in the blood of patients with T2D show a positive correlation with increasing severity of the disease [293]. Therefore, the involvement of activins in the development and onset of diabetes related male subfertility and/or infertility seems likely. Here it was shown that with blood glucose concentrations rising 2.9-fold from 76 ± 3 to 223 ± 8 mg/dl (4.2 ± 0.2 to 12.4 ± 0.4 mmol/l) testicular activin A levels are significantly upregulated in *Ins2*$^{Akita+/-}$ mice, but did not rise further with the higher magnitude of hyperglycaemia. It seems that the severely diabetic phenotype is not associated with a further increase as compared to mild diabetes indicating that testicular activin A levels may be linked more closely to moderate elevations of blood glucose concentrations and/or the genetic background of the *Ins2*$^{Akita+/-}$ mouse model.

In contrast to activin A levels, activin B production was significantly down regulated within *Ins2*$^{Akita+/-}$ mice at 12 weeks of age. While the role of activin B in the regulation of inflammation, as well as in testis function, is completely unknown, it was previously shown that levels of activin B within the testis of wild type mice appear to be about 10-fold higher than those of activin A. However, activin B is about 10-fold less potent than activin A in several of its effects, and activin B is suggested to act as a weak agonist of activin A [291]. Hence, the inverse regulation of activin A and activin B found in this study might suggest that each compensates for the effect of the other. This is further supported by the fact that neither of the main regulators of activin activity (inhibin and follistatin) was substantially affected by the diabetic conditions or elevated activin A levels. Most interestingly, only in diabetic *Ins2*$^{Akita+/-}$ mice were mRNA levels

of the activin receptor subunit *Acvr1b* significantly upregulated at 12 weeks of age, whereas the receptor subunits *Acvr2a* and *Acvr2b* were significantly downregulated at 24 or at both 12 and 24 weeks of age, respectively. This suggests that, even though the protein levels of activin A were equally increased in both *Ins*2$^{Akita+/-}$ genotypes, only within the diabetic mice was transmission of the activin signal disrupted. This is further supported by the finding that Smad4 was significantly upregulated in diabetic *Ins*2$^{Akita+/-}$ mice, likely due to an increased phosphorylation of Smad3 in this group. A selective use of Smad second messengers by activins has recently been proposed in insulin secretion studies [16,294]. However, these studies suggested that activin A favours Smad2, which is in contrast to our findings [16,294]. Nonetheless, overexpression of Smad3, as it was found in the present study, but not Smad2, was associated with a decrease in glucose stimulated insulin secretion in pancreatic islets [16,294]. This might suggest that the increase in pSmad3 further exacerbates the detrimental effects of hyperglycaemia within the *Ins*2$^{Akita+/-}$ mouse model. To strengthen this finding, future studies would benefit from interventions within the *Ins*2$^{Akita+/-}$ mice using follistatin treatment to revoke the dysregulation of the activins. If this approach would result in a normalized activin receptor expression as well as Smad phosphorylation, the activins could be considered major regulators of diabetes-induced male reproductive dysfunction. Another approach to explore this proposal would be a conditional activin knockout in T1D mice, to study the local molecular dysregulation of the activin signalling.

A scheme of the proposed mechanisms of activin action in different stages of hyperglycaemia is shown in Fig. 4-1.

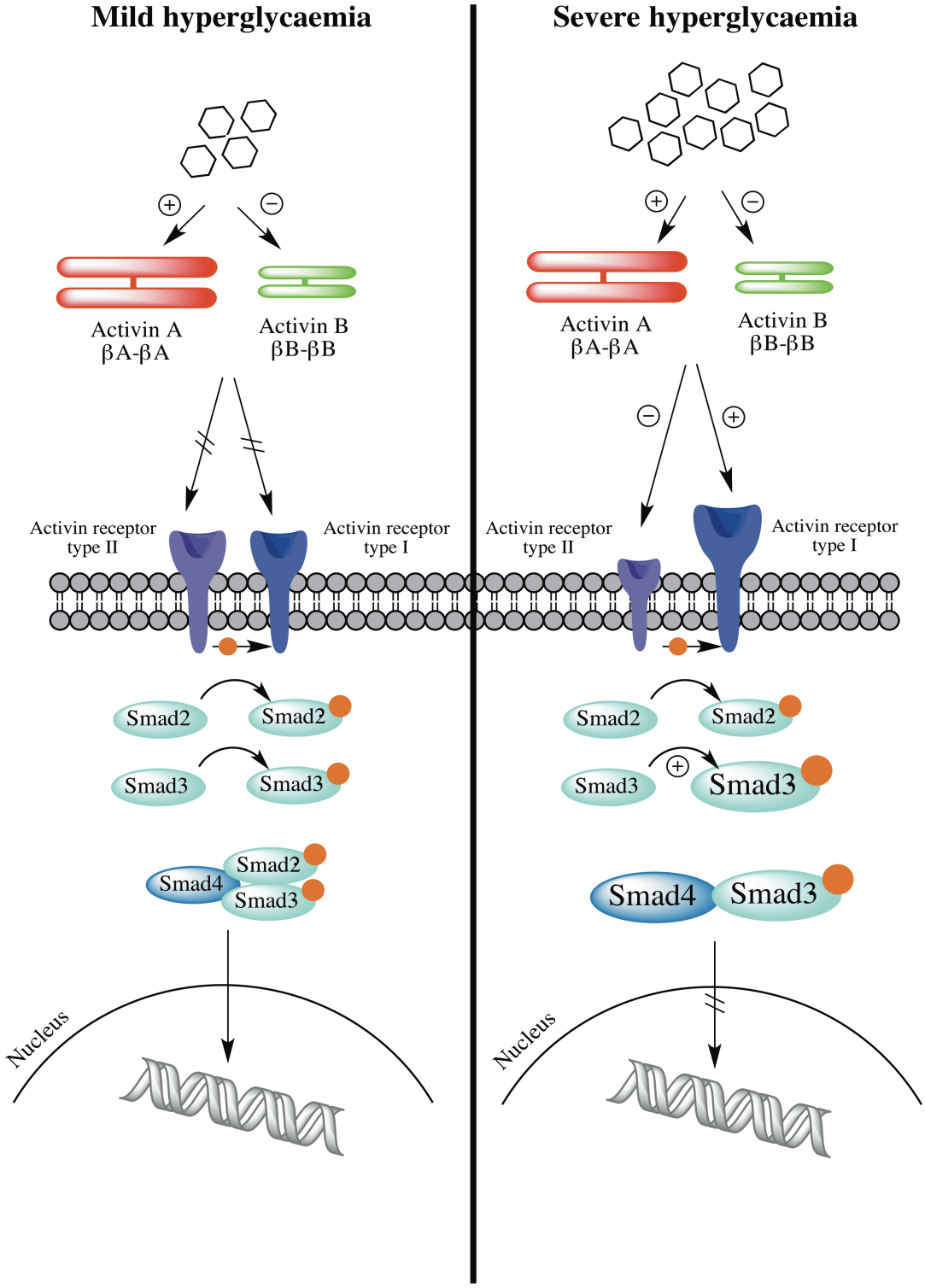

Fig. 4-1. Proposed actions of activin in the testis in different grades of hyperglycemia.

Mild hyperglycaemia (left panel), as investigated in non-diabetic *Ins2*$^{Akita+/-}$ mice, leads to an upregulation of activin A and a downregulation of activin B without further effect on the Smad signalling pathway. Severe hyperglycaemia (right panel), as investigated in diabetic *Ins2*$^{Akita+/-}$ mice, leads to an upregulation of activin A and a downregulation of

activin B, affecting activin receptor types II and I and promoting Smad signalling via an increase in phosphorylated of Smad3 and Smad4.

In spite of the increase in testicular activin A levels and the upregulation in Smad4, protein expression of the pro-inflammatory cytokine IL-6 and mRNA expression of the pro-inflammatory cytokines IL-1β and TNF-α remained unchanged in *Ins2*$^{Akita+/-}$ mice, suggesting no further inflammatory response to activin action.

Previous studies on T1D mice, including the *Ins2*$^{Akita+/-}$ mouse model, have suggested that the observed testicular damage results from impairment in production of FSH and LH by the pituitary, the latter being consistent with a loss of androgen support for spermatogenesis [30,166,235,236]. In contrast to these earlier findings, the present study shows that testicular damage in the heterozygous *Ins2*^{Akita} mouse model does not correlate with changes in the HPG axis as shown by protein levels for testosterone and LH.

Besides investigations on the testis, the activins were also examined in tissue homogenates of epididymides in order to investigate their actions along the reproductive tract. These data revealed that, in contrast to activin A production within the testis, its concentrations in epididymal samples show a significant upregulation in diabetic *Ins2*$^{Akita+/-}$ mice compared to controls, suggesting that, even though there seems to be no effect of diabetes on activin A production within the testis, there is a strong effect of diabetes within the epididymis of *Ins2*$^{Akita+/-}$ mice. In contrast to activin A production, neither activin B, nor inhibin, nor follistatin exhibited significantly different levels compared to the testis. It is further noteworthy, that the levels, for both activin A and activin B, are about 5 fold higher in the epididymis compared to the testis, which makes it likely that the actions of the activins within the epididymis are more pronounced, especially in terms of inflammation.

Taken together, these data show that in mice that are heterozygous for the *Ins2*^{Akita} gene, hyperglycaemia leads to an upregulation of activin A levels and a downregulation of activin B levels, while the levels of the antagonists FST and inhibin remain unchanged. These effects were already observed at moderate elevations of blood glucose concentrations. Of interest however was that activin downstream signalling, with regard to activin receptor expression and Smad signalling, was only affected in mice with extreme elevation of glucose (>14 mmol/l). These mice also exhibited progressive testicular disruption.

Moreover, the observed effects were not linked to a disruption in pituitary LH support or reduced testosterone production. The testicular damage may have been exacerbated by an upregulation of IL-6 and activin A, or dysregulation of activin signalling, as IL-6 and activin are involved in the fine control of Sertoli cell function during spermatogenesis [109].

Further, it is likely that the detrimental effects of activin become more pronounced in the distal parts of the reproductive tract, as diabetic *Ins2*$^{Akita+/-}$ mice showed an upregulation of activin A within the epididymis.

This is the first study to demonstrate that chronic elevation of glucose during diabetes may have a direct inhibitory effect on spermatogenesis. The activins are likely to be involved in diabetes-induced male infertility, but the mechanisms by which this occurs requires further investigation.

4.3 Impact of hyperglycaemia on Sertoli cell function

Changes in glucose metabolism as well as insulin signalling are known to disturb male reproduction by affecting the regulation of the energy metabolism of Sertoli cells by regulating the uptake of nucleotides (ATP, GTP, UTP), and the secretion of transferrin and lactate. Hence, both spermatogenesis and the blood testis barrier can be disturbed by these conditions [12,41,95,123,249].

Furthermore, glucose is a crucial energy substrate in order to maintain spermatogenesis, a metabolically active process, which requires tight cooperation among testicular cells [11]. In this context, the Sertoli cells play a crucial role in providing pyruvate and glycolytic converted lactate for developing germ cells [11,12]. Thus, disturbance in glucose metabolism, as in diabetic individuals, can lead to major disruptions in the cellular organisation, ranging from vacuolization to a high degree of degeneration. This in turn, has dramatic consequences for the cellular interaction during spermatogenesis [12].

Activins are known to be involved in the fine control of Sertoli cell function during spermatogenesis and were previously identified as a factor capable of reprogramming Sertoli cells to an immature, dedifferentiated phenotype [109,184]. With regard to diabetes, activins A and B, as well as their binding protein follistatin have been shown to be involved in the regulation of glucose metabolism and inflammation [15,62,104,191,260,293].

Therefore, the impact of hyperglycaemia on Sertoli cell function was investigated using *in vitro* approaches using primary mouse Sertoli cells as well as an immortalized mouse Sertoli cell line (WL-3). This allowed the compensation of disadvantages that are associated with the use of a single model, since primary mouse Sertoli cells can only be isolated from immature, juvenile mice and, thus, might lack the properties of adult Sertoli cells, whereas immortalised Sertoli cells show proliferation, which is not seen under physiological conditions in adult mice [264].

In order to examine the impact of hyperglycaemia cells were first treated with varying doses of glucose, insulin, testosterone, or FSH to determine optimal culture conditions. Thereafter, a treatment combination of glucose, insulin, and testosterone was chosen to mimic different stages of diabetes ranging from physiological to diabetic.

Of interest, none of the single treatments resulted in changes in activin A production. This observation was made in both primary and immortalised cells. Hence, further experiments were only conducted with the use of the cell line. With the combined treatment, however, WL-3 cells reacted with an increase in activin A production when low concentrations of testosterone were present. This was not accompanied by changes in protein levels of the activin antagonist inhibin. Furthermore, changing concentrations of glucose and insulin had no effect on either of the proteins.

This suggests that within Sertoli cells, activin A is regulated by changing concentrations of testosterone, but not glucose or insulin. This is in accordance with recent studies that show that the metabolic cooperation of testicular cells is tightly controlled by hormones, such as testosterone [13,90,209]. Therefore, any disruption in hormonal control of Sertoli cells can lead to changes in spermatogenesis [13].

Furthermore, the formation of tight junctions under diabetic conditions was investigated. Preliminary experiments showed that neither varying concentrations of glucose, nor the addition of activin A had an effect on tight junction formation in Sertoli cells. However, the majority of publications on this method uses primary cells to investigate tight junction formation, whereas here, immortalized WL-3 Sertoli cells were used. Thus, it is likely, that the experimental conditions need further optimization before the results can be evaluated.

Glucose is a crucial metabolite for the maintenance of spermatogenesis and blood-to-germ cells transport of glucose and other metabolic intermediates is highly controlled. This is mainly due to the presence of the blood–testis barrier [219], across which glucose transporters (GLUTs) ensure the passive transport of glucose. To date,

GLUT1, GLUT3 and GLUT8 isoforms have been identified and were shown to regulate glucose uptake by Sertoli cells [54,90]. In line with this, previous studies have demonstrated that disruptions in glucose or insulin metabolism lead to an adaptation within glucose transport machinery in order to ensure the appropriate lactate production [193,215]. Thus, it is likely that whilst changing concentrations of glucose and insulin had no effect on activin and inhibin production, Sertoli cell function is disrupted at the level of the glucose transport machinery.

A limitation of the use of an *in vitro* culture system is that, *in vivo*, Sertoli cells are highly sensitive to their environment and are surrounded by numerous germ cells at different stages of spermatogenesis. Further, they are under the influence of Leydig and peritubular myoid cells as well as the presence of local and endocrine factors. Thus, results derived from *in vitro* studies using Sertoli cell lines or primary Sertoli cells should be taken with caution since they may not necessarily reflect the *in vivo* situation.

5 Summary

Type 1 diabetes mellitus is a chronic, lifelong condition with worldwide increasing incidence. Furthermore, it affects a growing number of men of reproductive age since 90 % of these patients are diagnosed before the age of 30. Numerous studies have indicated that diabetes mellitus disrupts fertility at various levels including altered spermatogenesis, degenerative and apoptotic changes in testes, and altered glucose metabolism in Sertoli cells, but little is known about the underlying mechanisms.

In the present work, the *mev-1* mutant of the nematode *Caenorhabditis elegans*, the *Ins2*$^{Akita+/-}$ mouse model, as well as cultured Sertoli cells were used to investigate whether hyperglycaemia alters the secretory patterns and actions of the activin family of proteins.

It was found that glucose at a concentration of 100 mM significantly reduced brood size in *mev-1* nematodes. Most interestingly, diabetic *Ins2*$^{Akita+/-}$ mice showed progressive testicular disturbance, with a 30 % reduction in testis weight at 24 weeks of age, which correlated with blood glucose and HbA1c values. Diabetic mice showed significantly reduced seminiferous tubule diameters and increased spermatogenic disruption, although testes morphology appeared grossly normal. Serum LH and testosterone were similar in all groups. All *Ins2*$^{Akita+/-}$ mice showed elevation of the testicular inflammatory cytokines activin A and IL-6 at 12 and 24 weeks of age, while other key inflammatory cytokines were unaffected. Conversely, intratesticular activin B was downregulated at both time-points, while the activin regulatory proteins, follistatin and inhibin, were unchanged. At 24 weeks, activin type 2 receptor subunit expression was reduced in the diabetic mice, but Smad signalling was enhanced. Finally, investigations on *in vitro* cultured Sertoli cells did not show an effect of hyperglycaemia on activin A regulation or the formation of tight junctions.

In conclusion the present work demonstrates that hyperglycaemia disrupts fertility in both *mev-1* nematodes and the *Ins2*$^{Akita+/-}$ mouse model. Moreover, it was shown that prolonged exposure to elevated blood glucose in the *Ins2*$^{Akita+/-}$ mice leads to progressive testicular disruption, which may be exacerbated by dysregulation of testicular activin activity rather than by dysregulation of the hypogonadal pituitary gonadal-axis.

6 Zusammenfassung

Typ 1 Diabetes mellitus ist eine chronische, lebenslange Erkrankung mit weltweit steigender Inzidenz. Ferner ist eine steigende Zahl an Männern im reproduktiven Alter betroffen. Zahlreiche Studien weisen darauf hin, dass T1D die männliche Fertilität auf verschiedenen Ebenen, darunter Veränderungen in der Spermatogenese und ein veränderter Glucose Stoffwechsel in Sertoli Zellen, beeinflusst. Jedoch ist wenig über die zugrundeliegenden Mechanismen bekannt.

Im Rahmen dieser Arbeit wurden die *mev-1* Mutante der Nematode *Caenorhabditis elegans*, das *Ins2*$^{Akita+/-}$ Mausmodel sowie kultivierte Sertoli Zellen verwendet, um zu untersuchen, ob Hyperglykämie die Sekretionsmuster und Funktionen der Activin Proteinfamilie verändert.

Es konnte gezeigt werden, dass eine Glucosekonzentration von 100 mM die Wurfgröße in *mev-1* Nematoden erheblich vermindert. Darüber hinaus wiesen diabetische *Ins2*$^{Akita+/-}$ Mäuse eine progressive testikuläre Störung mit einer 30 %igen Reduktion des Hodengewichts im Alter von 24 Wochen auf. Diese korrelierte mit den Blutglucose und HbA1c Werten. Diabetische Mäuse zeigten signifikant reduzierte Tubulidurchmesser sowie vermehrte Störungen in der Spermatogenese. Serumwerte für LH und Testosteron waren in allen Gruppen ähnlich. Alle *Ins2*$^{Akita+/-}$ Mäuse hatten erhöhte Werte für die inflammatorischen Zytokine Activin A und IL-6, während andere Zytokine unbeeinträchtigt blieben. Im Gegensatz dazu war intratestikuläres Activin B herunterreguliert, während die regulatorischen Proteine Follistatin und Inhibin unverändert blieben. Im Alter von 24 Wochen wiesen diabetische Mäuse eine Reduktion des Activin Typ 2 Rezeptors auf, während der Smad Signalweg verstärkt war. Letztlich konnten die Untersuchungen an *in vitro* kultivierten Sertoli Zellen keine Wirkung von Hyperglykämie auf die Regulation von activin A oder die Formation von tight junctions nachweisen.

Zusammenfassend wurde in der vorliegenden Arbeit gezeigt, dass Hyperglykämie die Fertilität sowohl in *mev-1* Nematoden als auch in *Ins2*$^{Akita+/-}$ Mäusen beeinträchtigt. Ferner wurde nachgewiesen, dass, im *Ins2*$^{Akita+/-}$ Model, andauernde Einwirkung von erhöhtem Blutzucker zu progressiven Störungen im Hoden führt, welche möglicherweise durch eine Dysregulation der testikulären Activin Aktivität verstärkt wird.

List of abbreviations

ActRIIA	Activin receptor 2 A
ActRIIB	Activin receptor 2 B
A.D.	Anno Domini
AGE	Advanced glycation endproduct
ALX	Alloxan
ALK	Anaplastic lymphoma kinase
AMH	Anti-müllerian hormone
AR	Androgen receptor
APC	Antigen presenting cells
ATP	Adenosine-tri-phosphate
BG	Blood glucose
BMI	Body mass index
BMP	Bone morphogenetic protein
BSA	Bovine serum albumin
BTB	Blood-testis-barrier
BW	Body weight
C. elegans	Caenorhabditis elegans
CGC	Caenorhabditis Genetics Center
CGRP	Calcitonin gene-related peptide
CML	Carboxymethyl-lysine
C-peptide	Connecting peptide
CTS	Cataract-prone subline
CYB5A	Cytochrome *b*5A
CYP	Cytochromes P450
DAB	Diaminobenzidine
dbl-1	Drosophila decapentaplegic (Dpp) and bone morphogenetic protein (BMP)-like-1 gene, homologous to Smad-1 in humans
DHEA	Didehydroepiandrosterone
DM	Diabetes mellitus
DMEM	Dulbecco's Modified Eagle's Medium
DNA	Deoxyribonucleic acid
DR	Diabetic retinopathy

dsDNA	Double stranded deoxyribonucleic acid
E. coli	Escherichia coli
ED	Effective dose
ELISA	Enzyme-linked immunosorbent assay
ENU	N-ethyl-N-nitro-sourea mouse mutagenesis project
ER	Endoplasmic reticulum
ERG	Electroretinogram
ESRD	End-stage renal disease
FST	Follistatin
FDX1	Ferredoxin 1
FDXR	Ferredoxin Reductase
FSH	Follicle-stimulating hormone
GAD65	Glutamic acid decarboxylase 65
GAR	Goat anti-rabbit IgG
GnH	Gonadotropin
GnRH	Gonadotropin releasing hormone
GDF	Growth and differentiation factor
GDNF	Glial-cell-derived neurotrophic factor
GSIS	Glucose stimulated insulin secretion
GTP	Guanosine-tri-phosphate
HbA1c	Glycated hemoglobin, hemoglobin A1c
HLA	Human leukocyte antigen
HPG-axis	Hypothalamic-pituitary-gonadal axis
hr	Human recombinant
HRP	Horse reddish peroxidase
HSB	High saline bicarbonate buffer
HSD	Hydroxysteroid dehydrogenases
IA	Insulin antibodies
IA-2	Insulinoma antigen-2
ICSI	Intracytoplasmic sperm injection
IGF-1	Insulin-like growth factor-1
IgG	Immunoglobulin G
IFIH1	Interferon-induced with helicase C domain 1
IFNγ	Interferon γ

IL	Interleukin
IL2RA	Interleukin-2 receptor-α
Ins	Insulin gene
Ins1	Preproinsulin 1
Ins2	Preproinsulin 2
Insl3	Insulin-like growth factor 3
IT	Insulin therapy
IVF	*In vitro* fertilization
LH	Luteinizing hormone
LHCGR	Luteinizing hormone–chorionic gonadotropin receptor
LVMV	Left ventricular mass/ volume
MDA5	Melanoma differentiation-associated protein 5
Mev-1	Methyl viologen sensitive-1
MHC	Major histocompatibility complex
MI	Myocardial infarction
MODY	Maturity onset diabetes of the young
mtDNA	Mitochondrial deoxyribonucleic acid
nDNA	Nuclear deoxyribonucleic acid
NGM	Nematode growth medium
NOD	Non-obese diabetic mouse
NK-cells	Natural killer cells
OAD	Oral anti-diabetica
OD	Optical density
OGTT	Oral glucose tolerance test
OHdG	Hydroxydeoxyguanosine
PBS	Phosphate buffered saline
PEG	Polyethylene glycol
PenStrep	Penicillin-streptomycin
PC	Prohormone convertase
PCR	Polymerase chain reaction
POR	P450 Oxidoreductase
ppiA	*Peptidylpropyl isomerase A*
PTPN22	Protein tyrosine phosphatase, non-receptor type 22
PVDF	Polyvinylidene fluoride

qRT-PCR	Quantitative reverse transcriptase polymerase chain reaction
RAGE	Receptor for advanced glycation endproducts
RGC	Retinal ganglion cell
RIA	Radioimmunoassay
RNA	Ribonucleic acid
RNAi	Ribonucleic acid interference
ROS	Reactive oxygen species
RT	Room temperature
RT-PCR	Reverse transcriptase polymerase chain reaction
SAPE	Streptavidin-Phycoerythrin
SBTI	Soybean trypsin inhibitor
SDS	Sodium dodecyl sulphate
SDS-PAGE	Sodium dodecyl sulphate poly acrylamide gel electrophoresis
SI	Spermatogenesis index
SLC	Solute carrier family
Sma	small body size gene
Smad	Contraction of Sma (small body size) and Mad (Mothers against decapentaplegic)
SNP	Single-nucleotide polymorphisms
SOX-9	SRY-Box-9
SRP	Signal-recognition particle
SRY	Sex determining region of the Y chromosome
SSC	Spermatogonial stem cells
StAR	Steroidogenic acute regulatory protein
STZ	Streptozocin
TAC	Total antioxidant capacity
TAD	Triton assay diluent
TCR	T-cell receptor
TER	Transepithelial resistance
TGF-β	Transforming growth factor-β
Th1	Type 1 helper cells
Th2	Type 2 helper cells
TLR	Toll-like receptors
TMB	Tetramethylbenzidine

TNF-α	Tumor necrosis factor-α
T-reg	Regulatory T-cells
TUNEL	TdT-mediated dUTP-biotin nick end labelling
TW	Testis weight
T1D	Type 1 diabetes
T2D	Type 2 diabetes
UTP	Uridine-tri-phosphate
WHO	World Health Organization
WR	Working reagent
ZnT8	Zinc transporter 8

List of figures

List of tables

Bibliography

1. ADA. Diagnosis and classification of diabetes mellitus. *Diabetes Care* 2012; 35 Suppl 1: S64-71.

2. Agbaje IM, McVicar CM, Schock BC, et al. Increased concentrations of the oxidative DNA adduct 7,8-dihydro-8-oxo-2-deoxyguanosine in the germ-line of men with type 1 diabetes. *Reprod Biomed Online* 2008; 16(3): 401-9.

3. Agbaje IM, Rogers DA, McVicar CM, et al. Insulin dependant diabetes mellitus: implications for male reproductive function. *Hum Reprod* 2007; 22(7): 1871-7.

4. Ahmed AM. History of diabetes mellitus. *Saudi Med J* 2002; 23(4): 373-8.

5. Ahmed EA, Barten-van Rijbroek AD, Kal HB, et al. Proliferative activity in vitro and DNA repair indicate that adult mouse and human Sertoli cells are not terminally differentiated, quiescent cells. *Biol Reprod* 2009; 80(6): 1084-91.

6. Akira S, Uematsu S, Takeuchi O. Pathogen recognition and innate immunity. *Cell* 2006; 124(4): 783-801.

7. Aktas CK, M.; Erboga, M.; Timurkan, H. Effects of experimental diabetes on testis proliferations and apoptosis in rats. *Journal of Experimental and Clinical Medicine* 2011; 28(3): 94-8.

8. Ali ST, Shaikh RN, Ashfaqsiddiqi N, Siddiqi PQ. Serum and urinary levels of pituitary--gonadal hormones in insulin-dependent and non-insulin-dependent diabetic males with and without neuropathy. *Arch Androl* 1993; 30(2): 117-23.

9. Altun ZFH, L.A.; Wolkow, C.A.; Crocker, C.; Lints, R.; Hall, D.H. WormAtlas. 2002-2016. http://www.wormatlas.org (accessed 05.07. 2016).

10. Alvarez-Munoz P, Mauer M, Kim Y, et al. Cellular basis of diabetic nephropathy: V. Endoglin expression levels and diabetic nephropathy risk in patients with Type 1 diabetes. *J Diabetes Complications* 2010; 24(4): 242-9.

11. Alves MG, Martins AD, Cavaco JE, Socorro S, Oliveira PF. Diabetes, insulin-mediated glucose metabolism and Sertoli/blood-testis barrier function. *Tissue Barriers* 2013; 1(2): e23992.

12. Alves MG, Martins AD, Rato L, Moreira PI, Socorro S, Oliveira PF. Molecular mechanisms beyond glucose transport in diabetes-related male infertility. *Biochim Biophys Acta* 2013; 1832(5): 626-35.

13. Alves MG, Rato L, Carvalho RA, Moreira PI, Socorro S, Oliveira PF. Hormonal control of Sertoli cell metabolism regulates spermatogenesis. *Cell Mol Life Sci* 2013; 70(5): 777-93.

14. Amaral S, Mota PC, Lacerda B, et al. Testicular mitochondrial alterations in untreated streptozotocin-induced diabetic rats. *Mitochondrion* 2009; 9(1): 41-50.

15. Andersen GO, Ueland T, Knudsen EC, et al. Activin A levels are associated with abnormal glucose regulation in patients with myocardial infarction: potential counteracting effects of activin A on inflammation. *Diabetes* 2011; 60(5): 1544-51.

16. Andrzejewski D, Brown ML, Ungerleider N, Burnside A, Schneyer AL. Activins A and B Regulate Fate-Determining Gene Expression in Islet Cell Lines and Islet Cells From Male Mice. *Endocrinology* 2015; 156(7): 2440-50.

17. Aquila S, Gentile M, Middea E, Catalano S, Ando S. Autocrine regulation of insulin secretion in human ejaculated spermatozoa. *Endocrinology* 2005; 146(2): 552-7.

18. Arikave APD, A.O.; Udenze, I.C.; Akinwolere, F.M.; Olatunki-Bello, I.I.; Obika, L.F. Comparison of streptozotocin-induced diabetic and insulin resistant effects on spermatogenesis with proliferating cell nuclear antigen (PCNA) immunostaining of adult rat testis. *Journal of Experimental and Clinical Medicine* 2012; 29(3): 209-14.

19. Arya M, Shergill IS, Williamson M, Gommersall L, Arya N, Patel HR. Basic principles of real-time quantitative PCR. *Expert Rev Mol Diagn* 2005; 5(2): 209-19.

20. Askenasy N. Mechanisms of autoimmunity in the non-obese diabetic mouse: effector/regulatory cell equilibrium during peak inflammation. *Immunology* 2016; 147(4): 377-88.

21. Assoian RK, Komoriya A, Meyers CA, Miller DM, Sporn MB. Transforming growth factor-beta in human platelets. Identification of a major storage site, purification, and characterization. *J Biol Chem* 1983; 258(11): 7155-60.

22. Atkinson MA, Eisenbarth GS, Michels AW. Type 1 diabetes. *Lancet* 2014; 383(9911): 69-82.

23. Auchus RJ. Chapter 8 - Human Steroid Biosynthesis A2 - Plant, Tony M. In: Zeleznik AJ, ed. Knobil and Neill's Physiology of Reproduction (Fourth Edition). San Diego: Academic Press; 2015: 295-312.

24. Avruch J. Insulin signal transduction through protein kinase cascades. *Mol Cell Biochem* 1998; 182(1-2): 31-48.

25. Awad AS, You H, Gao T, Gvritishvili A, Cooper TK, Tombran-Tink J. Delayed Treatment with a Small Pigment Epithelium Derived Factor (PEDF) Peptide Prevents the Progression of Diabetic Renal Injury. *PLoS One* 2015; 10(7): e0133777.

26. Aybek H, Aybek Z, Rota S, Sen N, Akbulut M. The effects of diabetes mellitus, age, and vitamin E on testicular oxidative stress. *Fertil Steril* 2008; 90(3): 755-60.

27. Babaya N, Nakayama M, Moriyama H, et al. A new model of insulin-deficient diabetes: male NOD mice with a single copy of Ins1 and no Ins2. *Diabetologia* 2006; 49(6): 1222-8.

28. Baccetti B, La Marca A, Piomboni P, et al. Insulin-dependent diabetes in men is associated with hypothalamo-pituitary derangement and with impairment in semen quality. *Hum Reprod* 2002; 17(10): 2673-7.

29. Backes JM, Kostoff MD, Gibson CA, Ruisinger JF. Statin-Associated Diabetes Mellitus: Review and Clinical Guide. *South Med J* 2016; 109(3): 167-73.

30. Ballester J, Munoz MC, Dominguez J, Rigau T, Guinovart JJ, Rodriguez-Gil JE. Insulin-dependent diabetes affects testicular function by FSH- and LH-linked mechanisms. *J Androl* 2004; 25(5): 706-19.

31. Banting FG, Best CH, Collip JB, Campbell WR, Fletcher AA. Pancreatic Extracts in the Treatment of Diabetes Mellitus. *Can Med Assoc J* 1922; 12(3): 141-6.

32. Barakat B, Itman C, Mendis SH, Loveland KL. Activins and inhibins in mammalian testis development: new models, new insights. *Mol Cell Endocrinol* 2012; 359(1-2): 66-77.

33. Bartak V, Josifko M, Horackova M. Juvenile diabetes and human sperm quality. *Int J Fertil* 1975; 20(1): 30-2.

34. Benitez A, Perez Diaz J. Effect of streptozotocin-diabetes and insulin treatment on regulation of Leydig cell function in the rat. *Horm Metab Res* 1985; 17(1): 5-7.

35. Beumer TL, Kiyokawa H, Roepers-Gajadien HL, et al. Regulatory role of p27kip1 in the mouse and human testis. *Endocrinology* 1999; 140(4): 1834-40.

36. Beumer TL, Roepers-Gajadien HL, Gademan IS, et al. The role of the tumor suppressor p53 in spermatogenesis. *Cell Death Differ* 1998; 5(8): 669-77.

37. Biosystems A. Guide to Performing Relative Quantitation of Gene Expression Using Real-Time Quantitative PCR. 2004. http://www.gu.se/digitalAssets/1125/1125331_ABI_Guide_Relative_Quantification_using_realtime_PCR.pdf (accessed 27.07. 2016).

38. Blumensatt M, Greulich S, Herzfeld de Wiza D, et al. Activin A impairs insulin action in cardiomyocytes via up-regulation of miR-143. *Cardiovasc Res* 2013; 100(2): 201-10.

39. Boerner BP, George NM, Targy NM, Sarvetnick NE. TGF-beta superfamily member Nodal stimulates human beta-cell proliferation while maintaining cellular viability. *Endocrinology* 2013; 154(11): 4099-112.

40. Bondarenko LBS, G.M., Matvienko, A.V.; Kovalenko, V.M. Diabetes-mediated changes in rat type i collagen and spermatogenesis indices. *Romanian Journal of Diabetes Nutrition and Metabolic Diseases* 2012; 19(3).

41. Borland K, Mita M, Oppenheimer CL, et al. The actions of insulin-like growth factors I and II on cultured Sertoli cells. *Endocrinology* 1984; 114(1): 240-6.

42. Bose R, Adiga SK, D'Souza F, et al. Germ cell abnormalities in streptozotocin induced diabetic mice do not correlate with blood glucose level. *J Assist Reprod Genet* 2012; 29(12): 1405-13.

43. Bostrom KI, Jumabay M, Matveyenko A, Nicholas SB, Yao Y. Activation of vascular bone morphogenetic protein signaling in diabetes mellitus. *Circ Res* 2011; 108(4): 446-57.

44. Bottini N, Musumeci L, Alonso A, et al. A functional variant of lymphoid tyrosine phosphatase is associated with type I diabetes. *Nat Genet* 2004; 36(4): 337-8.

45. Bourne RB, Kretzschmar WA, Esser JH. Successful artificial insemination in a diabetic with retrograde ejaculation. *Fertil Steril* 1971; 22(4): 275-7.

46. Bretzel RG, Nuber U, Landgraf W, Owens DR, Bradley C, Linn T. Once-daily basal insulin glargine versus thrice-daily prandial insulin lispro in people with type 2 diabetes on oral hypoglycaemic agents (APOLLO): an open randomised controlled trial. *Lancet* 2008; 371(9618): 1073-84.

47. Brown J, Walker S, Steinman K. Endocrine manual for the reproductive assessment of domestic and non-domestic species. *Endocrine Research Laboratory, Department of Reproductive Sciences, Conservation and Research Center, National Zoological Park, Smithsonian Institution, Handbook* 2004: 1-93.

48. Brown ML, Kimura F, Bonomi LM, Ungerleider NA, Schneyer AL. Differential synthesis and action of TGFss superfamily ligands in mouse and rat islets. *Islets* 2011; 3(6): 367-75.

49. Brown ML, Ungerleider N, Bonomi L, Andrzejewski D, Burnside A, Schneyer A. Effects of activin A on survival, function and gene expression of pancreatic islets from non-diabetic and diabetic human donors. *Islets* 2014; 6(5-6): e1017226.

50. Burger HG, Lee VW, Rennie GC. A generalized computer program for the treatment of data from competitive protein-binding assays including radioimmunoassays. *J Lab Clin Med* 1972; 80(2): 302-12.

51. Burul-Bozkurt N, Pekiner C, Kelicen P. Diabetes alters aromatase enzyme levels in gonadal tissues of rats. *Naunyn Schmiedebergs Arch Pharmacol* 2010; 382(1): 33-41.

52. Cabrera SM, Henschel AM, Hessner MJ. Innate inflammation in type 1 diabetes. *Transl Res* 2016; 167(1): 214-27.

53. Cameron DF, Murray FT, Drylie DD. Interstitial compartment pathology and spermatogenic disruption in testes from impotent diabetic men. *Anat Rec* 1985; 213(1): 53-62.

54. Carosa E, Radico C, Giansante N, et al. Ontogenetic profile and thyroid hormone regulation of type-1 and type-8 glucose transporters in rat Sertoli cells. *Int J Androl* 2005; 28(2): 99-106.

55. Chabrolle C, Jeanpierre E, Tosca L, Rame C, Dupont J. Effects of high levels of glucose on the steroidogenesis and the expression of adiponectin receptors in rat ovarian cells. *Reprod Biol Endocrinol* 2008; 6: 11.

56. Chan SJ, Seino S, Gruppuso PA, Schwartz R, Steiner DF. A mutation in the B chain coding region is associated with impaired proinsulin conversion in a family with hyperproinsulinemia. *Proc Natl Acad Sci U S A* 1987; 84(8): 2194-7.

57. Chandel A, Dhindsa S, Topiwala S, Chaudhuri A, Dandona P. Testosterone concentration in young patients with diabetes. *Diabetes Care* 2008; 31(10): 2013-7.

58. Chandrashekar KN, Muralidhara. Evidence of oxidative stress and mitochondrial dysfunctions in the testis of prepubertal diabetic rats. *Int J Impot Res* 2009; 21(3): 198-206.

59. Chang MM, Lovett J. A laboratory exercise illustrating the sensitivity and specificity of Western blot analysis. *Biochem Mol Biol Educ* 2011; 39(4): 291-7.

60. Chaudhary J, Johnson J, Kim G, Skinner MK. Hormonal regulation and differential actions of the helix-loop-helix transcriptional inhibitors of differentiation (Id1, Id2, Id3, and Id4) in Sertoli cells. *Endocrinology* 2001; 142(5): 1727-36.

61. Chavakis E, Riecke B, Lin J, et al. Kinetics of integrin expression in the mouse model of proliferative retinopathy and success of secondary intervention with cyclic RGD peptides. *Diabetologia* 2002; 45(2): 262-7.

62. Chen WJ, Greulich S, van der Meer RW, et al. Activin A is associated with impaired myocardial glucose metabolism and left ventricular remodeling in patients with uncomplicated type 2 diabetes. *Cardiovasc Diabetol* 2013; 12: 150.

63. Choeiri C, Hewitt K, Durkin J, Simard CJ, Renaud JM, Messier C. Longitudinal evaluation of memory performance and peripheral neuropathy in the Ins2C96Y Akita mice. *Behav Brain Res* 2005; 157(1): 31-8.

64. Constant SL, Bottomly K. Induction of Th1 and Th2 CD4+ T cell responses: the alternative approaches. *Annu Rev Immunol* 1997; 15: 297-322.

65. Cooke HJ, Saunders PT. Mouse models of male infertility. *Nat Rev Genet* 2002; 3(10): 790-801.

66. Crespo D, Assis LH, Furmanek T, Bogerd J, Schulz RW. Expression profiling identifies Sertoli and Leydig cell genes as Fsh targets in adult zebrafish testis. *Mol Cell Endocrinol* 2016; 437: 237-51.

67. Czubak P, Bojarska-Junak A, Tabarkiewicz J, Putowski L. A modified method of insulin producing cells' generation from bone marrow-derived mesenchymal stem cells. *J Diabetes Res* 2014; 2014: 628591.

68. Dasu MR, Devaraj S, Zhao L, Hwang DH, Jialal I. High glucose induces toll-like receptor expression in human monocytes: mechanism of activation. *Diabetes* 2008; 57(11): 3090-8.

69. de Rooij DG, Russell LD. All you wanted to know about spermatogonia but were afraid to ask. *J Androl* 2000; 21(6): 776-98.

70. De Young L, Yu D, Bateman RM, Brock GB. Oxidative stress and antioxidant therapy: their impact in diabetes-associated erectile dysfunction. *J Androl* 2004; 25(5): 830-6.

71. Deusing DJ, Winter S, Kler A, et al. A catechin-enriched green tea extract prevents glucose-induced survival reduction in Caenorhabditis elegans through sir-2.1 and uba-1 dependent hormesis. *Fitoterapia* 2015; 102: 163-70.

72. Dias VL, Rajpert-De Meyts E, McLachlan R, Loveland KL. Analysis of activin/TGFB-signaling modulators within the normal and dysfunctional adult human testis reveals evidence of altered signaling capacity in a subset of seminomas. *Reproduction* 2009; 138(5): 801-11.

73. Dichmann DS, Miller CP, Jensen J, Scott Heller R, Serup P. Expression and misexpression of members of the FGF and TGFbeta families of growth factors in the developing mouse pancreas. *Dev Dyn* 2003; 226(4): 663-74.

74. Dodson G, Steiner D. The role of assembly in insulin's biosynthesis. *Curr Opin Struct Biol* 1998; 8(2): 189-94.

75. Donkin SG, Eiteman MA, Williams PL. Toxicity of Glucosinolates and Their Enzymatic Decomposition Products to Caenorhabditis elegans. *J Nematol* 1995; 27(3): 258-62.

76. Donmez YB, Kizilay G, Topcu-Tarladacalisir Y. MAPK immunoreactivity in streptozotocin-induced diabetic rat testis. *Acta Cir Bras* 2014; 29(10): 644-50.

77. Downes KP, M.; Angus, KL.; Hardy, M.; Nutland, S.; Smyth, DJ.; Walker, NM.; Wallace, C.; Todd, JA. Reduced expression of IFIH1 is protective for type 1 diabetes. *PLoS One* 2010; (Sep 9;5(9)): pii: e12646.

78. Enzlin P, Rosen R, Wiegel M, et al. Sexual dysfunction in women with type 1 diabetes: long-term findings from the DCCT/ EDIC study cohort. *Diabetes Care* 2009; 32(5): 780-5.

79. Eriksen MB, Glintborg D, Nielsen MF, et al. Testosterone treatment increases androgen receptor and aromatase gene expression in myotubes from patients with PCOS and controls, but does not induce insulin resistance. *Biochem Biophys Res Commun* 2014; 451(4): 622-6.

80. Eringsmark Regnell S, Lernmark A. The environment and the origins of islet autoimmunity and Type 1 diabetes. *Diabet Med* 2013; 30(2): 155-60.

81. Favaro WJ, Padovani CR, Cagnon VH. Ultrastructural and proliferative features of the ventral lobe of the prostate in non-obese diabetic mice (NOD) following androgen and estrogen replacement associated to insulin therapy. *Tissue Cell* 2009; 41(2): 119-32.

82. Fedder J, Kaspersen MD, Brandslund I, Hojgaard A. Retrograde ejaculation and sexual dysfunction in men with diabetes mellitus: a prospective, controlled study. *Andrology* 2013; 1(4): 602-6.

83. Fehmann H-C, Strowski MZ, Goeke B. Diabetes mellitus mit monogen determinierter Stoerung der Beta-Zell-Funktion: Maturity-onset Diabetes of the Young. *Dtsch Arztebl International* 2004; 101(13): 860-.

84. Fitzenberger E, Boll M, Wenzel U. Impairment of the proteasome is crucial for glucose-induced lifespan reduction in the mev-1 mutant of Caenorhabditis elegans. *Biochim Biophys Acta* 2013; 1832(4): 565-73.

85. Florio P, Luisi S, Marchetti P, et al. Activin A stimulates insulin secretion in cultured human pancreatic islets. *J Endocrinol Invest* 2000; 23(4): 231-4.

86. Fox R, Kim HS, Reddick RL, et al. Mitochondrial DNA polymerase editing mutation, PolgD257A, reduces the diabetic phenotype of Akita male mice by suppressing appetite. *Proc Natl Acad Sci U S A* 2011; 108(21): 8779-84.

87. Frandsen CS, Dejgaard TF, Madsbad S. Non-insulin drugs to treat hyperglycaemia in type 1 diabetes mellitus. *Lancet Diabetes Endocrinol* 2016.

88. Franko A, von Kleist-Retzow JC, Bose M, et al. Complete failure of insulin-transmitted signaling, but not obesity-induced insulin resistance, impairs respiratory chain function in muscle. *J Mol Med (Berl)* 2012; 90(10): 1145-60.

89. Friedman JE, Ishizuka T, Liu S, et al. Reduced insulin receptor signaling in the obese spontaneously hypertensive Koletsky rat. *Am J Physiol* 1997; 273(5 Pt 1): E1014-23.

90. Galardo MN, Riera MF, Pellizzari EH, et al. Regulation of expression of Sertoli cell glucose transporters 1 and 3 by FSH, IL1 beta, and bFGF at two different time-points in pubertal development. *Cell Tissue Res* 2008; 334(2): 295-304.

91. Garcia-Diez LC, Corrales Hernandez JJ, Hernandez-Diaz J, Pedraz MJ, Miralles JM. Semen characteristics and diabetes mellitus: significance of insulin in male infertility. *Arch Androl* 1991; 26(2): 119-28.

92. Gomez O, Ballester B, Romero A, et al. Expression and regulation of insulin and the glucose transporter GLUT8 in the testes of diabetic rats. *Horm Metab Res* 2009; 41(5): 343-9.

93. Gosmanov AR, Gosmanova EO, Dillard-Cannon E. Management of adult diabetic ketoacidosis. *Diabetes Metab Syndr Obes* 2014; 7: 255-64.

94. Griffeth RJ, Bianda V, Nef S. The emerging role of insulin-like growth factors in testis development and function. *Basic Clin Androl* 2014; 24: 12.

95. Griswold MD, Merryweather J. Insulin stimulates the incorporation of 32Pi into ribonucleic acid in cultured sertoli cells. *Endocrinology* 1982; 111(2): 661-7.

96. Grossmann M, Thomas MC, Panagiotopoulos S, et al. Low testosterone levels are common and associated with insulin resistance in men with diabetes. *J Clin Endocrinol Metab* 2008; 93(5): 1834-40.

97. Gumieniczek A, Wilk M. Nitrosative stress and glutathione redox system in four different tissues of alloxan-induced hyperglycemic animals. *Toxicol Mech Methods* 2009; 19(4): 302-7.

98. Gumienny TLS-D, C. TGF-β signaling in C. elegans. 10. July 2013. http://www.wormbook.org (accessed 06.07. 2016).

99. Gupta MKC, S. Y. Ovarian Hormones: Structure, Biosynthesis, Function, Mechanism of Action, and Laboratory Diagnosis. 2015. http://clinicalgate.com/ovarian-hormones-structure-biosynthesis-function-mechanism-of-action-and-laboratory-diagnosis/#bib114 (accessed 01.07. 2016).

100. Han Z, Guo J, Conley SM, Naash MI. Retinal angiogenesis in the Ins2(Akita) mouse model of diabetic retinopathy. *Invest Ophthalmol Vis Sci* 2013; 54(1): 574-84.

101. Handelsman DJ, Conway AJ, Boylan LM, Yue DK, Turtle JR. Testicular function and glycemic control in diabetic men. A controlled study. *Andrologia* 1985; 17(5): 488-96.

102. Haneda M, Chan SJ, Kwok SC, Rubenstein AH, Steiner DF. Studies on mutant human insulin genes: identification and sequence analysis of a gene encoding [SerB24]insulin. *Proc Natl Acad Sci U S A* 1983; 80(20): 6366-70.

103. Hartwig K, Heidler T, Moch J, Daniel H, Wenzel U. Feeding a ROS-generator to Caenorhabditis elegans leads to increased expression of small heat shock protein HSP-16.2 and hormesis. *Genes Nutr* 2009; 4(1): 59-67.

104. Hashimoto O, Funaba M. Activin in glucose metabolism. *Vitam Horm* 2011; 85: 217-34.

105. Hashimoto O, Ushiro Y, Sekiyama K, et al. Impaired growth of pancreatic exocrine cells in transgenic mice expressing human activin betaE subunit. *Biochem Biophys Res Commun* 2006; 341(2): 416-24.

106. Hassan AA, Hassouna MM, Taketo T, Gagnon C, Elhilali MM. The effect of diabetes on sexual behavior and reproductive tract function in male rats. *J Urol* 1993; 149(1): 148-54.

107. Hassan GA, Sliem HA, Ellethy AT, Salama Mel S. Role of immune system modulation in prevention of type 1 diabetes mellitus. *Indian J Endocrinol Metab* 2012; 16(6): 904-9.

108. Health WADo. Male reproductive system (labelled). https://gdhr.wa.gov.au/documents/10184/127993/Male+Repo+Senior+BW+Label.jpg/59632dc5-424b-4da9-a025-8fdb3844ec06?t=1405546236000 (accessed 28.07. 2016).

109. Hedger MP. Chapter 19 - The Immunphysiology of Male Reproduction. In: Plant TM, Zeleznik AJ, eds. Knobil and Neill's Physiology of Reproduction (Fourth Edition). San Diego: Academic Press; 2015: 805-92.

110. Hedger MP, Winnall WR. Regulation of activin and inhibin in the adult testis and the evidence for functional roles in spermatogenesis and immunoregulation. *Mol Cell Endocrinol* 2012; 359(1-2): 30-42.

111. Heier M, Margeirsdottir HD, Brunborg C, Hanssen KF, Dahl-Jorgensen K, Seljeflot I. Inflammation in childhood type 1 diabetes; influence of glycemic control. *Atherosclerosis* 2015; 238(1): 33-7.

112. Herbach N, Rathkolb B, Kemter E, et al. Dominant-negative effects of a novel mutated Ins2 allele causes early-onset diabetes and severe beta-cell loss in Munich Ins2C95S mutant mice. *Diabetes* 2007; 56(5): 1268-76.

113. Higuchi R, Fockler C, Dollinger G, Watson R. Kinetic PCR analysis: real-time monitoring of DNA amplification reactions. *Biotechnology (N Y)* 1993; 11(9): 1026-30.

114. Holstein A, Patzer O, Tiemann T, Vortherms J, Kovacs P. Number and sex ratio of children and impact of parental diabetes in individuals with Type 1 diabetes. *Diabet Med* 2012; 29(10): 1268-71.

115. Hombrebueno JR, Chen M, Penalva RG, Xu H. Loss of synaptic connectivity, particularly in second order neurons is a key feature of diabetic retinal neuropathy in the Ins2Akita mouse. *PLoS One* 2014; 9(5): e97970.

116. Hsu DR, Economides AN, Wang X, Eimon PM, Harland RM. The Xenopus dorsalizing factor Gremlin identifies a novel family of secreted proteins that antagonize BMP activities. *Mol Cell* 1998; 1(5): 673-83.

117. Huang C, Kim Y, Caramori ML, et al. Cellular basis of diabetic nephropathy: II. The transforming growth factor-beta system and diabetic nephropathy lesions in type 1 diabetes. *Diabetes* 2002; 51(12): 3577-81.

118. Husseini M, Wang GS, Patrick C, et al. Heme Oxygenase-1 Induction Prevents Autoimmune Diabetes in Association With Pancreatic Recruitment of M2-Like Macrophages, Mesenchymal Cells, and Fibrocytes. *Endocrinology* 2015; 156(11): 3937-49.

119. Hutson JC, Stocco DM, Campbell GT, Wagoner J. Sertoli cell function in diabetic, insulin-treated diabetic, and semi-starved rats. *Diabetes* 1983; 32(2): 112-6.

120. In't Veld P. Insulitis in human type 1 diabetes: The quest for an elusive lesion. *Islets* 2011; 3(4): 131-8.

121. Ishii N, Takahashi K, Tomita S, et al. A methyl viologen-sensitive mutant of the nematode Caenorhabditis elegans. *Mutat Res* 1990; 237(3-4): 165-71.

122. Itman C, Loveland KL. Smads and cell fate: distinct roles in specification, development, and tumorigenesis in the testis. *IUBMB Life* 2013; 65(2): 85-97.

123. Jain GC, Jangir RN. Modulation of diabetes-mellitus-induced male reproductive dysfunctions in experimental animal models with medicinal plants. *Pharmacogn Rev* 2014; 8(16): 113-21.

124. Jangir RN, Jain GC. Diabetes mellitus induced impairment of male reproductive functions: a review. *Curr Diabetes Rev* 2014; 10(3): 147-57.

125. Jax TJL. Mouse strain datasheet - 003548. 2016. https://www.jax.org/strain/003548 (accessed 08.03.2016 2016).

126. Jeon JY, Choi SE, Ha ES, et al. Association between insulin resistance and impairment of FGF21 signal transduction in skeletal muscles. *Endocrine* 2016; 53(1): 97-106.

127. Johnsen SG. Testicular biopsy score count--a method for registration of spermatogenesis in human testes: normal values and results in 335 hypogonadal males. *Hormones* 1970; 1(1): 2-25.

128. Jones KL, Mansell A, Patella S, et al. Activin A is a critical component of the inflammatory response, and its binding protein, follistatin, reduces mortality in endotoxemia. *Proc Natl Acad Sci U S A* 2007; 104(41): 16239-44.

129. Jutte NH, Jansen R, Grootegoed JA, Rommerts FF, van der Molen HJ. FSH stimulation of the production of pyruvate and lactate by rat Sertoli cells may be involved in hormonal regulation of spermatogenesis. *J Reprod Fertil* 1983; 68(1): 219-26.

130. Kakoki M, Sullivan KA, Backus C, et al. Lack of both bradykinin B1 and B2 receptors enhances nephropathy, neuropathy, and bone mineral loss in Akita diabetic mice. *Proc Natl Acad Sci U S A* 2010; 107(22): 10190-5.

131. Karimi J, Goodarzi MT, Tavilani H, Khodadadi I, Amiri I. Relationship between advanced glycation end products and increased lipid peroxidation in semen of diabetic men. *Diabetes Res Clin Pract* 2011; 91(1): 61-6.

132. Karimi J, Goodarzi MT, Tavilani H, Khodadadi I, Amiri I. Increased receptor for advanced glycation end products in spermatozoa of diabetic men and its association with sperm nuclear DNA fragmentation. *Andrologia* 2012; 44 Suppl 1: 280-6.

133. Kianifard D, Sadrkhanlou RA, Hasanzadeh S. The ultrastructural changes of the sertoli and leydig cells following streptozotocin induced diabetes. *Iran J Basic Med Sci* 2012; 15(1): 623-35.

134. Kiec-Wilk B, Matejko B, Razny U, et al. Hypoglycemic episodes are associated with inflammatory status in patients with type 1 diabetes mellitus. *Atherosclerosis* 2016; Aug; 251(251): 334-8.

135. Kim JJ, Hwang BH, Choi IJ, et al. Impact of diabetes duration on the extent and severity of coronary atheroma burden and long-term clinical outcome in asymptomatic type 2 diabetic patients: evaluation by Coronary CT angiography. *Eur Heart J Cardiovasc Imaging* 2015; 16(10): 1065-73.

136. Kim ST, Moley KH. Paternal effect on embryo quality in diabetic mice is related to poor sperm quality and associated with decreased glucose transporter expression. *Reproduction* 2008; 136(3): 313-22.

137. King AJ. The use of animal models in diabetes research. *Br J Pharmacol* 2012; 166(3): 877-94.

138. Knight PG, Muttukrishna S, Groome NP. Development and application of a two-site enzyme immunoassay for the determination of 'total' activin-A concentrations in serum and follicular fluid. *J Endocrinol* 1996; 148(2): 267-79.

139. Kolendorf K, Ross GP, Pavlic-Renar I, et al. Insulin detemir lowers the risk of hypoglycaemia and provides more consistent plasma glucose levels compared with NPH insulin in Type 1 diabetes. *Diabet Med* 2006; 23(7): 729-35.

140. Kubota H, Sasaki S, Kubota Y, et al. Cyclooxygenase-2 protects germ cells against spermatogenesis disturbance in experimental cryptorchidism model mice. *J Androl* 2011; 32(1): 77-85.

141. La Vignera S, Condorelli RA, Di Mauro M, et al. Reproductive function in male patients with type 1 diabetes mellitus. *Andrology* 2015.

142. Laimer M, Melmer A, Mader JK, et al. Variability of Basal Rate Profiles in Insulin Pump Therapy and Association with Complications in Type 1 Diabetes Mellitus. *PLoS One* 2016; 11(3): e0150604.

143. Landry D, Cloutier F, Martin LJ. Implications of leptin in neuroendocrine regulation of male reproduction. *Reprod Biol* 2013; 13(1): 1-14.

144. Lebel M, Mes-Masson AM. Establishment and characterization of testicular cell lines from MT-PVLT-10 transgenic mice. *Exp Cell Res* 1994; 213(1): 12-9.

145. Leiter EH, Prochazka M, Coleman DL. The non-obese diabetic (NOD) mouse. *Am J Pathol* 1987; 128(2): 380-3.

146. Leiter EH, Schile A. Genetic and Pharmacologic Models for Type 1 Diabetes. *Curr Protoc Mouse Biol* 2013; 3(1): 9-19.

147. Leng J, Liu G, Zhang C, et al. Physical Activity, Sedentary Behaviors and Risk of Gestational Diabetes Mellitus: A Population-Based Cross-Sectional Study in Tianjin, China. *Eur J Endocrinol* 2016.

148. Lenzen S, Drinkgern J, Tiedge M. Low antioxidant enzyme gene expression in pancreatic islets compared with various other mouse tissues. *Free Radic Biol Med* 1996; 20(3): 463-6.

149. Lequin RM. Enzyme immunoassay (EIA)/enzyme-linked immunosorbent assay (ELISA). *Clin Chem* 2005; 51(12): 2415-8.

150. Li HY, Oh YS, Choi JW, Jung JY, Jun HS. Blocking lysophosphatidic acid receptor 1 signaling inhibits diabetic nephropathy in db/db mice. *Kidney Int* 2017.

151. Li TT, Larrucea S, Souza S, et al. Genetic variation responsible for mouse strain differences in integrin alpha 2 expression is associated with altered platelet responses to collagen. *Blood* 2004; 103(9): 3396-402.

152. Linn T, Ortac K, Laube H, Federlin K. Intensive therapy in adult insulin-dependent diabetes mellitus is associated with improved insulin sensitivity and reserve: a randomized, controlled, prospective study over 5 years in newly diagnosed patients. *Metabolism* 1996; 45(12): 1508-13.

153. Linn T, Strate C, Federlin K, Papaccio G. Intercellular adhesion molecule-1 (ICAM-1) expression in the islets of the non-obese diabetic and low-dose streptozocin-treated mouse. *Histochemistry* 1994; 102(4): 317-21.

154. Lo CS, Shi Y, Chang SY, et al. Overexpression of heterogeneous nuclear ribonucleoprotein F stimulates renal Ace-2 gene expression and prevents TGF-beta1-induced kidney injury in a mouse model of diabetes. *Diabetologia* 2015.

155. Lopez-Alvarenga JC, Zarinan T, Olivares A, Gonzalez-Barranco J, Veldhuis JD, Ulloa-Aguirre A. Poorly controlled type I diabetes mellitus in young men selectively suppresses luteinizing hormone secretory burst mass. *J Clin Endocrinol Metab* 2002; 87(12): 5507-15.

156. Loveland KL, Hedger MP. 7 - Activins and inhibins in Sertoli cell biology: Implications for testis development and function A2 - Griswold, Michael D. Sertoli Cell Biology (Second Edition). Oxford: Academic Press; 2015: 201-32.

157. Ludlow H, Muttukrishna S, Hyvonen M, Groome NP. Development of a new antibody to the human inhibin/activin betaB subunit and its application to improved inhibin B ELISAs. *J Immunol Methods* 2008; 329(1-2): 102-11.

158. Maeda H, Hanazaki K. Pancreatogenic diabetes after pancreatic resection. *Pancreatology* 2011; 11(2): 268-76.

159. Makino A, Scott BT, Dillmann WH. Mitochondrial fragmentation and superoxide anion production in coronary endothelial cells from a mouse model of type 1 diabetes. *Diabetologia* 2010; 53(8): 1783-94.

160. Makino S, Kunimoto K, Muraoka Y, Mizushima Y, Katagiri K, Tochino Y. Breeding of a non-obese, diabetic strain of mice. *Jikken Dobutsu* 1980; 29(1): 1-13.

161. Malek H, Ebadzadeh MM, Safabakhsh R, Razavi A, Zaringhalam J. Dynamics of the HPA axis and inflammatory cytokines: Insights from mathematical modeling. *Comput Biol Med* 2015; 67: 1-12.

162. Mallidis C, Agbaje I, O'Neill J, McClure N. The influence of type 1 diabetes mellitus on spermatogenic gene expression. *Fertil Steril* 2009; 92(6): 2085-7.

163. Mallidis C, Agbaje I, Rogers D, et al. Distribution of the receptor for advanced glycation end products in the human male reproductive tract: prevalence in men with diabetes mellitus. *Hum Reprod* 2007; 22(8): 2169-77.

164. Mallidis C, Agbaje IM, Rogers DA, et al. Advanced glycation end products accumulate in the reproductive tract of men with diabetes. *Int J Androl* 2009; 32(4): 295-305.

165. Mallidis C, Green BD, Rogers D, et al. Metabolic profile changes in the testes of mice with streptozotocin-induced type 1 diabetes mellitus. *Int J Androl* 2007; 32(2): 156-65.

166. Maneesh M, Jayalakshmi H, Singh TA, Chakrabarti A. Impaired hypothalamic-pituitary-gonadal axis function in men with diabetes mellitus. *Indian J Clin Biochem* 2006; 21(1): 165-8.

167. Mangoli E, Talebi AR, Anvari M, Pourentezari M. Effects of experimentally-induced diabetes on sperm parameters and chromatin quality in mice. *Iran J Reprod Med* 2013; 11(1): 53-60.

168. Mather JP. Establishment and characterization of two distinct mouse testicular epithelial cell lines. *Biol Reprod* 1980; 23(1): 243-52.

169. McKnight AJ, Savage DA, Patterson CC, Sadlier D, Maxwell AP. Resequencing of genes for transforming growth factor beta1 (TGFB1) type 1 and 2 receptors (TGFBR1, TGFBR2), and association analysis of variants with diabetic nephropathy. *BMC Med Genet* 2007; 8: 5.

170. Mohasseb M, Ebied S, Yehia MA, Hussein N. Testicular oxidative damage and role of combined antioxidant supplementation in experimental diabetic rats. *J Physiol Biochem* 2011; 67(2): 185-94.

171. Morrison JF, Dhanasekaran S, Sheen R, Frampton CM, Mensah-Brown E. The effect of streptozotocin-induced diabetes on the rat seminal vesicle: A possible pathophysiological basis for disorders of ejaculation. *Ann N Y Acad Sci* 2006; 1084: 267-79.

172. Mueller SO, Korach KS. Immortalized testis cell lines from estrogen receptor (ER) alpha knock-out and wild-type mice expressing functional ERalpha or ERbeta. *J Androl* 2001; 22(4): 652-64.

173. Mulholland J, Mallidis C, Agbaje I, McClure N. Male diabetes mellitus and assisted reproduction treatment outcome. *Reprod Biomed Online* 2011; 22(2): 215-9.

174. Murakami M, Shirai M, Ooishi R, et al. Expression of activin receptor-like kinase 7 in adipose tissues. *Biochem Genet* 2013; 51(3-4): 202-10.

175. Naf S, Escote X, Ballesteros M, et al. Serum activin A and follistatin levels in gestational diabetes and the association of the Activin A-Follistatin system with anthropometric parameters in offspring. *PLoS One* 2014; 9(4): e92175.

176. Nakayama M. Insulin as a key autoantigen in the development of type 1 diabetes. *Diabetes Metab Res Rev* 2011; 27(8): 773-7.

177. Nakayama M, McDaniel K, Fitzgerald-Miller L, et al. Regulatory vs. inflammatory cytokine T-cell responses to mutated insulin peptides in healthy and type 1 diabetic subjects. *Proc Natl Acad Sci U S A* 2015; 112(14): 4429-34.

178. Nakayama M, Simmons KM, Michels AW. Molecular Interactions Governing Autoantigen Presentation in Type 1 Diabetes. *Curr Diab Rep* 2015; 15(12): 113.

179. Nanjo K, Sanke T, Miyano M, et al. Diabetes due to secretion of a structurally abnormal insulin (insulin Wakayama). Clinical and functional characteristics of [LeuA3] insulin. *J Clin Invest* 1986; 77(2): 514-9.

180. Navarro-Casado L, Juncos-Tobarra MA, Chafer-Rudilla M, de Onzono LI, Blazquez-Cabrera JA, Miralles-Garcia JM. Effect of experimental diabetes and STZ on male fertility capacity. Study in rats. *J Androl* 2010; 31(6): 584-92.

181. NCBI NCfBI. PubMed. 2016. http://www.ncbi.nlm.nih.gov/tools/primer-blast/ (accessed 27.07. 2016).

182. Neerman-Arbez M, Cirulli V, Halban PA. Levels of the conversion endoproteases PC1 (PC3) and PC2 distinguish between insulin-producing pancreatic islet beta cells and non-beta cells. *Biochem J* 1994; 300 (Pt 1): 57-61.

183. Nejentsev S, Walker N, Riches D, Egholm M, Todd JA. Rare variants of IFIH1, a gene implicated in antiviral responses, protect against type 1 diabetes. *Science* 2009; 324(5925): 387-9.

184. Nicholls PK, Stanton PG, Chen JL, et al. Activin signaling regulates Sertoli cell differentiation and function. *Endocrinology* 2012; 153(12): 6065-77.

185. Nishi M, Nanjo K. Insulin gene mutations and diabetes. *J Diabetes Investig* 2011; 2(2): 92-100.

186. Niven MJ, Hitman GA, Badenoch DF. A study of spermatozoal motility in type 1 diabetes mellitus. *Diabet Med* 1995; 12(10): 921-4.

187. Noble JA, Valdes AM. Genetics of the HLA region in the prediction of type 1 diabetes. *Curr Diab Rep* 2011; 11(6): 533-42.

188. O'Connor AE, McFarlane JR, Hayward S, Yohkaichiya T, Groome NP, de Kretser DM. Serum activin A and follistatin concentrations during human pregnancy: a cross-sectional and longitudinal study. *Hum Reprod* 1999; 14(3): 827-32.

189. O'Neill J, Czerwiec A, Agbaje I, et al. Differences in mouse models of diabetes mellitus in studies of male reproduction. *Int J Androl* 2010; 33(5): 709-16.

190. O'Shaughnessy P. Chapter 14 - Testicular Development. In: Plant TM, Zeleznik AJ, eds. Knobil and Neill's Physiology of Reproduction (Fourth Edition). San Diego: Academic Press; 2015: 567-94.

191. Ofstad AP, Gullestad L, Orvik E, et al. Interleukin-6 and activin A are independently associated with cardiovascular events and mortality in type 2 diabetes: the prospective Asker and Baerum Cardiovascular Diabetes (ABCD) cohort study. *Cardiovasc Diabetol* 2013; 12: 126.

192. Ogawa K, Abe K, Kurosawa N, et al. Expression of alpha, beta A and beta B subunits of inhibin or activin and follistatin in rat pancreatic islets. *FEBS Lett* 1993; 319(3): 217-20.

193. Oliveira PF, Alves MG, Rato L, et al. Effect of insulin deprivation on metabolism and metabolism-associated gene transcript levels of in vitro cultured human Sertoli cells. *Biochim Biophys Acta* 2012; 1820(2): 84-9.

194. Onichtchouk D, Chen YG, Dosch R, et al. Silencing of TGF-beta signalling by the pseudoreceptor BAMBI. *Nature* 1999; 401(6752): 480-5.

195. Oonk RB, Grootegoed JA, van der Molen HJ. Comparison of the effects of insulin and follitropin on glucose metabolism by Sertoli cells from immature rats. *Mol Cell Endocrinol* 1985; 42(1): 39-48.

196. Orban T, Sosenko JM, Cuthbertson D, et al. Pancreatic islet autoantibodies as predictors of type 1 diabetes in the Diabetes Prevention Trial-Type 1. *Diabetes Care* 2009; 32(12): 2269-74.

197. Owiredu WK, Amidu N, Alidu H, Sarpong C, Gyasi-Sarpong CK. Determinants of sexual dysfunction among clinically diagnosed diabetic patients. *Reprod Biol Endocrinol* 2011; 9: 70.

198. Padron RS, Dambay A, Suarez R, Mas J. Semen analyses in adolescent diabetic patients. *Acta Diabetol Lat* 1984; 21(2): 115-21.

199. Parajuli A, Liu C, Li W, et al. Bone's responses to mechanical loading are impaired in type 1 diabetes. *Bone* 2015; 81: 152-60.

200. Park D, Estevez A, Riddle DL. Antagonistic Smad transcription factors control the dauer/non-dauer switch in C. elegans. *Development* 2010; 137(3): 477-85.

201. Pellegrini S, Cantarelli E, Sordi V, Nano R, Piemonti L. The state of the art of islet transplantation and cell therapy in type 1 diabetes. *Acta Diabetol* 2016.

202. Perrard-Sapori MH, Chatelain PC, Rogemond N, Saez JM. Modulation of Leydig cell functions by culture with Sertoli cells or with Sertoli cell-conditioned medium: effect of insulin, somatomedin-C and FSH. *Mol Cell Endocrinol* 1987; 50(3): 193-201.

203. Peschon JJ, Behringer RR, Cate RL, et al. Directed expression of an oncogene to Sertoli cells in transgenic mice using mullerian inhibiting substance regulatory sequences. *Mol Endocrinol* 1992; 6(9): 1403-11.

204. Pfister F, Feng Y, vom Hagen F, et al. Pericyte migration: a novel mechanism of pericyte loss in experimental diabetic retinopathy. *Diabetes* 2008; 57(9): 2495-502.

205. Piccolo S, Sasai Y, Lu B, De Robertis EM. Dorsoventral patterning in Xenopus: inhibition of ventral signals by direct binding of chordin to BMP-4. *Cell* 1996; 86(4): 589-98.

206. Pitetti JL, Calvel P, Zimmermann C, et al. An essential role for insulin and IGF1 receptors in regulating sertoli cell proliferation, testis size, and FSH action in mice. *Mol Endocrinol* 2013; 27(5): 814-27.

207. Pontes DA, Fernandes GS, Piffer RC, Gerardin DC, Pereira OC, Kempinas WG. Ejaculatory dysfunction in streptozotocin-induced diabetic rats: the role of testosterone. *Pharmacol Rep* 2011; 63(1): 130-8.

208. Porto EM, Dos Santos SA, Ribeiro LM, et al. Lobe variation effects of experimental diabetes and insulin replacement on rat prostate. *Microsc Res Tech* 2011; 74(11): 1040-8.

209. Rato L, Alves MG, Duarte AI, et al. Testosterone deficiency induced by progressive stages of diabetes mellitus impairs glucose metabolism and favors glycogenesis in mature rat Sertoli cells. *Int J Biochem Cell Biol* 2015; 66: 1-10.

210. Rekittke NE AM, Rawat D, Khatri R, and Linn T. Regenerative Therapy of Type 1 Diabetes Mellitus: FromPancreatic Islet Transplantation to Mesenchymal Stem Cells. . *Stem Cells International* 2016.

211. Ren XJ, Guan GJ, Liu G, Zhang T, Liu GH. Effect of activin A on tubulointerstitial fibrosis in diabetic nephropathy. *Nephrology (Carlton)* 2009; 14(3): 311-20.

212. Resmini E, Minuto F, Colao A, Ferone D. Secondary diabetes associated with principal endocrinopathies: the impact of new treatment modalities. *Acta Diabetol* 2009; 46(2): 85-95.

213. Ribeiro DL, Marques SF, Alberti S, et al. Malignant lesions in the ventral prostate of alloxan-induced diabetic rats. *Int J Exp Pathol* 2008; 89(4): 276-83.

214. Ricci G, Catizone A, Esposito R, Pisanti FA, Vietri MT, Galdieri M. Diabetic rat testes: morphological and functional alterations. *Andrologia* 2009; 41(6): 361-8.

215. Riera MF, Galardo MN, Pellizzari EH, Meroni SB, Cigorraga SB. Molecular mechanisms involved in Sertoli cell adaptation to glucose deprivation. *Am J Physiol Endocrinol Metab* 2009; 297(4): E907-14.

216. Ringholm L, Juul A, Pedersen-Bjergaard U, Thorsteinsson B, Damm P, Mathiesen ER. Lower levels of placental growth hormone in early pregnancy in women with type 1 diabetes and large for gestational age infants. *Growth Horm IGF Res* 2015; 25(6): 312-5.

217. Robertson DM, Foulds LM, Prisk M, Hedger MP. Inhibin/activin beta-subunit monomer: isolation and characterization. *Endocrinology* 1992; 130(3): 1680-7.

218. Robertson DM, Hayward S, Irby D, et al. Radioimmunoassay of rat serum inhibin: changes after PMSG stimulation and gonadectomy. *Mol Cell Endocrinol* 1988; 58(1): 1-8.

219. Robinson R, Fritz IB. Metabolism of glucose by Sertoli cells in culture. *Biol Reprod* 1981; 24(5): 1032-41.

220. Roessner C, Paasch U, Kratzsch J, Glander HJ, Grunewald S. Sperm apoptosis signalling in diabetic men. *Reprod Biomed Online* 2012; 25(3): 292-9.

221. Romeo JH, Seftel AD, Madhun ZT, Aron DC. Sexual function in men with diabetes type 2: association with glycemic control. *J Urol* 2000; 163(3): 788-91.

222. Rosenberg HF GJ. Inflammation. In: WE P, ed. Fundamental immunology 5th ed: Lippincott, Williams and Wilkins; 2003: pp. 1151–69.

223. Russell LD, Ettlin RA, Hikim APS, Clegg ED. Histological and Histopathological Evaluation of the Testis. *International Journal of Andrology* 1993; 16(1): 83-.

224. Salim C, Rajini PS. Glucose feeding during development aggravates the toxicity of the organophosphorus insecticide Monocrotophos in the nematode, Caenorhabditis elegans. *Physiol Behav* 2014; 131: 142-8.

225. Sato Y, Yoshida K, Nozawa S, et al. Establishment of adult mouse Sertoli cell lines by using the starvation method. *Reproduction* 2013; 145(5): 505-16.

226. Sawant A, Chanda D, Isayeva T, Tsuladze G, Garvey WT, Ponnazhagan S. Noggin is novel inducer of mesenchymal stem cell adipogenesis: implications for bone health and obesity. *J Biol Chem* 2012; 287(15): 12241-9.

227. Scarano WR, Messias AG, Oliva SU, Klinefelter GR, Kempinas WG. Sexual behaviour, sperm quantity and quality after short-term streptozotocin-induced hyperglycaemia in rats. *Int J Androl* 2006; 29(4): 482-8.

228. Schiavi RC, Schanzer H, Sozio G, Setacci C, Stimmel B, Rayfield EJ. Erectile function and penile blood pressure in diabetes mellitus. *J Sex Marital Ther* 1994; 20(2): 119-24.

229. Schiavi RC, Stimmel BB, Mandeli J, Rayfield EJ. Diabetes mellitus and male sexual function: a controlled study. *Diabetologia* 1993; 36(8): 745-51.

230. Schiavi RC, Stimmel BB, Mandeli J, Rayfield EJ. Diabetes, sleep disorders, and male sexual function. *Biol Psychiatry* 1993; 34(3): 171-7.

231. Schiavi RC, Stimmel BB, Mandeli J, Schreiner-Engel P, Ghizzani A. Diabetes, psychological function and male sexuality. *J Psychosom Res* 1995; 39(3): 305-14.

232. Schmidt RE, Green KG, Snipes LL, Feng D. Neuritic dystrophy and neuronopathy in Akita (Ins2(Akita)) diabetic mouse sympathetic ganglia. *Exp Neurol* 2009; 216(1): 207-18.

233. Schneider CA, Rasband WS, Eliceiri KW. NIH Image to ImageJ: 25 years of image analysis. *Nat Meth* 2012; 9(7): 671-5.

234. Schoeffling K, Federlin K, Ditschuneit H, Pfeiffer EF. Disorders of Sexual Function in Male Diabetics. *Diabetes* 1963; 12: 519-27.

235. Schoeller EL, Albanna G, Frolova AI, Moley KH. Insulin rescues impaired spermatogenesis via the hypothalamic-pituitary-gonadal axis in Akita diabetic mice and restores male fertility. *Diabetes* 2012; 61(7): 1869-78.

236. Schoeller EL, Chi M, Drury A, Bertschinger A, Esakky P, Moley KH. Leptin monotherapy rescues spermatogenesis in male Akita type 1 diabetic mice. *Endocrinology* 2014; 155(8): 2781-6.

237. Schumacher V, Gueler B, Looijenga LH, et al. Characteristics of testicular dysgenesis syndrome and decreased expression of SRY and SOX9 in Frasier syndrome. *Mol Reprod Dev* 2008; 75(9): 1484-94.

238. Seethalakshmi L, Menon M, Diamond D. The effect of streptozotocin-induced diabetes on the neuroendocrine-male reproductive tract axis of the adult rat. *J Urol* 1987; 138(1): 190-4.

239. Setchell B, Breed W. Anatomy, vasculature, and innervation of the male reproductive tract. 2006.

240. Shayakhmetova GM, Bondarenko LB, Matvienko AV, Kovalenko VM. Correlation between spermatogenesis disorders and rat testes CYP2E1 mRNA contents under experimental alcoholism or type I diabetes. *Adv Med Sci* 2014; 59(2): 183-9.

241. Shiao MS, Liao BY, Long M, Yu HT. Adaptive evolution of the insulin two-gene system in mouse. *Genetics* 2008; 178(3): 1683-91.

242. Shibata H, Yasuda H, Sekine N, Mine T, Totsuka Y, Kojima I. Activin A increases intracellular free calcium concentrations in rat pancreatic islets. *FEBS Lett* 1993; 329(1-2): 194-8.

243. Shrilatha B, Muralidhara. Early oxidative stress in testis and epididymal sperm in streptozotocin-induced diabetic mice: its progression and genotoxic consequences. *Reprod Toxicol* 2007; 23(4): 578-87.

244. Shrivastav P, Swann J, Jeremy JY, Thompson C, Shaw RW, Dandona P. Sperm function and structure and seminal plasma prostanoid concentrations in men with IDDM. *Diabetes Care* 1989; 12(10): 742-4.

245. Silber SJ. Seminars in Reproductive Endocrinology. 1991. http://www.infertile.com/scientific-article-dr-silbers-findings-effects-age-male-fertility/ (accessed 29.06. 2016).

246. Silink M. Childhood diabetes: a global perspective. *Horm Res* 2002; 57 Suppl 1: 1-5.

247. Singh S, Malini T, Rengarajan S, Balasubramanian K. Impact of experimental diabetes and insulin replacement on epididymal secretory products and sperm maturation in albino rats. *J Cell Biochem* 2009; 108(5): 1094-101.

248. Sjoberg L, Pitkaniemi J, Haapala L, Kaaja R, Tuomilehto J. Fertility in people with childhood-onset type 1 diabetes. *Diabetologia* 2013; 56(1): 78-81.

249. Skinner MK, Griswold MD. Secretion of testicular transferrin by cultured Sertoli cells is regulated by hormones and retinoids. *Biol Reprod* 1982; 27(1): 211-21.

250. Smith LB, Walker WH. Chapter 16 - Hormone Signaling in the Testis A2 - Plant, Tony M. In: Zeleznik AJ, ed. Knobil and Neill's Physiology of Reproduction (Fourth Edition). San Diego: Academic Press; 2015: 637-90.

251. Smith-Garvin JE, Koretzky GA, Jordan MS. T cell activation. *Annu Rev Immunol* 2009; 27: 591-619.

252. Soudamani S, Malini T, Balasubramanian K. Effects of streptozotocin-diabetes and insulin replacement on the epididymis of prepubertal rats: histological and histomorphometric studies. *Endocr Res* 2005; 31(2): 81-98.

253. Steen E, Terry BM, Rivera EJ, et al. Impaired insulin and insulin-like growth factor expression and signaling mechanisms in Alzheimer's disease--is this type 3 diabetes? *J Alzheimers Dis* 2005; 7(1): 63-80.

254. Steiner DF, Cunningham D, Spigelman L, Aten B. Insulin biosynthesis: evidence for a precursor. *Science* 1967; 157(3789): 697-700.

255. Steiner DF, Oyer PE. The biosynthesis of insulin and a probable precursor of insulin by a human islet cell adenoma. *Proc Natl Acad Sci U S A* 1967; 57(2): 473-80.

256. Stiernagle T. Maintenance of C. elegans. *WormBook* 2006: 1-11.

257. Stoy J, Edghill EL, Flanagan SE, et al. Insulin gene mutations as a cause of permanent neonatal diabetes. *Proc Natl Acad Sci U S A* 2007; 104(38): 15040-4.

258. Sugino K, Kurosawa N, Nakamura T, et al. Molecular heterogeneity of follistatin, an activin-binding protein. Higher affinity of the carboxyl-terminal truncated forms for heparan sulfate proteoglycans on the ovarian granulosa cell. *J Biol Chem* 1993; 268(21): 15579-87.

259. Sullivan KA, Hayes JM, Wiggin TD, et al. Mouse models of diabetic neuropathy. *Neurobiol Dis* 2007; 28(3): 276-85.

260. Szabat M, Johnson JD, Piret JM. Reciprocal modulation of adult beta cell maturity by activin A and follistatin. *Diabetologia* 2010; 53(8): 1680-9.

261. Tager H, Given B, Baldwin D, et al. A structurally abnormal insulin causing human diabetes. *Nature* 1979; 281(5727): 122-5.

262. Taniguchi CM, Emanuelli B, Kahn CR. Critical nodes in signalling pathways: insights into insulin action. *Nat Rev Mol Cell Biol* 2006; 7(2): 85-96.

263. Tarulli GA, Stanton PG, Lerchl A, Meachem SJ. Adult sertoli cells are not terminally differentiated in the Djungarian hamster: effect of FSH on proliferation and junction protein organization. *Biol Reprod* 2006; 74(5): 798-806.

264. Tarulli GA, Stanton PG, Meachem SJ. Is the adult Sertoli cell terminally differentiated? *Biol Reprod* 2012; 87(1): 13, 1-1.

265. Teshiba E, Miyahara K, Takeya H. Glucose-induced abnormal egg-laying rate in Caenorhabditis elegans. *Biosci Biotechnol Biochem* 2016; 80(7): 1436-9.

266. Thayer TC, Delano M, Liu C, et al. Superoxide production by macrophages and T cells is critical for the induction of autoreactivity and type 1 diabetes. *Diabetes* 2011; 60(8): 2144-51.

267. Totsuka Y, Tabuchi M, Kojima I, Eto Y, Shibai H, Ogata E. Stimulation of insulin secretion by transforming growth factor-beta. *Biochem Biophys Res Commun* 1989; 158(3): 1060-5.

268. Totsuka Y, Tabuchi M, Kojima I, Shibai H, Ogata E. A novel action of activin A: stimulation of insulin secretion in rat pancreatic islets. *Biochem Biophys Res Commun* 1988; 156(1): 335-9.

269. Towbin H, Staehelin T, Gordon J. Electrophoretic transfer of proteins from polyacrylamide gels to nitrocellulose sheets: procedure and some applications. *Proc Natl Acad Sci U S A* 1979; 76(9): 4350-4.

270. Trindade AA, Simoes AC, Silva RJ, Macedo CS, Spadella CT. Long term evaluation of morphometric and ultrastructural changes of testes of alloxan-induced diabetic rats. *Acta Cir Bras* 2013; 28(4): 256-65.

271. Triplitt C, Solis-Herrera C, Reasner C, DeFronzo RA, Cersosimo E. Classification of Diabetes Mellitus. In: De Groot LJ, Beck-Peccoz P, Chrousos G, et al., eds. Endotext. South Dartmouth (MA); 2015.

272. Ueland T, Aukrust P, Aakhus S, et al. Activin A and cardiovascular disease in type 2 diabetes mellitus. *Diab Vasc Dis Res* 2012; 9(3): 234-7.

273. Venegas-Pino DE, Wang PW, Stoute HK, et al. Sex-Specific Differences in an ApoE(-/-):Ins2(+/Akita) Mouse Model of Accelerated Atherosclerosis. *Am J Pathol* 2016; 186(1): 67-77.

274. Verspohl EJ, Ammon HP, Wahl MA. Activin A: its effects on rat pancreatic islets and the mechanism of action involved. *Life Sci* 1993; 53(13): 1069-78.

275. Vigneri R, Goldfine ID, Frittitta L. Insulin, insulin receptors, and cancer. *J Endocrinol Invest* 2016.

276. Vignon F, Le Faou A, Montagnon D, et al. Comparative study of semen in diabetic and healthy men. *Diabete Metab* 1991; 17(3): 350-4.

277. Wada M, Shintani Y, Kosaka M, Sano T, Hizawa K, Saito S. Immunohistochemical localization of activin A and follistatin in human tissues. *Endocr J* 1996; 43(4): 375-85.

278. Walkin L, Herrick SE, Summers A, et al. The role of mouse strain differences in the susceptibility to fibrosis: a systematic review. *Fibrogenesis Tissue Repair* 2013; 6(1): 18.

279. Walther N, Jansen M, Ergun S, Kascheike B, Ivell R. Sertoli cell lines established from H-2Kb-tsA58 transgenic mice differentially regulate the expression of cell-specific genes. *Exp Cell Res* 1996; 225(2): 411-21.

280. Wang F, Dai S, Wang M, Morrison H. Erectile dysfunction and fruit/vegetable consumption among diabetic Canadian men. *Urology* 2013; 82(6): 1330-5.

281. Wang J, Cao H, Wang H, et al. Multiple mechanisms involved in diabetes protection by lipopolysaccharide in non-obese diabetic mice. *Toxicol Appl Pharmacol* 2015; 285(3): 149-58.

282. Wang J, Takeuchi T, Tanaka S, et al. A mutation in the insulin 2 gene induces diabetes with severe pancreatic beta-cell dysfunction in the Mody mouse. *J Clin Invest* 1999; 103(1): 27-37.

283. Wang Q, Guo T, Portas J, McPherron AC. A soluble activin receptor type IIB does not improve blood glucose in streptozotocin-treated mice. *Int J Biol Sci* 2015; 11(2): 199-208.

284. Weigert J, Neumeier M, Wanninger J, et al. Adiponectin upregulates monocytic activin A but systemic levels are not altered in obesity or type 2 diabetes. *Cytokine* 2009; 45(2): 86-91.

285. Wessel GM. Accessorizing the testis. Enrico Sertoli and the "mother cell" of the testis. *Mol Reprod Dev* 2011; 78(3): Fmi.

286. Wessells H, Penson DF, Cleary P, et al. Effect of intensive glycemic therapy on erectile function in men with type 1 diabetes. *J Urol* 2011; 185(5): 1828-34.

287. WHO. The Cost of Diabetes - Fact Sheet No. 236. 2000.

288. Wiebe JC, Santana A, Medina-Rodriguez N, et al. Fertility is reduced in women and in men with type 1 diabetes: results from the Type 1 Diabetes Genetics Consortium (T1DGC). *Diabetologia* 2014; 57(12): 2501-4.

289. Wild S, Roglic G, Green A, Sicree R, King H. Global prevalence of diabetes: estimates for the year 2000 and projections for 2030. *Diabetes Care* 2004; 27(5): 1047-53.

290. Winnall WR, Okuma Y, Saito K, Muir JA, Hedger MP. Regulation of interleukin 1alpha, activin and inhibin by lipopolysaccharide in Sertoli cells from prepubertal rats. *Mol Cell Endocrinol* 2009; 307(1-2): 169-75.

291. Winnall WR, Wu H, Sarraj MA, et al. Expression patterns of activin, inhibin and follistatin variants in the adult male mouse reproductive tract suggest important roles in the epididymis and vas deferens. *Reprod Fertil Dev* 2013; 25(3): 570-80.

292. World Health Organization DoRHaR. WHO laboratory manual for the examination and processing of human semen. In: T.C. C, editor. Fifth edition ed. Switzerland: WHO Press, World Health Organization; 2010. p. 287.

293. Wu H, Chen Y, Winnall WR, Phillips DJ, Hedger MP. Regulation of activin A release from murine bone marrow-derived neutrophil precursors by tumour necrosis factor-alpha and insulin. *Cytokine* 2013; 61(1): 199-204.

294. Wu H, Mezghenna K, Marmol P, et al. Differential regulation of mouse pancreatic islet insulin secretion and Smad proteins by activin ligands. *Diabetologia* 2014; 57(1): 148-56.

295. Wu H, Wu M, Chen Y, Allan CA, Phillips DJ, Hedger MP. Correlation between blood activin levels and clinical parameters of type 2 diabetes. *Exp Diabetes Res* 2012; 2012: 410579.

296. Xu X, Browning VL, Odorico JS. Activin, BMP and FGF pathways cooperate to promote endoderm and pancreatic lineage cell differentiation from human embryonic stem cells. *Mech Dev* 2011; 128(7-10): 412-27.

297. Yadav H, Devalaraja S, Chung S, Rane SG. TGF-beta1/Smad3 pathway targets PP2A-AMPK-FoxO1 to regulate hepatic gluconeogenesis. *J Biol Chem* 2017.

298. Yadav M, Bluestone JA, Stephan S. Peripherally induced Tregs – Role in immune homeostasis and autoimmunity. *Frontiers in Immunology* 2013; 4.

299. Yaguchi M, Nagashima K, Izumi T, Okamoto K. Neuropathological study of C57BL/6Akita mouse, type 2 diabetic model: enhanced expression of alphaB-crystallin in oligodendrocytes. *Neuropathology* 2003; 23(1): 44-50.

300. Yamanouchi J, Rainbow D, Serra P, et al. Interleukin-2 gene variation impairs regulatory T cell function and causes autoimmunity. *Nat Genet* 2007; 39(3): 329-37.

301. Yang J, Kan M, Wu GY. Bergenin ameliorates diabetic nephropathy in rats via suppressing renal inflammation and TGF-beta1-Smads pathway. *Immunopharmacol Immunotoxicol* 2016; 38(2): 145-52.

302. Yano H, Kitano N, Morimoto M, Polonsky KS, Imura H, Seino Y. A novel point mutation in the human insulin gene giving rise to hyperproinsulinemia (proinsulin Kyoto). *J Clin Invest* 1992; 89(6): 1902-7.

303. Yasuda H, Inoue K, Shibata H, et al. Existence of activin-A in A- and D-cells of rat pancreatic islet. *Endocrinology* 1993; 133(2): 624-30.

304. Yonezawa A, Ebiko M, Yoshizumi M, et al. Effects of insulin replacement on ejaculatory dysfunction in streptozotocin-induced diabetic rats. *Int J Urol* 2009; 16(2): 208-11.

305. Young JC, Wakitani S, Loveland KL. TGF-beta superfamily signaling in testis formation and early male germline development. *Semin Cell Dev Biol* 2015; 45: 94-103.

306. Yuill KH, Al Kury LT, Howarth FC. Characterization of L-type calcium channel activity in atrioventricular nodal myocytes from rats with streptozotocin-induced Diabetes mellitus. *Physiol Rep* 2015; 3(11).

307. Zhang YQ, Cleary MM, Si Y, et al. Inhibition of activin signaling induces pancreatic epithelial cell expansion and diminishes terminal differentiation of pancreatic beta-cells. *Diabetes* 2004; 53(8): 2024-33.

308. Zhang Z, Shao S, Meistrich ML. The radiation-induced block in spermatogonial differentiation is due to damage to the somatic environment, not the germ cells. *J Cell Physiol* 2007; 211(1): 149-58.

309. Zhao Y, Tan Y, Dai J, et al. Exacerbation of diabetes-induced testicular apoptosis by zinc deficiency is most likely associated with oxidative stress, p38 MAPK activation, and p53 activation in mice. *Toxicol Lett* 2011; 200(1-2): 100-6.

310. Zhao Z. Activin-A in diabetes-induced cardiac malformations in embryos. *Birth Defects Res B Dev Reprod Toxicol* 2013; 98(3): 260-7.

A Appendix: Materials

A.1 Consumables

Consumable material was purchased from Brand GmbH (Wertheim, Germany), Carl Roth GmbH & Co. KG (Karlsruhe, Germany), Duran Group GmbH (Wertheim/Main, Germany), Greiner Bio-One GmbH (Frickenhausen, Germany), ThermoScientific (MA, USA), Pechiney (Chicago, USA), Sarstedt AG & Co. (Nürnbrecht, Germany), Schleicher & Schuell (Dassel, Germany), and EMD Millipore (MS, USA).

Table A-1. List of consumables with order number and manufacturer

Consumables	Manufacturer
Beakers	Duran
Cell culture microplates 96 well	Greiner Bio-One
Cell culture tubes	Greiner Bio-One
Erlenmeyer flasks	Duran
Laboratory glass bottles	Duran
Measuring cylinders	Brand
Micro tubes (1.5 ml, 2 ml)	Sarstedt
Parafilm® M	Pechiney Plastic Packaging
Pasteur pipettes (150 mm)	Carl Roth
Petri dishes	Carl Roth
Pipette tips (10 µl, 200 µl, 1000 µl)	Sarstedt
Reagent and centrifuge tube (15 ml, 50 ml)	Sarstedt
Rotilabo ®-cryo boxes	Carl Roth
Rotilabo ®-disposable cuvettes semi-micro	Carl Roth
Rotilabo ®-inoculating loops	Carl Roth
Scalpel	Carl Roth
Serological pipette (2, 5, 10, 25 ml)	Sarstedt
Steristoppers ®	Carl Roth
Toothpicks	Carl Roth
Reaction tube (1.5 ml, 2 ml)	Sarstedt
Glass tubes	ThermoScientific

PVDF membrane Immobilon-P	EMD
GB002 gel-blotting-paper	Schleicher & Schuell
120 ml container	Sarstedt
Magpix Performance Verification Kit	EMD
Magpix Performance Calibration Kit	EMD

A.2 Instruments

Instruments that were used in the present work are listed in Table A-2. Instrument manufacturers were Carl Zeiss GmbH (Jena, Germany), Hettich (Tuttlingen, Germany), Eppendorf (Hamburg, Germany), Schott AG (Mainz, Germany), Gilson (Bad Camberg, Germany), Heraeus (Hanau, Germany), Lovibond (Dortmund, Germany), Binder (Tuttlingen, Germany), Hirschmann (Eberstadt, Germany), Kern & Sohn (Bailingen, Germany), neoLab (Heidelberg, Germany), Bandelin electronic (Berlin, Germany), Heidolph Instruments (Schwabach, Germany), Bosch (Gerlingen, Germany), Köttermann GmbH & Co KG (Uetze, Germany), Fried Electric (Haifa, Israel), IKA®-Werke GmbH & CO. KG (Staufen, Germany), Satorius (Göttingen, Germany), Leica Microsystems GmbH (Wetzlar, Germany), Apple Inc. (CA, USA), Brother Industries Ltd. (Nagoya, Japan), NanoDrop (DE, USA), Vilbert Lourmat (Eberhardzell, Germany), Von Keutz (Reiskirchen, Germany), Peqlab Biotechnologie GmbH (Erlangen, Germany), VWR International (Leuven, Netherlands), Lewis plastics PTY. LTD. (VIC, Australia), Applied Biosystems (CA, USA), John Lewis (Sheffield, UK), Hoefer scientific instruments (San Francisco, USA), Dell (TX, USA), ThermoScientific (MA, USA), MS major science (CA, USA), Ratek Instruments (Boronia, Australia), EMD Millipore (MS, USA), Labsystems (Vantaa, Finnland), Sigma Laborzentrifugen (Osterode am Harz, Germany), Industrial equipment & control PTY. LTD (VIC, Australia), Ohaus (Nänikon, Switzerland), Pharmacia (Uppsala, Sweden), and Stuart Scientific (Staffordshire, UK).

Table A-2. List of instruments with model description and manufacturers.

Instrument	Manufacturer
Axioskop 2 MOT microscope	Carl Zeiss
Benchtop centrifuge universal 320R	Hettich
Biophotometer Plus	Eppendorf

Cold light source KL200	Schott
Distriman®	Gilson
HERAsafe® KS safety cabinet	Heraeus
Incubator	Lovibond
Incubator	Binder
Pipetman® P	Gilson
Pipetus®	Hirschmann
Precision balance	Kern
Rotating shaker	neoLab
Ultrasonic bath	Bandelin
Vacuum pump	neoLab
Vortex mixer REAX control	Heidolph
Water bath	Bandelin
Hera Safe KS 12laminar flow cabinet	Heraeus
CO_2 incubator	Heraeus
fridge-freezer	Bosch
Universal 32R cooling table centrifuge	Hettich
Biofuge fresco	Heraeus
Biofuge 13	Heraeus
fume cupboard	Köttermann
WBS-8 water quench	Fried Electric
Type REAX 1R vortex mixer	Heidolph
RCH magnetic mixer	IKA
Typ L610D scale (d = 0,01 g)	Satorius
Labovert FS microscope (inverse)	Leica
freezer	Bosch
iMac	Apple
MFC-7820N printer	brother
ND-1000 Spectrophotometer	NanoDrop
Darkroom-CN-3000	Vilbert Lourmat
rocking shaker	Von Keutz
Power supply	Von Keutz
PCR Gel chambers Consort E844	Von Keutz

Double gel system PerfectBlue Twin S	peqLab
PCR Thermocycler 173L	VWR
StepOnePlus Real-time PCR System	Applied Biosystems
Smoothflow fume hood SF 2000 FK 1200	Lewis
Dual gel caster Mighty smallTM SE245	Hoefer
Eppendorf Pipette 20 μl	Eppendorf
Eppendorf Pipette 200 μl	Eppendorf
1000 μl pipette	ThermoScientific
Dry Bath incubator MD-01N-220	MS
Plate shaker MPS1	Ratek
ELISA plate reader, Labsystem Multiscan RC Type: 351	Labsystems
Dimension 1100 (Computer attached to ELISA scanner)	Dell
Magnetic stirrer N1471	Industrial equipment
Scales ARB120	Ohaus
Automated plate washer Wellwash 4 MK 2	ThermoScientific
Vortex mixer VM1	Ratek
Multipipette® Plus	Eppendorf
Multiple pipette (8-channel)	Labsystems
Centrifuge Model 1-15	Sigma Laborzentrifugen
Electrophoresis Power Supply EPS 500/400	Pharmacia
Roller SRT-1	Stuart Scientific
SE250 Western Blot electrophoresis chamber	Hoefer
L2CRD Western Blot Transfer Chamber	Plaztek Scientific
Western Blot Transfer Power Supply	Bio-Rad
Roller Mixer BTR10-12V	Ratek
Odyssey® Scanner	LI-COR
Hand held magnetic separation block for 96-well plate	EMD
Magpix (Milliplex Map Multiplex Assays)	EMD

A.3 Chemicals and reagents

Chemicals and reagents (Table A-3) were purchased from Bio-Rad Laboratories GmbH (München, Germany), Carl Roth GmbH & Co. KG (Karlsruhe, Germany), Life

Technologies GmbH (Darmstadt, Germany), Merck KGaA (Darmstadt, D), Sigma-Aldrich Chemie GmbH (Munich, Germany), Serva Electrophoresis GmbH (Heidelberg, Germany), VWR International (Leuven, Netherlands), Chem-Supply Pty. Ltd. (SA, Australia), AnalaR® (VIC, Australia), BD Biosciences (CA, USA), LI-COR (NE, USA), AppliChem GmbH (Darmstadt, Germany), Peqlab Biotechnologie GmbH (Erlangen, Germany), Calbiochem (CA, USA), Otto Fischar GmbH & Co. KG (Merchweiler, Germany), Amresko LLC (OH, USA), ThermoScientific (MA, USA), and Sanquin (Amsterdam, Netherlands).

Table A-3. List of chemicals with order number and manufacturer

Chemical	Order number	Manufacturer
2-Propanol	67-63-0	Roth
2- β -Mercaptoethanol (min. 98 %)	M3148	Sigma
30 % Acrylamide/ Bis solution, 37.5:1 (2.6 % C)	161-0158	Bio-Rad
Acetic acid 100%	64-19-7	Merck
Acetic acid-n-butylester (EBE)	123-86-4	Roth
Acetone	67-64-1	Roth
Agar Agar SERVA Kobe I	11392	Serva
Agarose	35-3020	peqlab
Ammoniumpersulfate (APS)	161-0700	Bio-Rad
Ammoniumpersulfate APS	A3678	Sigma
Ampicillin sodium salt	K029.1	Roth
Bovine serum albumin (BSA)	9048-46-8	Sigma
Bovine serum albumin (BSA)	A3294	Sigma
Bromphenolblue	8122	Merck
Calcium chloride dihydrat ($CaCl_2 \cdot 2\ H_2O$)	5239.2	Roth
Calciumchlorid-Dihydrate	10035-04-8	Roth
Calciumchloridedihydrate	10035-04-8	AppliChem
Carbenicillin disodium salt	C1389	Sigma
Cholesterol	C8667	Sigma
Citric acid monohydrate	5949-29-1	Roth
D(+) Mannose	M6020	Sigma
D(+)-Glucose monohydrate	6780.1	Roth

D(+)-Saccharose	57-50-1	Roth
Deoxycholic acid	D2510	Sigma
Di-Sodium hydrogen phosphate (Na_2HPO_4)	P030.1	Roth
Di-Sodiumhydrogenphosphate	7558-79-4	Roth
Dimethylsulfoxide (DMSO)	67-68-5	Roth
Dimethylsulfoxide (DMSO)	20385	Serva
Diphenylthiocarbazone	60-10-6	Sigma
Dithizone		Sigma
DPX mountant for microscopy	360294H	VWR
EDTA	11278.01	Serva
Ethanol (> 99.5 %)	5054.3	Roth
Ethanol 100 % undenaturated	EL043-20L-P	Chem-Supply
Ethanol 100%	64-17-5	
Formaldehyde 3.5-3.7%	50-00-0	Fischar
Fuchsin	21916	Serva
Glycin	0167	Amresco
Harris Hematoxylin	HHS16	Sigma
HCl (37 %, fuming)	K35557371 603	Merck
Hematoxyline	1051750500	Merck
Hepes	7365-45-9	Roth
Hepes buffer pH 7.5	A6916	AppliChem
Hydrochloric acid 1mol/L	110165	Merck
Hydrochloric acid 25 %	7647-01-0	Roth
Hydrochloric acid 37 % fuming	100317	Merck
Hydrochloric acid 6mol/L	0281.1	Roth
Hydrogen peroxide (30 %)	K44176709 304	Merck
Hypdrogenperoxide 30%	7722-84-1	Merck
Igepal CA-630	I3021	Sigma
Isopropanol (2-Propanol)	K43192934 232	Merck
Isopropyl- β -D-thiogalactopyranoside (IPTG)	59740	Sigma
KCl	PA054	Chem-Supply
KH_2PO_4	10203.4B	AnalaR®
L-Lactic acid-sodium-salt		Serva

Levamisol hydrochloride	46944	Sigma
Magnesium sulphate heptahydrate ($MgSO_4 \cdot 7 H_2O$)	P027.2	Roth
Magnesiumsulfateheptahydrate	10034-99-8	AppliChem
MassRuler DNA Ladder Mix	#SM0403	Thermo Scientific
MassRuler Low Range DNA Ladder	#SM0383	Thermo Scientific
Methanol	MA004-20L-P	Chem-Supply
Mouse IL-6 ELISA Set	555240	BD
Na_2CO_3	A0313192 211	Merck
Na_2HPO_4	F1786486 321	Merck
NaCl	SA046	Chem-Supply
$NaHCO_3$	K45372729 428	Merck
NaN_3		
NewBlot™ PVDF Stripping Buffer	928-40032	LI-COR
Nicotinamide	98-92-0	Sigma
Nystatin Suspension	N1683	Sigma
Odyssey® Blocking buffer	927-40000	LI-COR
Odyssey® protein molecular weight marker	928-40000	LI-COR
Omnipur Tris-HCl	1185-53-1	Calbiochem
Peptone ex soya	2365.1	Roth
Pikrinsäure 1.2%	88-89-1	AppliChem
Ponceau S Solution (0.2 %)	33427	Serva
potassium chloride	7447-40-7	AppliChem
Potassium dihydrogen phosphate (KH_2PO_4)	3904.1	Roth
Potassium hexacyanoferrate (II) 3- hydrate	14459-95-1	AppliChem
Pyruvic Acid	113-24-6	Sigma
Roti®-Histokitt	6638	Roth
Roti®-Histol	6640	Roth
Sodium chloride (NaCl)	3957.1	Roth
Sodium hydroxide (NaOH)	677.1	Roth
Sodium hydroxide 10%	1310-73-2	Roth

Sodium hydroxide 1mol/L	137031	Merck
Sodium hypochlorite solution (NaClO in H_2O, 12 % Cl)	9062.3	Roth
Sodium pyruvate	113-24-6	Sigma
Sodium-dodecyl-sulfate (SDS)	161-0301	Bio-Rad
Sodium-dodecyl-sulfate SDS	151-21-3	AppliChem
Sodiumchlorid	7647-14-5	AppliChem
sodiumhydrogencarbonate	144-55-8	Roth
Strepavidin Poly-HRP	M2051	Sanquin
SYTOX ® Green nucleic acid stain	S7020	Life Technologies
TEMED	161-0801	Bio-Rad
Tetracycline hydrochloride	T7660	Sigma
Tetramethylbenzidin (TMB)	002023	Life Technologies
Tris Buffer grade	77-86-1	AppliChem
Tris-base	648310	Calbiochem
Tris-hydrochloride	1185-53-1	Roth
Triton X-100	T-9284	Sigma
Trypanblue	T8154	Sigma
Tween®-20	P1379	Sigma

A.4 Buffers and solutions

Table A-4. List of buffers and solutions

Buffer	Ingredients
10x PBS stock solution (pH 7.5)	28.8 g Na_2HPO_4 + 4.8 g KH_2PO_4 + 160 g NaCl + 4 g KCl + 1.8 L MilliQ H_2O, pH to 7.5 then make up to 2 L with MilliQ H_2O
1x PBS	100 ml 10x PBS stock solution (pH 7.5) + 900 ml RO H_2O
2x YT-agar	2x YT-medium + 15 g agar, solution was autoclaved for 1 h at 121 °C, cooled for 1 h in a

	55°C water bath, + Ampicillin (final concentration 100 µg/ ml)
2x YT-medium	16 g Bacto-pepton + 10 g Bacto-Yeast-Extract + 5 g NaCl + 1 L MilliQ H_2O, adjust pH to 7.0, solution was autoclaved for 1 h at 121 °C and stored at RT afterwards
6 % SDS in 0.05 M PBS water for ELISA media samples	30 g SDS + 500ml 0.05 M PBS
6 % SDS in MilliQ water for ELISA sera samples	30 g SDS + 500ml MilliQ H_2O
Activin A ELISA Blocking buffer (50 mM Tris-HCl, pH 7.4)	7.88 g Tris-HCl (Omnipure) + 950 ml MilliQ Water, pH to 7.4 then make up to 1 L with MilliQ H_2O add 1 % BSA prior to use
Activin B ELISA Blocking buffer (1 % BSA-PBS-6 % Sucrose)	3 ml 10x PBS (pH 7.5) + 27 ml MilliQ H_2O + 1.8 g Sucrose, mix until sucrose is dissolved, 0.3 g BSA
Ammoniumpersulfate (10%)	250 mg Ammoniumpersulfate + 2500 µl RO H_2O
Ampicillin	100 mg dissolved in 1 ml of 50 % EtOH
Bicarbonate buffer	50 ml HS buffer + 0.063 g $NaHCO_3$
Bleaching-solution	0.5 ml NaClO (12 % Cl) + 0.5 ml NaOH (5 N) + 0.5 ml MilliQ H_2O
Bromphenolblue (0,5%)	0.05 g Bromphenolblue + 10 ml RO H_2O, filter solution
$CaCl_2$	0.1 M
Carbenicillin	25 mg dissolved in 1 ml 50 % EtOH
Carbonate buffer (pH 9.6) for ELISA	6.1.1.1.1.1.1 0.8 g Na_2CO_3 (acid) + 1.5 g NaHCO3 (alk) + 500 ml MilliQ H_2O
Casein colloid buffer	2 ml 5 % Casein + 8 ml 1x PBS + 2.5 µl Strept-poly-HRP
Cholesterin	5 mg dissolved in 1 ml 100 % EtOH
EBE solution I	EBE (1 part) + 99 % Ethanol (2 parts)

EBE solution II	EBE (2 parts) + 99 % Ethanol (1 part)
EBE solution III & IV	EBE (pure)
ELISA assay buffer	1 ml 10x PBS (pH 7.5) + 9 ml MilliQ water + 0.5 g BSA
ELISA stop solution – 0.3 M HCl	1 ml concentrated HCl + 59 ml MilliQ H_2O
ELISA Wash buffer	100ml 10x PBS (pH 7.5) + 900 ml MilliQ + 0.5 ml Tween-20
HS buffer	100 ml HS buffer stock solution + 0.3 g glucose + 4 ml HEPES (1 M, pH 7.4) + 0.5 ml lactate + 0.022 g pyruvate → fill up to 200 ml and adjust pH to 7.4
HS buffer stock solution	270 mM NaCl (15.77 g) + 10 mM KCl (0.745 g) + 2 mM $MgSO_4$ + 4 mM $CaCl_2$
HSB-buffer (pH 7.2)	5 ml bicarbonate buffer + 0.025 g BSA
IPTG	1 M
KH_2PO_4 (pH 6,0)	1 M
Levamisol (2 mM)	120.38 mg Levamisol-Hydrochlorid + 250 ml MilliQ H_2O; solution was stored at 4°C
M9-buffer	3 g KH_2PO_4 + 6 g Na_2HPO_4 + 5 g NaCl + 1 L MilliQ H_2O, solution was autoclaved for 1 h at 121 °C, cooled for 1 h in a 55°C water bath, + 1 ml $MgSO_4$ solution (1 M), pH was adjusted to 7.0, solution was stored at RT
M9-buffer/Tween®20	50 ml M9-buffer + 500 μl Tween®20
$MgSO_4$	0.1 M
NaCl-Pepton-solution (autoclaved for 15 minutes at 121.9°C)	3 g NaCl + 2.5 g Bacto-Pepton + 1 L MilliQ H_2O
NGM-Agar	3 g NaCl + 2.5 g Bacto-Pepton + 17 g Agar + 947 ml MilliQ H_2O, autoclaved for 15 minutes at 121.9°C, cooled for 1 h in a 55°C water bath, + 25 ml KH_2PO_4 (1 M) + 1 ml $MgSO_4$ (0.1 M) + 1 ml $CaCl_2$ (0.1 M) + 1 ml Cholesterol (5 mg/ 100 ml) + 10 ml Nyastatin (10000 U/ml)

	ca. 9 ml of the 55°C NGM-Agar were casted into 92 mm Petri dishes; dishes were left to solidify for 1 h under sterile conditions (slightly covered); afterwards plates were stored at RT
NGM-liquid-media (prepared freshly for every trail)	9.72 ml NaCl-Pepton-solution + 10 µl Cholesterol (5 mg/ 100 ml) + 10 µl $CaCl_2$ (0.1 M) + 10 µl $MgSO_4$ (1 M) + 250 µl KH_2PO_4 (1 M) + 10 µl Carbenicillin
Nystatin (10000 U/ml)	2.14 mg/ ml
Reagent Diluent (10 % BSA in TAD (Triton Assay Diluent) (Tris-buffered Saline, 25 mM Tris, 0.15 M NaCl, 5 % Triton X-100, 0,.1 % NaN_3 and 10 % BSA)	1.51 g Tris + 4.39 g NaCl + 25 ml Triton X-100 + 0.5 g NaN_3 + 475 ml MilliQ H_2O Adjust pH to 7.2 For use in assay add 10 % BSA prior to use (15 ml TAD + 1.5 g BSA)
RIPA-Buffer	0.438 g NaCl + 0.25 g Sodiumdeoxycholate + 0.05 g SDS + 0.5 ml Igepal CA 630 + 50 mL Tris buffer (50 mM, pH 8.0)
Running buffer (1x)	200 ml Running Buffer stock solution (5x) + 800 ml RO H_2O
Running Buffer Stocksolution (5x)	15 g Tris-base + 72 g Glycin + 800 ml RO H_2O, adjust to pH 8.3, fill up to 1000 ml with RO H_2O
Sample buffer (4x Laemmli)	2.4 ml 1 M Tris (pH 6.8) + 0.8 g SDS + 4 ml Glycerol (100 %) + 0.2 ml Bromphenolblue (0.5 %) + 1.9 ml ß-Mercaptoethanol + 2.8 ml RO H_2O, 500 µl aliquots stored at -20°C
SDS (10%)	50 mg SDS + 10 ml RO H_2O
SYTOX Green	5 mM
TAE (50-fold, 250 ml)	60.5 g TRIS base, 14.28 ml acetic acid (1 M), 4.65 g Tidiplex, Aqua dest.
Tetracyclin	25 mg dissolved in 1 ml 50 % EtOH
Transfer buffer (1x)	800 ml RO H_2O + 100 ml Transfer buffer stock

	solution (10x) + 100 ml Methanol
Transfer buffer Stocksolution (10x)	29 g Glycin + 58 g Tris-base + 3.7 g SDS + 1000 ml RO H_2O
TRIS 1 M	7.88 g TRIS-HCl + 40 ml RO H_2O, adjust to pH 6.8, fill up to 50 ml with RO H_2O
TRIS 1.5 M	18.18 g TRIS-base + 70 ml RO H_2O, adjust to pH 8.8, fill up to 100 ml with RO H_2O
Tris buffer (50 mM, pH 8.0)	0.606 g Tris base + 100 ml RO H_2O
TRIS stock solution (10-fold)	60.5 g TRIS base, 700 ml A. dest, adjust to pH 7.6 using 25 % HCl, fill up to 1 L using A. dest, add 90 g NaCl
TRIS-HCl (pH 8.2)	1.576 g TRIS-HCl dissolved in 100 ml
Triton assay buffer (0,1 M Tris – 5 % Triton X-100 – 0.9 % NaCl)	6.06 g Tris-base + 4.5 g NaCl + 25 ml Triton X-100 + 450 ml MilliQ H_2O, pH to 7.5 then make up to 500 ml with MilliQ H_2O Plate buffer: add 20 % BSA prior to use Antibody diluent: add 5 % BSA prior to use

A.5 Software

Table A-5. Software

Software	Company
ChemDraw Professional 15.0	PerkinElmer Inc., MA, USA
Genesis	Novell, UT, USA
ImageJ	Open source
Luminex Software XPonent42	EMD Millipore, MS, USA
Milliplex Analyst Software	EMD Millipore, MS, USA
Odyssey	LI-COR, NE, USA
OS X El Capitan Version 10.11.5	Apple Inc., CA, USA
Windows XP home edition on ELISA computer	Microsoft Corporation, WA, USA

B Appendix: Supplementary tables

Table B-6. Clinical studies on the effect of T1D on male reproductive function

Subjects	Mean Age	Reproductive Effects	References
27 patients with T1D	34 ± 2	• significant reduction in Semen volume in diabetic men • no differences in sperm concentration, total sperm output, percentage motility or percentage normal morphology • significantly higher levels of fragmented sperm nDNA and mtDNA sperm deletions in diabetic patients • authors conclude that the "significant differences lie at a 'molecular' and not at 'cellular' level"	[3]
11 male T1D patients	32.0 ± 1.6	• no changes with regard to semen volume, sperm concentration, motility, and morphology • significantly higher levels of sperm nDNA fragmentation • significant increase in 7.8-dihydro-8-oxo-2-deoxyguanosine (8-OHdG 10^{-5}dG) in sperm form T1D patients • 8-OHdG 10^{-5}dG was significantly associated with nDNA fragmentation • T1D is related to increased oxidative stress and nDNA damage in sperm	[2]
100 T1D patients	15-80 years of age	• significant increase in prolactin, FSH, and LH levels • significant decrease in testosterone levels • testicular dysfunction with intertubular fibrosis or tubular sclerosis, organic	[8]

		vascular disease (i.e. hypogonadotropic hypogonadism), and alteration in Leydig cell morphometry	
22 diabetic patients	38 ± 6	• no differences in basal hormonal levels (LH, FSH, testosterone), but reduced response to GnRH • no differences in seminal fluid volume, sperm, concentration or total sperm number • significantly lower sperm motility • abnormal acrosome shape in 78 % • reduced acrosome dimension in 57 % • abnormal nuclear shape in 74 % • incorrectly assembled mitochondria in 45 % • broken plasma membrane in 32 % of germinal cells	[28]
15 T1D patients	18.5 years	• lower sperm values in T1D group • significant changes in sperm motility and morphology	[33]
1 T1D patient	33 years of age	• retrograde ejaculation • poor sperm motility and density • acidic ejaculate • sperm motility and density were recovered by alkalinisation of the patient	[45]
10 diabetic patients	45.6 ± 4.1	• impotence, nocturnal tumescence • testicular sections show minimal to moderate pathology • germ cell depletion • maloriented spermatids • thickened seminiferous tubule walls	[53]

		• some tubules devoid of germ cells • altered apical Sertoli cell cytoplasm with vacuolization, discontinuity of cell membranes, mitochondrial lysis • cellular debris • abnormal or absent Sertoli cell junction specification • banded collagen in interstitial area	
38 male patients with T1D	26.45 ± 0.89	• mean total testosterone concentration (22.89 ± 1.23 nmol/l) mean free testosterone concentration (0.489 ± 0.030) in T1D patients was comparable to normal subjects • any observed hypogonadotrophic hypogonadism was related to BMI, but not to T1D	[57]
27 diabetic patients	26 – 74 years of age	• no changes in serum testosterone levels • 34.6 % of patients had retrograde ejaculation • no correlation of RE with HbA1c or testosterone levels	[82]
7 T1D patients	< 40 years of age	• significant decrease in seminal volume, sperm density, percentage of sperm with progressive forward movement, and viable sperm or sperm with normal morphology • incomplete arrest of sperm maturation • hypospermatogenesis • no difference in serum concentrations of FSH and LH • rise in plasma prolactin levels • decrease in plasma testosterone levels	[91]

643 diabetic patients (69 T1D, 574 T2D)	-	• 7 % of men with T1D had low total testosterone • 20.3 % of men with T1D had low calculated free testosterone • low testosterone levels were independently associated with insulin resistance	[96]
28 T1D patients	< 50 years of age	• reduction in testicular volume, semen volume, total and total motile sperm output • elevated plasma LH and FSH levels • no direct correlation of glycemic control and spermatogenesis	[101]
333 male patients with T1D	45.9 ± 16.4	• significantly fewer children in T1D individuals • no significant difference in sex ratio	[114]
32 male T1D patients	35.84 ± 8.89	• no significant differences in sperm concentration, morphology and motility between • no difference in lipid profiles • significantly elevated AGEs levels in the seminal plasma of diabetic men • no difference in CML levels • significant increase in lipid peroxidation in spermatozoa and seminal plasma • lower total antioxidant capacity (TAC) in seminal plasma • lipid peroxidation directly correlated with AGEs • inverse correlation between AGEs and TAC	[131]
32 diabetic	35.84 ±	• no significant differences in volume of	[132]

patients (17 T1D, 15 T2D)	8.89	semen, sperm concentration, morphology and motility of sperms • significantly higher levels of RAGE protein • significantly higher DNA fragmentation in spermatozoa • sperm RAGE was directly correlated to sperm DNA fragmentation in diabetic men	
32 patients with T1D	27	• diabetic patients had lower percentage of spermatozoa with progressive motility and a higher percentage of spermatozoa with abnormal mitochondrial function • greater post-ejaculatory diameters of caput and cauda epididymis • higher percentage of spermatozoa with low mitochondrial membrane potential • these changes correlated with fasting glycemia and disease duration • no changes in sperm volume or concentration • no changes in hormone levels of FSH, LH, testosterone • no correlation between HbA1c and conventional or biofunctional spermatozoa parameters and serum hormone concentrations	[141]
20 T1D patients		• serum LH levels were significantly decreased • observed pathologies correlated with the control of the diabetic status • no difference in serum testosterone levels	[155]

		• function of the HPG-axis is compromised in young men with poorly controlled T1D	
21 diabetic patients (14 T1D, 7 T2D)	37.6 ± 9.5	• no difference in sperm concentration, number, motility, or morphology • the receptor for advanced glycation endproducts (RAGE) was found throughout the testis, caput epididymis, particularly the apical region of principle cells, and on sperm acrosomes • significantly higher number of sperm displaying RAGE and overall protein amount in sperm and seminal plasma	[163]
13 T1D patients	33.0 ± 3.8	• no changes in sperm concentration, motility, and morphology • significant increase in total sperm count in diabetics • carboxymethyl-lysine (CML) was found throughout the seminiferous epithelium, the nuclei of spermatogonia and spermatocytes, in the basal and principle cell cytoplasm and nuclei of the caput epididymis and on most sperm tails, mid pieces and all cytoplasmic droplets • acrosomal cap, especially the equatorial band, was prominently stained for CML in diabetic samples • CML was significantly higher in sperm from non-diabetic men	[164]
12 patients with T1D	-	• no significant differences using routine light microscopy • all semen parameters above WHO reference values	[162]

		• perturbations in the expression of 285 genes involved in stress response, DNA metabolism, replication/ repair • 21 genes were related to oxidative stress, glycation, and AGE/RAGE metabolism	
35 patients with T1D	30.6 ± 4.7	• significantly low serum testosterone, accompanied by low LH, low FSH • diabetic patients also displayed hypercholesterolemia, hypertriglyceridemia, and hypoalbuminemia • increased oxidative stress	[166]
80 couples with a diabetic male of which 18 underwent assisted reproduction treatment, 3 patients were reported to be T1D	36.1 ± 6.8; median diabetes duration 17.1 years	• fertilization rates of diabetic patients (IVF 68 %, ICSI 62 %) similar to non-diabetic patients (IVF 70 %, ICSI 71 %) • no difference in embryo quality • some patients showed retrograde ejaculation, azoospermia, and reduced sperm motility • lower embryo transfers rate (5 % combined IVF/ICSI pregnancy rate/cycle to 28.8 %) • more couples with diabetic men sought fertility treatment • pregnancy rates were lower in couples with a diabetic male	[173]
17 T1D patients	36 years	• no correlations found between sperm motility and age, age of onset of diabetes, duration of diabetes or glycated haemoglobin • track speed, path velocity, progressive velocity, and lateral head displacement of sperm were not significantly different	[186]

274 diabetic patients	59.9 ± 11.3	• 69.3 % had sexual disorder related to infrequency (79.2 %), non-sensuality (74.5 %), dissatisfaction with sexual acts (71.9 %), non-communication (70.8 %), impotence (67.9 %), premature ejaculation (56.6 %), and avoidance (42.7 %) • Testosterone correlated negatively with HBA1c	[197]
32 T1D patients	18.6 years	• significantly smaller semen volume, lower motility, and lower normal morphology • lower sperm count • no alterations in testosterone levels • semen parameters correlated further with diabetic neuropathy	[198]
27 diabetic patients (13 T1D, 14 T2D)	-	• ejaculates of diabetic men contain significantly higher concentrations of spermatozoa with disrupted transmembrane mitochondrial potential, activated caspase 3, reactive oxygen species and fragmented DNA • more pronounced in men with T2D • all parameters were inversely correlated with the sperm fertilizing potential	[220]
9 T1D patients, 27 T2D patients	52.6 ± 7.2	• significant decrease in sexual desire, subjective arousal, erectile capacity, coital frequency and sexual satisfaction in diabetic patients • degree of nocturnal penile tumescent episodes • no differences between types of diabetes	[229]

		• significant correlation between lack of metabolic control, diabetic complications and impaired nocturnal tumescence • sexually non-functional diabetic men had significant nocturnal penile tumescence abnormalities	
9 T1D patients, 27 T2D patients	52.6 ± 7.2	• no significant difference between diabetic types • clinical penile tumescence in diabetic patients • 77,5 % showed erectile dysfunction • respiratory abnormalities during sleep are associated with erectile difficulties in diabetic men	[230]
37 diabetic patients (7 T1D, 22 T2D)	-	• significant negative correlation between age and the penile blood pressure as determined by penile-brachial-index (PBI) • PBI correlated with impotence in diabetic group • diabetic type, complications, and adequacy of metabolic control were not related to PBI	[228]
40 diabetic patients (type of diabetes not distinguished)	52.6 ± 7.2	• significantly lower levels of erotic drive, sexual arousal, enjoyment and satisfaction • no evidence that psychological distress or psychiatric disorders are associated with diabetes or its effects on sexual function	[231]
314 T1D patients	-	• 51 % observed sexual disturbance in terms of libido, potency, and fertility	[234]
18 T1D	20 – 40	• normal semen volume, sperm count, and	[244]

patients	years of age	spermatozoal motility • significantly greater numbers of abnormal spermatozoa • elevated concentrations of prostaglandins (E2, F2 α a, and I2 and thromboxane A2) in seminal plasma	
2819 male patients with T1D	T1D diagnosed before the age of 17	• diabetic men had a smaller number of live births • hazard ratio of having a first child was 0.77 (95 %CI 0.72, 0.83) • later age at onset of diabetes was associated with a higher rate of having a first child among men (p=0.04)	[248]
18 diabetic patients (15 T1D, 3 T2D)	34 ± 5.3	• diabetics show higher sperm and round cell concentrations/ml as well as a higher total spermatozoa count • higher percentage of abnormal sperm • diabetes was not a cause of subfertility	[276]
99 T1D patients	65.1 years	• a total of 4.94 % show erectile dysfunction	[280]
761 T1D patients	48.0 ± 5.9	• risk of erectile dysfunction was directly associated with mean HbA1c • intensive glycemic therapy reduced the risk of erectile dysfunction	[286]
3010 T1D affected and 801 unaffected adult siblings (49.7 % men)	T1D patients aged ≥ 18 (31.6 ± 11.3)	• mean number of offspring was higher in unaffected than in affected siblings • birth cohort and time of onset had a significant effect on the number of offspring (p=0.001) • no significant effect of disease duration	[288]

Table B-7. Animal studies on the effect of T1D on male reproductive function

Model	Reproductive Effects	References
STZ injected male Wistar rats	• seminiferous tubule diameter and Johnsen score values were significantly decreased • significant reduction in the expression of proliferating cell nuclear antigen • enhancement in the number of TUNEL positive cells in testis tissues	[7]
STZ injected Wistar rat	• alterations in spermatogenesis in both the testis and epididymis • overall results in mitochondrial parameters failed to reveal severe testicular mitochondrial dysfunction in diabetic animals • decrease in calcium load	[14]
STZ induced male Sprague-Dawley rats	• reduced tubular and testicular diameter • reduced proliferating cell nuclear antigen index	[18]
STZ injected Wistar rat	• elevated malondialdehyde • reduced superoxide dismutase, glutathione, and serum testosterone levels • no histopathologic changes in the testis tissue • pathologies were reversed by vitamin E treatment	[26]
STZ injected Wistar rat	• mean number of offspring was higher in unaffected than in affected siblings • decreased levels of serum insulin, testosterone, FSH, and LH • negative correlation between glucose and insulin and between glucose and testosterone • positive correlation between insulin and testosterone,	[30]

	insulin and FSH, testosterone and LH, and LH and FSH • significantly reduced reproductive performance, mating index, fertility, and libido • significantly reduced testis size, which was related to loss of interstitial tissue (less compact, increase in amorphous material, decrease in the total number of Leydig cells per interstitial space (4 ± 1) • no disruption in spermatogenesis • decreased expression of markers for testicular function (phosphorylated tyrosine, GLUT3, IGF-I receptor) • no changes in testicular expression of androgen receptors	
STZ injected male Sprague-Dawley rats	• significantly reduced pituitary and plasma LH • insulin treatment completely restored these levels • significantly decreased cyclic AMP content of interstitial cell incubation medium and plasma testosterone • decreased testicular steroidogenesis in the diabetic rat may represent a direct consequence of insulin deficiency at the hypothalamic and/or pituitary levels	[34]
STZ injected male Wistar albino rats	• lowering of sexual motivation and mating activity • testes were without any traces of oedema, with normal blood filling • reduction in relative testis weight • reduction in spermatozoa • changes in spermatogenetic epithelium • changes in spermatogenic index, number of spermatogonia, tubular epithelium, degenerating changes in the testis • changes in extracellular matrix proteins	[40]
STZ injected	• significant effects on serum testosterone level, sperm DNA integrity and DNA ploidy at 36 days with no	[42]

Swiss albino mice	changes in epididymal sperm concentration or germ cell methylation status • at the end of 76 days, no significant effects on serum testosterone level, sperm DNA integrity and DNA ploidy status, but altered epididymal sperm concentration and methylation status of preleptotene/zygotene cells • an attempt to find out the association between the blood glucose levels and the abnormalities in hyperglycemic group failed to demonstrate any correlation	
STZ induced male Sprague-Dawley rats	• aromatase expression levels in testis significantly decreased in a time dependant manner • no difference in aromatase immunoreactivity in vas deferens tissues • vas deferens smooth muscle responses were altered • altered smooth muscle responses did not correlate with tissue aromatase levels	[51]
STZ injected male Wistar-GFT strain rats	• reduction in testis size • testicular atrophy and marked oxidative damage • enhanced generation of reactive oxygen species, hydroperoxide and malondialdehyde levels • mitochondrial dysfunctions manifested as reduction in the activities of aldehyde dehydrogenase, tricarboxylic acid cycle enzymes, enhanced activities of oxidative phosphorylation enzymes, perturbations in calcium homeostasis and membrane potential	[58]
STZ injected male Sprague-Dawley rats	• significant decreased intracavernous pressure indicating erectile dysfunction • this was improved with phosphodiesterase type 5 (PDE5) inhibitor • improved nNOS, endothelial cell, and smooth muscle cell staining in diabetic mice after vitamin E plus	[70]

	sildenafil treatment • urine nitric oxide increased significantly in diabetic animals but was blunted with vitamin E • significant increase in positive staining for nitrotyrosine after vitamin E plus sildenafil treatment	
STZ injected male Sprague-Dawley rats	• diabetic animals showed reduced testis weights and seminiferous tubule diameter • the PCNA (proliferating cell nuclear antigen) index was significantly decreased in the diabetic animals • total (t)-ERK and phosphor (p)-ERK immunoreactivities were significantly decreased • t-JNK immunoreactivity was unchanged • p-JNK immunoreactivity was significantly increased	[76]
NOD mice	• structural disorganization in the ventral lobe of the prostate, which was more intense in the diabetic group • increased proliferation and apoptosis rate • diabetes disturbed the prostatic secretory activity • the association of insulin, testosterone and estrogen was crucial for glandular structural restoration	[81]
STZ injected male Wistar rats	• diabetic mice had reduced testicular weight and seminiferous tubule diameter • GLUT8 immunoreactivity in diabetic rats was mainly located associated to the acrosomic system of spermatids, and at low levels in Leydig cells • no difference in expression levels of GLUT8 • insulin was diffusely located in the cytoplasm of both Leydig cells and early elongated spermatids and concentrated in a cytoplasmic compartment in the more mature spermatids • testicular insulin protein levels were significantly reduced in diabetic rats • insulin and hyperglycemia do not regulate GLUT8	[92]

	expression	
Alloxan injected male New Zealand rabbits	• nitrotyrosine, a stable end-product of nitrosative stress, is unchanged in the testis • in the testis, the level of glutathione, glutathione peroxidase and catalase, and glutathione reductase activities were increased	[97]
STZ injected male Wistar rats	• diabetic animals showed reduced FSH, LH, PRL, and GH serum levels • insulin injections restored FSH levels • reduced testis, seminal vesicle, and epididymis weights in diabetic animals were increased by insulin injections and testis weights were fully restored • higher levels of epididymal ABP activity	[119]
STZ induced male Sprague-Dawley rats	• significantly reduced testicular weights, as well as plasma levels of testosterone, 17- β estradiol, progesterone, FSH, and LH • reduction in diameter of seminiferous tubules and germinal epithelium height • oedema in interstitial tissue, germ cell depletion, decrease in cellular population and activity with disruption of spermatogenesis • mitochondrial change and reduction of smooth endoplasmic reticulum in Sertoli cells • presence of lipid droplets in Leydig cells	[133]
Ins2^{Akita} mice (C57Bl/6 Background) and STZ injected B6XSJL	• no change in expression of SLC2A1, SLC2A3, and SLC2A5 in diabetic mice • reduced testicular expression of SLC2A8 and SLC2A9b • no testicular or sperm expression of SLC2A9a in Akita mice • significantly decreased expression of 3b-hydroxysteroid dehydrogenase (HSD3B) in Leydig cells from diabetic mice	[136]

mice	• lower sperm concentration and motility • disruption in sperm parameters normalised after insulin treatment • lower fertilization rates in Akita (17.9%) and STZ-injected mice (43.6%) • lower embryo developmental rates to the blastocyst stage	
STZ injected C57Bl/6 mice	• no differences in spermatogenic activity or testicular architecture after histological examination • changes in the testicular metabolome in T1D mice as shown by reduction in carnitine, creatine, and choline and increases in lactate, alanine and myo-inositol • variations in betain levels depending on the severity of the diabetic state	[165]
STZ injected male Syrian mice	• sperm count, rapid and total motilities, morphology and viability were significantly different • reduced quality and the quantity of sperm nuclear chromatin condensation/ DNA fragmentation • reduced degree of sperm nuclear DNA susceptibility to in-situ acid-induced denaturation • no changes in the degree of sperm chromatin protamination • no sperm chromatin condensation anomalies	[167]
STZ injected male albino rats	• mean values of malondialdehyde level and caspase activity were significantly elevated in diabetic animals • SOD and GPx specific activities were significantly lower • significantly lower testosterone levels • 30% of the tubules of diabetic mice showed incomplete spermatogenesis with arrest at the secondary spermatogenic stage • occasional sperm production	[170]

	• apoptotic figures at both primary and secondary spermatogenic stage forming small dense nuclei with clumped chromatin and fragmentation surrounded by clear hallow • interstitium was oedematous, vascular and congested with normal Leydig cells • abnormalities were restored by antioxidant treatment	
STZ injected Wistar rat	• major increases in noradrenaline concentration and content of the seminal vesicles • significant reductions in the concentration and content of dopamine • small reductions in the content of serotonin and adrenaline • increased uptake of tritiated noradrenaline • release of tritiated noradrenaline was increased in response to electrical field stimulation and high potassium solutions • raising calcium concentration caused increased release of tritiated noradrenaline at rest and during electrical stimulation • increased tyrosine hydroxylase • significant changes in the sympathetic innervation of the seminal vesicle during the course of STZ diabetes	[171]
STZ induced male Sprague-Dawley rats	• significant increase in teratozoospermia • decrease in serum testosterone, tubular, and testicular and epididymal weight • decrease in seminal volume and sperm density with no change in semen motility	[180]
STZ injected male	• CML was observed in the testes, epididymides and sperm • sperm from DM mice showed strong CML	[189]

C57Bl/6 mice; *Ins2*^{Akita} mice	immunolocalization in the acrosomal cap, the equatorial region, and cytoplasmic droplets • increased CML levels did not reach statistical significance • RAGE was present on the developing acrosome and epididymal sperm of all animals and in discrete regions of the epididymides of the diabetic animals • epididymal sperm of the *Ins2*^{Akita} mice had significantly increased nDNA damage	
STZ injected male Wistar albino rats	• reduced plasma testosterone levels • ejaculatory dysfunction • reduction in sexual activity • no difference in the sensitivity of the vas deferens to norepinephrine • increased sensitivity to methoxamine through the α 1-adrenoceptor • testosterone supplementation did not restore parameters to control values • in this experimental model, the lack of testosterone was not directly related to the diabetes-induced ejaculatory dysfunction	[207]
STZ injected male Wistar rats	• reduction in plasma testosterone (T) concentrations • normal dihydrotestosterone (DHT) levels • decreased gain in absolute prostatic weight • prostatic lobe weight was 100% higher, even at the beginning of the experiment • anterior lobe showed the highest weight gain in diabetic and insulin replacement conditions • epithelial cell proliferation was significantly reduced • this was recovered by insulin replacement • diabetes diminishes prostate growth during puberty	[208]
Alloxan	• decrease in prostatic weights	[213]

injected male Wistar rats	• decrease in testosterone levels • high variation in prostate morphology and stereology with intense epithelial atrophy, premalignant and malignant lesions • chronic inflammation, similar to proliferative inflammatory atrophy • high incidence of prostatitis, adenocarcinoma and prostatic intra-epithelial neoplasia • samples with adenocarcinoma had poorly differentiated acini with high levels of cellular proliferation and nuclear atypia • invasive feature showed Bcl-2-positive cells and interruptions in the basement membrane	
STZ injected male Wistar rats	• testes of diabetic animals showed frequent abnormal histology • seminiferous epithelium cytoarchitecture appeared altered • altered occludin distribution pattern • high number of damaged tubules, with early onset of diabetes • changes in spermatogenesis are more severe with early onset of diabetes • hypertrophic interstitial compartment of the testes • fully developed, but abnormally distributed Leydig cells • decrease in plasma testosterone levels • manganese superoxide dismutase was reduced in diabetic animals	[214]
STZ injected Wistar rat	• 59 % of animals showed no copulatory behaviour • reduced number of animals reaching ejaculation • decreased reproductive organ weights • diminished sperm counts in the testis and epididymis • reduction of plasmatic testosterone levels	[227]

	• decrease in the fertility after natural mating • distal cauda epididymal sperm from diabetic rats displayed normal fertilization ability using in utero insemination • no effects of hyperglycaemia on sperm transit time in the epididymis and on spermatogenesis	
FVB.B6-*Ins2*^{Akita}/MlnJ mice	• Akita homozygous male mice are infertile with reduced testis size and abnormal morphology • reduction in seminal vesicle weight • spermatogonial germ cells are still present but are unable to mature into spermatocytes and spermatids • significantly lower motile sperm as well as lower progressively and rapidly moving sperm • display fewer sperm cells in the epididymis • sperm cells obtained from the cauda epididymis undergo degeneration • caudal epididymal sperm display sperm lacking acrosomes, some cells with membrane blebbing, and numerous detached sperm heads as well as abnormal mitochondria • decreased levels of serum testosterone and LH • These effects were restored by exogenous insulin treatment • BTB remained intact	[235]
FVB.B6-*Ins2*^{Akita}/MlnJ mice	• leptin treatment resulted in larger total body size, testes, and seminal vesicles • Akita mice showed testes with no mature spermatozoa, a high degree of vacuolization, and large multinucleated cells • leptin treatment prevented testicular degeneration and rescued sperm • leptin-treated mice produced fertile sperm	[236]

	• critical reproductive hormones LH and testosterone were only modestly higher in leptin treated mice	
STZ injected rat	• decreased reproductive organ weights • diminished sperm counts and motility and prostatic acid phosphatase • increase in seminal fructose • significant decrease in serum LH, FSH and testosterone • reproductive changes, except for prostatic changes, were restored by insulin or testosterone treatment • in diabetic animals, there are both pituitary and testicular abnormalities	[238]
STZ injected male Wistar albino rats	• reduced spermatogenesis index • reduced number of spermatogonia • increased levels of epithelium exfoliation • increased CYP2E1 expression	[240]
STZ injected CFT-Swiss mice	• enhanced lipid peroxidation in testis (cytosol and mitochondria) and epididymal sperm (ES) • increased ROS production • significant perturbations in the activities of antioxidant enzymes in testis/ES • enhanced protein carbonyl content • oxidative damage in both compartments was amenable by antioxidative treatments • significant increase in testicular DNA damage • higher incidence of abnormal sperms • mating of STZ treated males resulted in a significant increase in the male mediated dominant lethal-type mutations	[243]
STZ injected male	• significantly reduced epididymal tissue concentrations of testosterone, androgen-binding protein, sialic acid, glycerylphosphoryl choline, and carnitine	[247]

Wistar rats	• adverse effects of diabetes on the secretory activity and concentrating capacity of epididymal epithelium • impaired cauda epididymal sperm motility and fertility (*in vivo*) • defective sperm maturation • insulin replacement prevented these changes either partially or completely	
STZ injected Wistar rat	• regression of epididymis, leading to a decrease in the absolute weight of caput, corpus, and caudal regions • reduction in the size of the tubule and lumen with an increase in interstitial stroma • tightly packed principal cells with clumping of nuclei • reduction in tubular diameter, volume, and surface density • epididymal lumen was totally devoid of spermatozoa • insulin replacement could only prevent some of the adverse effects in a region specific manner	[252]
Alloxan injected male Wistar rats	• decreased serum testosterone levels • reduced diameter, total area, epithelium area and epithelium thickness of seminiferous tubules • higher tubular density • ultrastructural changes compromising the whole testis including germ-, Sertoli-, and Leydig cells, mitochondria, and cellular nuclei • most frequently vacuolization and/or accumulation of lipid droplets and electron dense dark material in cell cytoplasm and/or in membranes, cellular degeneration, and apoptosis	[270]
STZ injected male Wistar-ST	• ejaculatory capacity deteriorated with time after the onset of diabetes • significantly decreased incidence of spontaneous seminal emission and the amount of ejaculated seminal	[304]

strain rats	material • reduced amount of seminal vesicle fluid • insulin replacement, when given before changes occurred, completely prevented these changes	
STZ injected FVB mice	• diabetes significantly decreased testicular Zn levels • significant induction of testicular apoptosis with increase in Bax/Bcl-2 ratio as an index of mitochondrial cell death pathway • diabetes induces ER-Stress via CHOP and caspase-12 activation • diabetic induction of oxidative stress via increased oxidative and nitrosative damage and depressed antioxidant Nrf2 expression • increase in p53 activation and phosphorylation of p38 MAPK	[309]

Table B-8. Association between diabetes and members of the activin family of proteins

Model	Results	Reference
20 T1D patients with nephropa-thy and proteinuria and 20 without	• expression of the activin antagonist endoglin is increased in skin fibroblasts of T1D patients without nephropathy • findings suggest a protective role for endoglin in diabetic nephropathy	[10]
115 patients with acute myocardial infarction (MI)	• serum levels of activin A were significantly higher in those with abnormal glucose regulation (AGR) • activin A levels were associated with the presence of AGR after 3 months • glucose enhanced the release of activin A in endothelial	[15]

without previously known diabetes	cells • activin A attenuated the release of interleukin (IL)-8 and enhanced the mRNA levels of the antioxidant metallothionine • activin A attenuated the suppressive effect of inflammatory cytokines on insulin release in islet cells • suggests a protective effect of activin A against hyperglycemia	
α-and β-cell lines, sorted mouse islet were treated with activin and related ligands	• activins A and B suppressed critical α-cell gene expression (Arx, glucagone, MafB) in the α-cell line • activins A and B enhanced β-cell gene expression in the α-cell line • activin A induced a significant increase in Pax4 (a fate determining β-cell gene) and insulin expression in β-cells • activins suppressed α-cell gene expression and enhanced Pax4 in β-cell in isolated islets • activin treatment resulted in Smad2 phosphorylation • activins A or B significantly inhibited proliferation of α-cells	[16]
primary adult rat cardiomyocytes (ARC) exposed to conditioned media generated from EAT biopsies (CM-EAT) from	• activin A induces miR-143 in cardiomyocytes and therefore inhibits insulin action released from epicardial adipose tissue (EAT) of T2D individuals • this interaction involves the inhibition of the Akt pathway through downregulation of the novel regulator of insulin action, ORP8, which regulates glucose uptake by insulin • activin A may contribute to the pathophysiology of diabetic cardiomyopathy via induction of myocardial insulin resistance	[38]

patients with and without T2D		
human pancreas and isolated islets	• nodal expression was confirmed on mRNA and protein level, with protein expression observed in β and α-cells • cripto expression was absent from human islets • exogenous Nodal stimulated modest β-cell proliferation and inhibited α-cell proliferation with no effect on cellular viability, apoptosis, or differentiation • nodal stimulated the phosphorylation of Smad2 • no effect on AKT or MAPK signalling • cripto had no effect on human islet cell proliferation, differentiation, or viability	[39]
HIP rats, $MGP^{tg/wt}$;*Ins2*$^{Akita/+}$ mice, db/db mice, human aortic endothelial cells (HAECs)	• high glucose augmented expression of BMP-2 and BMP-4; the BMP inhibitors matrix Gla protein (MGP) and Noggin; ALK 1, -2, -3 and -6; the BMP type 2 receptor; and the vascular endothelial growth factor in HAECs and in the aortic wall of *Ins2*$^{Akita/+}$ mice, db/db mice, and HIP rats • diabetic animals showed a dramatic increase in pSMAD1/5/8, which was prevented in transgenic *Ins2*$^{Akita/+}$ mice with increased aortic BMP inhibition	[43]
Rodent islets of male C57Bl/6J mice and Lewis rats	• activin A stimulates GSIS under hyperglycemic conditions • activin A and B are predominantly expressed in rodent islets • activins A and B are synthesized in mouse islets, primarily in α-cells and to a lesser degree in β-cells • non-islet activins were primarily localized in ductal epithelium	[48]

	• inhibin α-subunit mRNA and protein was undetectable in pancreatic cells	
Human islets of 26 normal and 7 T2D donors	• Inhba (the gene encoding activin A) was most highly expressed in normal, cultured islets • Inhba was expressed in both α- and β-cells • Inhbb and FSTL3 (activin antagonist follistatin-like-3) were primarily in α –cells • in cells from T2D donors both activin A and B protein expression were undetectable → suggests a functional role for these TGF-β superfamily members in islet cells • islets from T2D donors had significantly reduced expression of Inhba and significantly increased expression of TGF-β 2 and FSTL3 • activin A affects GSIS in human islets and restores glucose responsiveness in T2D islet cells • functional islets responded with increased activin A secretion after exposure to high glucose depending on functional and diabetic status • activin A improves viability of islet cells • activin A has a role in modulating several key islet functional (*Ins*, GCG, GLUT2, CACNA1C and CACNA1D) and survival genes (HIF1α), as well as, self-regulating the expression of Inhba	[49]
78 male T2D patients	• no difference in circulating activin A levels between T2D men and controls • activin A levels were negatively correlated with myocardial glucose metabolism, and positively with left ventricular mass/volume (LVMV)-ratio in T2D men • this suggests activin A has a negative effect in diabetic cardiomyopathy	[62]
Mesen-chymal	• activin A increases the percentage of differentiation from MSCs into insulin producing cells	[67]

stem cells (MSCs)		
human pancreatic islets	• activin A did not modify insulin secretion in the absence of glucose • glucose significantly increased insulin secretion in a dose dependent manner • in the presence of low glucose (3.3 mM), activin A significantly increased insulin secretion • in the presence of activin A glucose induced an additional effect of the dose-dependent glucose-mediated insulin secretion	[85]
Transgenic mice overexpressing activin βE subunit	• overexpression of activin βE in the pancreas decreased pancreas size and caused hypoplasia in pancreatic exocrine cells • activin βE might play a role in suppressing acinar cell growth in the pancreas	[105]
cultured skin fibroblasts (SFs) from T1D patients	• mRNA levels for TGF-β1, TGF-βRII, and thrombospondin-1 were unchanged • latent TGF-β binding protein-1 mRNA expression correlates with the development of diabetic nephropathy	[117]
272 T1D patients	• susceptibility to diabetic nephropathy is not related to suggest common single nucleotide polymorphism (SNP) variants in TGFB1, TGFBR1 and TGFBR2 genes	[169]
14 C57Bl/6J mice	• ALK7 is highly expressed in the pancreas of C57Bl/6J mice	[174]
207 pregnant women (129	• significantly lower serum follistatin levels in GDM women • serum FSTL3 and activin A levels were comparable between groups	[175]

without and 78 with gestational diabetes mellitus (GDM))	• serum follistatin concentrations were negatively correlated with insulin resistance and the diagnosis of gestational diabetes	
Pancreatic islets from female Wistar Imamichi rats	• α, β A, and β B subunits of inhibin/activin and follistatin mRNAs are expressed in pancreatic islets • follistatin was localized only in insulin-producing B cells	[192]
STZ treated male Wistar rats and high glucose-cultured HK-2 cells	• increased production of pSmad2/3 with duration of diabetes • activin βA was located in tubular epithelial cells, and significantly higher in diabetic animals • follistatin diminished gradually • high glucose facilitates the synthesis of activin bA, TGF-β, and pSmad2/3 in the human kidney proximal tubular epithelial cell line	[211]
Pancreatic islets from male Wistar rats	• activin A stimulated insulin secretion and reduced extracellular Ca^{2+} in pancreatic islets • activin A increased free intracellular Ca^{2+} concentration • this was abolished by the reduction of extracellular Ca^{2+} or the addition of Ca^{2+} channel blockers • activin A did not increase intracellular Ca^{2+} in the presence of diazoxide, an opener of ATP-sensitive K^{+} channels • activin A increases insulin secretion by stimulating Ca^{2+} entry	[242]
Human islets and	• activin A decreased the number of mature and increased the number of immature β-cells	[260]

islets from C57Bl/6J mice, Pdx1 labelled MIN6 cells	• activin A decreased the expression of insulin and genes associated with beta cell maturity (e.g. Pdx1, Mafa, Glut2) in primary islets and MIN6 cells • activin A upregulated genes (e.g. Mafb) in immature β-cells • activin A reduced insulin secretion	
Pancreatic islets from male Wistar rats	• activin A stimulated insulin secretion in a dose-dependent manner • activin A potentiated GSIS	[268]
Pancreatic islets from male Wistar rats	• TGF-β increased insulin release in a concentration-dependent manner • TGF-β1 and TGF-β2 were equally effective • stimulatory action of TGF-β was greater in the presence of stimulatory concentration of glucose	[267]
102 patients with T2D	• serum activin A and the activin A/follistatin ratio were increased • elevated activin A was associated with the severity of coronary atherosclerotic burden • no significant association between presence of coronary artery disease or extent score and activin A	[272]
Pancreatic islets from male Wistar rats	• activin A increased insulin and decreased glucagon secretion in a concentration dependant manner • effect on Ca^{2+} net uptake • activin A elevated Ins(1,4,5)-P 3 content • activin A inhibited the closing of K^+ channels	[274]
Human pancreas tissue of 10 donors (mean age 57 years)	• activin A strongly immunostained in islets of Langerhans • activin A was co-localized with insulin in B cells, but not with glucagon in A cells	[277]

STZ treated male C57BL/6Ncr mice	• soluble ACVR2B treatment elevated blood glucose	[283]
Primary human monocytes from T2D patients	• systemic activin A levels were not altered in T2D patients • activin A is upregulated by adiponectin via the p38 MAPK pathway • this was reversed by the adiponectin inhibitor Metformin	[284]
participants (34 males; 58 females) with diabetes or during an oral glucose tolerance test (OGTT)	• serum levels of activin A, activin B, or follistatin did not differ between subjects with normal OGTT, impaired glucose tolerance and/or fasting glucose, or T2D • activin A and activin B were positively correlated with parameters of insulin resistance and T2D (fasting glucose, fasting insulin, glycated haemoglobin, and homeostasis model assessment of insulin resistance (HOMA-IR)) • follistatin was positively correlated with HOMA-IR alone • activin A, B, or follistatin cannot discriminate risk for T2D, but display a positive relationship with clinical parameters	[295]
bone marrow-derived neutrophil precursors (BMNPs) from male C57BL6/J mice	• murine neutrophils are a source of stored activin A • activin A release was stimulated by TNF-a • LPS stimulated activin A release and production in total • activin A secretion was not enhanced by increased glucose and insulin • insulin pre-treatment blocked the TNF-a induced release of activin A	[293]
mice lacking activin B	• Inhbb$^{-/-}$ mice displayed elevated serum insulin levels and GSIS • injection of a soluble activin B antagonist phenocopied	[294]

(Inhbb$^{-/-}$), pancreatic islets derived from these mutants	these changes in wild-type mice • isolated pancreatic islets from Inhbb$^{-/-}$ mice showed enhanced GSIS - was rescued by exogenous activin B • activin B negatively regulated GSIS and ATP production in wild-type islets, activin A displayed the opposite effects • Smad3 responded preferentially to activin B in pancreatic islets and beta cells • Smad2 showed a preference for activin A • overexpression of Smad3, but not Smad2, decreased GSIS in pancreatic islets	
Human embryonic stem cells (hESC)	• activin A promoted the differentiation of hESCs to a mesendoderm fate • activin A treatment of hESCs resulted in strong induction of primitive-streak and definitive endoderm-associated genes (*MIXL1, GSC, SOX17, FOXA2*) • activin A, in combination with other signalling molecules (FGF, BMP), determines cell fate of hESCs towards pancreatic lineage cells	296
IFN-γ transgenic mice on NOD background	• activin βA and βB subunits and activin receptors (type I and II) are upregulated in duct epithelial cells during islet differentiation • βA subunit colocalized with glucagon, but not with insulin and only rarely with insulin in the regenerating pancreas • βB subunit colocalized with insulin and glucagon • inhibitors of activin signalling, follistatin and Cripto, were found to be augmented • activin inhibition significantly enhanced survival and expansion of pancreatic epithelial cells but decreased numbers of differentiated β-cells	307
STZ treated	• levels of inhibin βA expression and Smad2 and Smad3	310

female C57Bl/6J mice	activation were significantly reduced by maternal diabetes • activin A treatment significantly increased cell proliferation in the myocardium and migration of endocardial cells • activin A and Smad2/3 signalling system appears to play a role in diabetic embryopathy

List of publications

Original papers

Maresch CC, Stute DC, Ludlow H, Hammes HP, De Kretser DM, Hedger MP, Linn T. Hyperglycemia is associated with reduced testicular function and activin dysregulation in the *Ins2*$^{Akita+/-}$ mouse model of type I diabetes. Mol Cell Endocrinol. 2017 Feb 15. pii: S0303-7207(17)30107-7. doi:10.1016/j.mce.2017.02.020

Martin J, Geisel T, **Maresch C**, Krieger K, Stein J. Inadequate nutrient intake in patients with celiac disease: results from a German dietary survey. Digestion. 2013; 87(4):240-6. doi:10.1159/000348850

Review paper

Maresch CC, Stute DC, Alves MG, Oliveira PF, de Kretser DM, Linn T. Hyperglycemia-induced male reproductive dysfunction. (Under Revision – *Human Reproduction Update*)

Maresch CC, Theis S, Bosy-Westphal A, Linn T. Low glycemic index prototype isomaltulose – update of clinical trials. Nutrients 2017, 9(4), 381; doi:10.3390/nu9040381

Conference Paper

Maresch CC, Hedger M, de Krester DM, Wenzel U, Linn T. Glycation Adducts in sperm and activin regulation of inflammation induced by diabetes. Andrology. 2014; 2(S2): 2047-2927. doi:10.1111/andr.266

Declaration of honour

„I hereby declare that I have completed this work independently and without inadmissible assistance or the Doctorate Regulations of the Faculty of Medicine 23 August 2012 7.40.11 No 1 Page 9 use of other than the resources quoted. All texts that have been quoted verbatim or by analogy from published and non-published writings and all details based on verbal information have been identified as such. In the analyses that I have conducted and to which I refer in this thesis, I have followed the principles of good scientific practice, as stated in the Statute of Justus Liebig University Giessen for Ensuring Good Scientific Practice, as well as ethical principles and those governing data protection and animal welfare. I give my assurance that third parties have not received from me, either directly or indirectly, any financial remuneration for work in connection with the content of this doctoral thesis and that the work presented has not been submitted in the same or a similar form to another assessment authority in Germany or elsewhere for the purpose of being awarded a doctorate or another assessment procedure. All material taken from other sources and other persons and used in this thesis or to which direct reference is made has been identified as such. In particular, all those who took part directly and indirectly in the production of this study have been named. I agree to my thesis being subjected to scrutiny by plagiarism detection software or by an internet-based software programme.“

Acknowledgements

First and foremost I would like to extend my gratitude to my primary supervisor, Professor Dr. Thomas Linn. Thank you for giving me the opportunity to work on a project that has been challenging, but also inspired me to aim for scientific excellence and work towards providing valuable insights into diabetes-induced male infertility. Thank you for your enthusiasm and constant support, but most of all thank you for your trust in me from the very first moment on. Without this opportunity in which you have given me chance to learn every aspect of science I might not have ended up in science and I am very grateful I did.

I would also like to thank my co-supervisors, Associate Professor Mark Hedger and Professor David de Kretser, for their constant support and guidance throughout my PhD. Their on-going motivation, assistance, and constructive criticism made those last three years a great learning experience I will never forget.

I further want to thank my co-supervisor Prof. Wenzel for giving me the opportunity to work on such a fascinating model organism as *C. elegans* and for the insights into the working group of molecular nutritional research.

I would like to thank "my" RA's, Gundula, Birte, Doris, Julie, Sali, and Sue, for their assistance, technical expertise, and for helping me learn all the methods I needed from the very first step to the final result. You helped me not only by learning the methods, but also by making my life a cheerful one whenever I came into the lab – may it be by special "Lab-CD's" or by off-lab horse racing experiences – thank you so much!

To all my colleagues and friends at the JLU and the Hudson Institute for Medical Research. Special and hearty thanks to Dina, Kui, Christoph, Ally, Lexie, Fi, Cessy, Kirsten, Gavo, Steph, Cam, William aka Michael, V, Siv, Teisha, Nok, Ruki, and Julia – you guys really made my PhD an unforgettable time and took care that all the g's stay in "Giggles".

I would like to thank my family for giving me stability and support throughout my life. Thank you for always believing in me and encouraging me to chase my dreams.

I would like to finally thank my partner Steven Riedmüller. This experience would not have been the same without your continuous support and encouragement that has helped me to push through the hard times and believe in myself. You are my tower of strength and I do not want to miss you in my life. To say it with the words of our mutual favourite character: „You complete me.“ „I love you!“

I dedicate this work to my sister Nicole Maresch. My beloved big sister – without you I would not have studied nutritional sciences in the first place and I would never have gotten onto the scientific track, which I am absolutely passionate about. You seemed to always know which way I have to go and you always saw in me the person I would become, long before I did. Thank you for your love and support. I love you.

Danksagung

Mein ganz besonderer Dank gilt meinem Doktorvater, Professor Dr. Thomas Linn. Vielen Dank dafür, dass Sie mir die Möglichkeit gegeben haben an einem solchen herausfordernden Projekt zu arbeiten, welches mich inspiriert hat nach wissenschaftlicher Exzellenz zu streben und darauf hinzuarbeiten, wertvolle Einblicke in Diabetes vermittelter männlicher Infertilität zu erzielen. Vielen Dank für Ihren Enthusiasmus und Ihre fortwährende Unterstützung, jedoch vor allem vielen Dank für Ihr Vertrauen in mich, von dem ersten Moment an. Ohne diese Chance, durch welche Sie mir ermöglicht haben jeden Aspekt der Wissenschaft zu erlernen, wäre ich möglicherweise nicht in die Wissenschaft gelangt und dafür bin ich sehr dankbar.

Ich danke auch meinen Betreuern, Associate Professor Mark Hedger und Professor David de Kretser, für ihre fortwährende Unterstützung und Führung durch meine Doktorarbeit. Ihre stetige Motivation, Hilfe und konstruktive Kritik haben die letzten drei Jahre zu einer Erfahrung gemacht, die ich nie vergessen werde.

Desweiteren bedanke ich mich bei meinem Betreuer Prof. Wenzel, für die Gelegenheit an einem faszinierenden Modellorganismus wie *C. elegans* arbeiten zu dürfen sowie für die Einblicke in die Arbeit des Teams der molekularen Ernährungsforschung.

Ich danke „meinen“ MTA’s, Gundula, Birte, Doris, Julie, Sali und Sue, für ihre Hilfe, technische Expertise, und dafür, mir alle Methoden vom ersten Schritt bis zum finalen Ergebnis beizubringen. Doch nicht nur dafür, sondern auch dafür, dass ihr mich aufgeheitert habt wann immer ich ins Labor gekommen bin – sei es durch spezielle „Labor CD’s“ oder durch außerdienstliche Pferderennerfahrungen – Vielen Dank dafür!

Danke an all meine Kollegen und Freunde an der JLU und dem Hudson Institute for Medical Research. Besonderer Dank gilt Dina, Kui, Christoph, Ally, Lexie, Fi, Cessy, Kirsten, Gavo, Steph, Cam, William alias Michael, V, Siv, Teisha, Nok, Ruki, und Julia – ihr habt meine Zeit als PhD unvergesslich gemacht und immer darauf geachtet, dass alle g’s in “Giggles” bleiben.

Ich danke meiner wundervollen Familie für die Stabilität und Unterstützung, die sie mir schon mein ganzes Leben lang geben. Danke, dass ihr immer an mich glaubt und mich dabei unterstützt meine Träume wahr zu machen. Zu guter Letzt möchte ich meinem Partner Steven Riedmüller danken. Diese Erfahrung wäre nicht die Selbe gewesen ohne deine andauernde Unterstützung und Ermutigung, welche mir geholfen haben, auch die schwersten Zeiten zu überstehen. Du bist mein Fels in der Brandung und ich möchte dich in meinem Leben nie mehr missen. Um es mit den Worten unseres Lieblingsfilmcharakters zu sagen: „Du vervollständigst mich." „Ich hab dich lieb!". Ich liebe dich.

Ich widme diese Doktorarbeit meiner Schwester Nicole Maresch. Meine liebste große Schwester – ohne dich wäre ich womöglich nie auf die Idee gekommen Ernährungswissenschaften zu studieren und wäre so auch nie in der Wissenschaft, für die ich eine große Leidenschaft entwickelt habe, gelandet. Du schienst schon immer zu wissen, welcher Weg für mich der richtige ist und hast auch stets die Person in mir gesehen, zu der ich heranwachsen würde, noch lang bevor ich es tat. Vielen Dank für deine Liebe und Unterstützung. Ich liebe dich.